Investigation of the role of t(4;6) and 6q15 deletion in prostate cancer development and progression

Ling Shan

PhD Thesis

Institute of Cancer
Centre for Molecular Oncology & Imaging
Barts and the London School of Medicine and Dentistry
Queen Mary University of London
London EC1M 6BQ, UK

DECLARATION

I hereby declare that the material presented in this thesis is the result of original work done by the author, Ling Shan, at the Centre for Molecular Oncology and Imaging, and Medical Oncology, Barts and the London School of Medicine and Dentistry, Queen Mary University of London. All external sources have been properly acknowledged.

(Ling Shan)

September 2010

ACKNOWLEDGEMENTS

Firstly, I would like to thank my supervisors, Dr Yong-jie Lu and Prof. Bryan Young, for offering me the opportunity to work as a PhD student at the Institute of Cancer. My greatest appreciation and deepest gratitude are to my supervisor, Dr Yong-jie Lu, for his supervision, patience and guidance. Without his support, this project would not have been possible.

I wish to send a sincere thank you to the Transatlantic Prostate Group and Tissue Bank for supplying all the invaluable clinical samples for my project. Special thanks go to Dr Jeremy Clark, Dr Sandra Edwards and Ms Penny Flohr for technical support in fluorescence in situ hybridisation on prostate cancer tissue microarrays, Dr Phil East (CRUK) for analysing my Exon array data and the Pathology Lab for performing immunohistochemistry. I wish to express my sincere gratitude to Prof. Ian Hart, who read and corrected my thesis. Dr Lara Boyd, Kate Lines, Katrina Sweeney, Kevin Sharp and Marianne Baker also made effort to correct my thesis. As English is not my first language, the corrections from you all really mean a lot to me! Thank you very much!

I especially would like to thank all past and present colleagues in Medical Oncology and Molecular Oncology & Imaging whose help and support have been invaluable throughout my PhD. Very special thanks go to my team members: Elodie, Marc, Lara, Echo, Nuria and Kevin, whose support provided a constant source of strength, comfort and determination. I will never forget about my dear friends Chia-yu, Ka Yi and Nuria. Because of you, my PhD life became colourful. Apologies to the rest of my old friends, who are not mentioned here but the gratefulness of the friendship is always kept in my heart.

To my beloved family: Mum, Zhu-xian Liu, Dad, Jun-cai Shan, Sister, Jin Shan, I would like to say, your constant love and support has been inspirational. Finally, and above all, I would like to thank my husband, Li-gong Gao, for his unwavering support, patience and endearing love!

ABSTRACT

The recent identification of *TMPRSS2:ETS* gene fusions highlighted the importance of chromosomal rearrangement and fusion gene development in prostate tumourigenesis. We previously reported a recurrent translocation, t(4;6), in prostate cancer (PCa) with the breakpoints identified at 4q22 and 6q15 in the LNCaP cell line. A small deletion adjacent to the 6q15 breakpoint was found, which is consistent with the frequently lost chromosome region previously reported and detected by our micro-array analysis. Here I accessed the prevalence of the t(4;6)(q22;q15) and the 6q15 deletion and also looked for relevant candidate tumour suppressor genes (TSGs) in PCa. Using fluorescence *in situ* hybridisation (FISH) analysis, t(4;6)(q22;q15) was detected in 78 of 667 clinical, localised PCa samples. Statistical analysis showed it was not independently associated with patient outcome but occurred more frequently in high clinical T stage, high tumour volume specimens and in those with high baseline PSA (prostate-specific antigen) (P=0.001, 0.001 and 0.01 respectively). We hypothesised that both t(4;6)(q22;q15) and the 6q15 deletion contribute to the inactivation of TSGs at 6q15, which are associated with PCa development and progression. Therefore I investigated the TSGs located in this region. Using FISH analysis, this deletion was confirmed in 46% (13 in 28) of the PCa samples. Using Exon array to systematically detect inactivated genes in this region, four candidate genes, *CNR1*, *PNRC1*, *GJA10* and *BACH2* were identified with common down-regulation. The real-time PCR analysis validated these exon array results. However, with additional controls and clinical cancer samples, only two genes (*CNR1* and *BACH2)* still showed significant down-regulation. *CNR1* protein expression was absent in 76.8% (43 in 56) of PCa cases whereas its

expression was shown in 83.9% (26 in 31) of benign prostatic hyperplasia (BPH) samples as demonstrated by immunohistochemistry (IHC) analysis ($p<0.001$). In contrast, cytoplasmic expression of *BACH2* was slightly less in the examined PCa cases (14.0%, 12 in 86) compared with BPH samples (6.9%, 2 in 29). However, nuclear expression of *BACH2* was significantly higher in prostate cancer cases (45.3%) than it was in BPH samples (10.3%) ($p=0.001$). Five of the 43 PCa samples without *CNR1* expression were selected for sequencing and one of the five samples had insertion in the *CNR1* genomic DNA. The cellular function study of PCa cell lines indicated that the *CNR1* might function as a tumour suppressor involved in cell proliferation and invasion. In conclusion, both t(4;6)(4q22;6q15) and the 6q15 deletion are frequent events and the gene *CNR1* is a candidate TSG at this deletion region in PCa.

Publications

- **Shan L**, Ambroisine L, Clark J, Yáñez-Muñoz RJ, Fisher G, Kudahetti SC, Yang J, Kia S, Mao X, Fletcher A, Flohr P, Edwards S, Attard G, De-Bono J, Young BD, Foster CS, Reuter V, Moller H, Oliver TD, Berney DM, Scardino P, Cuzick J, Cooper CS, Lu YJ. The identification of chromosomal translocation, t(4;6)(q22;q15), in prostate cancer. ***Prostate Cancer And Prostatic Diseases.*** 2010;13(2):117-25

- Noel EE, Yeste-Velasco M, Mao X, Perry J, Kudahetti SC, Li NF, Sharp S, Chaplin T, Xue L, McIntyre A, **Shan L**, Powles T, Oliver RT, Young BD, Shipley J, Berney DM, Joel SP, Lu YJ. The association of CCND1 overexpression and cisplatin resistance in testicular germ cell tumours and other cancers. ***American Journal of Pathology.*** 2010;176(6):2607-15.

TABLE OF CONTENTS

LIST OF FIGURES

LIST OF TABLES

1 INTRODUCTION

1.1 Cancer

1.1.1 Definition and classification of cancer

Cancer is a collection of diseases that share common features. The two main characteristics of cancer are uncontrolled proliferation of the cells within a tissue type and the ability of these cells to invade from the original site and migrate to distant sites (Alison, 2002). Tumours can be divided, according to their cellular behaviour, into two major types: benign or malignant. Benign growths tend to be localised without invading surrounding tissue and histologically similar to the cell from which they arose. In contrast, malignant tumours are invasive, dissimilar to the parent tissue and become life threatening by spreading to other parts of the body (Alison, 2002).

Cancer arises from many specialised cell types. By classification of the cellular origin, cancers can be divided into four main categories: (1) **Carcinomas** arise in the epithelium and account for 90% of human cancers; (2) **Sarcomas** are cancers of the supporting/connective tissues; (3) **leukaemias** and **lymphomas** are originated from the blood and lymph glands respectively; (4) **Blastomas** arise from the outer cell layer of the early embryo. However, not all tumours fit into the major classifications (Alison, 2002). For example, **melanomas** derive from melanocytes, the pigmented cells of the skin and the retina (Weinberg, 2007).

Cancer is believed to be a monoclonal growth with accumulated genetic alterations. At the molecular level, six fundamental features (hallmarks) define malignant cells: self-sufficiency in growth signals, insensitivity to growth-inhibitory (antigrowth) signals, evasion of programmed cell death (apoptosis), limitless replicative potential, sustained angiogenesis and tissue invasion and metastasis (Hanahan and Weinberg, 2000). In recent years, deregulation of microRNA, suppressed cancer-related inflammation and increased genomic instability have been suggested as additional hallmarks of cancer (Colotta *et al.*, 2009; Negrini *et al.*, 2010).

1.1.2 Epidemiology of cancer

Cancer is a major cause of morbidity in the UK, with 297, 991 new cases diagnosed in 2007 (http://info.cancerresearchuk.org/cancerstats/index.htm). There are more than 200 different types of cancer, but more than half of the cases in the UK were from four major sites: breast (16%), lung (13%), colorectal (13%), and prostate cancer (12%). The risk of developing cancer increases with age. Nearly three quarters of cancer cases are diagnosed in individuals aged 60 and over, whereas less than 1% of all cases occur in children aged 0-14 years. Other risk factors related to cancer development include gender, ethnicity, family history, and lifestyle (http://info.cancerresearchuk.org/cancerstats/index.htm).

1.1.3 Aetiology of cancer

1.1.3.1 Genetic factors

Genetic factors associated with cancer are either germ-line mutations or somatic alterations, which cause cancer by eventually affecting two important classes of

genes: proto-oncogenes and tumour suppressor genes (Bower and Wasman, 2006).

Proto-oncogenes are genes coding for proteins that regulate cell growth, cell division, survival and differentiation. A proto-oncogene becomes an oncogene as a result of genetic alterations, such as mutations, gene amplifications or chromosomal translocations. Upon activation, oncogenes can cause cells to survive and proliferate instead of undergoing apoptosis (Croce, 2008). According to their different functions, products of oncogenes can be classified into five groups: growth factors (e.g. platelet-derived growth factor beta polypeptide, *PDGFB*); growth factor receptors (e.g. epidermal growth factor receptor, *EGFR*); signal transducers activated by growth factor binding to receptor (e.g. PI-3 and RAS/MAP kinase pathway); transcription factors (e.g. v-myc myelocytomatosis viral oncogene homolog, *c-Myc*); apoptosis regulators (e.g family members of B-cell CLL/lymphoma 2, *BCL2*) (Croce, 2008; Alison, 2002).

In contrast to oncogenes, the products of tumour suppressor genes have either a repressive effect on the regulation of the cell cycle or promote apoptosis; sometimes they do both. Thus tumour suppressor genes cause cancer by loss of their function, in most cases, through inactivation of both alleles (Knudson, 1971). In hereditary cancer syndromes, patients carrying one inactivated tumour suppressor gene in their germ line have a normal phenotype, but will develop cancer if the second gene is lost due to somatic mutation, loss of heterozygosity (LOH) or epigenetic modification. Tumour suppressor genes can be classified broadly into three groups according to their functions: (1) **Gatekeepers** include

all direct inhibitors of cell growth (suppressing proliferation, inducing apoptosis or promoting differentiation) such as adenomatous polyposis coli (*APC)*, retinoblastoma 1 (*Rb)* and tumour protein p53 (*TP53*) (van Heemst *et al.*, 2007). (2) **Caretakers** refer to the tumour suppressors that act indirectly to suppress cell growth by maintaining the integrity of the genome or repairing DNA (e.g. *MSH2*, *ATM* protein kinase and *TP53*) (van Heemst *et al.*, 2007). (3) **Landscapers** are cancer susceptibility genes that act by modulating the microenvironment in which cancer cells grow. The landscaper effect was first found in the juvenile polyposis syndrome (JPS) wherein the initiating lesions appeared to not occur in tumour cells but in the surrounding stromal cells. Loss of function of landscapers in stromal cells would induce abnormal growth of the adjacent epithelia (e.g. germline mutation of *PTEN* and *DPC4* in JPS) (Howe *et al.*, 1998; Kinzler and Vogelstein, 1997; Kinzler and Vogelstein, 1998; Lengauer *et al.*, 1998; Lynch *et al.*, 1997; Macleod, 2000; Olschwang *et al.*, 1998).

MicroRNAs (miRNAs), a class of non-coding small RNAs of 19-25 nucleotides in length, regulate the translation of about 30% of the protein coding genes through binding to complementary sequences in the 3' UTRs of target mRNAs (Lewis *et al.*, 2005), therefore miRNAs directly or indirectly affect most cellular pathways. The differential expression of miRNAs has been identified between tumours and normal tissue, indicating the association of miRNAs with tumourigenesis. So far a number of putative oncogenic and tumour-suppressive miRNA have been proposed (Medina and Slack, 2008). As an example of oncogenic miRNA, miR-17-92 cluster (13q31.3) frequently is over-expressed in B-cell lymphomas and other malignancies and acts cooperatively with *c-Myc* to

accelerate tumour development by increasing the tumour resistance to apoptosis (Medina and Slack, 2008; Ventura and Jacks, 2009). Regarding tumour-suppressive activity, lower expression of the *let-7* microRNA family has been implicated in lung cancer initiation (Yanaihara *et al.*, 2006) and correlated with a poor prognosis (Takamizawa *et al.*, 2004). *Let-7* performs its tumour suppressor role through regulating the oncogenes and proteins involved in the cell cycle, such as *RAS*, *HGMA2*, *myc*, *CDK6* and *CDC25* (Johnson *et al.*, 2007; Johnson *et al.*, 2005; Mayr *et al.*, 2007; Sampson *et al.*, 2007).

1.1.3.2 Environmental factors

The development of malignancy frequently is linked to environmental factors, which usually are divided into three groups: chemical, physical and biological factors. Certain kinds of cancers are associated with specific exposure to chemical carcinogens. Tobacco, particularly cigarette smoking, is the single greatest cause of cancer deaths in the UK. It accounts for more than a quarter (29%) of all deaths from cancer and 90% of deaths from lung cancer. Polycyclic aromatic hydrocarbons in the tar are carcinogenic. Other chemical agents, such as asbestos, wood, dust, soot, arsenic, aflatoxin , also are responsible for certain forms of human cancers (Neal and Hoskin, 2009).

The major physical carcinogen is radiation, which may either be ionising, like X-rays from medical imaging, α-particles from radon and γ-rays from cosmic radiation and isotope decay, or non-ionising like ultraviolet light from the sun. The physical carcinogen can cause direct damage to the genome, such as DNA strand breaks or point mutations. Skin and mucosal surfaces, which are exposed to the external environment, are most prone to physical carcinogenic influences.

Viruses, as biological factors, have been implicated as carcinogens. The integration of the virus genome with the infected host genome may lead to deregulation of oncogenes or inactivation of tumour suppressor genes. As a consequence, the normal cell can be malignantly transformed. For example, hepatitis B virus has been associated with hepatoma, Epstein-Barr virus (EBV) with nasopharyngeal carcinoma, B-cell and Burkitt's lymphomas and human papilloma virus (HPV) with cervical cancer (Damania, 2007).

1.1.3.3 Immune and endocrine factors

There is evidence that immunosuppression is related to development of some types of cancer. For example, the incidence of non-Hodgkin's lymphoma and Kaposi's sarcoma is increased significantly in patients with acquired immune deficiency syndrome (AIDS) (Caceres *et al.*, 2010; Gaidano *et al.*, 1996). Similarly, transplant recipients receiving drugs to induce immunosuppression have an increased incidence of Kaposi's sarcoma, non-Hodgkin's lymphoma and skin cancer (Neal and Hoskin, 2009).

Over-stimulation of receptors for hormones by endogenous or exogenous hormones can lead to excessive cell proliferation and sometimes result in malignancy. For instance, chronic severe iodine deficiency causes a rise in thyroid-stimulating hormone, leading to goitre and, in some cases, follicular carcinoma (Franceschi, 1998).

1.1.4 Multi-stage carcinogenesis

The development of cancer is a complex, multi-step process, which can be divided broadly into three sequential phases: (1) tumour initiation, (2) tumour promotion and (3) tumour progression (Trosko and Ruch, 1998). In the first phase, a cancer stem cell becomes initiated by acquiring irreversible genetic alterations leading to partial escape from homeostatic control of growth. The promotion phase refers to the process during which the initiated cell clonally expands and gives rise to a population of initiated cells. Finally, one of the initiated cells acquires additional genetic changes to transform into the malignant cell with the new properties of invasion and metastasis (Moolgavkar and Luebeck, 2003; Trosko and Ruch, 1998).

1.2 Genomic instability in cancer

1.2.1 Genomic instability in cancer

Genomic instability is a common feature of cancer cells and is present in all stages of cancer, from precancerous lesions through to disseminated disease. Underlying genomic instability might accelerate the accumulation of these mutations in oncogenes and tumour suppressor genes (Geigl *et al.*, 2008). Genomic instability refers to a series of spontaneous genomic changes occurring at a rate higher than in normal cells (Raptis and Bapat, 2006). There are various forms of genomic instability, including chromosomal instability (CIN), microsatellite instability (MIN) and CpG island methylator phenotype (CIMP) (Geigl *et al.*, 2008). The majority of human malignant tumours are characterised by CIN, defined as gain or loss of whole chromosomes or fractions of chromosomes with an increased rate. CIN can be classified as numerical and

structural instabilities. It has been suggested that CIN may represent an early event during carcinogenesis and might therefore be involved in tumour initiation (Coleman and Tsongalis, 1999, Geigl *et al.*, 2008). MIN refers to the expansion or contraction of the number of oligonucleotide repeats present in microsatellite sequences. Currently, genomic instability is best characterised for colorectal cancer. CIN and MIN occur in approximately 85% and 15% of colorectal cancer respectively (de la Chapelle, 2003) and their occurrence usually is mutually exclusive in colorectal cancer cell lines (Abdel-Rahman *et al.*, 2001). In colorectal cancer, about 10% of MIN-tumours occur sporadically and in most cases, this phenotype overlaps with CIMP, which is characterised by extensive promoter methylation (Weisenberger *et al.*, 2006). In fact, some colorectal cancers display none of CIN, MIN or CIMP. It might be because of the limitation of the detection method used, which might not detect subtle genomic changes (Mao *et al.*, 2008), or it is possible that other, as yet unknown, forms of instabilities might exist (Geigl *et al.*, 2008).

1.2.2 Mechanisms of genomic instability

In hereditary cancers, the presence of MIN is linked to mutations in DNA repair genes. Germline mutation in one of the mismatch repair genes (i.e. *MLH1*, *MSH2*, *MSH6* and *PMS2*) leads to MIN and causes hereditary nonpolyposis colorectal cancer, which occurs in approximately 5% of all colorectal cancers (de la Chapelle, 2003; Geigl *et al.*, 2008). Biallelic germline mutations in the DNA base excision repair gene, *MYH*, result in increased GC to TA transversion frequencies and account for hereditary MYH-associated polyposis colorectal cancer (Al-Tassan *et al.*, 2002). In sporadic colorectal cancers, MIN is found in most tumours with mutations in the *B-Raf* oncogene.

Compared with MIN, CIN is linked to more complex mechanisms. Numerical CIN appears to arise as a result of chromosome segregational defects, which have been shown to be caused by several factors, including multi-polar spindles, centrosome amplification, abnormal kinetochore-spindle interactions, premature chromatid separation and abnormal cytokinesis (Gollin, 2004; Gollin, 2005). Structural CIN results from chromosome breakage and rearrangement due to defects in cell cycle checkpoints, the DNA damage response and loss of telomere integrity. Human papillomavirus interferes with these processes, causing CIN and tumour formation in some of the epithelial cells that it infects (Feldser *et al.*, 2003; Gollin, 2004; Holland and Cleveland, 2009).

Currently it still is unclear whether genomic instability is the primary driving force for tumourigenesis, or whether the acquisition of genomic instability is a more passive secondary consequence, which occurs during the malignant process. However, it has been proposed that different cancers follow alternative pathways of initiation, thus the role of genomic instability in carcinogenesis may vary depending on the tumour type or nature of the transformed cell (Bayani *et al.*, 2007).

1.3 Chromosomal aberrations in cancer

1.3.1 Classification of chromosomal aberrations

Chromosomal aberration reflects an abnormal number of chromosomes or a structural abnormality in one or more chromosomes. Aneuploidy occurs when individual whole chromosomes are lost (monosomy) or extra whole chromosome(s) are gained (trisomy, tetrasomy, etc.) from the normal set of

chromosomes (46 chromosomes in human beings). Polyploidy arises when cells possess complete extra sets of chromosomes (triploidy, tetraploidy, etc.). It has been suggested that polyploidy cells are genetically unstable and precede the formation of aneuploid cells (Ganem *et al.*, 2007; Margolis *et al.*, 2003). Although it is clear today that aneuploidy is a common genetic feature of solid human tumours (Weaver and Cleveland, 2006), its role in malignant transformation remains unclear (Ricke *et al.*, 2008).

Structural chromosome abnormalities initiate when there are double strand breakages (DSB) in chromosomes, leading to loss, gain or abnormal rearrangement of one or more chromosomes. Structural abnormalities include deletion, amplification, ring chromosome, translocation, insertion, inversion and isochromosome, etc. (**Figure 1.1**). Unlike aneuploidy, structural abnormalities, especially deletions, amplifications and translocations, are an established cause of cancer (Holland and Cleveland, 2009).

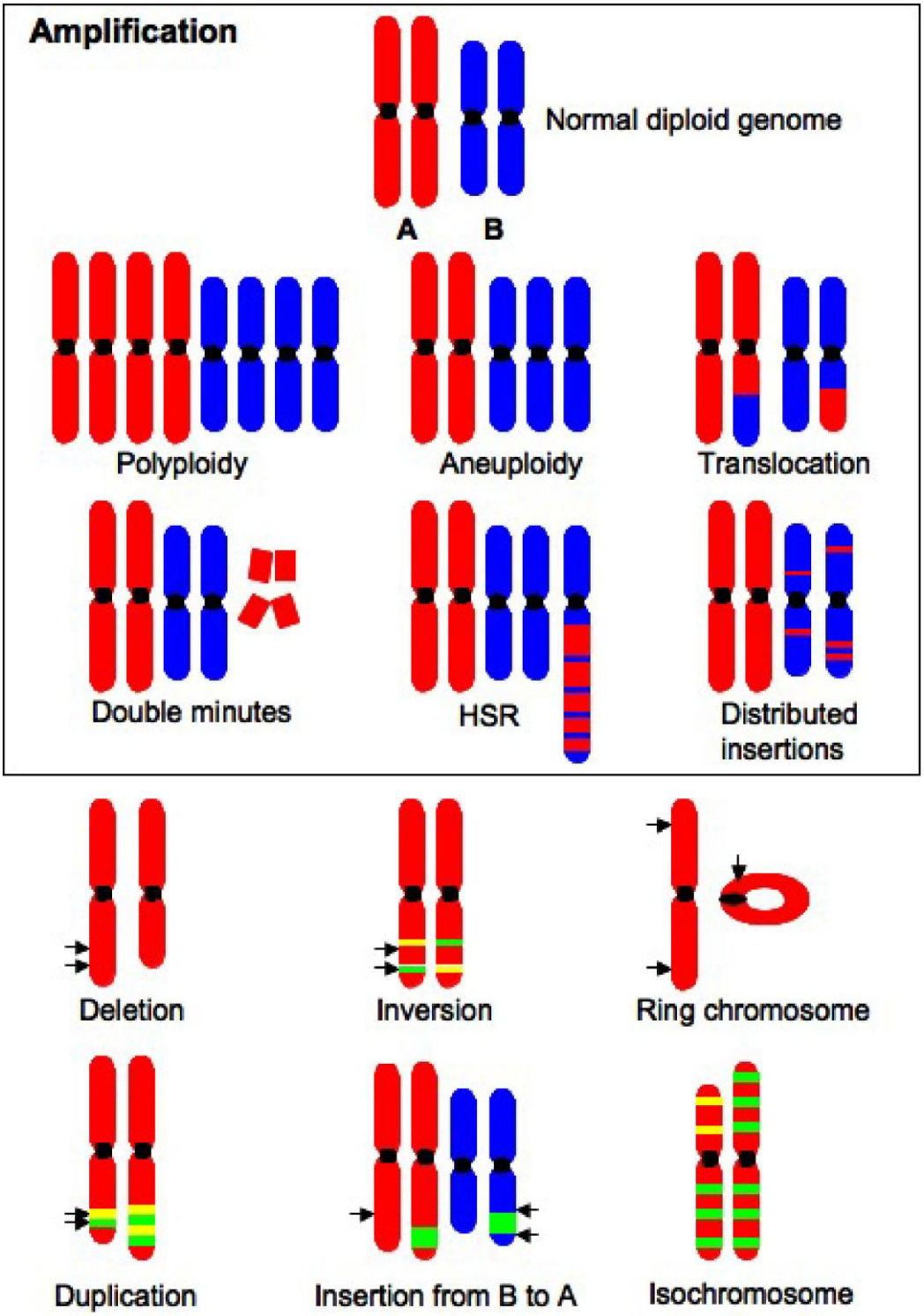

Figure 1.1 Numerical and structural changes leading to chromosomal aberrations.

Adapted from (Albertson *et al.*, 2003; Czepulkowski, 2001).

1.3.2 Deletion and amplification in cancer

Deletion is one of the most frequent genetic alterations detected in cancer cells. It can appear in the early stages of carcinogenesis, since deletion has been detected in normal cells (Deng *et al.*, 1996). Non-random deletions detected in certain regions have been widely interrogated to identify tumour suppressor genes. For example, deletions involving regions of chromosome 10 occur in the vast majority (>90%) of human glioblastoma multiforme as well as other cancers including prostate, renal, small cell lung, and endometrial carcinomas (Eagle *et al.*, 1995; Herbst *et al.*, 1994; Morita *et al.*, 1991; Peiffer *et al.*, 1995; Petersen *et al.*, 1997; Ransom *et al.*, 1992; Rempel *et al.*, 1993; Trybus *et al.*, 1996). *PTEN* was identified as the tumour suppressor gene located at 10q23−24 (Steck *et al.*, 1997). Neuroblastomas are characterised by hemizygous 1p deletions. *CHD5*, which was mapped to the smallest region of consistent deletion in a 2-Mb region of 1p36.31, was identified as the tumour suppressor (Fujita *et al.*, 2008). Deletion of tumour suppressor loci, containing *bona fide* tumour suppressor genes, such as 17p13/*TP53* and 9p21/ *p16INK4a*, has been reported in various cancers and these changes have contributed to the gene inactivation (Khayat *et al.*, 2009; Kohno and Yokota, 2006; Park *et al.*, 1996).

DNA amplification also is a frequent event in tumour cells, in which it plays a major role in oncogene activation, by causing an enhancement of gene expression (Albertson, 2006). Typical examples are amplification of oncogenes, *ERBB2*, *N-myc* and *EGFR*. *ERBB2* belongs to the epidermal growth factor receptor family. Amplification of *ERBB2* at 17q21 occurs in 10–35% of breast cancer cases and is linked to poor prognosis for patients with these tumours

(Ross and Fletcher, 1998; Slamon *et al.*, 1987; Slamon *et al.*, 1989). The increased expression of *ERBB2* in tumours led to the development of a therapy based on a specific antibody, Trastuzumab, directed against the extracellular domain of *ERBB2* (Carter *et al.*, 1992). *N-myc* belongs to the MYC proto-oncogene family and is fundamental in the development of the peripheral and central nervous systems. Amplification of *N-myc* has been reported to be present in 20% of neuroblastomas and associated with more aggressive disease (Pession and Tonelli, 2005; Savelyeva and Schwab, 2001). Amplification of *EGFR* occurs in 40% of gliomas and commonly is observed in malignant gliomas (Brandes *et al.*, 2008; Vogt *et al.*, 2004).

In recent years, miRNA has drawn great attention as more and more studies have shown that miRNAs are involved in the initiation and progression of cancer (Garzon *et al.*, 2009). It has also been shown that miRNAs are frequently located in minimal regions of loss of heterozygosity and minimal regions of amplification (Calin *et al.*, 2004). For example, miR-143 and miR-145 are located at 5q33, which frequently is deleted in myelodysplastic syndromes (Calin *et al.*, 2004). The miRNA cluster 17-92 is located at 13q31, a region commonly amplified in lymphomas (Ota *et al.*, 2004). Therefore miRNAs are now becoming the target candidates, together with tumour suppressors or oncogenes, to be searched for in recurrent deletion/amplification regions.

1.3.3 Chromosomal translocation and fusion genes

Chromosomal translocations have a causal effect in haematological malignancies. In 1960, Nowell and Hungerford reported the first consistent chromosomal abnormality, a small marker chromosome (Philadelphia

chromosome), which presents in 90% of chronic myelogenous leukaemias (CML) (Capdeville *et al.*, 2008). Philadelphia chromosome was characterised as a reciprocal translocation t(9;22), which creates a fusion gene, *BCR-ABL*, encoding a chimeric protein with increased tyrosine kinase activity (Warmuth *et al.*, 1999) and abnormal localisation (McWhirter and Wang, 1991). It has been shown that *BCR-ABL* is essential for the development of CML (Bruns *et al.*, 2009). Another important component of translocation events was the t(8;14), responsible for Burkitt's lymphoma. The fusion of the oncogene *c-Myc*, located at the breakpoint region of chromosome 8q24, with the 5' region of the immunoglobulin heavy chain (*IGH*) gene results in abnormal timing and levels of c-*Myc* expression (ar-Rushdi *et al.*, 1983; Dalla-Favera *et al.*, 1982). Accordingly, chromosomal translocation can play a causal role in malignancy through the generation of fusion genes. It can either cause juxtaposing of promoter/enhancer elements from one gene with the intact coding region of another gene, or cause recombining of the coding regions of two different genes.

Fusion genes have been causally implicated in sarcomas. Sarcomas have at least 50 different histological subtypes. Chromosomal translocations are present in about one fourth of sarcomas diagnosed, but gene fusions occur much more often in some subtypes than in others (Mertens *et al.*, 2009). For example, almost all of Ewing sarcomas, myxoid liposarcomas and synovial sarcomas harbour chimeric genes involving Ewing sarcoma breakpoint region 1 (*EWSR1*), DNA-damage-inducible transcript 3 (*DDIT3*) and synovial sarcoma X breakpoint 1, 2 or 4 (*SSX1*, *SSX2* or *SSX4*) genes, respectively, whereas no gene fusion has so far

been reported in osteosarcoma, conventional chondrosarcoma or leiomyosarcoma (Mertens *et al.*, 2009; Mitelman *et al.*, 2010).

Largely due to technical difficulties and the complexity of carcinoma karyotypes, cytogenetic analyses of carcinomas have lagged behind those of haematological malignancies and sarcomas (Edwards, 2010). It is now clear that carcinomas also have chromosomal abnormalities that result in the formation of fusion genes. The first example found in epithelial tumours was in papillary thyroid carcinoma (Pierotti *et al.*, 1992). The fusion gene joined the *RET* proto-oncogene, encoding a tyrosine kinase receptor, with the coiled-coil domain containing 6 (*CCDC6)* gene. So far, about ten fusions of *RET* and five of *NTRK1* (neurotrophic tyrosine kinase, receptor, type 1) have been found, which occur in up to 50% of papillary thyroid carcinomas. Unlike the fusion genes in haematological malignancies, which are generated by chromosomal translocation, the most prevalent fusion gene, *CCDC6/H4-RET*, is generated by inversion of a large section of chromosome, inv(10)(q11q21) (Pierotti *et al.*, 1992). Since the initial findings in thyroid cancers, other gene fusions have been discovered in less well-known carcinomas, such as the *CRTC1-MAML2* and *CRTC3-MAML2* fusions in mucoepidermoid carcinoma, the *ETV6-NTRK3* fusion in secretory breast cancer (a rare form of breast cancer) and translocations of Xp11.2, fusing the TFE3 gene, in a subset of renal cell carcinomas (Edwards, 2010; Mitelman *et al.*, 2007).

It was not until the identification of highly recurrent fusion genes in prostate and lung cancer that the pivotal role of fusion genes in common epithelial cancer was

recognised. The fusion of an androgen-responsive gene, transmembrane protease, serine 2 (*TMPRSS2*) with *ETS* transcription factor family genes has been commonly found in prostate cancer and in some cases of prostatic intraepithelial neoplasia (PIN) (Tomlins *et al.*, 2005; Clark *et al.*, 2008; Perner *et al.*, 2007; Shah and Chinnaiyan, 2009). The most prevalent fusion gene, *TMPRSS2-ERG*, was caused by either inversion or by interstitial deletion, as the two genes are about 3 Mb apart on chromosome 21 (Prensner and Chinnaiyan, 2009; Rabbitts, 2009). A variety of other fusions mostly are formed by chromosome translocations. More detail of fusion genes in prostate cancer is illustrated in section **1.6**, regarding the genetic alterations in prostate cancer.

Recurrent gene fusions have also been reported in non-small cell lung cancer (NSCLCs). The fusion between the anaplastic lymphoma kinase gene (*ALK*) and the echinoderm microtubule-associated protein-like 4 gene (*EML4*), which was created by an inversion of chromosome 2p, has been detected in a subset of NSCLCs (Soda *et al.*, 2007). Another tyrosine kinase ROS (highly expressed in NSCLCs) also becomes part of a fusion protein in lung tumours, fusing with the transmembrane portions of either SLC34A2 or CD74, to create a chimeric kinase (Rikova *et al.*, 2007).

The identification of fusion genes in prostate and lung cancer indicates that there are more undefined fusion genes in common epithelial cancers. With new technologies in sequencing, microarrays analysis and bioinformatics, it is a promising time for gene fusion discovery and characterisation of recurrent gene fusions in major epithelial cancers (Edwards, 2010).

1.4 Technologies for the detection of chromosomal aberrations

Chromosomal aberrations characterise various cancers and have been commonly studied in genetic research. The identification of chromosomal aberrations largely depends on available techniques. From low resolution banding techniques to molecular cytogenetic methods and more recent high-resolution microarray techniques, the detection of chromosomal aberrations has been constantly improved. Especially, the very recent introduction of a new generation of DNA sequencers opens a new era for the systematic discovery of chromosomal rearrangements and genomic alterations (Barrett, 2010).

1.4.1 Banding technology

Karyotyping is a classical cytogenetic tool to identify chromosomal aberrations in cell metaphases (Mitelman, 1995). It usually involves the use of dyes to stain individual chromosomes and produce a pattern of alternated dark and light bands for each chromosome. Darkness or lightness of bands depends on chromosomal condensation. In classic G-banding techniques, with Giemsa as the dye mixture, light bands appear to be early replicating, guanosine/cytosine (GC) and gene-rich, whereas the dark ones are late replicating, adenosine/thymine (AT) rich and gene-poor regions. Other alternative banding methods have also been developed. However all banding methods fall into two principal groups: (1) bands distributed along the whole chromosome, such as G-, Q- (similar banding pattern to G-banding), and R-banding (reverse band pattern of G-banding); (2) a restricted number of bands with staining on specific chromosome structures, including C-

banding (reveal constitutive heterochromatin), T-banding (visualise telomeric), and NORs (show nucleolus organising regions) (Mitelman, 1995).

Banding techniques were used to identify the first translocations in human cancer, which is the Philadelphia chromosome in CML (Nowell and Hungerford, 1960). However, as banding methods have low resolution and require good quality metaphases, they are no longer commonly used for the analysis of genetic alterations.

1.4.2 Molecular cytogenetic technology

1.4.2.1 Fluorescence *in situ* hybridisation (FISH)

FISH is a relatively simple and reliable method, which is routinely applied for the study of molecular cancer cytogenetics. It allows the identification and localisation of genetic alterations by using specific DNA probe(s) with incorporated reporter molecules (Price, 1993). In brief, the DNA probes are hybridised to chromosomal loci containing the complementary sequences. Then the reporter molecules are detected under a fluorescence microscope. The reporter molecule can be a protein, such as biotin or digoxigenin, or a fluorescent molecular such as rhodamine or fluoroisothiocyanate. The reporter molecule, as labelled nucleotides is incorporated into the probe by nick translation or primer extension (Price, 1993).

The FISH technique has been used intensively in both basic research and clinical diagnosis for detecting specific translocations, gene amplifications and deletions. Recently, the application of the FISH method on paraffin-embedded tissue

microarrays has been optimised (Lu *et al.*, 1999; Summersgill *et al.*, 2008). This combination of methods enables the detection of specific genetic alterations on a large number of clinical samples in parallel. Therefore, it is becoming a promising approach to be applied widely in clinical research.

1.4.2.2 Multiplex fluorescence *in situ* hybridisation (M-FISH) and Spectral karyotyping (SKY)

The development of M-FISH and SKY technology provides an accurate overview of the chromosomes present in a tumour, so that they have been used to detect translocations not recognisable by traditional banding analysis (Bayani and Squire, 2004). M-FISH use fluorescent dyes that label each chromosomal DNA in a different colour combination. As different chromosomes have unique spectral characteristics, they are hybridised with varying amounts of the dyes (Kearney, 2006). The slight variations of colour are detected by computer and the different ratios of colour combinations are translated to a pseudocolour. Therefore, each chromosome has one colour. If translocation occurs, more than one colour will appear on a chromosome. Spectral karyotyping (SKY) is a similar technique to M-FISH. The only difference between M-FISH and SKY is the imaging system used to discriminate the fluorophore combination (Bayani and Squire, 2004).

Due to the limited resolution, M-FISH and SKY, however, cannot detect translocation breakpoints accurately. In addition, metaphases are required for these techniques; therefore M-FISH and SKY are used mostly on cell lines rather than on clinical samples.

1.4.2.3 Comparative genomic hybridisation (CGH)

CGH is another molecular cytogenetic approach, which detects DNA copy number changes. Equal amounts of control and test DNA (e.g. tumour DNA), that are differentially fluorophore labelled, are hybridised simultaneously to normal metaphases. The ratio of the colours on each chromosomal segment reflects the ratio of test DNA to control DNA on that segment. The decreased and increased ratios of fluorescent intensities for the test DNA probes represent the deletion (losses) and amplification (gains) of the chromosomal regions in the cancer genome, respectively (Kallioniemi *et al.*, 1992). The CGH technique does not require metaphase spreads but has low resolution. It scans the entire genome to detect gains and losses of DNA sequences at a megabase level of resolution.

1.4.3 Microarray technology

1.4.3.1 Array Comparative genomic hybridisation

Based on CGH technology, array CGH was developed. Instead of human metaphases, array CGH uses an array of cloned DNAs or synthesised oligonucleotides immobilised on a solid surface to achieve the higher resolution (Solinas-Toldo *et al.*, 1997). Currently a commercialised CGH array can consist of 42 million probes distributed uniformly across the entire human genome, allowing detection of DNA copy number variations down to ~500 bp resolution (http://www.roche.com). Array CGH can find the breakpoints of unbalanced rearrangements but does not detect balanced rearrangements, such as reciprocal translocations.

1.4.3.2 Single nucleotide polymorphism genotyping (SNP) arrays

SNP array is a new generation of micro-array technique, which apply SNPs probes on array chips. SNPs are the most frequent genetic variation in the human genome (Dutt and Beroukhim, 2007). According to the NCBI SNP databases, the total number of SNPs currently known is around 10 million, thus the average overall frequency of SNPs is approximately one per 300 bp. Although SNPs are not evenly distributed across the whole genome, they are still the most powerful markers to detect genomic alterations. Among the different proposed platforms, Affymetrix Human Mapping arrays allow genome-wide studies using 25 nucleotide long probes and the latest SNP6.0 array chips provide very high coverage, that is, the median distance between probes is 1.7 Kb (www.invitrogen.com). SNP array has been widely used to detect genome-wide genotyping, loss of heterozygosity and DNA copy number changes (Dutt and Beroukhim, 2007).

1.4.4 Next generation sequencing technology

Next generation of DNA sequencing technology has been developed recently and it has provided a different route to systematic discovery of genome rearrangements. The new sequencers typically sequence very large numbers of DNA fragments simultaneously. In most published work, two instruments, the Roche 454 and the Illumina (formerly Solexa)1G, were applied. Briefly, the next generation of DNA sequencers work by amplifying individual DNA molecules in droplets or bound to glass, respectively, then sequencing them by adding nucleotides sequentially, monitoring the addition by light emission or fluorescence (Mardis, 2008). So far, DNA sequencing is used to discover

genome rearrangements in two main ways. Pieces of genome or cDNA can simply be sequenced at random and compared to the reference genome and transcriptome. This has worked quite well when applied to cDNA (Guffanti *et al.*, 2009; Maher *et al.*, 2009), but will not detect genomic fusion without a fusion transcript. The second way is the paired end read approach, which fragments the genome to a defined size and sequences just the ends. The paired end approach is very well suited to discovering genome rearrangements (Campbell *et al.*, 2008).

The sequencing-based methods are probably already superior for the discovery of genome rearrangements, but the molecular cytogenetic tools will remain essential for some time yet because of the analysis simplicity (Edwards, 2010).

1.5 Human prostate cancer

1.5.1 Prostate histology

Prostate develops from the urogenital sinus and is comprised of three major prostatic zones: the peripheral zone, the central zone and the transition zone, which take up 70%, 25% and 5% of the prostatic volume, respectively (McNeal, 1981). The vast majority of prostate cancers are adenocarcinomas (malignant cancer of epithelia originating in glandular tissue). Approximately 75% of prostate adenocarcinomas develop in the peripheral zone and 15% in the transition zone. Benign prostate hyperplasia (BPH) commonly arises in the central zone. The prostate gland is mainly constituted by two distinct cell types: basal cells and luminal cells. The basal cells form a layer along the basement membrane of each duct, and the luminal cells form a layer above the basal cells.

The presence of an intact basal cell layer distinguishes the non-cancerous from the cancerous gland.

1.5.2 Epidemiology

1.5.2.1 Incidence of prostate cancer in the UK

Prostate cancer is the most common cancer in men in the UK. Each year about 36,000 new cases are diagnosed with prostate cancer in the UK. Over the last 30 years, the incidence of prostate cancer has increased dramatically, although much of the increase is due to increased detection through widespread use of the PSA test. The incidence of prostate cancer is strongly related to age. More than half of prostate cancer cases are diagnosed in men aged over 70 years (www.cancerresearchuk.org).

1.5.2.2 Mortality and survival of prostate cancer patients in the UK

Prostate cancer is the second most common cause of cancer death in men in the UK, following lung cancer. In 2008 there were 10,168 deaths in the UK from prostate cancer (http://info.cancerresearchuk.org/cancerstats/).

Survival rates for prostate cancer have been successfully improved over 30 years. For men diagnosed with prostate cancer in England, the relative five-year survival rate was raised from 31% in 1971–1975 to 77% in 2001-2006 (http://info.cancerresearchuk.org/cancerstats/) This may reflect the detection of a greater proportion of latent, earlier, slow-growing tumours in more recent time periods, which would be expected to have a beneficial effect on survival rates. There may also have been genuine improvements in survival due to more

effective treatment, both for early, aggressive prostate cancers and for advanced cases.

Survival from prostate cancer is strongly related to the stage of the disease at diagnosis. For localised prostate cancer, five-year relative survival for patients in England is 90% or more in 1999-2002, but for the metastatic cancer, five-year relative survival is lower, at around 30% (http://info.cancerresearchuk.org/cancerstats/).

1.5.2.3 Risk factors

Prostate cancer is caused by multiple factors. Epidemiological studies of potential genetic, environmental and social issues have provided some clues to these underlying factors. The strongest known risk factor of prostate cancer is age. According to post-mortem results, approximately 80% of men by age 80 were shown to have cancer cells in their prostate (Sakr *et al.*, 1996). Although prostate cancer can be found in men as young as age 30, prostate cancer incidence in men under the age of 40 is extremely rare (Powell *et al.*, 2010). Ethnicity is another significant risk factor. The rate of prostate cancer differs by as much as 90-fold between populations. The lowest rates are usually in Asian men while the highest rates are in African-American population (Gronberg, 2003). Migration studies have shown that when Japanese people move from Japan to the USA, the incidence of prostate cancer in these people increases; however, the increase is only to about 50% of the rate for white people and to 25% of that for African-American people in the USA, indicating the real difference between ethnic populations (Reviewed by Gronberg, 2003). Family history plays an important role in the incidence of prostate cancer.

Approximately 5-10% of all prostate cancer patients have a family history of the disease (Bratt, 2002). Men with a family history of prostate cancer have higher risk and those whose families have an increased risk of breast cancer are also at higher risk of prostate cancer. The association between prostate cancer and breast cancer in the same family may be explained, in part, by the suggested increase in the risk of prostate cancer among men with *BRCA1/2* mutations, which are main risk factors in hereditary breast cancer (Gayther *et al*., 2000; Mitra *et al*., 2010).

Other risk factors include diet, sexual behaviour, alcohol consumption, exposure to ultraviolet radiation and occupational exposure. Red and processed meats have been reported as having a strong association with significantly increased risk of prostate cancer or death from prostate cancer (Rodriguez *et al.*, 2002; Walker *et al.*, 2005). The foods containing lycopenes and selenium probably have a protective effect while diets high in calcium may increase risk (McMichael, 2008).

1.5.3 Screening

Prostate cancer is incurable when diagnosed at a late stage. An accurate method for early detection therefore is highly desirable. However, no single, effective screening test for early prostate cancer is available at the moment. Serum PSA measurement alone is used in the USA for men over 50, or men over 45 thought to be at high risk of prostate cancer. In general, a PSA value less than 4 ng/mL is considered as normal; levels above 10 ng/mL indicate high risk; values between 4 and 10 ng/mL are the most ambiguous. Men in this range may benefit most from refinements in the PSA test, e.g. the PSA density (total serum PSA per cubic centimetre of prostatic volume), PSA velocity (change in PSA value

overtime) and percentage of free (non-protein-bound) PSA (Alison, 2002; McNeal, 1988).

The PSA test alone is not recommended for screening in the UK. There are three main reasons: 1) around 15% of men with a normal PSA level have prostate cancer (Thompson *et al.*, 2004); 2) about two-thirds of men with an elevated PSA level do not have prostate cancer; 3) there is uncertainty about the best way to treat early prostate cancer (http://www.cancerhelp.org.uk/type/prostate-cancer/). A randomized European study of prostate cancer screening recently reported that PSA-based screening reduced the rate of death from prostate cancer by 20% but was associated with a high risk of over-diagnosis (Schroder, et al., 2009).

A few new biomarkers discovered have shown some clinical value for detecting prostate cancer. Of these novel biomarkers, including human kallikrein 2 (hK2), urokinase-type plasminogen activator receptor (uPAR), prostate-specific membrane antigen (PSMA), early prostate cancer antigen (EPCA), prostate cancer antigen 3 (PCA3), alpha-methylacyl-CoA racemase (AMACR) and glutathione S-transferase pi (GSTP-1) hypermethylation, the most promising is the PCA3 test (Nogueira *et al*., 2010; Berney, 2010). PCA3 (9q21-22) is a prostate-specific non-coding mRNA, which is over-expressed 60–100 times in 95% of prostate cancers and prostate metastatic specimens than in benign prostate tissue (de Kok, *et al*., 2002). It has been shown that use of PCA3 in combination with PSA significantly increased diagnostic accuracy (Aubin *et al*., 2010). Although not approved by the FDA (USA Food and Drug Administration)

for prostate cancer detection, a commercial PCA3 test is available (Bostwick Laboratory, Glen Allen, VA, USA). Additional clinical research trials are required to provide further guidelines for widespread application of the urinary PCA3 test (Nogueira *et al*., 2010).

1.5.4 Diagnosis and tumour grade

The PSA test and digital rectal examination are routine initial tests for the diagnosis of prostate cancer, but prostate cancer can only be confirmed by biopsy. Systematic transrectal core biopsy, with guidance by transrectal ultrasound, is the most common urologic procedure used to obtain the tissue specimen. For grading adenocarcinoma of the prostate, the Gleason method is the one in most widespread usage (Gleason, 1966; Gleason and Mellinger, 1974). This system relies on the architectural assessment of tumour growth according to histological grades (grades 1-5). The grades 1, 2 and 3 represent tumours that most closely resemble normal prostate glands, and grade 4 and 5 tumours show increasingly abnormal glandular architecture (Lotan and Epstein, 2010). The Gleason score is the sum of the two most common grades. For example, if the most common tumour pattern was grade 3, and the next most common tumour pattern was grade 4, the Gleason score would be 3+4 = 7. Gleason score ranges from 2 to 10, with 2 being the least aggressive and 10 the most aggressive. For Gleason score 7, a Gleason 4+3 is a more aggressive cancer than a Gleason 3+4.

1.5.5 TNM system for tumour stage

The TNM System is the staging system most commonly used in prostate cancer **Table 1.1**. The TNM system separately assesses the tumour (T), lymph nodes (N) and secondary cancer or metastases (M).

Table 1.1 TNM Staging for Prostate Cancer*

STAGE	DEFINITION
T1	Clinically inapparent tumour, not detected by digital rectal examination nor visible by imaging
T2	Confined within the prostate
T3	Tumour extends through the prostate capsule but has not spread to other organs
T4	Tumour is fixed or invades adjacent structures other than seminal vesicles

STAGE	DEFINITION
NX	Regional lymph nodes can not be assessed
N0	No regional lymph node metastasis
N1	Regional lymph node metastasis

STAGE	DEFINITION
MX	Distant metastasis can not be assessed
M0	No distant metastasis
M1a	Non-regional lymph node(s)
M1b	Bones
M1c	Metastasis at other site(s)

* Adapted from CRUK webpage, http://www.cancerhelp.org.uk, with modifications

1.5.6 Clinical management

The latest detailed guidelines for clinical treatment of prostate cancer are published in the website of the National Institute for Health and Clinical Excellence (http://www.nice.org.uk/Guidance/CG58). In brief, prostate cancer cannot be cured when it has metastasised. Immediate hormonal therapy is recommended for patients with metastatic disease, which could extend their lives by several years. Prostate cancer can be cured when treated early. Patients diagnosed with locally advanced prostate cancer should be given dose-escalated radiotherapy or a combination of radiotherapy and adjuvant hormonal therapy. For the large group of patients diagnosed with apparently localised prostate cancer of low-to-intermediate risk, the choice of treatment (active monitoring, radical prostatectomy, or any type of radiotherapy) is adapted according to tumour characteristics and the patient's life expectancy. Because most cases of prostate cancer have an indolent course during the first 10 to 15 years, they even can be left without active treatment (Albertsen *et al.*, 2005; Johansson *et al.*, 2004). Men with a life expectancy of less than 10 years should be monitored actively as the first step in the treatment. The main difficulty that clinicians face is the small number of men diagnosed with localised prostate cancer who will have cancer progression and ultimately die if not treated. This progression is possible because of future random mutations in the tumour, or some aggressive cells that are already present but undetectable (Klein, 2009).

1.5.7 Prognostic factors

Prognostic factors provide information about the natural history (outcome) of the cancer in an individual and also can be used to estimate probable survival years

of patients after treatment. Generally, patients with a high tumour burden have a poorer prognosis, whereas patients with a low tumour burden will do much better. The prognosis is not linked strongly to the chosen treatment (Damber and Aus, 2008). For patients with localised prostate cancer, prognostic risk factors, which include clinical T stage, serum concentration of PSA, and biopsy grade or Gleason score, are commonly used (Humphrey, 2004; Montironi *et al.*, 2006). For patients with stage N1 disease, the median survival is 8 years (Aus *et al.*, 2003), better than for those with distant metastasis. For patients with distant metastases, the prognosis is poor, with an average survival of 24-48 months. More metastases on bone scan, raised serum PSA concentrations and high concentrations of bone-turnover markers indicate poorer prognosis. After treatment of patients with stage M1 disease, the PSA nadir after castration provides prognostic information; the lower the PSA, the better the prognosis. Circulating tumour cell (CTC) number has been shown to be the most accurate and independent predictor of overall survival in castration-resistant prostate cancer (de Bono *et al.*, 2008; Scher *et al.*, 2009). So far, there are no other informative risk factors to aid in the prognosis and treatment decisions to be taken for patients. Efforts to identify prostate cancer prognosticators must continue.

1.6 Genetic alterations in prostate cancer

As previously illustrated, cancer is caused by an accumulation of genetic alterations, which cause inactivation of tumour suppressor genes and/or over-expression of oncogenes. With emerging genetic and genomic technologies, extensive studies have been applied to investigate genetic alterations occurring in

prostate cancer. So far, the identification of germline variations and somatic alterations of prostate cancer have improved our understanding of molecular mechanism of prostate cancer initiation and progression.

1.6.1 Germline variations in prostate cancer

In the last decade, linkage analyses largely have been undertaken to unravel common germline mutations, which account for families with a significantly increased risk of prostate cancer. Several strong candidate genes, such as the ribonuclease L 2,5-oligoisoadenylate synthase-dependent gene (*RNAseL*, formally termed hereditary prostate cancer 1 [*HPC1*]) at 1q25, elaC homolog 2 gene (*ELAC2/HPC2*) at 17p11 and the macrophage scavenger receptor 1 gene (*MSR1*) at 8p22, have been reported to be associated with prostate cancer. However, most of the studies have not been well replicated (Schaid, 2004). So far, no gene has been identified for prostate cancer, which is equivalent to the breast cancer gene *BRCA1* or the adenomatous polyposis coli gene *APC* in colon cancer with respect to frequency or penetrance. Therefore it is believed that much of the genetic basis of prostate cancer arises from multiple, low-risk genes.

In contrast to linkage analysis, which is best suited to studying rare variants with high penetrance, genome-wide association studies (GWAS) provide greater power to detect small to modest effects on disease risk (Jorgenson and Witte, 2007). In recent years, GWAS in prostate cancer have revealed over a dozen highly replicated, independent germline loci for the disease (**Table 1.2**) (Duggan *et al.*, 2007; Eeles *et al.*, 2008; Gudmundsson *et al.*, 2007a; Gudmundsson *et al.*, 2008; Haiman *et al.*, 2007b; Thomas *et al.*, 2008a; Witte, 2007; Yeager *et al.*, 2007). Among all the loci, three regions, including 8q24, 10q and 17q, have

received the most attention. The association of 8q24 with prostate cancer was first identified through linkage and admixture studies (Amundadottir *et al.*, 2006; Freedman *et al.*, 2006) and has also been confirmed through GWAS (Eeles *et al.*, 2008). At least three distinct prostate cancer susceptibility regions have been identified within a ~ 1 Mb segment of 8q24 (Eeles *et al.*, 2008; Gudmundsson *et al.*, 2007a; Haiman *et al.*, 2007b). A meta-analysis suggests that the SNPs within 8q24 may result in a 25-50% increased risk of prostate cancer (Cheng *et al.*, 2008). SNPs in the 8q24 region have also been associated with colorectal, breast, ovarian and bladder cancer (Ghoussaini *et al.*, 2008; Haiman *et al.*, 2007a; Kiemeney *et al.*, 2008; Zanke *et al.*, 2007). No known genes reside within the 8q24 region, but the oncogene *MYC* is approximately 200 Kb downstream. Although no evidence of association between risk alleles in the 8q region and expression of *MYC* in prostate or colorectal cancer has been found (Pomerantz *et al.*, 2009b), recent functional studies have described possible mechanisms by which SNP rs6983267 increases cancer risk. It has been shown that, in colorectal cancer cells, rs6983267 differentially binds transcription factor 7-like 2 (*TCF7L2*), which is the main transcriptional effector of Wnt signalling, and the partner for β-catenin coactivation, while it physically interacts with MYC (Pomerantz *et al.*, 2009a). Whether other 8q24 risk loci also interact with MYC, and the mechanisms underlying the association of these loci with prostate cancer risk, remains unknown.

Two risk alleles were identified on chromosome 10. rs10993994 lies 2 bp upstream of the transcription start site of the β-microseminoprotein gene (*MSMB*). This risk allele has been shown to down-regulate *MSMB* expression by

approximately 70% (Buckland *et al.*, 2005). *MSMB* encodes β-microseminoprotein (PSP94), which is one of the most abundant proteins in the prostate. *MSMB* is a tumour suppressor and loss of its expression has been demonstrated to result in unregulated cell growth and tumourigenesis in prostate cancers (Whitaker *et al.*, 2010).

Two distinct loci on chromosome 17 (17q12 and 17q24) have been identified to be associated with prostate cancer and the corresponding variants increase the prostate cancer risk by approximately 20% independently (Eeles *et al.*, 2008; Gudmundsson *et al.*, 2007b; Sun *et al.*, 2008; Thomas *et al.*, 2008a). The chromosome 17q12 prostate cancer risk variant rs4430796 decreases the risk of type 2 diabetes (T2D) by approximately 10%, which is consistent with the finding that there is an inverse association between T2D and prostate cancer (Gudmundsson *et al.*, 2007b). rs4430796 locates in intron 4 of the HNF1 homeobox B gene, *HNF1B*. It might suggest that there is a common mechanism underlying both prostate cancer and T2D, such as in a hormonal or metabolic pathway, or *HNF1B* has pleitropic effects across different tissue (Gudmundsson *et al.*, 2007b).

Because of the fact that many risk loci were identified in a few years, it is possible that, with larger cohorts of prostate cancer samples, more alleles associated with the risk of developing prostate cancer and with the clinical behaviour of prostate cancer will be identified in the near future. It is challenging to identify the causal variants underlying the associations, because typically there are many strongly correlated variants in a given region and also most of the

variants do not lie within coding regions of the genome (Varghese and Easton, 2010). However, it is plausible to believe that, with more risk loci being discovered, our knowledge of the mechanisms of carcinogenesis will be expanded considerably in the near future (Manolio, 2010).

Table 1.2 Common susceptibility loci for prostate cancer identified through GWAS*

Locus	SNP	Allele (-/+)	Nearby genes and potential function	Reference
2p15	rs721048	G/A	*EHBP1*: endocytic trafficking	(Gudmundsson *et al.*, 2008)
3p12	rs2660753	C/T	Intergenic	(Eeles *et al.*, 2008)
6q25	rs9364554	C/T	*SLC22A3*: elimination of drugs and toxins	(Eeles *et al.*, 2008)
7q21	rs6465657	T/C	*LMTK2*: endosomal membrane trafficking	(Eeles *et al.*, 2008)
8q24 (region 2)	rs16901979	C/A	Intergenic	(Haiman *et al.*, 2007b)
8q24 (region 3)	rs6983267	T/G	Intergenic	(Haiman *et al.*, 2007b) (Eeles *et al.*, 2008)
8q24 (region 1)	rs1447295	C/A	Intergenic (the oncogene *MYC* is 200 kb downstream)	(Gudmundsson *et al.*, 2007a) (Haiman *et al.*, 2007b) (Eeles *et al.*, 2008)
10q11	rs10993994	C/T	*MSMB*: tumour suppressor properties	(Thomas *et al.*, 2008a) (Eeles *et al.*, 2008)
10q26	rs4962416	T/C	*CTBP2*: antiapoptotic activity	*(Thomas et al., 2008a)*
11q13	rs7931342	T/G	Intergenic	(Thomas *et al.*, 2008a) (Eeles *et al.*, 2008)
17q12	rs4430796	G/A	*HNF1B*: tumour suppressor properties, epithelial differentiation	(Gudmundsson *et al.*, 2007b) (Thomas *et al.*, 2008a) (Eeles *et al.*, 2008)
17q24	rs1859962	T/G	Intergenic	(Gudmundsson *et al.*, 2007b) (Eeles *et al.*, 2008)
19q13	rs2735839	A/G	*KLK2* and *KLK3*: serine protease that affects PSA concentrations, androgenic	(Eeles *et al.*, 2008)
Xp11	rs5945619	T/C	*NUDT10* and *NUDT11*: apoptosis, DNA repair, stress response	(Gudmundsson *et al.*, 2008) (Eeles *et al.*, 2008)

* Adapted from (Dianat *et al.*, 2009; Varghese and Easton, 2010).

1.6.2 Epigenetic alterations in prostate cancer

Somatic epigenetic alterations are an increasingly recognised phenomenon in the development of human cancers, including prostate cancer (Jones and Baylin, 2002; Jones and Baylin, 2007; Bastian *et al.*, 2004). During prostatic carcinogenesis, epigenetic changes appear to be the earliest somatic changes yet recognised in human prostate cancer, linking the appearance of epigenetic alterations to prostate cancer initiation.

Hypermethylation of glutathione S-transferase (*GSTP1*) is one of the most frequently observed epigenetic alterations, occurring in 72–100% of clinical specimens in more than 50 independent analyses (Bastian *et al.*, 2004). *GSTP1* (11q13) encodes an enzyme responsible for detoxifying electrophiles and oxidants (Lee *et al.*, 1994). Loss of *GSTP1* function likely occurs at the initiation of prostatic carcinogenesis, with *GSTP1* methylation evident in some 5–10% of proliferative inflammatory atrophy (PIA) lesions, the earliest prostate cancer precursors, and in more than 70% of prostatic intraepithelial neoplasia lesions (Nakayama *et al.*, 2003) (Brooks *et al.*, 1998).

A recent review summarised the genes that frequently are methylated in prostate cancer (Phe *et al.*, 2010). Since then, frequent methylation of a few more genes has been identified in prostate cancer (**Table 1.3**). The methylation of paired-like homeodomain 2 (*PITX2*) gene has been reported as a prostate specific antigen recurrence predictor in patients with post-radical prostatectomy prostate cancer (Banez *et al.*, 2010; Schatz *et al.*, 2010). B-cell CLL/lymphoma 2 (*BCL2*) gene was found to be silenced frequently in prostate cancer due to aberrant promoter

methylation, possibly indicating a future role of apoptosis-targeted therapy in prostate cancer (Carvalho *et al.*, 2010).The methylation of homeobox D3 (*HOXD3*) has been identified to distinguish low-grade prostate cancers from intermediate and high-grade ones and may have prognostic value when considered together with pathological stage (Kron *et al.*, 2010).

It is now clear that epigenetic regulation plays an important role in the development and progression of prostate cancer; however, the relative importance of the individual genes identified still needs to be clarified.

Table 1.3 Genes that are frequently methylated in prostate cancer *

Gene	Location	Name
GSTP-1	11q13	Glutathione S-transferase P1
CDKN2A	9p21	Cyclin-dependent kinase inhibitor 2 A (p16)
CCND2	12p13	Cyclin D2
p14b		
MGMT	10q26	O-6-methylguanine DNA methyltransferase
ASC	16p11.2	Apoptosis-associated Speck-like protein containing a CARD
AR	Xq12	Androgen receptor
ESR1	6q25.1	Oestrogen receptor 1
ESR2	14q23.2	Oestrogen receptor 2
RARβ	3p24	Retinoic acid receptor β
EDNRB	13q22	Endothelin receptor type B
RASSF1A	3p21.3	Ras association domain family protein 1 isoform A
MDR1	7q21.12	Multidrug resistance receptor 1
CDH13	16q23.3	Cadherin 13
APC	5q21-q22	Familial adenomatous polyposis
TIMP3	22q12.3	TIMP metallopeptidase inhibitor 3
CDH1	16q22.1	E-cadherin
CD44	11p13	CD44 molecule
RARRES1	3q25.32	Retinoic acid receptor responder (tazarotene induced) 1
LAMA3	18q11.2	α-3 laminin
LAMB3	1q32	β-3 laminin
LAMC2	1q25-q31	γ-3 laminin
CAV 1	7q31.1	Caveolin 1
PTGS2	1q25.2-q25.3	Prostaglandin endoperoxide synthase 2
RUNX3	1p36	Runt-related transcription factor 3
WIF1	12q14.3	WNT inhibitory factor 1
COX2	1q25.2-q25.3	Cyclo-oxygenase 2

* Adapted from (Phe *et al.*, 2010) with modifications.

1.6.3 Somatic DNA alterations

1.6.3.1 Somatic DNA copy number changes in prostate cancer

Various technologies have been used to detect somatic DNA copy number alterations in prostate cancer, including conventional cytogenetic evaluation of chromosomal aberrations, DNA polymorphism analysis for detecting LOH, CGH and microarray approaches (aCGH and SNP array) for genome-wide investigation of segmental copy number changes.

A number of chromosomal regions have been identified for their frequent alterations in prostate cancer. **Table 1.4** lists the chromosomal deletions detected by conventional cytogenetic analysis.

Application of genome-wide approaches, including CGH, aCGH and SNP array, to investigate somatic DNA copy number changes has identified more, and confined, regions with gain and loss in prostate cancer. Sun et al. performed a combined analysis of 41 studies (including 872 prostate tumours), which applied CGH/aCGH approaches to detect DNA copy number variations reported before April 2006 (Sun *et al.*, 2007). Eight deletions and five gains in prostate tumour genomes were defined as being frequently altered regions since they were observed in more than 10% of the examined tumours. In addition, three deletions and three gains were found in more than 10% of advanced tumours (**Table 1.5**)

Since April 2006, ten more studies have performed aCGH or SNP array analysis in a total number of 238 prostate tumours to examine the genome-wide DNA

copy number alterations. In each study, the frequent gain/loss regions (at least in more than 10% of examined prostate tumours) were described. All the frequent loss/gain regions revealed by the previous 41 studies have been confirmed by at least one of the ten studies. **Table 1.6** and **Table 1.7** list the gain/loss regions, which have been reported in at least two of the ten studies. One gain region on 8q and seven loss regions on 6q, 8p, 10q, 13q, 16q, 17p and 17q respectively were reported by more than five of the ten studies.

Chromosome 8q is the most commonly gained region in prostate cancer. It has been suggested that 8q gains are associated with prostate cancer progression and poor prognosis (Ribeiro *et al.*, 2006b; El Gammal *et al.*, 2010; Holcomb *et al.*, 2009). *c-MYC* is the well-defined oncogene located at 8q24. The *c-MYC* protein is a nuclear transcription factor that regulates cell proliferation, autophagy, and apoptosis. Over-expression of *c-MYC* has been identified in the majority of clinical prostate cancers and high-grade PIN samples (Gurel *et al.*, 2008). Other genes on chromosome 8q have also been implicated as potential targets of amplification. Amplification of *EIF3S3* (8q23) has been identified to be associated with advanced stage in prostate cancer. A recent study reported a target gene, *TCEB1* (8q21.11), that promotes invasion of prostate cancer cells and is involved in development of hormone-refractory prostate cancer (Jalava *et al.*, 2009).

Chromosome 8p is the region most commonly lost in prostate cancer. Allelic loss on 8p also has been demonstrated in many prostate tumours by LOH analysis (Crundwell *et al.*, 1996; Deubler *et al.*, 1997; Oba *et al.*, 2001). Several genes

located on chromosome 8p have been examined as candidate tumour suppressors, with one of the most promising being *NKX3.1*. *NKX3.1* encodes a prostate restricted homeobox protein that is involved in the regulation of prostate development (Shen and Abate-Shen, 2003). The *NKX3.1* protein is expressed in normal prostate epithelium and often is decreased in PIN lesions and in prostate tumour cells (Bethel *et al.*, 2006).

Other strong candidate tumour suppressors and oncogenes corresponding to the loss/gain regions are detailed in **Table 1.8**. It is notable that loss of 6q14-6q21 was one of the most frequent genetic alterations in prostate cancer; however, no known strong candidate genes have yet been identified in this region.

Our team recently identified differences in the somatic genomic alterations in prostate cancers from two different ethnic populations, suggesting that genetic changes might be induced by specific environmental and/or genetic risk factors (Mao *et al.*, 2010).

Table 1.4 Chromosomal deletions detected by cytogenetic analysis*

Band	No. of cases	No. of studies	Reference
1q12	5	2	(Carvalho-Salles *et al.*, 2000) (Qi *et al.*, 1996)
3p13	2	2	(Gibas *et al.*, 1985) (Jones *et al.*, 1994)
7q22	6	5	(Atkin and Baker, 1985) (Azar *et al.*, 1997) (Lundgren *et al.*, 1988) (Lundgren *et al.*, 1992) (Milasin and Micic, 1994)
8p21	3	2	(Lundgren *et al.*, 1992) (Webb *et al.*, 1996)
10q24	10	3	(Atkin and Baker, 1985) (Lundgren *et al.*, 1992)
16q22	2	2	(Webb *et al.*, 1996) (Zitzelsberger *et al.*, 1996)
17p11	3	3	(Konig *et al.*, 1998) (Molenaar *et al.*, 1996) (Teixeira *et al.*, 2000)

* Data were collected primarily from the Mitelman Database of Chromosome Aberrations and Gene Fusions in Cancer (Mitelman *et al.*, 2010). Only the chromosomes with at least two cases showing deletions and reported in at least two studies are listed.

Table 1.5 Frequently altered chromosomal regions in prostate cancer detected by CGH/aCGH analysis reported before April 2006

	Band	Peak	Peak frequency (%)	Tumour related genes
Loss	2q21.2-2q22.3*	2q22.2	12.42	*TTL, ERCC3, BIN1*
	4q21.3-4q31.1*	4q27-4q28.1	7.55	*MAD2L1, SYNPO2, MAPK10*
	5q13.1-5q21.3	5q15	13.06	*APC, MCC*
	6q14.1-6q21	6q15	22.24	*FOXO3A, GOPC, MAP3K7*
	8p21.3-8p21.1	8p21.3	34.09	*WRN, WHSC1L1, FGFR1, LZTS1, TUSC3, MSR1, NKX3.1, DLC1*
	10q23.1-10q25.3	10q23.2	11.76	*PTEN, TNFRSF6, SUFU, FGFR2*
	12p13.32-12p11.23*	12p13.1	6.02	*CDKN1B, RECQL, CCND2*
	13q14.13-13q22.2	13q21.33	28.04	*RB1, FOXO1A, LCP1, RFP2, DLEU1, DLEU2, KLF5*
	15q21.1-15q25.3*	15q23	6.66	*TCF12, BUB1B, THBS1*
	16q13-16q24.3	16q22.1	17.85	*ERCC4, CYLD, CBFB, CDH1, ATBF1, CDH11, CBFA2T3, FANCA, RBL2*
	18q12.1-18q23	18q21.33-18q22.1	12.80	*SERPINB5, SMAC, SMAD4, MALT1, DCC*
Gain	1q24.1-1q42.3*	1q32.2	7.46	*SIL, ABL2*
	3q23-3q26.33	3q26.1	10.24	*GMPS, PIK3CA, MLF1, SKIL, CCNL1, ECT2*
	4q21.21-4q27*	4q26	6.99	*NFKB1*
	7q11.21-7q33	7q21.11	12.48	*CDK6, SMOH, TIF1, HIP1, ABCB1, MET*
	8q21.3-8q24.3	8q22.2	25.09	*CBFA2T1, WISP1, MYC*
	9q32-9q34.2*	9q33.3	8.07	*ABL1, SET*
	17q24.1-17q25.3	17q24.1	11.65	*MAFG, BCAS3*
	Xq11.1-Xq23	Xq11.1	10.86	*AR*

* Regions with altered copy number frequencies below 10% in all tumours but above 10% in advanced tumours.

Table 1.6 Frequently observed regions of chromosomal loss in prostate cancer detected by aCGH/SNP array analysis reported after April 2006.

Chro.	Band	Reference
2	2q14.2	(Watson *et al.*, 2009) (Saramaki *et al.*, 2006)
	2q31.1	(Watson *et al.*, 2009) (Saramaki *et al.*, 2006)
	2q22.2	(Saramaki *et al.*, 2006) (Liu *et al.*, 2006)
3	3p12.2	(Liu *et al.*, 2006) (Kobayashi *et al.*, 2008)
	3q26.33	(Kim *et al.*, 2007) (Liu *et al.*, 2006)
4	4p16.3-4p16.1	(Holcomb *et al.*, 2009) (Saramaki *et al.*, 2006) (Holcomb *et al.*, 2008)
	4q28.2-4q31.1	(Saramaki *et al.*, 2006) (Liu *et al.*, 2006) (Saramaki *et al.*, 2006) (Kobayashi *et al.*, 2008)
5	5p15.32-5q15.2	(Holcomb *et al.*, 2008) (Watson *et al.*, 2009)
	5q12.3-5q13.2	(Ishkanian *et al.*, 2009) (Holcomb *et al.*, 2009)
	5q13.2-5q13.3	(Kim *et al.*, 2007) (Ishkanian *et al.*, 2009) (Kobayashi *et al.*, 2008)
	5q14.2	(Watson *et al.*, 2009) (Holcomb *et al.*, 2009)
	5q23.1	(Holcomb *et al.*, 2009) (Liu *et al.*, 2006)
6	**6q14-6q21**	(Saramaki *et al.*, 2006) (Holcomb *et al.*, 2009) (Ishkanian *et al.*, 2009) (Watson *et al.*, 2009) (Jiang *et al.*, 2008) (Kobayashi *et al.*, 2008) (Holcomb *et al.*, 2008) (Kim *et al.*, 2007) (Liu *et al.*, 2006) (Paris *et al.*, 2006)
8	**8p23.3-8p12**	(Kim *et al.*, 2007) (Paris *et al.*, 2006) (Kobayashi *et al.*, 2008) (Holcomb *et al.*, 2008) (Watson *et al.*, 2009) (Holcomb *et al.*, 2009) (Saramaki *et al.*, 2006) (Liu *et al.*, 2006)
10	**10q23.31**	(Kim *et al.*, 2007) (Ishkanian *et al.*, 2009) (Holcomb *et al.*, 2008) (Watson *et al.*, 2009) (Liu *et al.*, 2006)
12	12q13.13	(Watson *et al.*, 2009) (Jiang *et al.*, 2008)
13	**13q14.13-13q21.31**	(Kim *et al.*, 2007) (Ishkanian *et al.*, 2009) (Holcomb *et al.*, 2008) (Watson *et al.*, 2009) (Liu *et al.*, 2006) (Saramaki *et al.*, 2006)
16	**16q12.2-16q24.1**	(Kim *et al.*, 2007) (Ishkanian *et al.*, 2009) (Holcomb *et al.*, 2008) (Watson *et al.*, 2009) (Liu *et al.*, 2006) (Saramaki *et al.*, 2006) (Kobayashi *et al.*, 2008) (Holcomb *et al.*, 2008) (Holcomb *et al.*, 2009)
17	**17p13.1-17q13.1**	(Ishkanian *et al.*, 2009) (Watson *et al.*, 2009) (Liu *et al.*, 2006) (Holcomb *et al.*, 2009) (Saramaki *et al.*, 2006) (Jiang *et al.*, 2008)
	17q21.31	(Kim *et al.*, 2007) (Ishkanian *et al.*, 2009) (Watson *et al.*, 2009) (Liu *et al.*, 2006) (Holcomb *et al.*, 2009)
18	18q21.2-18q21.33	(Kim *et al.*, 2007) (Watson *et al.*, 2009) (Saramaki *et al.*, 2006) (Kobayashi *et al.*, 2008)
21	21q21.3	(Saramaki *et al.*, 2006) (Holcomb *et al.*, 2008)
	21q22.2	(Ishkanian *et al.*, 2009) (Watson *et al.*, 2009) (Holcomb *et al.*, 2009)
22	22q11.2	(Saramaki *et al.*, 2006) (Ishkanian *et al.*, 2009) (Watson *et al.*, 2009) (Holcomb *et al.*, 2009)
	22q13.33	(Saramaki *et al.*, 2006) (Holcomb *et al.*, 2009)

Note: Cytobands that were found in more than five of the ten studies are indicated in bold.

Table 1.7 Frequently observed regions of chromosomal gain in prostate cancer detected by aCGH/SNP array analysis reported after April 2006.

Chro.	Band	Reference
1	1q21.2-1q43	(Holcomb *et al.*, 2009) (Holcomb *et al.*, 2008) (Saramaki *et al.*, 2006) (Liu *et al.*, 2006)
2	2p23.3	(Kim *et al.*, 2007) (Holcomb *et al.*, 2008)
	2p25.1	(Kim *et al.*, 2007) (Holcomb *et al.*, 2009)
3	3q26.32	(Kim *et al.*, 2007) (Liu *et al.*, 2006) (Paris *et al.*, 2006)
	3q26.2	(Paris *et al.*, 2006) (Liu *et al.*, 2006) (Kobayashi *et al.*, 2008)
	3q25.1-3q25.2	(Jiang *et al.*, 2008) (Kobayashi *et al.*, 2008)
	3q29	(Saramaki *et al.*, 2006) (Holcomb *et al.*, 2008)
5	5p15.33	(Holcomb *et al.*, 2008) (Saramaki *et al.*, 2006) (Liu *et al.*, 2006)
	5q35.3	(Holcomb *et al.*, 2008) (Liu *et al.*, 2006)
7	7p21.3-7p13	(Kobayashi *et al.*, 2008) (Kim *et al.*, 2007) (Holcomb *et al.*, 2009)
	7q21.2-7q33	(Liu *et al.*, 2006) (Holcomb *et al.*, 2009) (Kobayashi *et al.*, 2008)
	7q36.1	(Kim *et al.*, 2007) (Kobayashi *et al.*, 2008)
8	**8q21.13-8q24.3**	(Kim *et al.*, 2007) (Paris *et al.*, 2006) (Kobayashi *et al.*, 2008) (Holcomb *et al.*, 2008) (Watson *et al.*, 2009) (Holcomb *et al.*, 2009) (Saramaki *et al.*, 2006) (Liu *et al.*, 2006) (Ishkanian *et al.*, 2009) (Jiang *et al.*, 2008)
9	9q33	(Kim *et al.*, 2007) (Watson *et al.*, 2009) (Holcomb *et al.*, 2008) (Holcomb *et al.*, 2009)
11	11q13.4-11q13.5	(Paris *et al.*, 2006) (Holcomb *et al.*, 2008) (Holcomb *et al.*, 2009) (Liu *et al.*, 2006)
16	16p13.3	(Holcomb *et al.*, 2008) (Saramaki *et al.*, 2006)
17	17q25.3	(Paris *et al.*, 2006) (Holcomb *et al.*, 2008) (Saramaki *et al.*, 2006)
21	21q22.3	(Saramaki *et al.*, 2006) (Watson *et al.*, 2009)
X	Xq12-Xq13.1	(Holcomb *et al.*, 2009) (Jiang *et al.*, 2008)
	Xq28	(Holcomb *et al.*, 2008) (Saramaki *et al.*, 2006)

Note: Cytobands that were found in more than five of the ten studies in bold.

Table 1.8 Summary of the most frequently reported loss/gain regions, and associated key genes, in prostate cancer.

Band	No. of studies	Key Gene
Loss		
6q14-6q21	10	
8p23.3-8p12	9	*NKX3.1* (8p21)
10q23.31	5	*PTEN* (10q23)
13q14.13-13q21.31	6	*KLF5* (13q21)
16q12.2-16q24.1	9	*ATBF1* (16q22)
17p13.1-17q13.1	6	*P53* (17p13)
17q21.31	5	
Gain		
8q21.13-8q24.3	10	*c-MYC* (8q24)

1.6.3.2 Fusion genes in prostate cancer

The first fusion gene reported in prostate cancer was *TPC-HPR* in the LNCaP cells caused by chromosome translocation, t(6; 16)(p21; q22) (Veronese *et al.*, 1996). As this fusion was an isolated example from one cell line and therefore of unknown wider significance, it attracted little attention (Edwards, 2010). One of the most important recent findings in prostate cancer is the identification of recurrent gene fusions involving the ETS family of transcription factor genes (Tomlins *et al.*, 2005). Initially, androgen-responsive gene *TMPRSS2* was identified as being able to fuse with *ERG* (12q23) and *ETV1* (12q22), leading to the over-expression of these two genes in many prostate tumours. Additional ETS gene fusions including *ETV4* (17q21) and *ETV5* (3q27) were discovered shortly after. ETS fusions in prostate cancer exhibit a variety of 5' binding partners that drive over-expression of the ETS transcription factors. So far, ten 5′ binding partners have been identified (**Table 1.9**). *TMPRSS2-ERG* is the most common of the known fusions, accounting for approximately 90% of all the fusions, followed by *TMPRSS2-ETV1*. Other fusions feature prostate-specific genes (*KLK2, C15orf21, CANT1, SLC45A3*), endogenous retroviral elements (*HERV_K_22q11.23, FLJ35294*), a fatty-acid chain ligase (*ACSL3*), a DEAD box helicase (*DDX5*) and a housekeeping gene (*HNRPA2B1*). With the exception of *HNRPA2B1*, *C15ORF21*, and *DDX5*, all the other 5' partners are androgen-responsive.

Table 1.9 The 5′ binding partners of ETS family genes in prostate cancer

5'-fusion partners	Oncogenic ETS transcription factors			
	ERG	*ETV1*	*ETV4*	*ETV5*
TMPRSS2-ETS	*TMPRSS2**	*TMPRSS2**	*TMPRSS2**	*TMPRSS2**
Other androgen-inducible	*SLC45A3**	*SLC45A3**, *HERV-K**, *FLJ35294*	*CANT1**, *KLK2**	*SLC45A3**
Androgen-repressed		*C15orf21**		
Androgen-irrelevant		*HNRPA2B1* *ACSL3*	*DDX5*	

* Prostate specific gene

Recent studies have revealed part, if not all, of the mechanisms underlying androgen-induced *TMPRSS2-ERG* fusion. First of all, androgen receptors (AR) bind to multiple intronic regions near break sites in *TMPRSS2* and *ERG* genes and juxtapose the translocation loci by triggering intra- and interchromosomal interactions. AR then promotes site-specific DNA double-stranded breaks (DSBs) at the translocation loci by recruiting multiple enzymatic activities, including that of topoisomerase II beta (TOP2B) in the case of intrinsic androgen signaling and other nucleases (including activation-induced cytidine deaminase (AID) and the LINE-1 repeat-encoded ORF2 endonuclease) in the case of exogenous genotoxic stress. Under regulation of DSB repair machinery, DSBs are recombined and the *TMPRSS2-ERG* fusion gene is generated (Mani *et al*., 2009; Lin *et al*., 2009; Haffner *et al*., 2010).

Although *TMPRSS2-ERG* fusion occurs in 50-80% of prostate cancer patients, the role of the fusion in prostate carcinogenesis is still unclear. Over-expression of *ERG* and *ETV1* has been shown to contribute to cellular invasiveness in benign prostate epithelial cells (Tomlins *et al.*, 2008) (Cai *et al.*, 2007). However, *TMPRSS2-ERG* fusion is insufficient for the initiation of carcinogenesis in mouse models (Tomlins *et al.*, 2008). Therefore it has been suggested that over-expression of *ERG* needs to cooperate with other early genomic alterations in prostate cancer, such as loss of the tumour suppressor *PTEN*, to induce an invasive phenotype (Tomlins *et al.*, 2008).

Clinically, the association of *TMPRSS2:ERG* gene rearrangement with Gleason score, aggressive disease, and prognosis is unclear, as multiple studies with

conflicting findings have been described (Yoshimoto *et al.*, 2008; Rajput *et al.*, 2007; Demichelis *et al.*, 2007; Attard *et al.*, 2008; Gopalan *et al.*, 2009). However, it has been shown that *TMPRSS2-ERG* fusions generated by intrachromosomal deletions tend to correspond with worse prognoses than do those created by inversions (Attard *et al.*, 2008). Furthermore, prostate cancer with two or more copies of the 3′ *ERG* region showed much worse clinical behaviour than those lacking this amplification (Attard *et al.*, 2008).

Recent transcriptome sequencing analysis revealed many more fusion genes and chromosomal alterations occurring in prostate cancer cells. It has been shown that a particular cancer cell line or tissue can harbour multiple gene fusions (Maher *et al.*, 2009). With application of next generation sequencing technology, there is no doubt that more and more fusion events will be discovered in prostate cancer, which will improve our understanding of genetic causes of prostate cancer development and further contribute to clinical prostate cancer diagnosis and treatment.

2 MATERIALS AND METHODS

2.1 Cell lines and culture conditions

Six prostate cancer cell lines: LNCaP, DU145, PC3, VCaP, 22RV1 and MDA PCa 2b, four immortalised prostate cell lines: PNT1A, PNT2, PNT2C2 and RWPE, and the human embryonic kidney (HEK) 293 cell line were stored in liquid nitrogen. All the cell lines were thawed at 37 °C immediately after removal from liquid nitrogen. The suspension was then mixed with 10 mL relevant culture media, pelleted by centrifugation at 1,200 g for 5 mins and re-suspended in relevant media prior to transfer into tissue culture flasks. With the exception of MDA PCa 2b and HEK293 cells, which were maintained in high glucose DMEM media (Gibco), all prostate cancer and immortalised cells were maintained in RPMI-1640 media (Gibco). Both DMEM and RPMI-1640 were supplemented with 10% foetal bovine serum (FBS) and 1% penicillin/streptomycin (CRUK). Cells were grown in incubators containing 5% CO_2 at 37 °C and split at 80% confluence by trypsinisation.

2.2 Primary tissue samples and tissue microarray (TMA) construction

2.2.1 Clinical fresh frozen samples

15 fresh clinical prostate cancer and 23 BPH specimens were collected from Barts and The London Hospital by the Orchid tissue bank. All samples were freshly frozen in dry ice immediately after removal from the patients and stored

in liquid nitrogen prior to use. The collection of these specimens was approved by the Local Ethical Committee.

2.2.2 Formalin-fixed paraffin embedded (FFPE) clinical samples

A large number of formalin-fixed and paraffin embedded (FFPE) clinical samples were used to construct six batches of tissue microarrays (TMAs), including a total of 1182 prostate cancer samples, 50 BPH and 16 non-prostate non-malignant samples.

The first TMA contained 16 cases of non-prostate non-malignant controls from a variety of human tissue types (**Table 3.1**). The second TMA was constructed from 34 benign prostate hyperplasia (BPH) samples collected from the Barts and The London Hospital following transurethral resection of prostate (TURP) specimens. The third comprised two TMAs constructed from 68 archival anonymous prostate cancer samples from radical prostatectomy specimens and 6 morphologically non-malignant prostate samples obtained from the Barts and The London Hospital. These three batches of TMAs were constructed in 35x22x4 mm blocks of paraffin wax using a manual tissue microarrayer (Beecher Instruments, Sun Prairie, WI, USA). Triplicate cores of 1 mm diameter were taken from each sample. The fourth batch included three TMAs containing 124 archival anonymous prostate cancer radical prostatectomy specimens collected from Whipps Cross Hospital (London, UK). This batch of TMAs was constructed in 35x22x4 mm blocks of paraffin wax. Triplicate cores of 0.6 mm

diameter were taken from each sample. The collection of these specimens was approved by the Local Ethical Committee.

The fifth batch comprised 24 TMAs constructed from a large cohort of 808 cases of TURP prostate cancer specimens. These samples were provided by the Transatlantic Prostate Group, which represents a collaboration between Barts and The London Hospital, (London, UK), Royal Marsden Hospital, (London, UK) and Memorial Sloan-Kettering Cancer Centre, (New York, USA). All the patients were managed conservatively without initial treatment except early hormone management. Clinical outcome data were available for all cases. The median follow-up time was 121 months (8–203 months) and more than 80% of the men were diagnosed after the age of 65. The 10-year survival rate of the patients was 50% and 17% of the patients died due to prostate cancer (Cuzick *et al.*, 2006). TMAs were constructed using a manual tissue microarrayer into 35x22x7 mm paraffin wax blocks. Up to four tumour cores of 0.6 mm diameter were taken from each prostate sample. Ethical approval was obtained from the Northern Multi-Research Ethics Committee for the collection of the cohort and followed by Local Research Ethics Committee approval at individual collaborating hospitals.

A pathologist (D. Berney) examined all samples and graded each cancer specimen with Gleason scores. The samples on the fourth batch of TMAs were also centrally reviewed by pathologists (D. Berney, C. S. Foster and V. Reuter) in the Transatlantic Prostate Group (TAPG).

The sixth batch comprised three TMAs with 182 prostate cancer and 10 BPH cases obtained from the Changhai Hospital, The Second Military Medical University (Shanghai, China). The TMA was constructed in 35x22x7 mm paraffin wax blocks. 1.5 mm diameter cores were taken from each sample. Collection of this batch of specimens was approved by local ethics committee.

2.3 Fluorescence in situ hybridisation (FISH)

2.3.1 FISH probe preparation

2.3.1.1 DNA extraction from bacterial artificial chromosomes (BACs)

Thirteen BAC clones, including RP11-18N21, RP11-681L8, RP11-240J11, RP11-111J1, RP11-595C20, RP1-214H13, RP1-44N23, RP1-154G14, RP11-104N3, RP1-102H19, RP1-249N8, RP1-72A23 and RP3-322A2, were obtained from the Wellcome Trust Sanger Institute (Hinxton Hall, Cambridge, UK). Details of the BACs can be seen in **Table 2.1.**

Table 2.1 Location and length of BAC clones.

Chr.	Location	BAC clone	Region	Length (bps)	Antibiotic
4	Distal 4q	RP11-18N21	98,354,298-98,515,689	63,210	Chloramphenicol
		RP11-681L8	98,513,689-98,622,889	161,392	Chloramphenicol
		RP11-240J11	98,832,380-98,895,589	109,201	Chloramphenicol
6	Proximal 6q	RP11-111J1	87,249,921-87,344,749	97,534	Chloramphenicol
		RP11-595C20	87,344,650-87,442,183	59,031	Chloramphenicol
		RP1-214H13	87,576,952-87,635,982	94,829	Kanamycin
6	6q15 Deletion	RP1-44N23	90,814,536-90,843,275	28,740	Kanamycin
		RP1-154G14	91,251,386-91,352,280	100,895	Kanamycin
		RP11-104N3	91,549,094-91,609,835	60,742	Chloramphenicol
6	6q15 Deletion	RP1-44N23	90,814,536-90,843,275	28,740	Kanamycin
		RP1-154G14	91,251,386-91,352,280	100,895	Kanamycin
6	Distal *CNR1*	RP1-102H19	88,009,641-88,111,280	101,640	Kanamycin
		RP1-249N8	88,688,904-88,750,812	61,908	Kanamycin
6	Proximal *CNR1*	RP1-72A23	89,632,912-89,781,452	148,540	Kanamycin
		RP3-322A2	90,145,402-90,277,901	132,499	Kanamycin

The method for BAC DNA extraction was modified based on a standard Qiagen-Tip method without organic extractions or columns. To initiate single clone culture, BAC clones were cultured on the lysogeny broth (LB) agar containing chloramphenicol (20 μg/mL) or kanamycin (25 μg/mL) (Sigma) and incubated overnight at 37 °C in an incubator. A single isolated bacterial colony was inoculated into 5 mL LB media supplemented with 12.5 μg/ml chloramphenicol or kanamycin. The bacteria were then cultured for 12 h on an oscillating incubator shaking at 225-300 rpm at 37 °C. 1.5 mL of bacterial culture was harvested by centrifugation for 5 mins at 10,000 rpm in a tabletop centrifuge. The bacterial pellet was re-suspended in 150 μL P1 solution (**Table 2.2**) and lysed with 150 μL of P2 solution. The bacterial lysis solution was mixed gently by inverting the tube 4 times and left at RT for 5 mins until the cell suspension cleared. 150 μL of P3 neutralisation solution was added slowly and the tube was gently inverted 4 times before being placed on ice for 10 mins. The tube was then centrifuged at 13,000 rpm for 20 mins. The supernatant was transferred to a fresh tube and centrifuged again at 13,000 rpm for 5 mins. The supernatant was then mixed with 0.8-volume ice-cold isopropanol at -20 °C for 15-30 mins (or overnight). The BAC DNA was ultimately precipitated after spinning the tube at 13,000 rpm for 15 mins. The DNA pellet was washed with 0.5 mL fresh 80% ethanol and then centrifuged at 13,000 rpm for 5 mins. The supernatant was carefully aspirated off and the DNA pellet was left to air-dry at RT before dissolving in 30 μL Tris-EDTA (TE) buffer. The concentration and quality of the DNA was assessed by spectrophotometer ND-1000 (Nanodrop, USA) as well as running a 1% agarose gel (Invitrogen, Paisley, UK).

Table 2.2 Solutions for plasmid extraction

Buffer	Ingredient	Concentration
P1	Tris	50 mM (pH 8)
	EDTA	10 mM
	RNase A	100 μg/ml
P2	NaOH	0.2N
	SDS	1%
P3	KOAc	3M (pH 5.5)

2.3.1.2 BAC DNA amplification

BAC DNA was amplified before labelling. The amplification was achieved using the GenomiPhi amplification V2 kit (GE Healthcare) following the manufacturer's guidelines. Briefly, BAC DNA was heated to 55 °C for 5 mins and then centrifuged at 13,000 rpm for 10 mins. 1 μL BAC DNA (10 ng -1 μg) was taken from the top of the supernatant and then added to 9 μL sample buffer before heating at 95 ºC for 3 mins. After cooling on ice for 5 mins. 1 μL polymerase and 9 μL reaction buffer were added to DNA/sample buffer mix and kept at 30 ºC for 1.5 h for amplification. The polymerase was then inactivated at 65 ºC for 10 mins. A DNA smear should be seen after running 1 μL of amplified DNA on a 1% agarose gel, to confirm the amplification. 10 μL of amplified DNA was purified using standard phenol/chloroform extraction. Simply, 90 μL 1x TE (10 mM TrisHCl pH7·5/1 mM EDTA) was added to 10 μL DNA. Then 100 μL (1 volume) 1:1 phenol/chloroform was added and mixed before being centrifuged at 13,000 rpm for 1-2 mins. The top aqueous phase was transferred to 100 μL (1 volume) chloroform followed by spinning at 13,000 rpm for 1-2 mins. The aqueous phase was then transferred and mixed with 5 μL (1/20 volume) 4 M NaCl and 100 μL isopropanol (2.5 volume ethanol). After incubation at -20 °C

for 20 mins, the DNA was precipitated by centrifugation at 13,000 rpm for 20 mins. The DNA pellet was washed with 1 volume fresh 80% ethanol and centrifuged at 13,000 rpm for 10 mins. The supernatant was discarded and the DNA pellet was left to air-dry at RT before dissolving in 15 µL TE. The concentration of DNA was determined by the Nanodrop technique.

2.3.1.3 BAC DNA labelling

300 ng amplified DNA was added to distilled water to reach the final volume of 24 µL. 20 µL random primer (BioPrime labelling kit, Invitrogen) was added and the tube was heated up to 95 ºC for 5 mins before cooling on ice for 10 mins. Probes for FISH analysis were labelled either by Biotin or digoxigenin (DIG). For biotinylated probes, 5 µL of 10 x dNTP (BioPrime labelling kit, Invitrogen) was added to DNA/primer mix, whereas for DIG labelled probes, 1.75 µL DIG-11-dUTP (pH 7.5, Roche) and 5 µL special DIG 10x dNTP (1 mM dATP, dGTP, dCTP, and 0.65 mM dTTP) was used. After 1 µL Klenow (BioPrime labelling kit, Invitrogen) was added, the tubes were incubated in a water bath at 37 ºC for 3 h. This was followed by the addition of 5 µL stop buffer (BioPrime labelling kit, Invitrogen). All labelled probes were cleaned up using Microspin G50 columns (GE Healthcare, UK). Briefly, G50 columns were spun at 3,500 rpm for 1 min and then washed twice with 200 µL 1x TE at 3,500 rpm. DNA was added to the centre of the column and spun at 3,500 rpm for 2 mins. The concentration of DNA was then measured (expect ~90-150 ng/µl). 30 µL Cot-1 DNA (1 µg/µl) and 1 µL salmon sperm (10 µg/µl) were added and the DNA was precipitated by adding 4 µl 4 M NaCl and 222 µL 100% ethanol and spinning at 13,000 rpm for 10-20 mins. The pellet was rinsed with 100-200 µL fresh 80% ethanol and air dried before being dissolved in 20 µL H_2O.

2.3.1.4 Preparation of metaphase slides

Slides (HV Skan Ltd) were immersed in acetic acid over night and then washed with distilled water prior to use. The slides were stored in fresh distilled water at 4 ºC prior to use.

Metaphase slides were prepared from human lymphocytes. Briefly, 0.5 mL of fresh blood collected from a male or female healthy donor was mixed to 10 mL of cell culture medium containing phytohaemagglutinin in a small cell culture flask and incubated at 37 ºC for 72 h. Colcemid (Invitrogen) was added into the flask for 2-4 h at a final concentration of 0.04 μL/mL, in order to maintain lymphocytes in metaphase. Lymphocytes subsequently were pelleted through centrifugation and then re-suspended in 10 mL of 0.075 M potassium chloride (KCl), which is a hypotonic solution used to enlarge cells for adequate spreading of metaphase chromosomes. After 10 mins incubation at 37 ºC, 10 mL of fixation solution, acetate/methanol (1:3, v/v), was added drop-wise to the pellet. Cells were pelleted through centrifugation for 6 mins at 1,000 rpm. This step was repeated twice before final re-suspension of the pellet into a small volume of fix solution. The lymphocyte suspension was then dropped on pre-cleaned slides and left to air-dry. The slides were kept at - 20 ºC until further use.

2.3.2 FISH analysis

2.3.2.1 Confirmation of BAC clone location and probe labelling efficiency

The location of BAC clones and probe labelling efficiency was examined by FISH hybridisation (as described below) to normal human lymphocyte

metaphase slides, prepared as described above. Subsequently, the probes producing sharp FISH signals in the correct regions were applied for FISH analysis on TMAs.

2.3.2.2 Hybridisation and post-hybridisation washes

4 µm TMA sections were cut onto SuperFrostPlus glass slides (VWR International, Poole, UK) and baked at 65 °C over night. TMA slides were dewaxed in Xylene at 55 °C three times, each for 7 mins, followed by washing in 100% ethanol twice, 3 mins each. Then the tissue was fixed with boiling ethanol and washed twice in H_2O, 3 mins each. The slides were washed in pre-treatment buffer (SPoT-light tissue pre-treatment kit, Zymed, South San Francisco, CA, USA) at ≥ 98 °C for 15 mins and digested with pepsin solution (Digest All-3, Invitrogen, Paisley, UK) for 4.5 mins at 28 °C. Then the slides were washed in water twice, 3 mins each, and air-dried. For each slide, 300 ng probes (1.5 µL) were needed and they were mixed with 1 µL COT-1/sperm (10 µg/ µL COT-1, 2 µg/ µL sperm) and 9.6 µL hybridisation buffer (**Table 2.3**). Each slide was co-denatured with 13 µL such probe/hybridisation buffer mix at 98 °C for 7 mins at 37 °C overnight for hybridisation.

Table 2.3 FISH Hybridisation buffer

Components	Volume
DI formamide	600 µL
dextran sulphate	120 mg
20x SSC	120 µL
EDTA (500 mM, pH 8)	0·28 µL
Salmon sperm (10 mg/ml)	40 µL

2.3.2.3 Post-hybridisation wash and hybridisation signal detection by adding fluorescent antibodies

The cover slip was removed from the slide before it was rinsed 3 times in 2x SSC at 42 °C. The slide was then washed twice in 50% formamide/2x SSC at 42 °C, 4 mins each. After the slide was washed twice in 2x SSC at 42 °C, 5 mins each, it was washed in SSCT (4x SSC, 0.5% Tween) once at RT.

Before adding fluorescent antibodies, the slide was incubated with 200 μL SSCTM (0·5 g Marvel milk powder dissolved in 10 mL SSCT, then the mix solution was filtered by 0·45 μm filter) at 37 °C for 15 mins. The slide was washed in SSCT for 3 mins at RT. For each slide, 200 μL SSCTM with 1 μL Streptavidin-Cy3 conjugate (Sigma-Aldrich, Poole, UK) and 200 μL SSCTM with 1 μL anti-DIG-FITC (Roche, Welwyn Garden City, UK) were required. The slide firstly was incubated with 200 μL streptavidin-Cy3/SSCTM and then with 200 μL anti- DIG-FITC/SSCTM under the same conditions at 37 °C for 10 mins. The slide was washed by phosphate buffered saline (PBS) solution twice, 5 mins each, and shortly dehydrated in 70% ethanol. 20 μL Vectashield anti-fade containing DAPI (Vector labs, Burlingame, CA, USA) was mounted on each slide and a 22x50 mm cover slip was placed on the top. Slides were stored at 4 °C before scanning.

2.3.2.4 Re-hybridisation

For some slides, that needed to be re-hybridised with different probes, the previous signal was removed first. Briefly, the cover slip was removed by soaking in SSCT for 5 mins and then the slide was washed in 2x SSC twice with

agitation, each for 10 mins. After being washed in 2x SSC at 68 °C for 2 mins, the slide was soaked in 70% formamide/2x SSC at 68 °C for 4 mins to remove hybridised probes. The slide was washed in 2x SSC for 2 mins at RT and then in water for 3 mins. The slide and probes were co-hybridised and incubated as illustrated in **2.3.2.1**.

2.3.2.5 Image scanning and analysis

All the TMA slides were scanned at 40x magnification with seven 0.5 µm z-stacks using an Ariol SL-50 system (Applied Imaging, San Jose, CA, USA) with an upright fluoresence microscope (Olympus BX61). Images were then stored for future analysis.

Evaluation of the FISH results in each core was performed in a double blind manner. A minimum of 50, and in most cases (80%), out of 100 cells with both green and red signals in a continuous tissue area were counted. FISH signal co-localisation was defined as a red and a green signal overlapping or separated by a distance of less than one signal-diameter. For FISH signal break-apart assay, chromosome split was defined as a red and a green signal separated by a distance of more than two signal-diameters. Cores with high background or very weak signals that affected the signal assessment were excluded from analysis. Cases with less than 50 scorable cells were excluded from data interpretation.

2.4 Genomic DNA sequence analysis

2.4.1 Genomic DNA extraction from FFPE prostate cancer specimens

Twelve 10 µm slices of paraffin-embedded tissue sections of each prostate cancer sample were cut onto mega twinfrost slides (MAD-1400-02A, CellPath, UK) using a microtome (LEICA, UK). The first and last sections of each sample were stained with haematoxylin and eosin (H&E). A pathologist (L.Y. Xue) examined the H&E sections and marked the tumour area on the first section after confirming that the last sections of each sample had a similar size of tumour tissue area as with the first sections. Tumour tissues from each sample were macro-dissected using scrapers and directly collected in 1.5 mL micro-tube containing 1 mL xylene. The tubes were kept for 10 mins at 65 °C and then the supernatants were discarded after centrifugation at 13,620 g for 5 mins. The procedure was repeated three times and the last round of centrifugation was performed at maximum speed. The pellet was washed in a descending series of ethanol dilutions (100%, 95% and 75%). Every change was preceded by homogenisation and centrifugation at maximum speed for 5 mins. The pellet was washed in 1 mL of Tris-NaCl-EDTA (TNE) buffer followed by centrifuging at maximum speed for 5 mins. A volume of 490 µL of lysis solution (440 µl TNE, 50 µL of 10% SDS) and 10 µL of proteinase K (25 mg/mL) (0.5 mg/mL) was added to the pellet and vortexed for 5 s, followed by an overnight incubation at 55 °C. 10 µL of proteinase K (25 mg/mL) was added on the second day and the third day followed by overnight incubation at 55 °C. After incubation, 5.2 µl of RNase A (10 mg/ml) (final concentration, 100 µg/mL) was added to each tube

followed by incubation at 37 °C for 1 h. Following the addition of another 10 µL of proteinase K (25 mg/mL), the samples were incubated at 55 °C for 1.5 h. The genomic DNA was then purified using phenol (Sigma) and chloroform (Fluke). Briefly, an equal volume of phenol/chloroform (1:1, v/v) was added to each reaction tube. The samples were then vortexed at slow speed for 5-10 s and centrifuged at 4,000 rpm for 15 mins. The aqueous phase was transferred into a new 1.5 mL tube. The phenol/chloroform extraction was repeated once. The equal volume of chloroform was then added and the aqueous phase (upper layer) was transferred into a 1.5 mL tube after repeating the vortex and centrifuging step. Equal volume of isopropanol and 1/10 volume of 3 M NaOAc (pH5.2, Invitrogen) were added. The tube was kept at -80 °C for 30 mins, and then centrifuged at 13,000 rpm at 4 °C for 10 mins. The pellet was washed by 1 mL of 70% ethanol. After centrifugation at 13,000 rpm at 4 °C for 5 mins, ethanol was removed and the pellet was left to air dry at RT. DNA was dissolved in distilled water and the concentration was measured using a Nanodrop.

2.4.2 Polymerase chain reaction (PCR) analysis

All primers applied were ordered from Sigma. PCR reactions with genomic DNA template, extracted from paraffin-embedded samples, were all performed using Phusion DNA polymerase (Finnzymes), 5x GC buffer (Finnzymes) and dNTP (10 mM each) (Invitrogen). Primer sequences, PCR working conditions (temperature and time of annealing and extension) and expected sizes in reference human genome are listed in **Table 2.4**. All reactions were preceded by initial heating at 98 °C for 2 mins and ended with heating at 72 °C for 10 mins. Each reaction was 35 cycles with denaturing at 98 °C for 10 s. PCR products

were purified using a PCR purification kit (Qiagen) according to manufacturer's instruction. The concentration of each purified sample was tested using a Nanodrop and then the concentration was adjusted to around 100 ng/µL. Sequence analysis service was provided by the Genome Centre (William Harvey Research Instititute, Queen Mary). The BigDye Terminator v3.1 Cycle Sequencing Kit (Applied Biosystem) was applied. Briefly, the sequencing reaction mix was made as described in **Table 2.5**. The reaction was performed in a thermo-fast 96-well semi-skirted plate (ABgene) under the following conditions: 96 ºC for 30 s, 50 ºC for 15 s and 60 ºC for 1 min for 25 cycles and 4 ºC for 2 mins. Unincorporated Big Dye was removed through the following procedures: 30 µL of 96% Ethanol: 7.5 M Ammonium Acetate (27.9:2.1, v/v) was added to each sample well. The plate was sealed with a new PCR seal and inverted 5 to 10 times to mix. Then the plate was spun at 4,388 rpm at 4 °C for 35 mins. The supernatant was tipped off immediately onto tissue paper. The plate was inverted on fresh tissue paper and then spun again at 1,246 rpm for 30 s. 100 µL of chilled 70% ethanol was added to each well. Then the plate was spun at at 4,388 rpm at 4 °C for 6 mins. The supernatant was tipped off immediately and the plate was spun upside down on tissue paper at 1,246 rpm for 30 s. The plate was left to air dry for 10 mins. 10 µL of distilled H_2O was added to each well to re-suspend the amplified PCR products. 8 µL of highly deionised formamide (Applied Biosystem) was added to each well before the plate was sealed. The plate was pulse-centrifuged to at 4,388 rpm and placed assembly on the ABI3730xl machine for sequencing. **Table 2.6** lists the sequencing primers for the gene *CNR1*. PCR products, which could not generate sequencing data, were cloned into a T-vector (Invitrogen) according to the manufacturer's instructions

and sequenced with a T7 promoter primer and M13 reverse primer. The detailed procedure for cloning is described in the plasmid construction section, **2.7.3**.

Table 2.4 PCR primers for *CNR1* sequencing and breakpoint mapping

No.	PCR Primer	Sequence	Condition	Expected size	Genome position
1	Full fwd	5'-GAGGTTATGAAGTCGATCCTAG ATGGC	65°C-30s 72°C-1.5 mins	1415bp	21268-22692
	full rvs	5'-TCACAGAGCCTCGGCAGACGTG			
2	P1 fwd	5'- CCTTCCTACCACTTCATCG	55°C-30 s 72°C-1 min	681bp	21724-22404
	P1 rvs	5'- CGTCTTAATGAGCTTGTTCA			
3	P2 fwd	5'-CCTGTGGGTCACTTTCTCAGTC	60°C-30 s 72°C-1 min	897bp	21219-22115
	P2 rvs	5'-CCGATCCAGAACATCAGGTAG			
4	P3 fwd	5'-TGGCCTATAAGAGGATTGTCACC	61°C-30 s 72°C-1 min	787bp	21938-22724
	P3 rvs	5'-TCTTTTCCTGTGCTGCCAG			
5	P4 fwd	5'- AAGTCTCTCTCGTCCTTCAAG	56°C-30 s 72°C-30 s	286bp	21523-21808
	P4 rvs	5'- CGTGGAAGTCAATGAAGC			
6	P2 fwd	5'-CCTGTGGGTCACTTTCTCAGTC	58°C-30 s 72°C-30 s	590bp	21219-21808
	P4 rvs	5'- CGTGGAAGTCAATGAAGC			
7	P6 fwd	5'- AAGGGTAAGACCTGGCAGAGTTG	64°C-30 s 72°C-15 s	134bp	742-875
	P8 rvs	5'- AAACACCGACGCACGATTCG			
9	P10 fwd	5'-GCTTCCTCAGTTCTCACTAGCTC	60°C-30 s 72°C-20 s	337bp	20619-20955
	P10 rvs	5'-TCAGTGTGTGAATCCAGGAAGG			
10	P11 fwd	5'-ACGCCATCCCTGAACTTTG	60°C-30 s 72°C-20 s	229bp	21010-21238
	P11 rvs	5'-CTGAGAAAGTGACCCACAGG			
11	P12 fwd	5'-TTCTCACCATTCGGCTTATTTG	60°C-30 s 72°C-30 s	396bp	21173-21569
	P12 rvs	5'-CCACACTGGATGTTCTCCTC			
12	P13 fwd	5'-AGCTTTCATTCCCTGCTGAA	60°C-30 s 72°C-25 s	345bp	3459-3804
	P13 rvs	5'-GAAAAATCAGCAAAGCAGGC			
13	P14 fwd	5'-TTGCAAGTGCTTTGGTCAAC	61°C-30 s 72°C-15 s	192bp	10860-11051
	P14 rvs	5'-TCTGCATAATTCAAAGCCCC			
14	P15 fwd	5'-ACAAGAGCCTGAGGGTCAGA	61°C-30 s 72°C-15 s	293bp	18607-18900
	P15 rvs	5'-TCTCATCACTGCTCACCAGG			
15	P16 fwd	5'-GCAGCTACATCCCCCAAAGCCT	67°C-30 s 72°C-15 s	152bp	13681-13833
	P16 rvs	3'-GGCAGGAAAACTGCTCTCTGCAT			
16	P17 fwd	5'-TCTGGGTGCAGTGCTTGCTC	64°C-30 s 72°C-15 s	163bp	15330-15493
	P17 rvs	3'-TGGACTGGTGACACTGAGCCT			
17	P18 fwd	5'-GTGGGAGGGGCTGGTCAGGA	69°C-30 s 72°C-15 s	174bp	16768-16941
	P18 rvs	3'-TGGCCCTGAGTGACTTGCTGC			
18	P19 fwd	5'-GAGCAGCAAGTCACTCAGG	59°C-30 s 72°C-20 s	317bp	16919-17236
	P19 rvs	5'-CCTTAGGTTCCCTGTTCATCTG			
19	P20 fwd	5'-CAGACAGATGAACAGGGAACC	59°C-30 s 72°C-25 s	353bp	17211-17564
	P20 rvs	5'-TGAACCAGTTCTGCACACC			
20	P21 fwd	5'-CTGGTTCAGAAGCCCAGAC	58°C-30 s 72°C-30 s	407bp	17557-17964
	P21 rvs	5'-AAGGGATCTAGCCTGGAGAG			
21	P22 fwd	5'-TCTCCAGGCTAGATCCCTTG	60°C-30 s 72°C-25 s	354bp	17946-18300
	P22 rvs	5'-GAACACCCTTTCTGGGCTC			
22	P23 fwd	5'- TCTGTTTGGGTATTCTGGGAG	59°C-30 s 72°C-2 mins	3381bp	18264-21645
	P23 rvs	5'-GAGGGACAGGACTGCAATG			
23	P24 fwd	5'-GAGCAGCAAGTCACTCAGG	58°C-30 s 72°C-3 mins	4726bp	16919-21645
	P24 rvs	5'-GAGGGACAGGACTGCAATG			
24	P25 fwd	5'-GAGCAGCAAGTCACTCAGG	58°C-30 s 72°C-3 mins	4691bp	16919-21610
	P25 rvs	5'-GGTTCAGGACCATGAAACACTC			

Table 2.5 BigDye sequencing reaction mix

Components	Volume
PCR product	4 μL (100 ng)
Sequencing primer	1 μL
BigDye Terminator Master Mix v 3.1	0.5 μL
Better buffer	3.5 μL
DMSO	0.5 μL

Table 2.6 Sequence of the primers for *CNR1* sequencing

No.	Sequence
1	5'- AAGTCTCTCTCGTCCTTCAAG
2	5'- ACCGCAAAGATAGCCGCAAC
3	5'- TCTGTTCATCGTGTATGCG
4	5'- ATGCTCTGCCTGCTGAACTC
5	5'- TCTCCCGCAGTCATCTTCTC
6	5'-GAGGTTATGAAGTCGATCCTAGATGGC
7	5'-TCACAGAGCCTCGGCAGACGTG
8	5’- CCTTCCTACCACTTCATCG
9	5’- CGTCTTAATGAGCTTGTTCATC
10	5’- CCTCTGCTTGCAATCATGG
11	5’– ACACGTGGAAGTCAATGAAGC

2.4.3 Genome walking assay

The Genome walking assay was performed mainly according to the GenomeWalker universal Kit user manual (Clontech) with slight alterations. All genome walking related primers and their sequences are listed in **Table 2.5**. First of all, 2.5 µg of genomic DNA from each sample was digested with 80 units of blunt-end restriction enzymes, *PvuII*, *DraI*, *StuI* and *EcoRV* (Promega), respectively, in 100 µL reaction volumes in 0.5 mL tubes at 37 ºC for 2 h. The tubes were vortexed at slow speed for 5-10 s before returning to 37 ºC overnight (16-18 h). The genomic DNA was then purified using phenol and chloroform as described in **2.4.1** with slight alteration. Briefly, an equal volume (100 µL) of phenol was added to each reaction tube followed by vortexing at slow speed for 5-10 s and centrifuging at 13,000 rpm for 1 min at room temperature (RT). The aqueous phase was transferred into a 0.5 mL tube. An equal volume (100 µL) of chloroform was then added to the tube. Following vortexing and centrifuging again, the aqueous phase was transferred into a 0.5 mL tube. 2.5 volumes (250 µL) of ice-cold 100% ethanol and 1/10 volume (10 µL) of 3 M NaOAc were then added and the tube was placed at -20 ºC for at least 20 mins. The tube was then centrifuged at 13, 000 rpm for 20 mins at 4 ºC and the DNA pellet was washed twice with 500 µL 80% of ice-cold ethanol. The pellet was air dried before dissolving in 20 µL of sterilised deionised water. Following the digestion and purification steps, 4 µL genomic DNA from each tube was ligated to 1.9 µL adaptors (25 µM) in 8 µL reaction volume using 0.5 µL T4 DNA ligase (6 units/µL) (Promega). The adaptors were made through annealing two primers, AL and AS (**Table 2.7**). 25 µM AL and AS primers were mixed in 100 µL sterilised deoinised water before they were denatured at 98 ºC for 2 mins in a

PCR machine. The primers were annealed after the machine was switched off and the temperature in the PCR block was gradually dropped down over 1 hr. After the ligation of genomic DNA and adaptor at 16 ºC overnight, the reaction was stopped through incubation at 70 ºC for 5 mins.

The primary and secondary nested PCRs were then carried out. For primary PCR, 1 µL of each library was used as a template; 1 µL adaptor-binding primer 1 (AP1) (10 µM) and 1 µL gene-specific primer were used as a primer pair. The PCR reaction was performed in a 50 µL volume under the following two-step cycle parameters: 98 ºC-25 s, 72 ºC-3 mins for 7 cycles; 98 ºC-25 s, 67 ºC-3 mins for 32 cycles and 67 ºC for an additional 7 mins after the final cycle. 5 µL of the primary PCR products were analysed on a 1.5% agarose/EtBr gel. For the secondary nested PCR, 1 µL of the primary PCR product was used as the template; 1 µL adaptor-binding primer 2 (AP2) (10 µM) and 1 µL gene-specific nested primer were used as a primer pair. The PCR reaction was performed in 50 µL volume under the following two-step cycle parameters: 98 ºC-25 s, 72 ºC-3 mins for 5 cycles; 98 ºC-25 s, 67 ºC-3 mins for 24 cycles and 67 ºC for an additional 7 mins after the final cycle. 5 µL of the secondary PCR products were analysed on a 1.5% agarose gel.

Table 2.7 Primers for genome walking analysis

Genome walking primers		Short name	Sequence
Adaptor related primers	Adaptor long	AL	5'-GTAATACGACTCACTATAGGGCACGCGTGGT CGACGGCCCGGGCTGGT
	Adaptor short	AS	5'-[Phos]ACCAGCCC[Amine]-3'
	Adaptor primer 1	AP1	5'-GTAATACGACTCACTATAGGGC-3'
	Nested adaptor primer 2	AP2	5'-ACTATAGGGCACGCGTGT
Gene specific primers	CB1 down-stream breakpoint primer 1	CB1DBP1	5'-GTTCAGGACCATGAAACACTCTATGTC
	CB1 down-stream breakpoint nested primer 2	CB1DBP2	5'-TCATTCTCCTTGAAGGACGAGAGAGAC
	CB1 up-stream breakpoint primer 1	CB1UBP1	5'-CTATCATGCTATCAGGCTGGTAAACCACT
	CB1 up-stream breakpoint primer 2	CB1UBP2	5'-AACTCCTGATTATACGACGTGATGAGG

2.5 DNA methylation analysis

Genomic DNA from 10 BPH and 48 prostate cancer samples, which were extracted from macro-dissected clinical fresh frozen materials, were available in our group. These 58 DNA samples were sent to the Molecular Epidemiology Laboratory, Wolfson Institute of Preventive Medicine (http://www.wolfson.qmul.ac.uk/ems/research/Molecular_Epidemiology_Laboratory.html), for *CNR1* methylation analysis.

2.5.1 Bisulfite conversion

120 – 300 ng of genomic DNA from each sample was used in the bisulfite conversion reactions, where unmethylated cytosines were converted to uracil with the EpiTect Bisulfite kit (Qiagen) according to manufacturer's instructions. Briefly, DNA was mixed with water, DNA protect buffer and bisulfite mix and then the conversion was run in a thermocycler (Biometra, Goettingen, Germany) at the recommended cycle conditions. Converted DNA was purified and eluted into a total 40 µl Buffer EB and further diluted into 20 µl aliquots of 100 cell-equivalents/µl (the cell genome-equivalents of DNA calculations assumed 6 pg DNA per diploid cell).

2.5.2 PCR and Pyrosequencing

Primer set with reverse biotin-labelled primer at the 5' end was used to amplify the bisulfite converted DNA. Primers for the gene amplification *CNR1* F 5' – GTTTAGTTTAGGGGTTGGTTG – 3', BCNR1 R 5' – B-CTTCCTTCTCCACTTCTTTTCC – 3' and the pyrosequencing *CNR1* S 5' – GAGTTTTGTAGGGAGT -3' were designed using PyroMark Assay Design

software version 2.0.1.15 (Qiagen); The size of the amplicons was restricted to a maximum of 210 bp. The primers were located in promoter or first exon CpG islands identified by MethPrimer (http://www.urogene.org/methprimer/index1.html), depending on where the design of the assay allowed for optimal primers. Due care was taken to avoid any primer overlapping CG dyads to prevent amplification biases. PCRs were performed using a converted genomic DNA genome-equivalent of 200 to 400 cells employing the PyroMark PCR kit (Qiagen). Briefly, 12.5 µl master mix, 2.5 µl Coral red, 5 pmol of each primer, 7 µl of water and 2 µl sample were mixed for each reaction and run at thermal cycling conditions: 95 °C for 15min and then 45 cycles: 30 sec at 94 °C; 30 sec at 56 °C; 30 sec at 72 °C and a final extension for 10 min at 72 °C. The correct amplified DNA was confirmed by the QiaExel capillary electrophoresis instrument (Qiagen). A standard pyrosequencing sample preparation protocol was applied (Tost and Gut, 2007). 3 µl streptavidin beads (GE Healthcare, UK), 37 µl PyroMark binding buffer (Qiagen), 20 µl PCR product and 20 µl water were mixed and incubated for 10 min on a shaking table at 1300 rpm. Using the Biotage Q96 Vacuum Workstation, amplicons were separated, denatured, washed and added to 45 µl annealing buffer containing 0.33 µM of pyrosequencing primer. Primer annealing was performed by incubating the samples at 80 °C for 2 min and allowed to cool to room temperature prior to pyrosequencing. PyroGold reagents were used for the pyrosequencing reaction and the signal was analysed using the PSQ 96MA system (Biotage, Uppsala, Sweden). Target CGs were evaluated by instrument software (PSQ96MA 2.1), which converts the pyrograms to numerical values for peak heights and calculates proportion of methylation at each base as a C/T ratio. All runs

contained standard curves, which comprised a range of control methylated DNA (0%, 25%, 50%, 75%, and 100%) to allow standardised direct comparisons between different primer sets. For the standard curves a total of 300 ng of unmethylated (Qiagen) and hypermethylated DNA (Millipore, Billerica, MA, USA) were mixed to obtain the different ratios of DNA methylation and then bisulfite converted as described above.

2.6 RNA expression analysis

2.6.1 Total RNA extraction

2.6.1.1 Total RNA isolation from cell lines

Total RNA was extracted using TRIzol® reagent (Invitrogen) according to the manufacturer's recommendations. 1 mL TRIzol was used per 5 x 10^5 cells for lysis. The lysate was incubated at RT for 5 mins to permit the complete dissociation of nucleoprotein before 0.2 mL chloroform per 1 mL of TRIzol was added. Tubes were shaken vigorously for 15 s and incubated 2-3 mins at RT before centrifugation at 11,900 g for 15 mins at 4 °C. The aqueous phase (about 60% volume) was transferred to a fresh tube, and 0.5 mL of isopropanol was added per 1 mL of TRIzol. The tube was incubated for 10 mins at RT before centrifugation at 11,900 g for 10 mins at 4 °C. The supernatant was removed and the pellet was washed with 1.5 mL 75% ethanol. RNA was dissolved in 50 µL RNase-free water and stored at -80 °C.

2.6.1.2 Total RNA isolation from fresh frozen sliced tissues

Slides were washed with RNaseZap (Ambian, Applied Biosystem) to remove RNases and then rinsed with diethylpyrocarbonate (DEPC) water before being

left to air-dry. Ten 15 µm slices of fresh frozen tissue sections of each clinical sample were cut onto the pre-treated slides. The slides were placed in a plastic slide box, which was kept on dry ice. The first and the last sections of each sample were stained with H&E. A pathologist (LY Xue) examined the H&E sections and marked the tumour or BPH area on the first section after confirming that the last section of each sample had a similar size of tumour or BPH tissue area as the first sections. Tumour or BPH tissue from each sample were macro-dissected using scrapers and directly collected in a 1.5 mL micro-tube containing 1 mL TRIzol (Invitrogen). Tissue was homogenised with a syringe. Following homogenisation, the same procedure was performed as detailed in **2.5.1.1**

2.6.1.3 Residual DNA removal and RNA quantification

In order to remove the residual genomic DNA from RNA samples, DNase I (Ambion, Applied Biosystems) treatment was applied following the manufacturer's instructions. 1 µL (2 U) DNase I was used to treat ≤ 10 µg RNA in 50 µL volume with DEPC-treated water. After incubation at 37 °C for 30 mins, RNA was purified using phenol/chloroform to inactivate the DNase I as illustrated in **2.3.1.2**. To reduce the volume, and also to improve the RNA quality, RNA was re-precipitated by adding 1/10 volume of 3 M NaOAc (pH 5.2, Gibco, Invitrogen) and 2.5 volumes of 100% ethanol to the samples. Following incubation at -20 °C for 20 mins, RNA was precipitated by centrifugation at 12,000 g for 20 mins at 4 °C. The RNA pellet was washed by 80% ethanol and re-suspended in RNase-free water. The quality and quantity of RNA were assessed using the spectrophotometer ND-1000 and Agilent 2100 Bioanalyser (Agilent Technologies).

2.6.2 Affymetrix Exon array

Affymetrix GeneChip® Human Exon 1.0 ST Array was applied to investigate expression variations of whole transcripts. The experiment was performed by Sharon James following the manufacturer's protocol as described below. This protocol can be downloaded from Affymetrix website (http://www.affymetrix.com/Auth/support/downloads/manuals/wt_sensetarget_label_manual.pdf). **Figure 2.1** shows the whole transcript sense target labelling assay schematic.

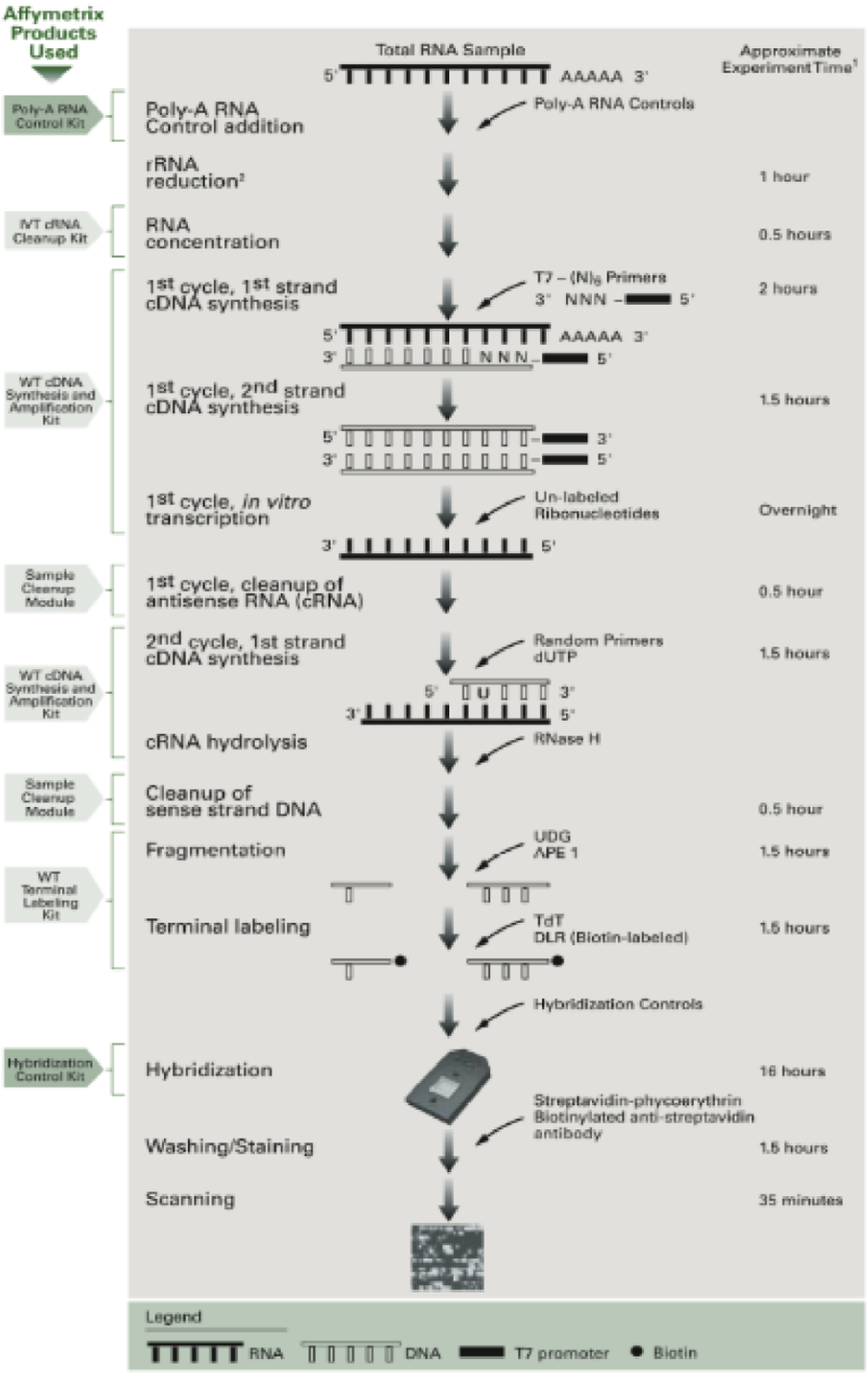

Figure 2.1 Whole transcript sense target labelling assay schematic

Adapted from Affymetrix GeneChip® Whole Transcript Sense Target Labelling Assay Manual.

2.6.2.1 rRNA reduction

2.6.2.1.1 Preparation of dilutions of poly-A RNA controls

GeneChip® Poly-A RNA Control Kit was used for this step. 2 µL of Poly-A RNA Control Stock was added to 38 µL of Poly-A Control Dil Buffer to make the first dilution (1:20). After mixing and spinning, 2 µL of the first dilution was added to 98 µL Poly-A Control Dil Buffer to make the second dilution (1:50). Then 2 µL of the second dilution was added to 98 µL of Poly-A Control Dil Buffer to make the third dilution (1:50). 2 µL of the third dilution was added to 1 µg of total RNA for each reaction to finally make up the total RNA/Poly-A RNA Control Mix.

2.6.2.1.2 rRNA reduction

For rRNA reduction, the RiboMinus™ Human/Mouse Transcriptome Isolation Kit (Invitrogen) was used. First of all, 54 µL betaine (5 M) and 126 µL hybridisation buffer were mixed to give a total volume of 180 µL hybridisation buffer with betaine for a single total RNA sample. Then 3 µL of total RNA/Poly-A RNA Control Mix and 20 µL of hybridisation buffer with betaine were mixed with 0.8 µL of RoboMinus probe (100 pmol/µL) in a 0.2 mL strip tube and incubated at 70 °C for 5 mins. The tube was then placed on ice while magnetic beads were prepared. 50 µL of bead suspension was transferred to a 1.5 mL non-stick RNase-free tube. After spinning and placing on the magnetic stand for 1 min, the supernatant was gently aspirated off and discarded. The beads were then washed by 50 µL of RNase-free water and placed on the magnetic stand for 1 min before the supernatant was discarded. This washing step was repeated twice, once with 50 µL of RNase-free and once with 50 µL of the hybridisation buffer.

The beads were finally re-suspended in 30 µL of the hybridisation buffer with betaine, and kept at 37 °C for 1-2 mins. After beads preparation, ice-cold hybridised sample (prepared previously) was transferred to the tube containing the beads and incubated at 37 °C for 10 mins. The tube was placed on the magnetic stand for 1-2 mins to obtain the rRNA-probe pellet. The supernatant was transferred to a 1.5 mL non-stick, RNase-free tube and left on ice while the beads were washed in 50 µL of hybridisation buffer with betaine and incubated at 50 °C for 5 mins. The beads were than placed on the magnetic stand for 1 to 2 mins. Finally, the supernatant was combined with the supernatant, which was left on ice. The total volume of the rRNA-reduced sample was approximately 100 µL.

2.6.2.2 RNA concentration

The GeneChip® IVT cRNA Cleanup Kit was required for measurement of the RNA concentration. 350 µL of cRNA binding buffer was added to each rRNA-reduced sample from the previous step and vortexed for 3 s. 250 µL of 100% ethanol was added to each reaction and flicked to mix well. The sample was then applied to the IVT cRNA Cleanup Spin Column sitting in a 2 mL collection tube. Following centrifugation for 15 s at ≥ 8,000 g, the flow-through was discarded and the IVT cRNA Cleanup Spin Column was transferred to a new 2 mL collection tube. The 500 µL of cRNA Wash Buffer was added and then the tube was centrifuged for 15 s at ≥ 8,000 g, the flow-through again was discarded. The tube was centrifuged at ≤ 25,000 g for 15 s with the cap left open. After transferring to a new 1.5 mL collection tube, 11 µL of RNase-free Water was directly added to the membrane of the IVT cRNA Cleanup Spin Column and then centrifuged at ≤ 25,000 g for 1 min. The eluted rRNA-Reduced Total

RNA/Poly-A RNA Controls Mix was approximately 9.8 µL. The quality of rRNA-Reduced Total RNA/Poly-A RNA was checked using the Agilent 2100 Bioanalyser.

2.6.2.3 First-strand cDNA synthesis

The GeneChip® WT cDNA Synthesis Kit was used for first strand DNA synthesis. The T7- $(N)_6$ primer was diluted in RNase-free water to a 500 ng/ µL working solution and mixed with the concentrated rRNA-reduced sample. After the mixture was mixed well and spun, it was incubated at 70 °C for 5 mins followed by 4 °C for at least 2 mins. The sample was stored on ice until further use. The First-Cycle, First-Strand Master Mix was prepared as shown in **Table 2.8** below. 5 µL of the First-Cycle, First-Strand Master Mix was added to the tube containing the Concentrated rRNA-Reduced Total RNA/Poly-A RNA controls/ T7- $(N)_6$ Primers Mix giving a total reaction volume of 10 µL. The tube was then incubated sequentially at 25 °C for 10 mins, 42 °C for 60 mins, 70 °C for 10 mins and 4 °C for at least 2 mins before immediately continuing to the First-Cycle, Second-Strand cDNA synthesis.

Table 2.8 First-Cycle, First-Strand Master Mix

Component	Volume in 1 reaction
5 x 1st Strand Buffer	2 µL
DTT, 0.1 M	1 µL
dNTP Mix, 10 mM	0.5 µL
RNase Inhibitor	0.5 µL
SuperScript™ II	1 µL
Total Volume	5 µL

2.6.2.4 First-cycle, Second-Strand cDNA synthesis

The GeneChip® WT cDNA Synthesis Kit was also used in this procedure. 2 µL of 1 M $MgCl_2$ was mixed with 112 µL of RNase-free water first. Then the First-Cycle, Second-Strand Master Mix was prepared as described in **Table 2.9** below. 10 µL of the First-Cycle, Second-Strand Master Mix was mixed with the reaction tube from the First-Strand cDNA Synthesis Reaction for a total reaction volume of 20 µL. The tube was incubated in a thermal cycler at 16 °C for 120 mins without a heated lid and at 75 °C for 10 mins with a heated lid before being cooled for at least 2 mins at 4 °C.

Table 2.9 First-Cycle, Second-Strand Master Mix

Component	Volume in 1 Rxn
$MgCl_2$, 17.5 mM	4 µL
dNTP Mix, 10 mM	0.4 µL
DNA Polymerase I	0.6 µL
RNase H	0.2 µL
RNase-free Water	4.8 µL
Total Mix Volume	10.0 µL

2.6.2.5 First-cycle, cRNA synthesis and cleanup

The GeneChip® WT cDNA Amplification Kit and the GeneChip® Sample Cleanup Module were used for this step. In a separate tube, the IVT Master Mix was assembled at RT as listed in **Table 2.10** below.

Table 2.10 First-Cycle, cRNA Synthesis

Component	Volume in 1 Reaction
10x IVT Buffer	5 μL
IVT NTP Mix	20 μL
IVT Enzyme Mix	5 μL
Total Volume	30 μL

30 μL of the IVT Master Mix to each First-Cycle cDNA Synthesis Reaction sample from the previous step was transferred to a final volume of 50 μL and briefly spun in a centrifuge before incubation at 37 °C for 16 h. 50 μL of RNase-free water was added to each IVT reaction to a final volume of 100 μL and then 350 μL of cRNA Binding Buffer was added to each sample. The tube was vortexed for 3 s before 250 μL 100% ethanol was added. The sample was then applied to the IVT cRNA Cleanup Spin Column sitting in a 2 mL collection tube. 500 μL of cRNA Wash Buffer was added and the tube was centrifuged for 15 s at ≥ 8,000 g. The flow-through was discarded, 500 μL of 80% (v/v) ethanol was added to wash again and then the tube was centrifuged at the same speed for 15 s before discarding the flow-through. After spinning at ≤ 25,000 g for 5 mins with the column cap open, the IVT cRNA Cleanup Spin Column was transferred to a new 1.5 mL collection tube and 12 μL of RNase-free water was added directly to the membrane. The tube was centrifuged at 25,000 g for 1 min. The eluted cRNA is approximately 10.5 μL. The cRNA yield was determined by Nanodrop ND-100.

2.6.2.6 Second-cycle, first-strand cDNA synthesis

The GeneChip® WT cDNA Synthesis Kit was used in this step. cRNA was first mixed with the Random Primers as listed in **Table 2.11** below. The tubes were

flick-mixed and spun down before being incubated at 70 °C for 5 mins and 25 °C for 5 mins. After cooling at 4 °C for at least 2 mins, 12 µL of the Second-Cycle, First-Strand cDNA Synthesis Master Mix, as described in **Table 2.12**, was transferred to the Second-Cycle, cRNA/Random Primers Mix for a total reaction volume of 20 µL. After mixing and centrifuging, the tubes were incubated sequentially at 25 °C for 10 mins, 42 °C for 90 mins, 70 °C for 10 mins and 4°C for at least 2 mins.

Table 2.11 Second-Cycle, cRNA/Random Primers Mix

Component	Volume in one reaction
cRNA, 8 µg	Variable
Random Primers (3 µg/ µL)	1.5 µL
RNase-free water	Up to 8 µL
Total Volume	8 µL

Table 2.12 Second-Cycle, First-Strand cDNA Synthesis Master Mix

Component	Volume in one reaction
5 x 1st Strand Buffer	4 µL
DTT, 0.1 M	2 µL
dNTP+dUTP, 10 mM	1.25 µL
SuperScript^{TM} II	4.75 µL
Total Volume	12 µL

2.6.2.7 Hydrolysis of cRNA and cleanup of single-stranded DNA

For this step, the GeneChip® WT cDNA Synthesis Kit and the GeneChip® Sample Cleanup Module were used. First of all, 1 µL of RNase H, 2 U/µL was added to each of the samples. The samples were then incubated sequentially at 37 °C for 45 mins, 95 °C for 5 mins and 4 °C for 2 mins. 80 µL of RNase-free

water and 370 μL of cDNA Binding Buffer were added to each sample. After vortexing for 3 s, the entire sample (the total volume is 471 μL) was applied to a cDNA Spin Column sitting in a 2 mL collection tube and spun at ≥ 8,000 g for 1 min. The flow-through was discarded and the columns were placed in 1.5 mL collection tubes. After 15 μL of the cDNA Elution Buffer was directly added to the column membrane, the columns were incubated at RT for 1 min and centrifuged at ≤ 25, 000 g for 1 min. The cDNA elution step was repeated. The yield of single-stranded DNA was determined by NanoDrop ND-1000.

2.6.2.8 Fragmentation of single-stranded DNA

The GeneChip® WT Terminal Labeling Kit was used in this step. The fragmentation mix was prepared as described in **Table 2.13** below and added to each sample. The samples were incubated at 37 °C for 60 mins, 93 °C for 2 mins, 4 °C for at least 2 mins. After being flick-mixed and spun down, 45 μL of each sample was transferred to a new tube. The remainder of the samples was used for size analysis using Agilent 2100 Bioanalyser. The range in peak size of the fragmented samples should be approximately 40 – 70 nt.

Table 2.13 Fragmentation mix of Single-Stranded DNA

Component	Volume/Amount in one reaction
Single-Stranded DNA	5 μg
10x cDNA Fragmentation Buffer	4.8 μL
UDG, 10 U/μL	1 μL
APE 1, 1,000 U/ μL	1 μL
RNase-free Water	Up to 48 μL
Total Volume	48 μL

2.6.2.9 Labelling of fragmented single-stranded DNA

The GeneChip® WT Terminal Labeling Kit was used in this step. The labelling reaction was prepared as listed in **Table 2.14** below. After adding the labelling reagents, the fragmented DNA samples were flick-mixed and spun down. The samples were then incubated at 37 °C for 60 mins, 70 °C for 10 mins and 4 °C for at least 2 mins.

Table 2.14 Labelling Master Mix

Component	Volume/Amount in one reaction
Fragmented Single-Stranded DNA	45 µL
5x TdT Buffer	12 µL
TdT	2 µL
DNA labelling Reagent, 5 mM	1 µL
Total Volume	60 µL

2.6.2.10 Preparation of the hybridisation cocktail

The hybridisation cocktail was prepared in a 1.5 mL RNase-free tube as shown in **Table 2.15** below. At this point, samples were consigned to the Affymetrix operator (Mrs T.Chaplin), who was in charge of performing hybridisation, washing, staining, and scanning of the samples on chips.

Table 2.15 Hybridisation Cocktail

Component	Volume for a single 49 format array	Final concentration or Amount
Fragmented and labelled DNA target	~ 60 µL	~ 5 µg
Control Oligonucleotide B2	3.3 µL	50 pM
20x Eukaryotic Hybridisation Controls (bioB, bioC, bioD, cre)	10 µL	1.5, 5, 25 and 100 pM, respectively
Herring Sperm DNA (10 mg/mL)	2 µL	0.1 mg/mL
Acetylated BSA (50 mg/mL)	2 µL	0.5 mg/mL
2x Hybridisation Buffer	100 µL	1x
DMSO	14 µL	7%
RNase free H_2O	Up to 200 µL	
Total Volume	200 µL	

2.6.2.11 Hybridisation, washing, staining and scanning

The Affymetrix Exon 1.0 ST Array chips were stored at 4 °C. Prior to use, they were equilibrated to RT while the hybridisation cocktail was heated at 99 °C for 5 mins, cooled down to 45 °C for 5 mins and then centrifuged at maximum speed for 1 min. Subsequently, the samples were added to the chip and incubated at 45 °C for 16 h in a hybridisation oven at 60 rpm. After overnight hybridisation, the hybridisation cocktail was removed and replaced by Non-stringent Wash Buffer. Once placed in a GeneChip® 450 Fluidics wash station, chips were washed to remove non-hybridised probes and stained with Streptavidin Phycoerythrin (SAPE) to localise the biotiylated targets using the protocol EukGE_WS2v5. In the end, chips were scanned using the GeneChip® 3000 scanner.

2.6.3 Exon array data analysis

2.6.3.1 Bioinformatics analysis

Microarray analysis generates large sets of data and, therefore, requires the use of bioinformatics and additional analytical tools. For global analysis of expression alterations, raw Exon array data were statistically analysed by Phil East (bioinformatics software specialist, CRUK). First of all, probe level intensities were background corrected using the anti-genomic probe groups and then quantile normalised. Core level probeset and gene level signal estimates, along with probeset detection p-values (DABG), were generated using Iter-plier. Quantification was further carried out using apt-1.10.0 from Affymetirx with a '-a' option of 'quant-norm.pm-gcbg.iter-plier'. For each of the pairwise comparisons, probesets displaying a greater than 0.05 detection p-value in more than half of the samples, in both conditions, were removed from the analysis. In addition, entire transcript clusters were removed if more than half the member probesets had a detection p-value above 0.05 across one condition. This step was implemented since it is impossible to infer a translocation event against an unexpressed transcript. Once filtered each probeset was scaled to its corresponding gene level intensity estimate to remove any gene effect present in the comparison. Scaled probesets displaying differential behaviour were detected via Anova analysis using a 0.05 fdr (false discovery rate) threshold. T-statistics were moderated using empirical Bayes shrinkage to increase statistical power. The analysis was then carried out using the Limma package from Bioconductor (Gentleman *et al.*, 2004). Finally, transcript clusters with differential probesets were inspected visually for expression profiles indicative of translocations.

2.6.3.2 Exon array data analysis with commercial software

2.6.3.2.1 Integrated Genomic Browser (IGB)

IGB is an interactive software programme which can be used to visualise and explore genome-scale data sets from multiple data sources. All data viewed in IGB, regardless of its source, were organised into distinct genomes and chromosomes. IGB was downloaded from the Affymetrix website (www.affymetrix.com/partners_programs/_developer/_tools/download_igb.affx). The Exon array data text file generated via ExACT software, (beta test software, Affymetrix) was uploaded to IGB. The expression variations of the probes representing individual genes were visualised in the browser.

2.6.3.2.2 Ingenuity Pathway Analysis (IPA)

In order to identify biologically relevant pathways, Ingenuity Pathway Analysis (IPA version 4.0), a web-based application (www.Ingenuity.com) that enables building signalling networks from gene expression data, was applied. According to the introduction from IPA website (www.Ingenuity.com), IPA is based on IPKB (Knowledge Base database), which is currently the largest curated database containing millions of computable relationships between genes, proteins, drugs and diseases. IPA's curation is performed by PhD-level scientists that manually curate the data and assess their quality. IPA's knowledge base ontology contains 12 major branches, ~580, 000 classes, as well as pathway interaction domains. IPA's biological process relationships describe the impact of gene on the process (for example, increases apoptosis or decreased migration etc), and has more than 15,000 gene-to-disease associations.

A data set containing Affymetrix probe identifiers and their corresponding 'fold change' values was uploaded in Excel. Each probe identifier was mapped to its corresponding object in the IPK base. To build a network, IPA searches the IPKB for interactions between focus genes/proteins and all other gene objects stored in the Knowledge base ('Focus genes' show direct interaction with other genes in the knowledge base). It then generates a set of networks with a maximum of 35 genes, and computes a score for each network. The score shows the likelihood that a gene is placed in a network due to random chance (for example, a score of 2 gives a 99% confidence that the focus genes are not being generated by random chance). In addition, IPA's Global Functional Analysis feature provides an overview of biological functions associated with a set of dysregulated genes/proteins, with functions displaying a p-value <0.05 being significant. The significance values for these analyses are calculated using the right-tailed Fisher's Exact test.

2.6.4 Synthesis of complementary DNA

1 µg of total RNA and 1.5 µL of random hexamers (50 µM) were co-denatured at 70 °C for 5 mins. 6 µL of M-MLV RT 5x synthesis buffer (Promega, UK), 10 µL of dNTPs (2.5 mM each) and 2 µL of M-MLV RT RNase H minus, Point mutant (200 U/µL) (Promega) were added and then the reactions were incubated for 1 h at 42 °C followed by 5 mins at 95 °C. Following the addition of 2 µL of RNase H (1 U/µL) (Promega), tubes were placed back at 42 °C for 10 mins and subsequently stored at -20 °C.

2.6.5 Real-time quantitative reverse transcription PCR (qRT-PCR) analysis

2.6.5.1 cDNA quality confirmation using β-actin control PCR

Following the cDNA synthesis, a standard PCR using β-actin primers (Forward sequence: 5'-GCGGGAAATCGTGCGTGCGTGACATT-3'; Reverse sequence: 5'-GATGGAGTTGAAGGTAGTTTCGTG-3') (Sigma) was performed. β-actin is a commonly used housekeeping gene for PCR-based techniques and Western blotting. Here, β-actin was used as a positive control to determine the quality of the cDNA synthesised by checking for the presence or absence of PCR product.

For each sample, the PCR reaction was performed in 25 µL volume. A mixture of 2 µL of cDNA, 2.5 µL 10X buffer (Invitrogen), 0.5 µL of dNTPs (10 mM), 0.75 µL of $MgCl_2$ (50 mM, Invitrogen), 1 µL of each β-actin primer (10 µM each, Sigma), 0.2 µL of Taq DNA polymerase (5 U/µL, Invitrogen) and 17.05 µL of molecular biology-grade water was used. The PCR was carried out under the following conditions: 95 ºC-1 min; 95 ºC-30 s, 62 ºC-30 s and 68 ºC-90 s for 35 cycles; 72 ºC for an additional 1 min after the final cycle. PCR products were analysed on a 1.5% agarose/EtBr gel and bands of 250 bp were expected.

2.6.5.2 Real-time quantitative reverse transcription PCR

Relative expression of genes, which were selected from Exon array data, was determined using either Taqman-based or SYBR-Green based real-time quantitative reverse transcription PCR analysis.

2.6.5.2.1 Taqman-based gene expression detection

Taqman gene expression probes were ordered from Applied Biosystems (ABI) (**Table 2.16** and **Table 2.17**) and the qRT-PCR reactions were performed using an ABI 7900 Real Time PCR System (Applied Biosystems, ABI) keeping the default settings for baselines and thresholds. The housekeeping gene (*GAPDH*) was used as an endogenous control. The standard reaction volume (20 µL) and cycling conditions were applied to assess all Taqman probes in MicroAmp® fast optical 96-well reaction plates (Applied Biosystem). The reaction mix is listed in **Table 2.18**. The cycling conditions were as follows: 2 mins at 50 °C, 10 mins at 95 °C, 40 cycles of 15 s at 95 °C and 1 min at 60 °C. All measurements were performed in triplicate and a no template control (NTC) was included to detect any possible contamination.

Each probe generated an expression curve from which the cycle threshold (C_t) values were extracted. For each triplicate, a mean C_t value was calculated, making sure to remove any aberrant values. Each target mRNA was normalised against the housekeeping gene by subtracting the C_t value of *GAPDH* from the C_t value of the target probe (ΔC_t). This compensates for the variability in the amount of starting material. To ensure that results processed on different plates were comparable to a unique calibrator (positive control, P129), the ΔC_t for the control sample was subtracted from the ΔC_t for the target sample ($\Delta\Delta$Ct). Fold change compared with control was calculated by $2^{-\Delta\Delta Ct}$.

$\Delta C_t = \Delta C_{t\ target} - \Delta C_{t\ housekeeping\ gene}$

$\Delta\Delta C_t = (\Delta C_{t\ target} - \Delta C_{t\ housekeeping\ gene})_{sample} - (\Delta C_{t\ target} - \Delta C_{t\ housekeeping\ gene})_{control}$

Expression fold change $=2^{-\Delta\Delta Ct}$

Table 2.16 ABI Taqman gene expression probes ordered for target validation

Probes ordered from www.appliedbiosystems.com

Gene Name	Assay ID	Interrogated sequence (Refseq)	Exon boundary
CNR1	Hs00275009_s1	NM_033181.2	2-2
PNRC1	Hs00199095_m1	NM_006813.1	1-2
GJA10	Hs01087606_s1	NM_032602.1	1-1
ARMCX1	Hs01849556_s1	NM_016608.1	4-4
SRD5A2	Hs00936406_m1	NM_000348.3	2-3
	Hs03003722_m1		4-5
KRT23	Hs01119993_m1	NM_015515.3	3-4
	Hs01119997_m1		8-9
UNC5C	Hs01031779_m1	NM_003728.2	9-10
GAPDH	Hs99999905_m1	NM_002046.3	3-3

Table 2.17 Custom TaqMan® Gene Expression Assays

Gene name	Interrogated sequence (Refseq)	Forward primer	Reverse primer	Reporter sequence	Exon boundary
SRD5A2	NM_000348.3	GGCACTGGCCTTGTACGT	AGCCGCCGGCTTCAG	CTCTCCGTGTGCTTCC	1-1
KRT23	NM_015515.3	AGGTGTGCTGGGATGAAAGG	GGTATCTTTCTAATCTTGCCGTGAAGT	CTGGAAGTGGAAGGTAAAT	1-2

Table 2.18 Reaction mix for Taqman Real-time quantitative reverse transcription PCR

Component	Volume for one reaction
2x Universal PCR Master Mix	10 μL
20x ABI probe/primer mix	1 μL
cDNA	1 μL
Water	8 μL

2.6.5.2.2 SYBR-Green based detection

To ensure that primers are specific for the target sequence, free of internal secondary structure, and to avoid complementation at 3′-ends, primers for SYBR-Green gene expression analysis were designed using the online software Primer3 (http://frodo.wi.mit.edu/primer3/) . In addition, primers were designed to ensure that the amplicon length was approximately 80–120 bp to optimise the

efficiency of qPCR and also the primers span different exons to avoid amplification from residual genomic DNA. The primers were ordered from Sigma and the SYBR® Green PCR Master Mix was purchased from Applied Biosystems, ABI (**Table 2.19**). Prior to the detection of gene expression, a standard curve for each primer pair was created by performing qRT-PCR on a serial of five-fold serial dilutions of a cDNA template (1, 1/5, 1/25, 1/125, 1/625, 1/3125). Ct values (>8 and <35) were plotted against log10 of the dilution factor. The amplification efficiency was assessed using the slope of the regression line in the standard curve. A slope of – 3.3 indicates 100% PCR amplification efficiency and 10-fold increase of products for every 3.3 cycles. The specificity of the primers was determined through dissociation peak and further confirmed on a 1.5% agarose gel with a single band at the correct size. Primers, which had a PCR efficiency and R^2 values (correlation coefficiency) >98% and that also demonstrated specificity, were applied for further analysis.

The SYBR-Green qRT-PCR reactions were performed on a ABI PRISM 96-well optical plate using an ABI 7500 Real Time PCR System (Applied Biosystems, ABI). The housekeeping gene (β-actin) was used as an endogenous control. The standard reaction volume (20 μL) was applied as listed in **Table 2.20**. The cycling conditions were as follows: 2 mins at 50 °C, 10 mins at 95 °C, 50 cycles of 15 s at 95 °C, 1 min at 60 °C, 15 s at 95 °C, 1 min at 60 °C and 15 s at 95 °C. All measurements were performed in triplicate and a no template control (NTC) was included to detect any possible contamination. The threshold cycle (Ct) data were determined using default threshold settings. The qRT-PCR data analysis was the same as illustrated **2.2.6.2**

Table 2.19 SYBR Green gene expression primers

Target gene	Primer	Sequence
CNR1	Forward	5'-AAGACCCTGGTCCTGATCCT
	Reverse	5'-CGCAGGTCCTTACTCCTCAG
CNR2	Forward	5'-ATCATGTGGGTCCTCTCAGC
	Reverse	5'-GATTCCGGAAAAGAGGAAGG
β-actin	Forward	5'-AGAAAATCTGGCACCACACC
	Reverse	5'-AGAGGCGTACAGGGATAGCA
SULF	Forward_1	5'-AGAGCGTGGAAGGACCATAA
	Reverse_1	5'-TTATGGTCCTTCCACGCTCT
SULF	Forward_2	5'-GAAGGAGAAGAGACGGCAGA
	Reverse_2	5'-CAGAAAGATCCCAGGTTCCA
PTGIS	Forward_1	5'-CATCCCCTGGTTGGGGTATG
	Reverse_1	5'-CGTCGTAGGAGTGTGGGTC
PTGIS	Forward_2	5'-CACGAGGATGAAGGAGAAGC
	Reverse_2	5'-GTCCAGGAGAACGGTGACAT

Table 2.20 Reaction mix for SYBR Green Real-time quantitative reverse transcription PCR

Component	Volume for one reaction
2x SYBR® Green PCR Master Mix	10 μL
Forward primer (10 μM)	0.6 μL
Forward primer (10 μM)	0.6 μL
cDNA	1 μL
Water	7.8 μL

2.7 Protein expression analysis

2.7.1 Western blot analysis

2.7.1.1 Total protein isolation from cell lines

Media was removed before cells were washed with cold PBS. 100 µl of lysis buffer (1% Triton X-100 and 1x protease inhibitor cocktail (Roche) in PBS) was applied to 1 well of a 6-well plate. Cells were scraped and centrifuged at 1000 rpm for 2 mins. The supernatant was stored at – 80 °C.

2.7.1.2 Total protein isolation from clinical fresh frozen tissue

All clinical fresh frozen samples were cut onto slides and marked with tumour or BPH area before being macro-dissected to 2 mL tubes as illustrated in **2.5.1.2**. 500 µL of lysis buffer was added to each tube. Tissue was homogenised using a homogeniser. The tissue was then sonicated on ice with 2x 10 s pulses. The tubes were centrifuged at 14,000 rpm for 15 mins at 4 °C. Supernatants were transferred to pre-chilled 1.5 mL tubes and kept at – 80 °C prior to use.

2.7.1.3 Protein quantification

Protein concentrations of whole cell extracts were quantified in duplicate, using the Bradford Protein Assay (BioRad) in a 96-well microplate (Greiner Bio-One). Protein was quantified by diluting the whole cell extract (1:10) in double distilled H_2O, adding 190 µl of 1x BioRad reagent (5x) diluted in distilled H_2O. In addition, 10 µl of 0.1, 0.2, 0.3, 0.4, 0.5, 0.8, 1 mg/ml of bovine serum albumin (BSA; Sigma-Aldrich) were added to 190 µL 1x BioRad reagent respectively. After incubation at RT for 5 mins, absorbance of samples at 595 nm was measured using an Opsys MR 96-well microplate reader (DYNEX). A standard

curve of absorbance versus concentration was constructed for the different concentrations of BSA and the protein concentration in each sample was calculated using this graph.

2.7.1.4 Sodium dodecyl sulphate polyacrylamide gel electrophoresis (SDS-PAGE) and protein detection

30 µg of protein from each sample was used for Western-blot analysis. The protein was combined with SDS-PAGE loading buffer and reducing buffer and then heated to 100 °C for 5 mins before separation by electrophoresis. The Bio-Rad mini-PROTEAN Tetra gel electrophoresis system was used (Bio-Rad Laboratories Ltd). Depending on the molecular weight of the protein of interest, different concentrations of resolving gel were prepared: 7.5-8% gels were cast for high molecular weight proteins (i.e. more than 100 kD) and 10-12% gels for lower molecular weight proteins (i.e. 20-100 kD) (**Table 2.21**). After the resolving gel was loaded in between the gel plates, double distilled water was overlaid to exclude air. Once set, water was poured off and the stacking gel was added. The desired comb was inserted to form wells within the stacking gel. Once set, the gel was transferred into a Bio-Rad reservoir tank filled with 1x Tris-Glycine-SDS PAGE buffer (National Diagnosis). The protein samples and 15 µL spectra multicolour broad range protein ladder (Fermentas) were loaded. The gel was run at 100 V for protein stacking and 120 V for protein separation. Then proteins were transferred onto a PVDF membrane at 0.25 mA for 90 mins in a transfer tank filled with 1x Tris-Glycine electroblotting buffer (National Diagnosis) and surrounded by an ice-box.

Table 2.21 SDS-Polyacrylamide Gel Formulations

	Resolving gel				Stacking gel
	7.5%	10%	12%	15%	5%
Acrylamide/Bisacrylamide (40%)	2.85 mL	3.8 mL	4.5 mL	5.7 mL	625 µL
Tris-HCl (1.5M, pH 8.8)	3.75 mL	3.75 mL	3.75 mL	3.75 mL	—
Tris-HCl (1M, pH 6.8)	—	—	—	—	625 µL
SDS (10%)	170 µL	170 µL	170 µL	170 µL	50 µL
H_2O (MiliQ)	8.15 mL	7.17 mL	6.472 mL	5.27 mL	3.67 mL
TEMED	10 µL	10 µL	10 µL	10 µL	5 µL
Ammonium persulphate (1.5%)	100 µL	100 µL	100 µL	100 µL	25 µL

After the proteins were transferred, the membrane was blocked with 5% (w/v) non-fat milk and 0.01% Tween-20 in PBS (PBST) for 1 h at RT. The membrane was incubated with primary antibody, which was diluted in 10% bovine serum albumin (BSA) in PBST, overnight at 4 °C before being washed with PBST for 10 mins at RT. After the secondary antibody, which was diluted in PBST, was added to the membrane and incubated for 50 mins, the membrane was washed three times with PBST, 10 mins per wash. Protein was detected by chemoluminescent detection of the horseradish peroxidase-conjugated secondary antibody using the enhanced chemiluminecence (ECL) Western Blotting Detection Reagent (Amersham Biosciences). Signal was visualised with Super RX Fuji Medical X-Ray Film (Fujifilm) developed in a Curix 60 Developer (Agfa, Middlesex, UK).

2.7.2 Immunohistochemistry (IHC)

2.7.2.1 Paraffin-embedment of cells

In order to perform IHC analysis on cells, which were cultured *in vitro,* the cells were first fixed in formalin and embedded in paraffin. Cells were harvested and

washed with PBS before being re-suspended in 2% (w/v) low melting temperature soft agar, which was dissolved in PBS and kept at 40 ºC in a water bath prior to use). The cell/soft agar suspension was transferred to a 5 mL syringe, which was cut at the bottom, and then kept at 4 °C for 1 hr. After the agar had solidified, it was fixed in 10% formalin for 24 h and then transferred to 70% ethanol. Paraffin embedment was performed by the pathology services of the Institute of Cancer (QMUL, London) .

2.7.2.2 IHC analysis

IHC analysis of *CNR1* was performed by the Institute of Cancer (QMUL, London) pathology service using the Ventana Discovery™ System (Illkirch, France) following the manufacturer's protocol 088. Simply, all slides were deparaffinised and processed for antigen retrieval with standard SSC. After blocking, the slides were incubated with the *CNR1* primary antibody from Abcam (ab23703, synthetic peptide: MSVSTDTSAEAL, corresponding to C-terminal amino acid 461-472) or *CNR1* antiserum (2824.3) for 60 mins and anti-rabbit secondary antibody for 16 mins. Staining for *CNR1*, was performed using the 3-3' diaminobenzidine (DAB) detection kit (Ventana). Slides were counterstained with H&E.

Rabbit polyclonal antibody (F69-2) of *BACH2* was a kind gift from Prof. Igarashi (Division of Biochemistry, Tohoku University Graduate School of Medicine). IHC of *BACH2* was performed manually by a pathologist, Y.W. Yu. All slides were deparaffinised and antigen retrieval was performed by heating the sections immersed in Target Retrieval Solution, high pH (DAKO), in a pressure cooker for 15 mins. The primary antibody (at a dilution of 1:500) was incubated

for 40 mins at RT followed by secondary biotinylated universal antibody (Vectastain universal ABC kit, Vector Laboratory) for 30 mins at RT. Tissue slides were incubated in DAB at RT until the brown colour appeared. Slides were then counterstained with H&E.

2.7.2.3 Evaluation of staining

The stained tissue sections were scored by a pathologist (L.Y. Xue, Cancer Hospital, Peking Union Medical College, Beijing, China) with the criteria of combined intensity with the rate of positive cells. The staining intensity was graded on a 0-3 scale: 0, negative; 1, weak; 2, moderate; 3, strong. The rate of positive cells was scored according to the percentage of stained cells in relation to the entire section as 0 point for <5%; 1 point, 5~25%; 2 points, 26~50%; 3 points, 51%~75%; 4 points, >75%. A final score was achieved by multiplication of the two scores above. Scores of 0~4 were defined as negative expression (-); scores of 5~8 as weakly positive expression (+), and scores of 9~12 as strongly positive expression (++).

2.8 Plasmid construction

2.8.1 Commercial plasmids

Two plasmids containing the Kozak sequence and coding sequence of the gene *CNR1* were purchased from Missouri S&T cDNA Resource Center (USA). The vector backbone of these plasmids is pcDNA3.1(+) (Invitrogen). pcDNA-CNR1, contains the *CNR1* open reading frame sequence (1419 bp). pcDNA-3HA_CNR1, contains *CNR1* open reading frame sequence with three HA-tags at

the N-terminal of *CNR1* (1503 bp). The vector, pmaxCloning, was purchased from Lonza, Germany.

2.8.2 Plasmid construction

2.8.2.1 pcDNA-CNR1_Flag plasmid construction

In order to over-express *CNR1* in prostate cancer cell lines, first of all, the open reading frame sequence of *CNR1* (1419 bp) was PCR amplified from the cDNA of a BPH sample (P129), which was shown with high *CNR1* expression at the RNA level. In the forward primer, *Hind III* restriction enzyme cutting site (AAGCTT) was incorporated; in the reverse primer, *XbaI* restriction enzyeme cutting site (TCTAGA) was included and a Flag-tag sequence (GATTACAAGGATGACGACGATAAG) was also added before the stop codon (TGA). The forward sequence was 5'-AGTAAGCTTGAGGTTATGAAGTCGATC CTAGATGGC, and the reverse sequence was 5'-ACTTCTAGATCACTTATCGTC GTCATCCTTGTAATCCAGAGCCTCGGCAGACGTG. The PCR was performed using the high fidelity Phusion DNA polymerase (Finnzymes). The PCR was preceded by initial denaturation at 98 °C for 2 mins followed by 35 cycles of denaturing at 98 °C for 10 s, annealing at 65 °C for 30 s, extension at 72 °C for 90 s. The reaction followed by extension at 72 °C for 10 mins. The PCR product was purified using a PCR purification kit (Qiagen) before being digested with both *Hind III* and *XbaI* at 37 °C for 1 h. The plasmid pcDNA3.1 (+) (Invitrogen) was also digested with the same restriction enzymes under the same conditions. Digested PCR and pcDNA3.1 fragments were separated by agarose gel electrophoresis and purified using a Gel extraction kit (Qiagen). The PCR

product was ligated with pcDNA3.1 (+) using T4 DNA ligase (NEB) at 16 °C overnight.

2.8.2.2 pmaxCNR1 plasmid construction

The open reading frame sequence of *CNR1* (1419bp) with Kozak sequence (gccaccatgc) was inserted between the *KpnI* (ggtacc) and the *SacI* (gagctc) sites of the pmaxCloning multiclonal site (MCS). For gene cloning, the forward primer sequence is 5'-AGTGGTACCGCCACCATGAAGTCGATCCTAGATGGC and reverse primer sequence is 5'-ACTGAGCTCTCACAGAGCCTCGGCAGACGT G. The PCR was performed by initial denaturation at 98 °C for 2 mins and 35 cycles with denaturing at 98 °C for 10 s, annealing at 65 °C for 30 s, extension at 72 °C for 90 s. The reaction was ended with an extension step at 72 °C for 10 mins. The following procedures, including PCR product purification, restriction enzyme digestion and ligation with pmaxCloning plasmid, were completed as described in **2.8.2.1**.

2.8.2.3 Plasmid transformation

The ligated plasmid was transformed into TOP10 chemically competent bacteria (Invitrogen) through co-incubation for 5 mins on ice, heat shock at 42 °C for 40 s and incubation for 10 mins on ice. Then the transformed bacteria were spread on an LB agar plate containing 100 ng/mL ampicillin overnight. Single colonies were picked and cultured in LB media on an oscillating incubator shaking at 225-300 rpm at 37 °C overnight. The plasmids were extracted using a miniprep kit (Qiagen) and then sent to the Genome Centre (QMUL, London) for sequencing. The plasmid, which was confirmed to contain the correct cDNA sequence of the gene *CNR1*, was applied for further study.

2.9 Cell transfection

2.9.1 Over-expression

In order to study the cellular function of the gene *CNR1*, a potential tumour suppressor gene in prostate cancer, over-expression of *CNR1* in prostate cancer cells *in vitro* is essential. In this study, *CNR1* was over-expressed transiently in 22RV1 and 293 cells; In addition, stably transfected 22RV1 cells were established.

2.9.1.1 Transient transfection

Cell transfection can be accomplished through several different methods. In this study, chemical reagents and electroporation (nucleofection) were attempted to deliver the plasmids into cells. For transfection with chemical reagents, the plasmid, pcDNA-GFP, was used to optimise the transfection protocol for each of the reagents used. pcDNA-GFP was a gift kindly provided by Dr Gunnel Hallden's group (Institute of Cancer, QMUL, London). This is a plasmid with the *GFP* open reading frame sequence inserted into the pcDNA3.1 (+) vector. For nucleofection transfection, pmaxGFP, a commercial control plasmid, with a *GFP* open reading frame sequence inserted to the pmaxCloning vector, was used to optimise the electrical transfection conditions. For different transfection reagents, cell density and the ratio of plasmid/reagent were used according to the manufacturer's recommendation.

2.9.1.1.1 Transfection with JetPEI™-RGD reagent

jetPEI™-RGD (Poly-Plus, Illkirch, France) is a Arg-Gly-Asp (RGD) peptide-conjugated linear polyethylenimine (PEI). It allows selective and efficient

transfection of integrin-expressing epithelial (i.e. prostate cancer cells) and endothelial cells as many integrins bind multiple RGD peptide sequences present in serum and extracellular matrix proteins. Three different conditions were used for transfection with JetPEI-RGD. 2.5 x 10^5 of 22RV1 cells were seeded per well in a 6-well plate with 1.8 mL culture media one day before transfection. 3 μg of DNA and 6 μL of jetPEI™-RGD solution were diluted separately into 100 μL of 150 mM NaCl. 100 μL of diluted jetPEI™-RGD solution was added to the 100 μL DNA solution, followed by incubation for 30 mins at RT. Then 200 μL jetPEI™-RGD/DNA mixture was added to each well. Cells were incubated at 37 °C in a CO_2 incubator for 24-48 h prior to testing for transgene expression.

2.9.1.1.2 Transfection with Effectene reagent

Effectene transfection kit (Qiagen) is routinely used in our lab for transfection of HEK293 cells with, in our experience, approximately 50% transfection efficiency. 1.5 x 10^5 HEK293 cells were seeded per well in a 6-well plate and cultured overnight. 0.4 μg of plasmid was diluted in 100 μL of buffer EC and then 3.2 μL of enhancer solution was added followed by incubation for 5 mins at RT. 10 μL of Effectene transfection reagent was then added to the mixture and incubation was carried out for another 10 mins at RT to allow transfection-complex formation. In the meanwhile, cells were washed with PBS and refed with 1.6 mL growth media. Then 0.6 mL growth media was added to the transfection complexes before the whole mixture was applied to the cells. Cells were incubated for 24-48 h prior to testing for transgene expression.

2.9.1.1.3 Transfection with Lipofectamine reagent

One day before transfection, 5 x 10^5 of 22RV1 cells in 2 mL of growth media without antibiotics were plated in 6-well plates so that cells reached 90-95% confluency at the time of transfection. For each transfection, complexes were prepared as follows: 4 μg DNA was diluted in 250 μL of serum-free/antibiotic free growth media; 10 μL of Lipofectamine™ 2000 (Invitrogen) was diluted in 250 μL of serum-free/antibiotic free growth media. After incubation for 5 mins at RT, the diluted DNA was combined with diluted Lipofectamine™ 2000 followed by incubation for 20 mins at RT. 250 μL of complexes were added to each well. Cells were incubated at 37 °C in a CO_2 incubator for 24-48 h prior to testing for transgene expression.

2.9.1.1.4 Transfection with Nucleofector

Cells were transfected using Nucleofector technology with the Amaxa cell line nucleofector kit V (Amaxa Biosystems, Gaithersburg, MD) according to the manufacturer's instructions. 1x10^6 22RV1 cells and 4 μg of Amaxa's pmaxGFP vector, as well as the built-in programme, A-020, was found to result in approximately 100% transfection efficiency, thus it was selected for consecutive studies. Cells were split 48 h before transfection to obtain 70-80% confluency. Cells were then trypsinised and counted. 1x10^6 cells were centrifuged at 100 g for 10 mins. Cell pellets were resuspended in 100 μL Nucleofector solution L provided in the kit (Amaxa). Upon the addition of 4 μg DNA, the cell-plasmid mix was electroporated on the nucleofector apparatus using programme A-020. Immediately after electroporation, 500 μL of pre-warmed cell culture media supplemented with 10% FBS was added and the cell-plasmid solution was transferred to a 6-well plate, which contained 1 mL of pre-warmed medium.

Cells were incubated at 37 °C in a CO_2 incubator for 24-48 h prior to testing for transgene expression.

2.9.1.2 Stable transfection

In order to obtain cells expressing *CNR1* stably, transient transfected cells were cultured under geneticin G418 (1 mg/mL) (Sigma-Aldrich) selection. G418 is a toxin but can be neutralised by the product of the neomycin resistance gene, which is constructed in the pcDNA3.1 (+) vector. Therefore, only cells that have the plasmid integrated into the nuclear genome would survive. Simply, cells were passaged into fresh growth media 24 h after transfection and G418 was add the following day to a final concentration of 1 mg/mL. Cells were maintained under this selection. Media was changed every 3 to 5 days until successful selection was achieved. Stably transfected 22RV1 cells were maintained in RPMI-1640 supplemented with 10% FCS and G418 at 1 mg/mL.

2.9.2 siRNA transfection

CNR1 siGENOME SMARTpool (5 nmol) that targets the 3'UTR/ORF of *CNR1* transcript was purchased from Dharmacon. *CNR1* siRNA (5 nmol) and non-targeting siRNA (NT siRNA) was dissolved in 500 μL of 1x siRNA buffer, which was diluted from 5x siRNA buffer (Dharmacon) in DEPC water, to reach 20 μM concentration. The dissolved siRNA was incubated for 30 mins at RT with rotation. The siRNA solution was stored as 50 μL aliquots at -20 °C prior to use.

1.2×10^5 of 22RV1 cells were seeded per well in a 6-well plate at 40-50% confluence. Cells were cultured overnight in RPIM-1640 media supplemented

with 10% FBS without antibiotics. 5 μL of each *CNR1* siRNA and non-targeting (NT) siRNA was diluted in 180 μL unsupplemented media respectively; 10 μL oligofectamine (Invitrogen) was diluted in 40 μL unsupplemented media followed by incubation for 10 mins at RT. 25 μL of oligofectamine mix was added to *CNR1* and NT siRNA mix respectively and incubated for 25 mins at RT. Cells in each well were washed with PBS and covered with 790 μL unsupplemented media. After the incubation, 210 μL transfection mixture was then added to each well and an additional 500 μL RPIM-1640 media, supplemented with 30% FBS, was added after 4 h.

2.10 Cellular functional analysis

2.10.1 MTS assay

5x 10^3 of 22RV1 cells in 100 μL growth media were seeded in each well of 96-well plates. Media alone was used as control. MTS assay kit CellTitre 96 AQ_{ueous} Non-Radioactive Cell Proliferation Assay (Promega, WI, USA) was used to determine cell proliferation/viability every 24 h for 5 days. The MTS assay is a colourimetric method for determining cell proliferation/viability, by using the tetrazolium compound (3-(4,5-dymethylthiazol-2-yl)-5 (3carboxymethoxyphenyl)-2-(4-sulphophenyl)2H-tetrazolium; MTS) combined with phenazine methosulphate (PMS), an electron coupling reagent. Mitochondrial enzymatic activity of viable cells reduces MTS to formazan that is water-soluble. The number of living cells is directly proportional to the concentration of formazan in the sample, determined by the absorbance at 490 nm. 2 mL of MTS and 100 μL PMS were mixed and 20 μL of the mixture was added to each well of the 96-well plate. Absorbance at 490 nm was measured after 3 h of incubation at 37 °C and

5% CO_2, using an OpsysMR plate reader (Dynex Technologies Inc, Chantilly, US).

2.10.2 Colony formation assay

3000, 2000, 1000, 100, 10 of 22RV1 cells were plated per well in a 6-well plate in growth media. Cells were cultured for 14 days with media changed every three days. Media was removed and the colonies from each well were stained with 3 mL of 1% crystal violet (0.5g dissolved in 500 mL of methanol) for 1 h at RT. The excess stain was removed with running water and the plate was left to dry. Experiments were carried out in triplicate. The stained colonies were captured using a camera. Analysis took place by measuring the area covered by colonies using ImageJ software. For each well, the same size of measuring area (230x236 pixels) was set and the area covered by colonies was measured under the same defined thresholds.

2.10.3 Invasion assay

Invasion assays were performed using BD Biocoat Matrigel Invasion Chambers with 8-micron pores (BD Biosciences, Oxford, UK) in which the upper and bottom chambers were separated by a membrane coated with Matrigel. Invasion chambers were equilibrated for 2 h at RT and hydrated for 2 h with 500 µL serum-free media at 37 °C. After rehydration of the Matrigel, 750 µL RPMI-1640 media, supplemented with 10% FBS, was added to the lower chamber as a chemoattractant. 2.5 x 10^4 cells in 500 µL serum-free media were added to the upper chamber. The chamber was incubated for 48 or 72 h at 37 °C. Cells that had invaded through the pores onto the lower surface of the filters were fixed with 100% methanol for 30 s. After washing the membrane with double distilled

H_2O, non-invaded cells at the top of the Matrigel membrane were removed. Cells present on the bottom of the membrane represented the invading cells. The membranes were stained with 1% Giemsa Blue (Sigma-Aldrich) and the total number of invading cells was counted under an Olympus CX41 microscope at 40x magnification. Each experiment was repeated in triplicate.

2.11 Statistical analysis

The statistical analyses regarding t(4;6)(q22;q15) were carried out by a statistician (L Ambroisine, CRUK). Associations between t(4;6)(q22;q15) status and categorical data were examined using the χ^2 test. Associations between t(4;6)(q22;q15) status and numerical variables were assessed using analysis of variance. Univariate and multivariate analyses using proportional hazard regression (Cox and Oakes, 1984) were applied to determine the impact of t(4;6)(q22;q15) on prostate cancer specific death and death for any cause. For the multivariate analyses the variables used were age at diagnosis, Gleason score, baseline PSA and tumour volume in the biopsy. For IHC analysis of *CNR1* and *BACH2*, the statistical analyses were done by a pathologist (L.Y. Xue, Cancer Hospital, Peking Union Medical College, Beijing, China). The χ^2 test performed with SPSS 10.0 for Windows (SPSS, Chicago, IL, USA) was used to compare the immunoreactivity of *CNR1* and *BACH2* protein among prostate cancer and BPH samples. Regarding the DNA methylation analysis of *CNR1*, the statistical analyses were performed by Dr N Vasiljevic (Cancer Research UK Centre for Epidemiology, Mathematics and Statistics, Wolfson Institute of Preventive Medicine). The analyses were based on mean values of the four CG analysed. Methylation differences between normal and cancer were examined by Wilcoxon

signed-rank and Mann-Whitney test for matched or unmatched specimens respectively. The statistical calculations were conducted using software R version 2.9.2 (Team, 2009).

3 THE IDENTIFICATION OF CHROMOSOMAL TRANSLOCATION, T(4;6)(q22;q15), IN PROSTATE CANCER

3.1 Introduction

In 2005, identification of recurrent fusion genes, *TMPRSS2:ERG* and *TMPRSS2:ETV1*, in prostate cancer addressed the importance of chromosomal translocation and fusion genes in prostate cancer development. Our group has a long-standing interest in attempting to identify chromosomal translocation and fusion genes in prostate cancer. In 2007, we reported a recurrent chromosomal translocation, t(4;6), which was detected in three out of six prostate cancer cell lines and four of 25 primary tumours using M-FISH analysis (Lane *et al.*, 2007). The breakpoints of the translocation were mapped in the LNCaP cell line using FISH analysis (Lane *et al.*, 2007). It showed that the breakpoints locate at 4q22 and 6q15. In addition, micro-deletions were identified adjacent to both of the breakpoints. Therefore there were two breakpoints at each of the 4q22 and 6q15 locations. At distal breakpoint of 4q22, the gene unc-5 homolog C (*UNC5C*) lost its promoter and the first exon. *UNC5C* is one of the netrin-1 receptors and it belongs to the functional dependence receptor family, members of which share the ability to induce apoptosis in the absence of their ligands. *UNC5C* has been reported as a putative tumour suppressor gene (Thiebault *et al.*, 2003). At proximal breakpoint of 4q22 and two breakpoints of 6q15, no known gene has been identified. Interestingly, copy number loss has been detected frequently on 4q and 6q in prostate cancer as described in **1.6.3**. 6q15, particularly, is one of

the most frequently deleted regions in prostate cancer, indicating that tumour suppressor gene(s) might locate in this region.

Chromosomal translocation has a causal effect in haematological malignancy. A classic example is the Philadelphia chromosome, which is caused by t(9;22)(q34;q11), which presents in 95% of CML patients. The Philadelphia chromosome serves as a diagnostic marker, therapeutic target as well as a prognosis marker to predict the therapeutic outcome (Sessions, 2007). If t(4;6) is correlated with any clinical feature or patient outcome, it could, potentially, be used as a biomarker. The clinical prevalence of t(4;6) and its correlations with clinical outcome in prostate cancer were investigated in this study.

3.2 Aims

In this study, I aimed to examine the frequency of t(4;6)(q22;q15) using FISH analysis on prostate cancer tissue microarrays (TMAs) with probes located on 4q22 and 6q15 and then correlate the translocation status with clinical features.

3.3 Results

3.3.1 Probe selection

The t(4;6) can be examined by FISH signal co-localisation or splitting analysis. For signal co-localisation analysis, two probes binding to 4q22 or 6q15 were labelled as green or red respectively. In t(4;6) negative cases, red and green signals appeared to be apart from each other as they bind to different

chromosomes; whereas in t(4;6) positive cases, red and green signals appeared to be adjacent to each other (co-localised). For signal splitting analysis, two probes were utilised, which bind to each side of the breakpoint on 4q22 or 6q15. In t(4;6) negative cases, red and green signals were expected to be located adjacent to each other, whereas in t(4;6) positive cases, splitted red and green signals were expected to be observed. FISH signal co-localisation analysis was preferred initially as, in general, co-localised signals were easier to distinguish visually than splitting signals. Therefore we decided to apply FISH signal co-localisation analysis to investigate the t(4;6) fusion in large prostate cancer samples first and then perform signal splitting analysis to confirm the co-localised signals, which is caused by t(4;6) rather than random adjacent localisation of two chromosomes, in certain samples.

Dual-colour probes that separately bind to the regions flanking the breakpoints on chromosome 4 and 6 were selected for FISH signal co-localisation analysis. Probes that separately bind to the regions flanking the distal breakpoint on chromosome 6 were selected for FISH signal splitting analysis. There were two different probe combinations: one was to use the probes binding to distal 4q22 and proximal 6q15; the other was to use the probes binding proximal 4q22 and distal 6q15. Both combinations were tested in our group's previous study. The first probe combination showed co-localised signals in LNCaP cells and one primary prostate cancer sample, whereas the other pair did not. Further study demonstrated that, besides the translocation, the 6q15-25.3 fragment was inverted, which leads to the fusion of 4q22 to 6q25.3 in LNCaP cells; therefore there was a gap between the proximal 4q22 and the proximal 6q15 signals.

Although the inversion might only be specific to LNCaP cells, we preferred to investigate the t(4;6) using the first combination in primary prostate cancer samples.

In order to generate good signals on FFPE TMAs, probe sets with a combination of more than one probe were considered. It has been reported that three overlapping BAC clones showed 400 times magnified signal intensity, with little increase of background noise, on FFPE tissue sections (Lambros *et al.*, 2006). Therefore three probes were selected to hybridise simultaneously to distal 4q22 or proximal 6q15. The probe information and their corresponding regions are shown in **Table 3.1**. For the co-localisation analysis of the t(4;6)(q22;q15), probe set I on distal 4q22 location (**Figure 3.1a**) was labelled with biotin; probe set II on 6q14.3 (**Figure 3.1b**) was labelled with DIG. For the 6q15 break-apart assay, probe set III (**Figure 3.1c**), corresponding to the 6q15 deleted region in LNCaP, was labelled with biotin and was used in combination with the DIG-labelled probe set II on proximal 6q15. For each location, one probe set was generated from three BACs. In addition to the probe sets I and II, a third probe set (set III) was generated in order to confirm the translocation. All the BACs listed in the **Table 3.1** have been validated on metaphases of normal lymphocytes with chromosomal location specificities.

Table 3.1 Probe sets for t(4;6) detection and confirmation.

Probe set	Chr.	Location	BAC clone	Region	Length (bps)	Labelled	Signal colour
I	4	Distal 4q	RP11-18N21	98,354,298-98,515,689	63,210	Biotinylate	Red
			RP11-681L8	98,513,689-98,622,889	161,392		
			RP11-240J11	98,832,380-98,895,589	109,201		
II	6	Proximal 6q	RP11-111J1	87,249,921-87,344,749	97,534	DIG	Green
			RP11-595C20	87,344,650-87,442,183	59,031		
			RP1-214H13	87,576,952-87,635,982	94,829		
III	6	Deleted	RP1-44N23	90,814,536-90,843,275	28,740	Biotinylate	Red
			RP1-154G14	91,251,386-91,352,280	100,895		
			RP11-104N3	91,549,094-91,609,835	60,742		

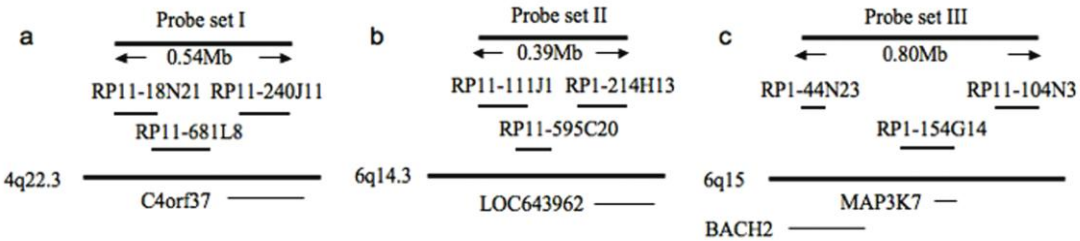

Figure 3.1 Maps showing the position of the BACs used as probes in FISH assays.

(a) Probe set I includes three BACs, RP11-18N21, RP11-681L8 and RP11-240J11, corresponding to a 0.54Mb region of distal 4q22 breakpoint. (b) Probe set II includes three BAC clones, RP11-111J1, RP11-595C20 and RP1-214H13, corresponding to a 0.39Mb region of 6q14.3 (proximal to 6q15 breakpoint). (c) Probe set III includes three BACs, RP1-44N23, RP1-154G14 and RP11-104N3, corresponding to a 0.80Mb region of 6q15 deleted in LNCaP cells.

3.3.2 Co-localisation analysis

3.3.2.1 Defining the cut-off for t(4;6) on control TMAs

As co-localisation of the 4q22 and 6q14.3 probes can also be caused by co-localisation of these two chromosomes by chance rather than translocation, we expected to see a low frequency of co-localised signals in normal tissue cells. Therefore, we determined the frequency of signal co-localisation on 16 morphologically normal tissues (**Table 3.2**). The co-localised signals in all the normal samples occurred at a low frequency, ranging from 1% to 6% with the mean of 2.7094 and standard deviation (SD) of 1.2151. A sample area without co-localised signal is shown in **Figure 3.3a**. Although it is widely accepted that the diagnostic cut-off is calculated as the mean plus three times SD of false-positive findings in at least five normal controls, we used a higher cut-off of 15% which is considered a reasonable cut-off for single co-localisation analysis (Ventura *et al.*, 2006). We subsequently scored prostate tumour samples as positive for t(4;6)(q22;q15) if 15% or more co-localised signals were detected within a cancer lesion containing more than 50 cells with both green and red signals.

Table 3.2 Scoring of non-malignant control samples on the TMAs for co-localisation of probes on 4q22 and 6q14.3

Sample	Total cells	Co-localisation positive	Percentage
Appendix	98	5	5.10
Breast	60	2	3.30
Cervix 1	104	4	3.80
Cervix 2	67	1	1.49
Colon	59	1	1.69
Foreskin	57	2	3.51
Inflamed gall bladder	54	1	1.90
Kidney	53	1	1.89
Lung	50	1	2.00
Placenta	60	2	3.30
Prostate	65	1	1.50
Small Intestine	59	3	5.10
Stomach	55	1	1.80
Testis	50	1	2.00
Tonsil	63	2	3.17
Uterus	55	1	1.80

3.3.2.2 Recurrence of t(4;6)(q22;q15) in primary tumour samples

Applying the above criteria, we firstly screened for t(4;6)(q22;q15) on the BPH and prostate cancer samples on the Barts TMAs using FISH probe co-localisation analysis. Out of the 68 prostate cancer samples on the two Barts tissue arrays, 56 were scorable and 4 out of these samples (7.2%) were considered positive for t(4;6)(q22;q15). A representative FISH image is shown in **Figure 3.3b**. A similar screening of the 34 BPH cases did not detect any positive samples. Cells with co-localisation signals in these samples range from 0% to 9.7% with median of 3.1%.

After confirming the re-occurrence of the t(4;6)(q22;q15) chromosomal translocation in prostate cancer, we further investigated a large cohort of localised prostate cancers, initially managed conservatively, on 24 TMAs using the FISH probe co-localisation assay. Out of the 808 cancers, 667 cases could be analysed and 78 (11.7%) samples were t(4;6)(q22;q15) positive. The chromosomal translocations were confirmed using the signal break-apart approach on two randomly selected TMAs, which were re-hybridised for FISH analysis using probes either side of the 6q15 centromeric breakpoint of LNCaP cells (**Figure 3.2c-e**). Of the five t(4;6)(q22;q15) positive cases, all of them were confirmed with the break-apart assay: three cases with splitting signals and two cases showing loss of 6q15 probe red signals, indicating deletion of this chromosome region as shown in **Figure 3.2e**. **Figure 3.4a** and **c** show examples of cells with co-localised signals in the probe co-localisation analysis; **Figure 3.4b** and **d** show the same cells but detected with the signal break-apart assay.

The cell with split red and green signals is indicated in **Figure 3.2d** and the cell with missing red signal was indicated in **Figure 3.2e**.

During our FISH analysis, we also revealed that the t(4;6)(q22;q15) status was heterogeneous within each case of cancer. The t(4;6)(q22;q15) fusion was only found in some patched areas of each section. The high frequency of signal co-localisations in one cancer area but lack of co-localisations in the other cancer areas indicates the heterogeneity of t(4;6)(q22;q15) in prostate cancer cells within individual samples.

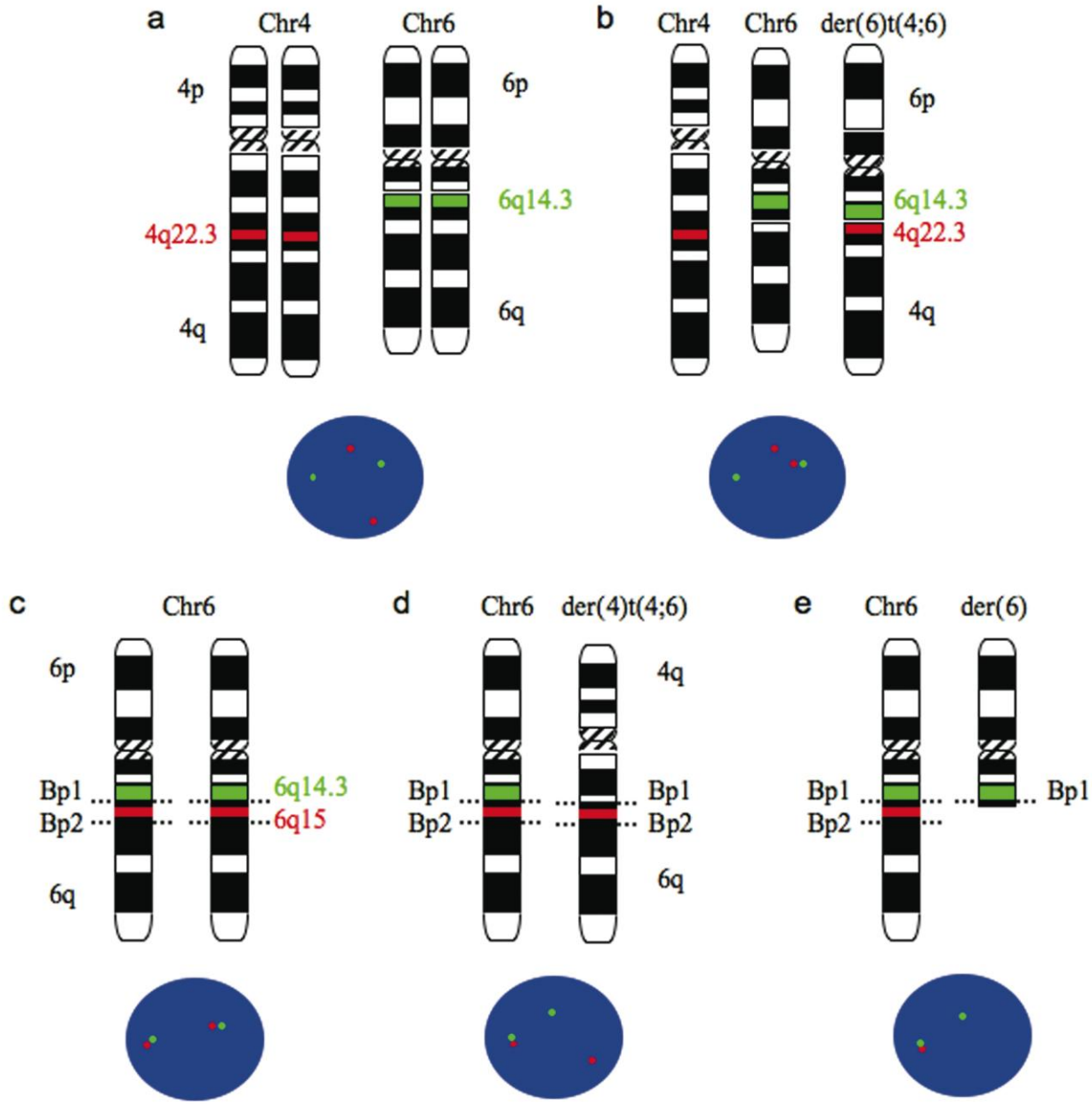
a
Chr4
Chr6
4p
6p
6q14.3
4q22.3
6q
4q
b
Chr4
Chr6
der(6)t(4;6)
6p
6q14.3
4q22.3
4q
c
Chr6
6p
Bp1
Bp2
6q14.3
6q15
6q
d
Chr6
der(4)t(4;6)
4q
Bp1
Bp2
Bp1
Bp2
6q
e
Chr6
der(6)
Bp1
Bp2
Bp1

Figure 3.2 Schematic representation of FISH detection of t(4;6)(q22;q15).

In the signal co-localisation study (a-b), probe set I and II were used and in the signal split apart analysis (c-e), probe set II and III were used. (a) In a normal cell, there are two pairs of normal chromosome 4 and 6 carrying hybridised red (probe set I) and green (probe set II) signals respectively. In an interphase nucleus, it shows two pairs of separated green and red signals. (b) In a cancer cell with t(4;6)(q22;q15), there are one of each normal chromosome 4 and 6 carrying hybridised red and green signals. The translocation brings probe set I on chromosome 4 and probe set II on chromosome 6 together. In an interphase nucleus, it shows one pair of separated red and green signals and one pair of co-localised red and green signals. (d) In a normal cell, one pair of chromosome 6 carry hybridised green (probe set II) and red (probe set III) signals. In an interphase nucleus, it shows two pairs of co-localised green and red signals. Bp1: centromeric breakpoint; bp2: telemetric breakpoint. (d) In a cancer cell with t(4;6)(q22;q15), one chromosome 6 carries hybridised green and red signals, but on the chromosome 6 with translocation, the signals are split apart. In an interphase nucleus, it shows one pair of co-localised green and red signals and another pair of separated red and green signals. (e) In the case of the telemeric part of 6q being lost or two breakpoints (bp1 and bp2) occurs due to the t(4;6) rearrangement, besides the normal chromosome 6 carrying hybridised red and green signals, only one green signal is left on the abnormal chromosome 6 fragment(s). In an interphase nucleus, it shows one pair of co-localised green and red signals and a single green signal.

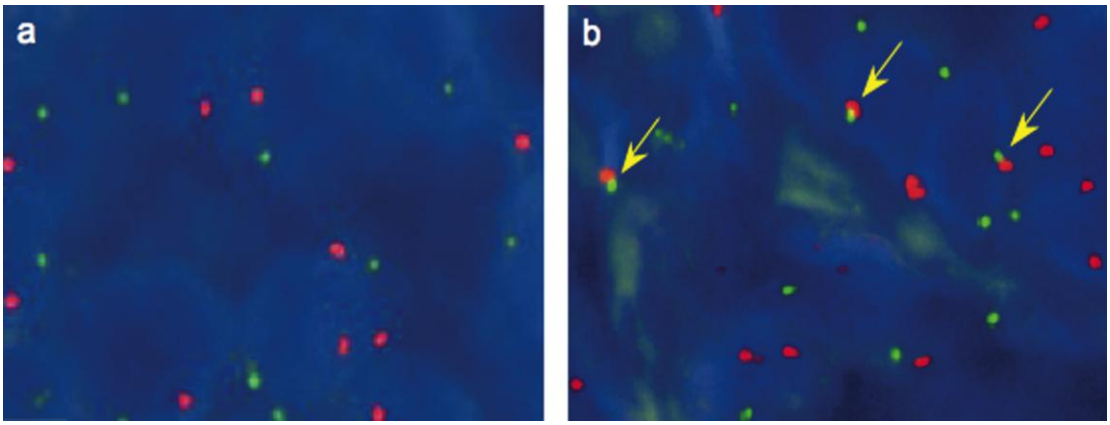

Figure 3.3 Examples of FISH signals using the probe co-localisation analysis as illustrated in Figure 3.2a and b.

(a) A co-localisation negative area in a normal control prostate sample where red signals were seen separated from the green signals. (b) In a prostate cancer sample, co-localisation of red (4q22 probes) and green (6q14.3 probes) signals (arrow) was found in many cells.

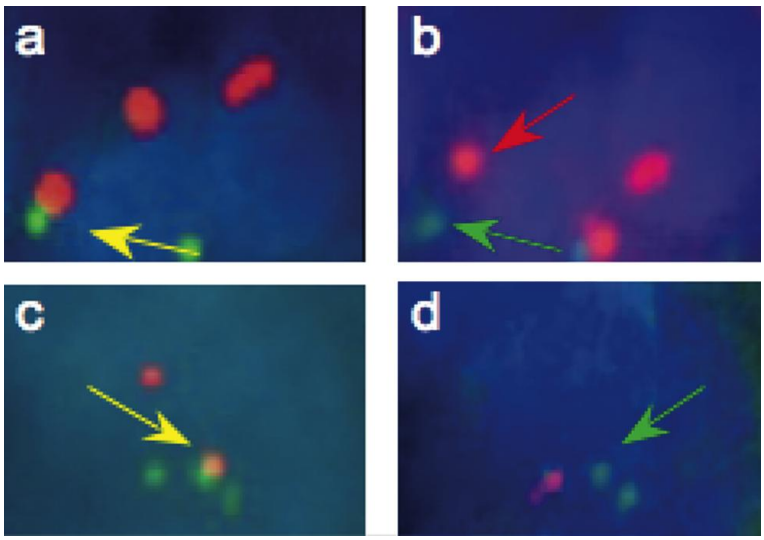

Figure 3.4 Confirmation of the t(4;6) positive cells using the split signal approach.

(a) and (c) The co-localised signals generated by probes on 4q22 (probe set I, red) and 6q14.3 (probe set II, green) are indicated by yellow arrows. (b) and (d) The nuclei from (a) and (b), respectively, were re-hybridised with probes on 6q14.3 (green) and 6q15 (probe set III, red). (b) The signals generated by probes on 6q14.3 and 6q15 showed split green and red signal (green and red arrows respectively), indicating translocation break point at 6q15 region as illustrated in **Figure 3.2d**. (d) A single green signal generated by the probe on 6q14.3 was detected (green arrow), whilst the red signal (probe on 6q15) was lost, indicating deletion at this region as illustrated in **Figure 3.2e**.

3.3.3 Clinical Significance of t(4;6)(q22;q15)

As the clinical and patient outcome data are available for the large cohort of surveillance-managed cancers, we studied the correlation between the t(4;6)(q22;q15) status and these clinical data. The univariate Cox model analysis showed that t(4;6)(q22;q15) was not a significant prognostic factor of either cause-specific survival (χ^2=1.01, p=0.30) or overall survival (χ^2=0.16, p=0.69) (**Figure 3.5a** and **b**). The translocation was not significantly associated with patient age using χ^2 test for trend (**Table 3.3**). However, it presented at a higher frequency in tumours with higher Gleason score, clinical stage, baseline PSA and larger tumour volume in the biopsy (p=0.04, 0.001, 0.01 and 0.001 respectively).

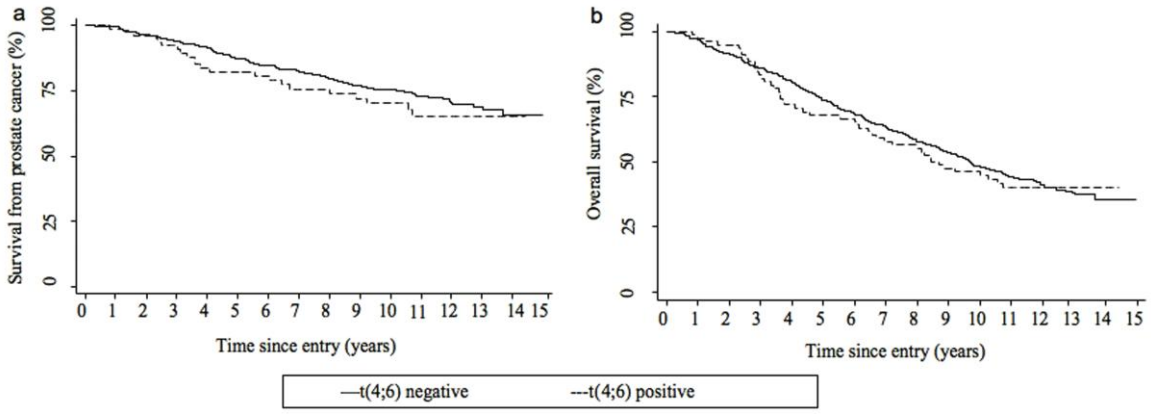

Figure 3.5 Kaplan-Meier analysis comparing prostate cancer patient outcomes with the t(4;6)(q22;q15) status.

(a) and (b) Cause-specific survival and overall survival respectively.

Table 3.3 Relationship of t(4;6)(q22;q15) (as a binary variable) with demographics and tumour characteristics using a 15% cut-off to define negative and positive cases

Variable	t(4;6) % of positive cells		p-value [a]
	<15% (n=589)	≥15% (n=78)	
Mean age ± SD (years)	69 ± 5	70 ± 5	0.93
Classes of age (years)			0.93
≤ 65	113 (90%)	13 (10%)	
> 65 - 70	159 (86%)	25 (14%)	
> 70 - 73	152 (89%)	19 (11%)	
> 73 - 76	165 (89%)	21 (11%)	
Gleason score [b]			0.04
<7	311 (91%)	29 (9%)	
=7	140 (83%)	28 (17%)	
>7	136 (87%)	21 (13%)	
Clinical stage [c]			0.001
T1	163 (93%)	12 (7%)	
T2	132 (90%)	15 (10%)	
T3	56 (78%)	16 (22%)	
Baseline PSA			0.01
≤ 10	221 (92%)	18 (8%)	
> 4 - 10	123 (88%)	17 (12%)	
> 10 - 25	112 (86%)	18 (14%)	
> 25 - 50	85 (84%)	16 (16%)	
> 50 - 100	48 (84%)	9 (16%)	
Cancer in biopsy (%) [d]			0.001
≤ 6	180 (93%)	14 (7%)	
> 6 - 20	143 (89%)	18 (11%)	
> 20 - 40	86 (91%)	8 (9%)	
> 40 - 75	70 (82%)	15 (18%)	
> 75 - 100	99 (81%)	23 (19%)	

[a] Test for trend in "≥15%" group (except for mean age).

[b] Restricted to patients for which Gleason score was available.

[c] Restricted to patients for which clinical T stage was available.

[d] Restricted to patients for which extent of disease was available.

Abbreviations: SD, standard deviation; PSA, prostate specific antigen.

3.3.4 Association of t(4;6)(q22;q15) with ERG gene rearrangements

Since the translocation status of *ERG* was already defined in this large cohort of prostate cancers (Attard *et al.*, 2008), we assessed whether there was an association between t(4;6)(q22;q15) and *ERG* gene rearrangements. In 510 cases of the cancer samples, both t(4;6)(q22;q15) and *ERG* gene rearrangement status were available. Although no correlation between t(4;6)(q22;q15) and *ERG* gene rearrangements was identified in these samples, t(4;6)(q22;q15) occurred more frequently in 2+Edel (two or more *ERG* deletion signals) positive, than negative, samples (26.5% vs. 14.5%) (**Table 3.4**).

Table 3.4 Relationship of t(4;6) with *ERG* status (n=510 patients)

	t(4;6) status	
ERG status	**Negative (n=442)**	**Positive (n=68)**
Normal	295 (67%)	40 (59%)
1Esplit	36 (8%)	7 (10%)
2+Esplit	17 (4%)	2 (3%)
1Edel	60 (14%)	10 (15%)
2+Edel	34 (8%)	9 (13%)

1Esplit: one *ERG* split signal; 2+Esplit: two or more *ERG* split signals; 1Edel: one *ERG* deletion signal; 2+Edel: two or more *ERG* deletion signals.

3.4 Discussion

Recent discovery of recurrent fusion genes in a range of carcinomas, (Choi *et al.*, 2008; Liu and Adams, 2007; Mitelman *et al.*, 2007; Soda *et al.*, 2007; Tognon *et al.*, 2002) including prostate cancer, (Maher *et al.*, 2009; Tomlins *et al.*, 2007; Tomlins *et al.*, 2005) suggests an important role for chromosomal rearrangements in solid tumours (Mitelman *et al.*, 2007). Here we have confirmed the frequent occurrence of a novel chromosomal translocation in human prostate cancer. Previously, we reported the t(4;6) translocation in prostate cancer cell lines and a small set of primary prostate tumours, without definition of the chromosome breakpoints in these samples, except in LNCaP cells (Lane *et al.*, 2007). Using BAC clones flanking the 4q22 and 6q15 translocation breakpoints defined in LNCaP cells, we have now confirmed a similar translocation occurs in a considerable proportion of primary prostate cancers.

In the current study, t(4;6)(q22;q15) translocation was not independently associated with prognostic potential, specifically not with poor patient outcome. However, it was significantly associated with tumours of high tumour volume and relatively late clinical T stage (p=0.001). The *TMPRSS2:ERG* fusion, previously linked to high clinical stage and more aggressive cancers (Mehra *et al.*, 2007b; Perner *et al.*, 2006; Wang *et al.*, 2006), is not generally associated with prostate cancer patient outcome, except the amplified fusion genes with deletion between *TMPRSS2* and *ERG* (Attard *et al.*, 2008; Gopalan *et al.*, 2009). In our previous analysis of factors affecting patient outcome in this cohort,

Gleason score was shown as the strongest predictor while the clinical T stage had little impact (Cuzick *et al.,* 2006). Therefore, t(4;6)(q22;q15) itself may affect cancer cell proliferation locally in the prostate, but not contribute much to tumour metastasis or other features associated with poor patient outcome. In this study, the correlation between *ERG* gene rearrangements and t(4;6)(q22;q15) was determined. It showed that t(4;6)(q22;q15) occurred more frequently in 2+Edel positive than negative prostate cancer samples. It has been shown that prostate cancers with 2+Edel are associated with a bad prognosis (Attard *et al.*, 2008). There might be a subtype of t(4;6) which is associated with 2+Edel positive and bad prognosis cancers.

The recurrent chromosomal rearrangements previously identified mainly lead to gains of function of genes located at the breakpoints (Mitelman *et al.*, 2007). However, the mechanism of action of the t(4;6)(q22;q15) translocation is less clear. In LNCaP cells, a small deletion adjacent to the translocation breakpoints occurred at both chromosomes 4 and 6 leading to four breakpoints instead of two (Lane *et al.*, 2007). *UNC5C* located at the distal breakpoint on 4q22 was the only known gene interrupted by these four breakpoints. No currently known genes were located at the other three breakpoints. In our group's previous study, we failed to identify *UNC5C* fusion transcripts by RT-PCR in LNCaP cells and no fusion transcripts involved in *UNC5C* or corresponding to this chromosomal rearrangement have been identified in this cell line by deep sequencing using the next generation sequencing technology (Maher *et al.*, 2009). Therefore, t(4;6)(q22;q15) might cause the inactivation of *UNC5C.* Down regulation of *UNC5C* occurs in various human tumours, including colorectal, breast, ovary,

uterus, stomach, lung, or kidney cancers. (Arakawa, 2004; Furuta *et al.*, 2006; Latil *et al.*, 2003; Thiebault *et al.*, 2003). Aberrant methylation of *UNC5C* has been detected frequently in advanced colorectal cancer and inactivation of *UNC5C* has been demonstrated to be associated with colorectal cancer progression (Hibi *et al.*, 2009) (Bernet *et al.*, 2007). 4q and 6q are among the most frequently deleted chromosome regions in human tumours and 6q15 deletion has been associated with a subtype of prostate cancer (Konishi *et al.*, 2003; Lapointe *et al.*, 2007; Liu *et al.*, 2007). The 6q15 chromosome region has been proposed to harbour candidate tumour suppressor genes in prostate cancer, such as the *MAP3K7* (Liu *et al.*, 2007). The subsequent effect of t(4;6)(q22;q15) may be a consequence of the inactivation of candidate tumour suppressor genes located either at the breakpoints or within the adjacent deleted regions. Inactivation of genes through chromosomal translocations has been reported previously (Belloni *et al.*, 2004; Berger *et al.*, 2006; Fernandez *et al.*, 2008; Karenko *et al.*, 2005; Mitelman *et al.*, 2007; Panagopoulos *et al.*, 2006; Popovici *et al.*, 2002). The high resolution provided by recently developed microarray technology allows detection of sub-microscopic deletions associated with cytogenetically balanced translocations (Mao *et al.*, 2007; Watson *et al.*, 2007). In a wide range of leukaemias, including CML, AML and ALL, these microdeletions coupled with chromosomal translocations are associated with poor prognosis (Kolomietz *et al.*, 2001). Therefore we hypothesise that the t(4;6)(q22;q15) may contribute to prostate cancer development through inactivation of tumour suppressor genes rather than gain of function by forming fusion genes.

A second possibility is that the translocation is a reflection of genomic instability. Genomic instability is an important mechanism in carcinogenesis (Cahill *et al.*, 1999; Mao *et al.*, 2008) and there is evidence that genomic instability, particularly chromosomal instability which occurs as early as at the precursor stage, is involved in prostate cancer development and progression (De Marzo *et al.*, 2003; Joshua *et al.*, 2008; Karan *et al.*, 2003). Prostate cancer frequently presents as multiple foci lesions and different genomic alterations, including multiple forms of *TMPRSS2:ETS* fusions, frequently occur in different foci within the same case of prostate cancer. This indicates that these multiple foci arise independently (Attard *et al.*, 2009a; Clark *et al.*, 2008; Joshua *et al.*, 2008; Mehra *et al.*, 2007a). This independent generation of multiple foci within the same prostate, together with the identification of genetic alterations in the normal prostate epithelial cells adjacent to cancer lesions, suggests that there is an underlying mechanism leading to genomic instability in the prostate cells (Joshua *et al.*, 2008). This genomic instability may induce multiple genomic alterations and chromosomal rearrangements, among them the t(4;6) translocation. This genomic instability induced t(4;6) translocation may explain why the t(4;6)(q22;q15) was identified in only a proportion of cancer cells in each specimen. The occurrence of genetic alterations in a proportion of cancer cells has been observed previously in prostate cancer, including the commonly deleted *PTEN* genes (Attard *et al.*, 2009b; Klein *et al.*, 2002). Heterogeneity of *PTEN* deletions has also been observed in our FISH analysis of prostate cancer samples from prostatectomy (unpublished data). While the t(4;6) translocation may represent genomic instability in the translocation positive samples, the frequent detection of t(4;6)(q22;q15) may also indicate that 6q15 and 4q22 are

unstable genomic regions in prostate cancer cells, which correlates with the frequent genomic copy number changes of these regions as discussed above. Further investigations are now required to understand the biological mechanism of the t(4;6)(q22;15) translocation.

In summary, t(4;6)(q22;q15) is a frequent chromosomal translocation in prostate cancer, which has now been confirmed in a large series of prostate cancer clinical samples. While it does not affect patient outcome independently, it does not occur in non-malignant prostatic epithelium and hence it may define the development of a specific cohort of prostate cancers. The consequence of this genomic alteration and affected genes should be studied further. In **Chapter 4**, the potential tumour suppressor genes in 6q15 deletion region associated with the t(4;6)(q22;q15) are investigated.

4 6q15 DELETION AND GENE EXPRESSION ALTERATIONS IN PROSTATE CANCER

4.1 Introduction

As illustrated in the previous chapter, we identified a recurrent translocation, t(4;6)(q22;q15), in prostate cancer. We hypothesised that this translocation may contribute to prostate cancer development through inactivation of tumour suppressor gene(s). The first supporting evidence for this hypothesis is that the putative tumour suppressor gene *UNC5C* was identified to be disrupted by the distal breakpoint of the translocation on 4q22 in LNCaP cells. At the genomic level, *UNC5C* lost its promoter and the first exon caused by the t(4;6)(q22;q15) fusion as well as the micro-deletion on 4q22; at the transcriptional level, the expression of *UNC5C* could not be detected using RT-PCR analysis, indicating that *UNC5C* might have lost its expression due to the disruption of the genomic DNA.

The second line of evidence is as described earlier: the micro-deletion on 4q22 and 6q15 is another characteristic of t(4;6) in LNCaP cells. 6q15 is one of the most frequently deleted regions reported in prostate cancer (Cooney *et al.*, 1996; Konishi *et al.*, 2003; Liu *et al.*, 2007). Our SNP array data are consistent with this identification showing that 6q15 was deleted in 53% (35 in 66) of prostate cancer patients (unpublished data). It is believed that there are one or more tumour suppressor gene(s) in 6q15. Liu et al. reported that loss of *MAP3K7* gene in 6q15 was associated with high-grade prostate cancer (Liu *et al.*, 2007).

MAP3K7 encodes Tak1, a mitogen activated protein kinase kinase kinase family member. *MAP3K7* is the first gene distal to the telomeric breakpoint of t(4;6)(q22;q15) in the LNCaP cell line. Whilst there is evidence to suggest that the *MAP3K7* gene is involved in augmenting transforming growth factor β (TGF-β)-induced apoptosis in prostate cancer cells (Edlund *et al.*, 2003), it has yet to be determined if *MAP3K7* plays a role in prostate cancer pathogenesis. Other putative genes have been identified within the 6q15 deletion region, including *CX62*, *MDN1*, caspase 8 associated protein A2 (*CASP8A2*) and BTB and CNC homology 1, basic leucine zipper transcription factor 2 (*BACH2*) (Liu *et al.*, 2007). *CASP8A2* is involved in CD95-induced apoptosis via caspase 8 activation. Therefore, deletion of this gene would be detrimental in terms of the cells' ability to undergo apoptosis. One study has shown that *CASP8A2* is frequently mutated in mismatch repair-deficient colorectal cancer cell lines (Park *et al.*, 2002). *BACH2* is a B-cell specific transcription factor, which has been implicated as a putative tumour suppressor gene. There have been several reports demonstrating high frequency of LOH in human B-cell lymphomas (Sasaki *et al.*, 2000; Vieira *et al.*, 2001). Over-expression of *BACH2* in the Raji cell line (which does not express endogenous *BACH2*) results in enhanced apoptosis upon exposure to cytotoxic drugs, which are oxidative stressors, such as etoposide, doxorubicin and cytarabine (Kamio *et al.*, 2003). Although these genes are considered as putative target genes in the 6q15 deletion region, no detailed analysis of these genes has been made relating to prostate cancer.

Minimisation of the commonly deleted region on 6q may facilitate the identification of the putative tumour suppressor genes. According to our group's

previous SNP array data (unpublished), the minimum overlapping deleted region was on 6q15, detected in 33 out of 71 clinical prostate cancer samples within 87.21-90.35 Mbp. 34 out of 71 cancer samples were detected covering 90.88-91.35 Mbp, which was overlapped with the deleted region in LNCaP cells (88.55-91.7 Mbp).

In this study, I examined the frequency of 6q15 deletion in primary prostate cancer samples using FISH analysis and investigated the potential tumour suppressor genes, for which the RNA expression was down-regulated. Expression microarray is one of the ideal approaches to examine the expression alterations of all the genes located at 6q15 systematically in prostate cancer. The application of the high resolution, high throughput Exon Array has facilitated the systematic interrogation of genome-wide differentially expressed genes as well as alternative splicing variants in various types of cancer (Gardina *et al.*, 2006; Moller-Levet *et al.*, 2009; Thorsen *et al.*, 2008). In this study, Exon Array was applied to investigate the commonly down-regulated genes located at 6q15 in six prostate cancer cell lines and one clinical prostate cancer sample.

4.2 Aim

The aim of this study was to determine the frequency of 6q15 deletion in primary prostate cancer samples and identify commonly down-regulated genes caused by 6q15 deletion in prostate cancer. At the same time, I aimed to reveal differentially expressed genes and cancer specific alternative splicing in prostate cancer using this Exon Array data.

4.3 Results

4.3.1 Frequency of 6q15 deletion in primary prostate cancer samples

In order to examine the frequency of 6q15 deletion in primary prostate cancer samples, FISH analysis was applied with a probe set (**Table 4.1**) spanning the region between 90.82-91.25 Mbp.

Table 4.1 Probe set for 6q15 deletion detection

Location	BAC clone	Region	Length (bps)	Labelled	Signal colour
6q15	RP1-44N23	90,814,536-90,843,275	28,740	DIG	Green
	RP1-154G14	91,251,386-91,352,280	100,895		

A commercially available centromere probe for chromosome 6 (labelled as red) was used as a control. FISH analysis was performed on two TMAs containing 68 prostate cancer samples and six morphologically non-malignant prostate samples. According to the criteria described in **2.3.2.4**, 28 prostate cancer samples and four non-malignant control samples were considered informative. Among the four control samples, one sample showed 6.25% more red signal than green, while the other three showed 4.5%, 0% and 0% respectively (**Table 4.2**). Based on this ratio and consideration of the hybridisation efficiency and possibility of artificial truncation of the cells during the slide-cutting process, a higher cut-off of 20% was set for detection of the 6q15 deletion. That is, TMA cores with more than 20% more red than green signals in all counted cells (≥ 50 cells) were considered deletion-positive. Thirteen of 28 (out of 68) prostate cancer samples (46%) were assessed as 6q15-deletion positive. The Gleason

score of the 28 informative samples was distributed as follows: 16 of them were between 2-6 and 37.5% (6 of 16 cases) were deletion positive; seven had a Gleason score of 7 with 57.1% (4 of 7 tumours) were deletion-positive; three of them were between 8-10 with 75% (3 of 4 tumours) deletion-positive. This suggests that 6q15 deletion may associate with high-grade disease but, since there was only a small number of patient samples, chi-square test showed no statistical significance ($P > 0.05$).

Table 4.2 Frequency of 6q15 deletion using prostate cancer TMAs

Case No.	6q15 Negative/ Positive	Core No.	Red Signal	Green Signal	Gleason Score
PC1	N	A	208	184	3+2
PC2	N	A	67	63	5+4
PC3	N	A	97	99	4+3
PC4	P	A	120	75	3+4
PC6	P	A	50	29	3+4
PC7	N	A	62	65	3+3
PC8	P	A	76	29	4+5
PC9	N	A	80	75	3+3
PC10	P	A	75	39	4+4
PC11	N	A	154	124	2+2
PC12	N	A	86	88	1+2
PC13	N	A	69	70	1+2
PC14	N	A	87	76	3+4
		A	36	34	
PC16	N	B	82	81	3+3
		A	65	64	
PC17	N	B	54	50	3+3
		A	137	125	
PC18	N	B	38	27	3+3
		A	104	69	
PC19	P	B	148	91	3+3
		A	24	13	
PC20	P	**B**	**102**	**51**	3+3
		A	**177**	**110**	
PC21	P	B	58	47	2+2
		A	41	34	
		B	**71**	**44**	
		B	15	11	
PC22	P	B	8	2	3+4
		A	52	49	
		B	13	9	
PC25	N	B	21	9	-
		A	199	205	
		B	142	138	
PC27	N	C	105	107	3+4
		A	**110**	**63**	
		B	**254**	**140**	
PC28	P	C	115	97	3+4
		A	**140**	**68**	
		B	37	34	
PC29	P	C	59	56	4+4
		A	9	7	
		B	60	55	
PC30	N	C	4	4	2+3
		A	**122**	**89**	
		B	26	15	
PC31	P	**C**	**51**	**29**	3+2
		A	6	3	
		B	**92**	**47**	
PC32	P	C	95	39	2+2
		A	**305**	**188**	
		B	155	147	
		C	138	125	
PC33	P	D	24	17	3+3
N1		A	47	50	
N2		A	75	78	
		A	140	134	
N3		B	141	144	
N4		A	85	80	

PC- prostate cancer; N- normal prostate;

4.3.2 Expression of *UNC5C* and 6q15 deletion associated genes in prostate cancer

As micro-deletion in 6q15 was confirmed in 46% of prostate cancer samples using FISH analysis, the genes down-regulated in the deletion region were investigated using Exon Array analysis. Affymetrix Exon 1.0 ST Array analysis was applied to six prostate cancer cell lines (LNCaP, PC3, 22RV1, DU145, VCaP and MDA PCa 2b), one clinical prostate cancer sample (p127) and two BPH samples (p143 and p2) as a control.

4.3.2.1 Down-regulated genes in the 6q15 region

Within the 4.14 Mbps region (87.21-91.35 Mbps), there are 29 protein-coding genes, 12 pseudo-genes and one non-protein coding RNA according to the NCBI database (Human genome, build 36.3) (**Table 4.3**). No known ESTs or microRNAs have been identified in this region. IGB software was used to visualise the expression variations of individual genes in all the tested samples. Three genes, cannabinoid receptor 1 (*CNR1*), proline-rich nuclear receptor coactivator 1 *(PNRC1)* and gap junction protein, alpha 10 (*CX62),* were found to be down-regulated in prostate cancer cell lines and the clinical prostate cancer sample compared to the two BPH controls (**Figure 4.1**, **Figure 4.2** and **Figure 4.3**). Partek software was also used to examine all genes within 88.8-92.9 Mbp. Apart from the three genes *CNR1*, *PNRC1* and *CX62*, the gene *BACH2* was also commonly down-regulated in prostate cancer cells and the cancer sample compared to the BPH controls.

Table 4.3 Genes located within 87.21- 91.35 Mbps in 6q15

Gene Symbol	Gene type	Region (bps)	Description
LOC643971	Pseudo	87680152-87680976	Similar to 60S ribosomal protein L7
HTR1E	Protein coding	87647024-87726397	5-hydroxytryptamine (serotonin) receptor 1E
CGA	Protein coding	87795333-87804824	Glycoprotein hormones, alpha polypeptide
LOC442234	Pseudo	87831411-87832406	Similar to Reticulocalbin-1 precursor
ZNF292	Protein coding	87865269-87973406	Zinc finger protein 292
LOC644016	Pseudo	88008490-88010180	Similar to heat shock protein 1 (chaperonin)
GJB7	Protein coding	87992697-88038996	Gap junction protein, beta 7, 25kDa
C6orf162	Protein coding	88032306-88052043	Chromosome 6 open reading frame 162
C6orf163	Protein coding	87992697-88174183	Chromosome 6 open reading frame 163
TAF13P	Pseudo	88057220-88299735	TAF13 RNA polymerase II, TATA box binding protein (TBP)-associated factor, pseudogene
C6orf165	Protein coding	88117721-88174183	Chromosome 6 open reading frame 165
SLC35A1	Protein coding	88182643-88222057	Solute carrier family 35 (CMP-sialic acid transporter), member A1
RARS2	Protein coding	88224096-88299735	Arginyl-tRNA synthetase 2, mitochondrial
ORC3L	Protein coding	88299843-88377169	Origin recognition complex, subunit 3-like (yeast)
AKIRIN2	Protein coding	88384578-88411985	Akirin 2
NCRNA00120	MiscRNA	88410020-88410933	Non-protein coding RNA 120
SPACA1	Protein coding	88,814,226-88,833,269	Sperm acrosome associated 1
CNR1	Protein coding	88,906,302-88,932,385	Cannabinoid receptor 1 (brain)
ACTBP8	Pseudo	89,043,958-89,769,338	Actin, beta pseudogene 8
LOC100130179	Pseudo	89,435,019-89,437,344	Similar to env protein
RNGTT RNA	Protein coding	89,730,067-89,376,708	Guanylyltransferase and 5'-phosphatase
CYCSP16	Pseudo	89,769,338-89,769,168	Cytochrome c, somatic pseudogene 16
LOC100131124	Pseudo	89,826,066-89,826,773	Similar to adaptor-related protein complex 4, sigma 1 subunit
PNRC1	Protein coding	89,487,216-89,851,598	Proline-rich nuclear receptor coactivator 1
SRrp35	Protein coding	89,884,519-89,862397	Serine-arginine repressor protein
PM20D2	Protein coding	89,912,488-89,932,003	Peptidase M20 domain containing 2
GABRR1	Protein coding	89,983,779-89,944,691	Gamma-aminobutyric acid (GABA) receptor, rho 1
GABRR2	Protein coding	90,081,686-90,023,958	Gamma-aminobutyric acid (GABA) receptor, rho 2

UBE2J1	Protein coding	90,119,338-90,093,063	Ubiquitin-conjugating enzyme E2, J1
RRAGD	Protein coding	90,178,497-90,134,313	Ras-related GTP binding D
LOC100128021	Pseudo	90,239,358-90,188,537	Similar to mCG17022
ANKRD6	Protein coding	90,199,616-90,400,124	Ankyrin repeat domain 6
LYRM2	Protein coding	90,405,195-90,398,664	LYR motif containing 2
MDN1	Protein coding	90,586,163-90,409,952	Midasin homolog (yeast)
LOC100132736	Pseudo	90,581,116-90,581,903	Similar to family with sequence similarity 64, member A
CASP8AP2	Protein coding	90,596,379-90,640,876	Caspase 8 associated protein 2
LOC644269	Pseudo	90,652,055-90,654,295	Hypothetical LOC644269
CX62	Protein coding	90,660,909-90,662,540	Gap junction protein, alpha 10
LOC100129711	Protein coding	90,716,538-90,718,429	Similar to mCG1050952
BACH2	Protein coding	91,063,182-90,692,969	BTB and CNC homology 1, basic leucine zipper transcription factor 2
MAP3K7	Protein coding	91,353,628-91,282,074	Mitogen-activated protein kinase kinase kinase 7
LOC100129847	Pseudo	92,582,852-92,582,279	Hypothetical LOC100129847

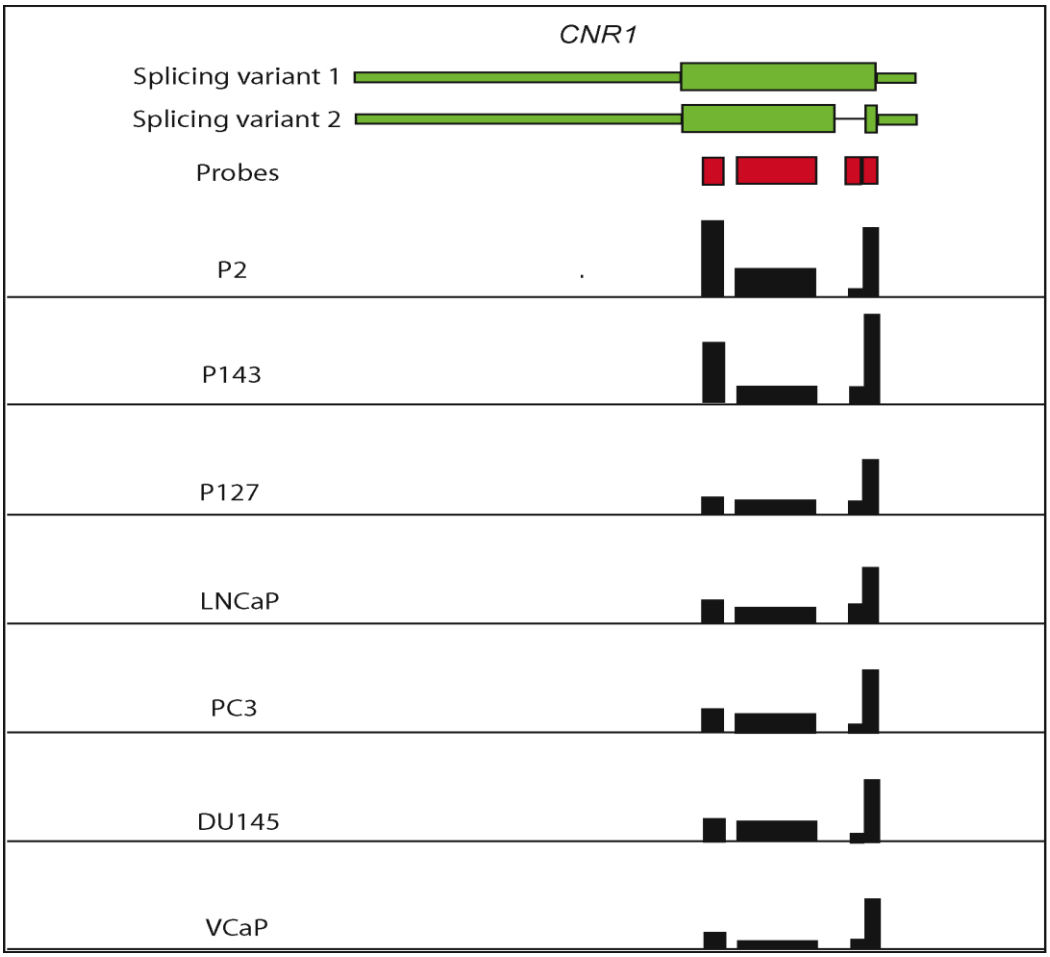

Figure 4.1 Graphical representation of comparison of the *CNR1* expression levels in different samples viewed with IGB

Green bars represent two transcript isoforms of *CNR1*. The narrow part of the green bars indicates untranslated region (UTR) with the wider part indicating exon(s). The red bars represent the probe sets that detect the expression of the corresponding region of the gene *CNR1*. Seven samples including four prostate cancer cell lines (DU145, LNCaP, PC3, VCaP) and one primary prostate cancer sample (P127), plus two control BPH samples (P143 and P2) are shown in this figure. The height of the black bars indicates the expression level detected by the corresponding probes. The average expression level of each sample detected by four probe sets is compared visually with the average level of two controls. The average expression levels of all the prostate cancer cell lines and the cancer sample are lower compared to the controls. The lowest expression was found in PC3 and LNCaP cells.

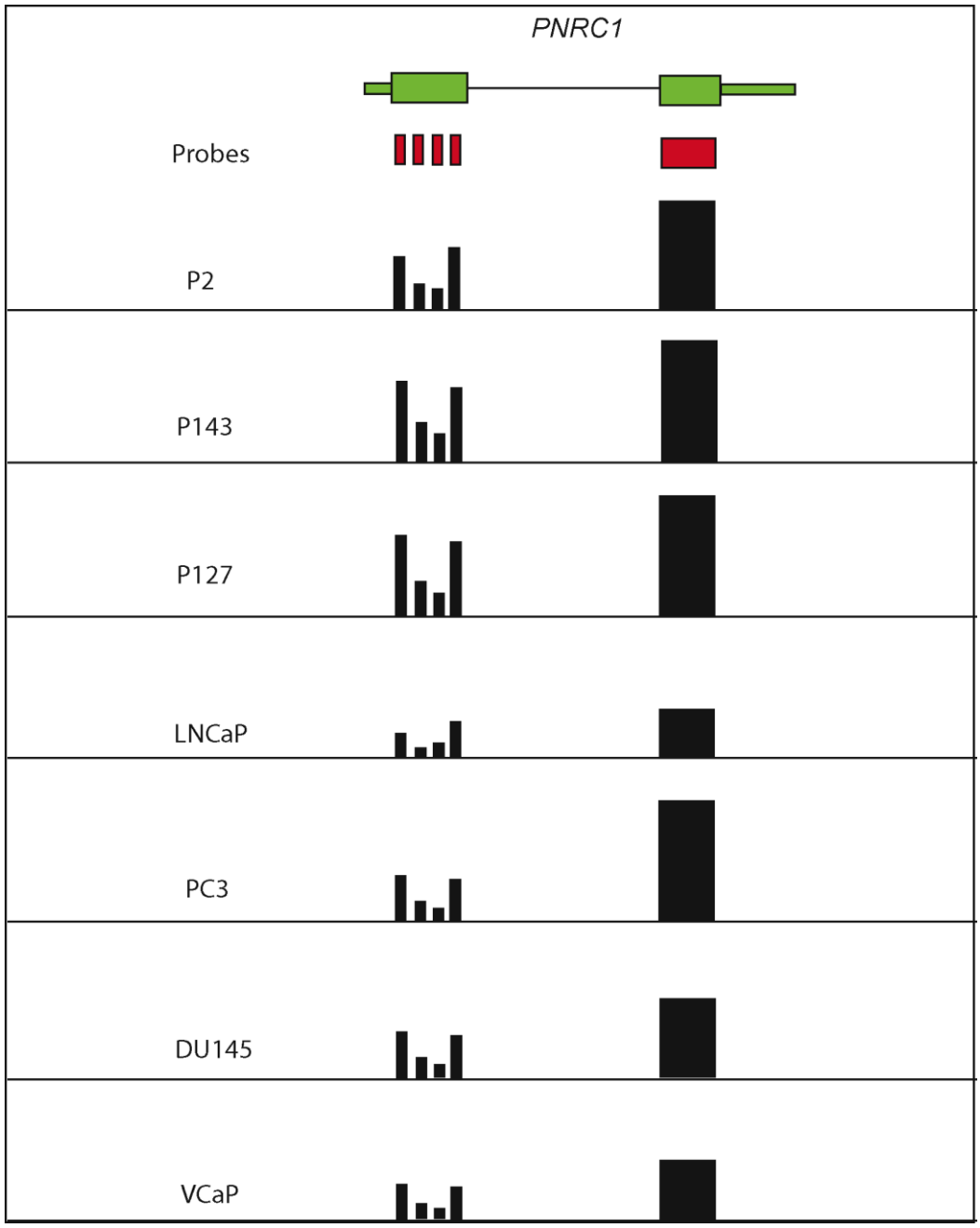

Figure 4.2 Graphical representation of comparison of the *PNRC1* expression levels in different samples viewed with IGB

PNRC1 has only one transcript isoform. The detailed illustration of the common features of the figures is described in the legend of **Figure 4.1**. The average expression levels of all the prostate cancer cell lines and the cancer sample detected by five probe sets are lower compared to the average level of the two controls. The lowest expression is shown in LNCaP cells.

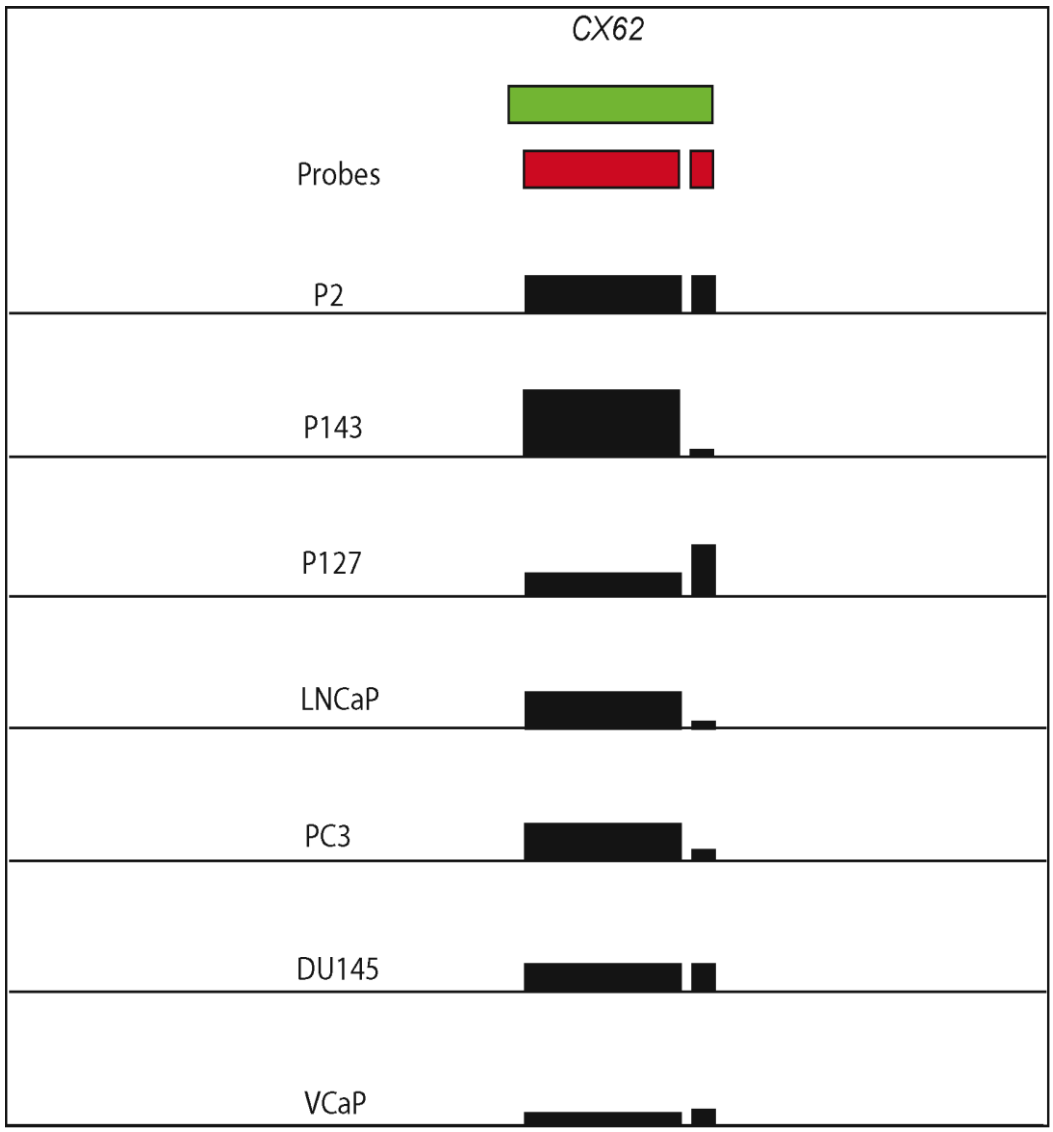

Figure 4.3 Graphical representation of comparison of the *CX62* (*GJA10*) expression levels in different samples viewed with IGB

CX62 has one transcript isoform with one exon. The detailed illustration of the common feature of the figures is described in the legend of **Figure 4.1**. The average expression levels of all the prostate cancer cell lines and the cancer sample detected by two probes are lower compared to the average level of the two controls. The lowest expression is in VCaP cells.

4.3.2.2 Down-regulation of *UNC5C*

As the Exon Array data were available, the expression of the gene *UNC5C* was examined using IGB. It showed that *UNC5C* was down-regulated in the clinical prostate cancer sample and all the cell lines.

4.3.2.3 qRT-PCR validation of down-regulated genes

qRT-PCR analysis was applied to validate the down-regulation of the four genes, located in the 6q15 region (*CNR1, PNRC1, CX62* and *BACH2*), and the gene *UNC5C*, using the pre-designed TaqMan® gene expression probes detailed in **2.6.6.2**.

The housekeeping gene *GAPDH* was used as control for gene validation by qRT-PCR. RNA extracted from the BPH samples, p129, was used as an internal calibrator to obtain comparative results (Custom TaqMan® gene expression assay protocol at http://www.appliedbiosystems.com).

Relative expression of four genes (*CNR1, PNRC1, BACH2* and *UNC5C*) was measured by qRT-PCR from one BPH sample (p143) and the six prostate cancer cell lines plus one clinical prostate cancer sample (p127) used for the Exon Array study. Relative expression of these four genes measured by qRT-PCR was consistent with the Exon Array data, showing down-regulation in all prostate cancer cell lines and the clinical sample (p127) compared to the BPH sample (p143) (**Figure 4.4, Figure 4.5, Figure 4.6** and **Figure 4.7**)

As the amount of cDNA from the BPH sample p143 was insufficient, the relative expression of *CX62* was measured in another BPH sample, p125, instead. The qRT-PCR result showed that the expression level of *CX62* was too low to be detected in all the examined samples including the six prostate cancer cell lines, the clinical prostate cancer sample (p127) and the BPH sample p125 (**Figure 4.8**). Because the different BPH sample was applied to correlate the Exon Array data and relative expression of the gene *CX62*, it is difficult to draw a conclusion as to on whether the qRT-PCR result correlated with the Exon Array data or not.

Additional control samples, including five BPH samples (p125, p6, p112, p37, p61) and two primary prostate cancer samples (p105 and p98), were applied to further examine the expression alterations of the five genes in clinical samples. With the additional samples, *CNR1* and *BACH2* still showed common down-regulation in prostate cancer samples. The average expression level of *UNC5C* in the three prostate cancer samples was lower than the average level in seven BPH samples (**Figure 4.7**), but there was only a small number of patient samples, one-tailed Student's t-test showed no statistically significant difference (p=0.0509). In contrast, *PNRC1* and *CX62* did not show common down-regulation in prostate cancer samples. The expression of *PNRC1* in prostate cancer sample p127 was higher than the additional five BPH samples (**Figure 4.5**). The expression level of *CX62* was still too low to be detected in all the additional BPH samples (**Figure 4.8**).

The expression levels of *CNR1* and *BACH2* were further examined in more clinical samples. Thirteen prostate cancer and 24 BPH samples were macro-

dissected to obtain relatively pure cancer and benign prostate tissue respectively as described in **2.6.1.2**. qRT-PCR analysis was then applied to examine the relative expression of *CNR1* and *BACH2* in these samples. In total, 28 BPH samples and 16 clinical prostate cancer samples were applied to examine *CNR1* expression. It showed that the expression of *CNR1* was significantly down regulated in 16 prostate cancer samples compared to the 28 BPH samples (p=0.0201) (**Figure 4.4**). As for studies with the gene *BACH2*, its expression was measured in 19 BPH samples and 14 clinical prostate cancer samples. It showed that the expression of *BACH2* was significantly down regulated in the 14 prostate cancer samples compared to the 19 BPH samples (p=0.0156) (**Figure 4.6**).

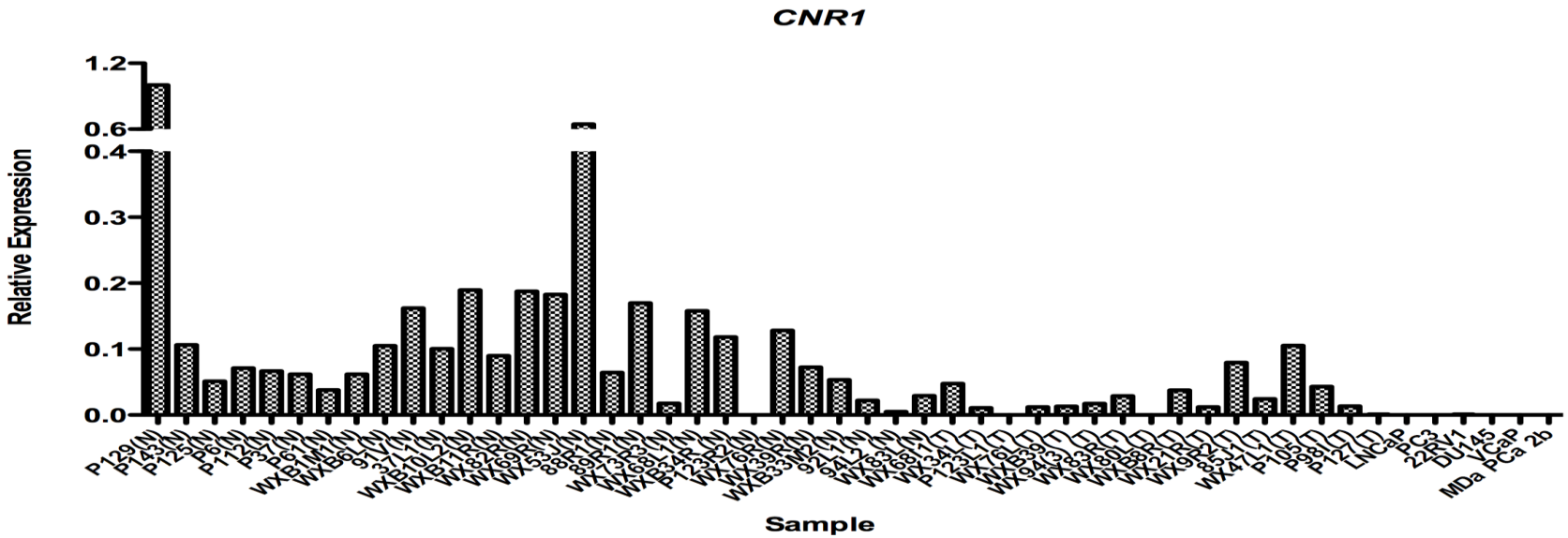

Figure 4.4 Relative expression of *CNR1* in fresh frozen clinical tissue samples and prostate cancer cell lines as measured by qRT-PCR.

The expression of the gene *CNR1* was measured by qRT-PCR relative to the expression of the housekeeping gene *GAPDH* and normalised to the p129 as a positive control. N stands for normal BPH sample and T stands for tumour sample.

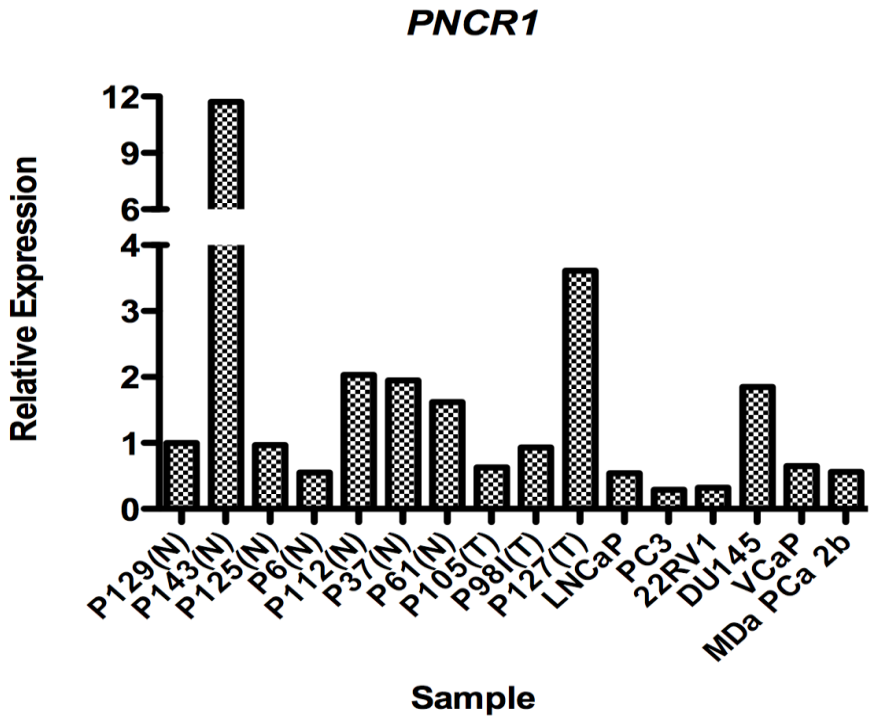

Figure 4.5 Relative expression of *PNRC1* in fresh frozen tissue samples and prostate cancer cell lines as measured by qRT-PCR.

The expression of *PNRC1* was measured by qRT-PCR relative to the expression of the housekeeping gene *GAPDH* and normalised to the BPH sample p129 as a positive control. N stands for normal BPH sample and T stands for tumour sample.

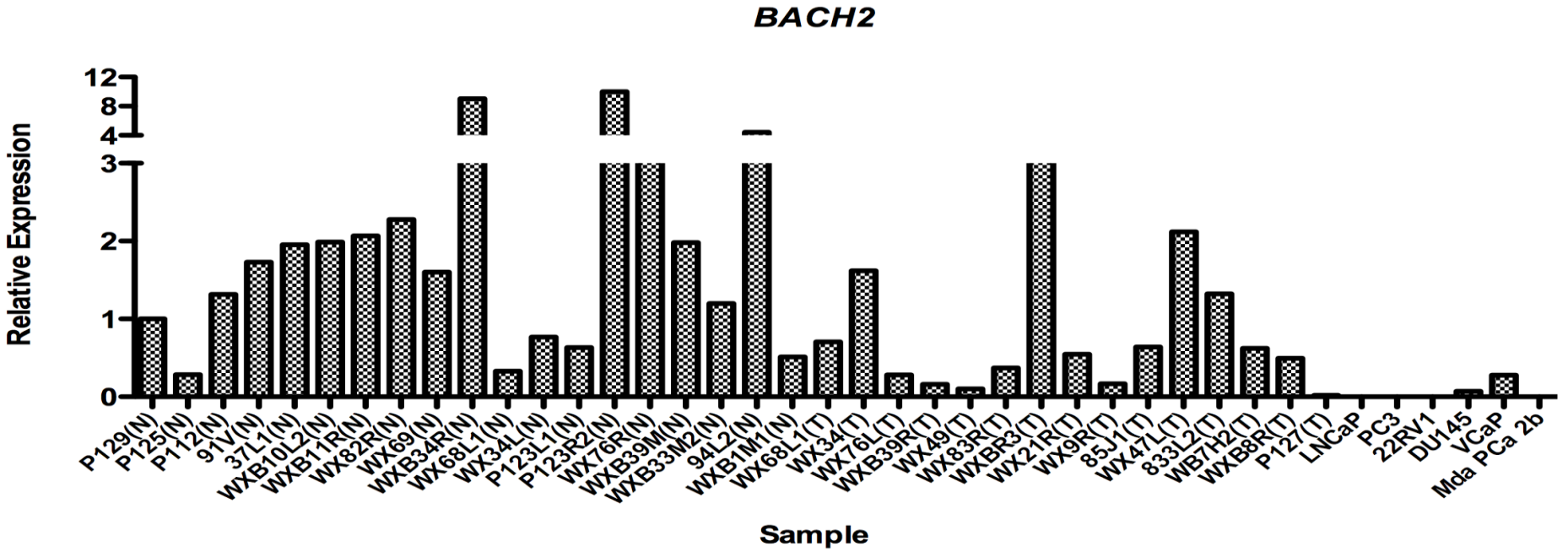

Figure 4.6 Relative expression of *BACH2* in fresh frozen clinical tissue samples and prostate cancer cell lines as measured by qRT-PCR.
The expression of the gene *BACH2* was measured by qRT-PCR relative to the expression of the housekeeping gene *GAPDH* and normalised to the p129 as a positive control. N stands for normal BPH sample and T for tumour sample.

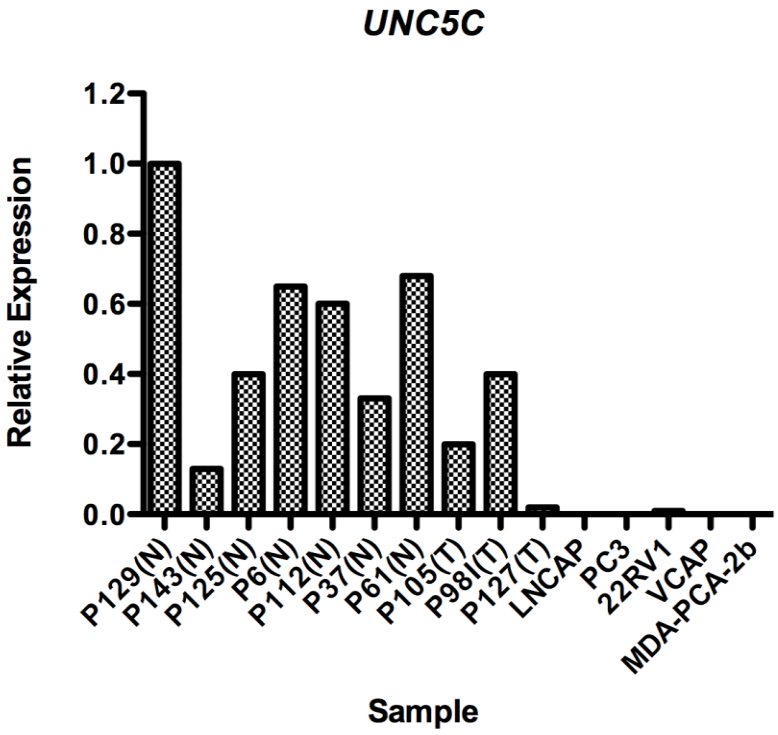

Figure 4.7 Relative expression of *UNC5C* in fresh frozen tissue samples and prostate cancer cell lines as measured by qRT-PCR.

The expression of *UNC5C* was measured by qRT-PCR relative to the expression of the housekeeping gene *GAPDH* and normalised to the BPH sample p129 as a positive control. N stands for normal BPH sample and T stands for tumour sample.

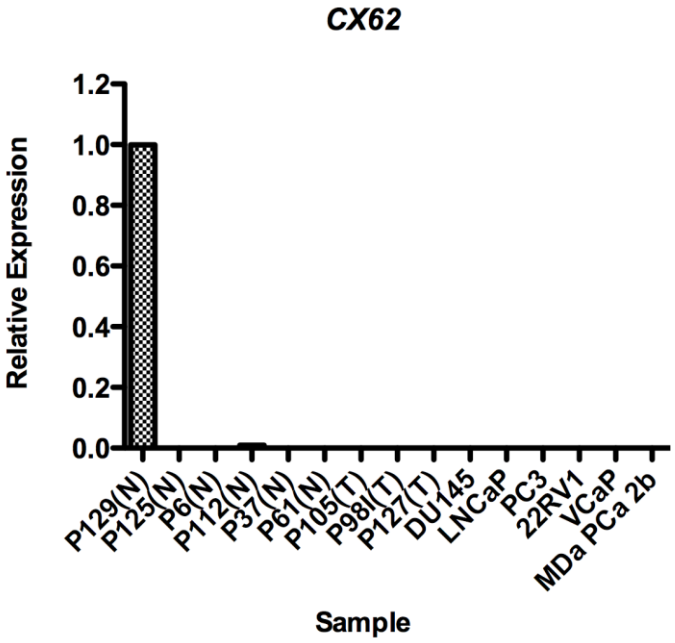

Figure 4.8 Relative expression of *CX62* in fresh frozen tissue samples and prostate cancer cell lines as measured by qRT-PCR.

The expression of *CX62* was measured by qRT-PCR relative to the expression of the housekeeping gene *GAPDH* and normalised to the BPH sample p129 as a positive control. N stands for normal BPH sample and T stands for tumour sample.

4.3.3 qRT-PCR validation of other genes in prostate cancer

As the Exon Array data were available, it was possible to investigate the genes with abnormally spliced/truncated mRNA forms or showing consistent over-/under-expression.

As mentioned earlier, our group has been dedicated to identifing chromosomal translocations and fusion genes ever since it was established. Exon Array data can be applied to identify potential fusion genes. Using bioinformatic analysis as described in **2.6.3.1**, two genes: 5 alpha-reductase type 2 gene (*SRD5A2*, 2p23) and keratin 23 (*KRT23*, 17q21.2), were shown to have a truncated expression pattern in all the prostate cancer cell lines and the clinical cancer samples as compared to BPH controls. As shown in **Figure 4.9**, the expression intensity of the first exon of the gene *SRD5A2*, which was detected by four probe sets (2547250, 2547249, 2547248 and 2547247), is similar in all prostate cancer cell lines and two BPH samples. Conversely the expression intensity of the remaining four exons, which were detected by probe set 2547241 for exon 2, 2547240 for exon 3, 2547238 and 2547237 for exon 4, 2547236 and 2547235 for exon 5, were shown to be lower in all prostate cancer cell lines as compared to the BPH controls. The expression pattern of *KRT23* (**Figure 4.10**) was similar to *SRD5A2*. The expression intensity of exon 1 of *KRT23*, which was detected by three probe sets (3756612, 3756611 and 3756610), was similar in all prostate cancer samples and two BPH control samples. However the expression intensity of the other eight exons, which were detected by probe sets 3756610 and 3756609 for exon 2, 3756605 for exon 3, 3756604 for exon 4, 3756603 for exon 5, 3756602 for exon 6, 3756597 for exon 7, 3756596 for exon 8, 3756594, 3756593 and 3756592 for

exon 9, was lower in cancer samples as compared to the BPH controls. This expression pattern could be caused by genomic alterations, such as translocation, deletion, inversion, in which the breakpoint could disrupt *SRD5A2* and *KRT23* and lead to the truncated expression pattern of these two genes.

qRT-PCR analysis was performed to validate the expression of different exons in these two genes. For each gene, three different TaqMan® gene expression probes (described in **2.6.6**) were used to investigate the expression of different exons. For *SRD5A2* the expression levels of exon 1, exons 2-3 and exons 4-5 were compared. For *KRT23* the expression levels of exon 1-2, exons 3-4 and exons 8-9 were evaluated. Results showed that the overall expression of the gene *SRD5A2* was down-regulated dramatically in all prostate cancer cell lines, although there was an indication of differential expression between different exons (**Figure 4.11**). Similar to *SRD5A2*, the expression of *KRT23*, as examined by three different probes, was not detected with 40 cycles of qRT-PCR reaction in all prostate cancer cell lines (**Figure 4.12**). This demonstrated that down-regulation of *SRD5A2* and *KRT23* were the dominant events in gene expression alterations in prostate cancer cell lines. In order to examine the expression of these two genes in clinical samples, five BPH samples (p125, p6, p112, p37, p61) and three primary prostate cancer samples (p105, p98 and p127) were used to examine the expression of *SRD5A2* using qRT-PCR analysis. Using a TaqMan® probe binding to the exon 2-3 boundary, the expression of *SRD5A2* was shown to be down-regulated in prostate cancer samples as compared to BPH controls (**Figure 4.13**). Using a TaqMan® probe binding to the exon 3-4 boundary, the expression of *KRT23* was examined in five BPH samples (p125, p6, p112, p37, p61) and

two primary prostate cancer samples (p105 and p127). It showed that the expression of *KRT23* was down-regulated in prostate cancer samples as compared to BPH controls (**Figure 4.14**).

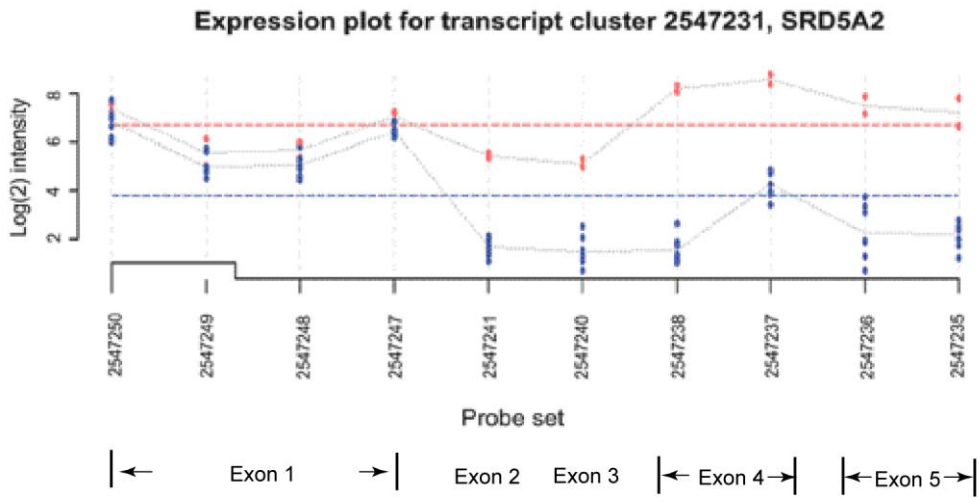

Figure 4.9 Expression plot of the gene *SRD5A2* as detected by a series of probe sets.

The expression intensities of five exons detected by ten probe sets, showed differential expression between prostate cancer cell lines and BPH controls in exon 2-5 but not exon 1. Red dots represent two BPH control samples and blue dots represent six prostate cancer cell lines and the clinical prostate cancer sample. The red and blue lines indicate the average expression intensity of the BPH samples and cancer samples respectively.

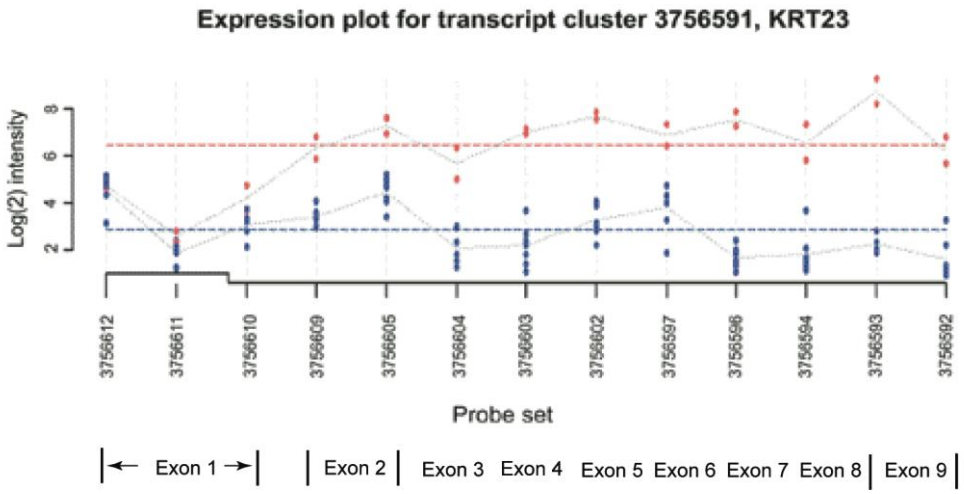

Figure 4.10 Expression plot of the gene *KRT23* as detected by a series of probe sets.

The expression intensities of nine exons, detected by 13 probe sets, showed differential expression between prostate cancer cell lines and BPH controls in exons 3-9 but not exons 1-2. Red dots represent two BPH control samples and blue dots represent six prostate cancer cell lines and the clinical prostate cancer sample. The red and blue lines indicate the average expression intensity of the BPH samples and cancer samples respectively.

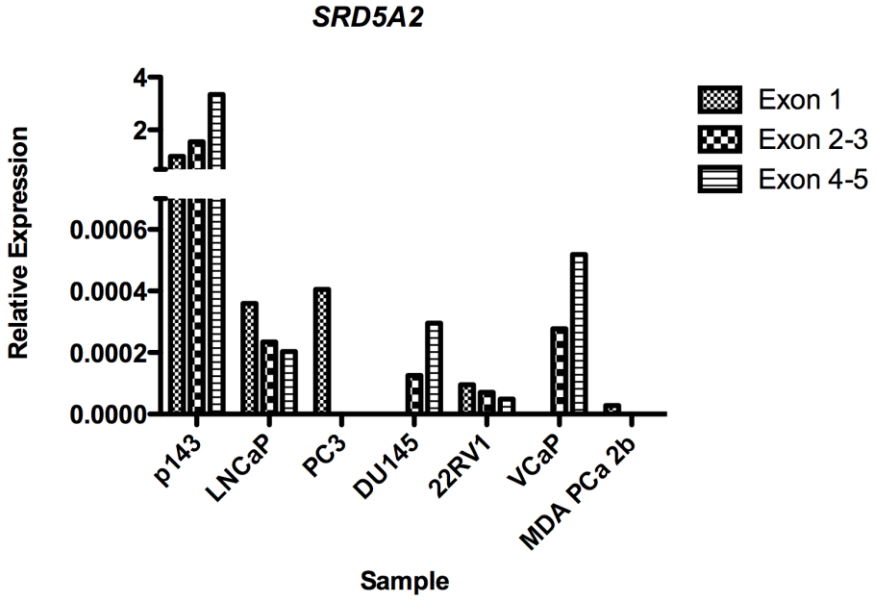

Figure 4.11 Relative expression of *SRD5A2* exons in BPH and prostate cancer cell lines as measured by qRT-PCR

Using a BPH (p143) and six prostate cancer cell lines (LNCaP, PC3, DU145, VCaP, 22RV1 and MDA PCa 2b), the expression levels of exon 1, exon 2-3 and exon 4-5 were measured by qRT-PCR relative to the expression of the housekeeping gene *GAPDH* and normalised to the exon 1 of p143 as a positive control.

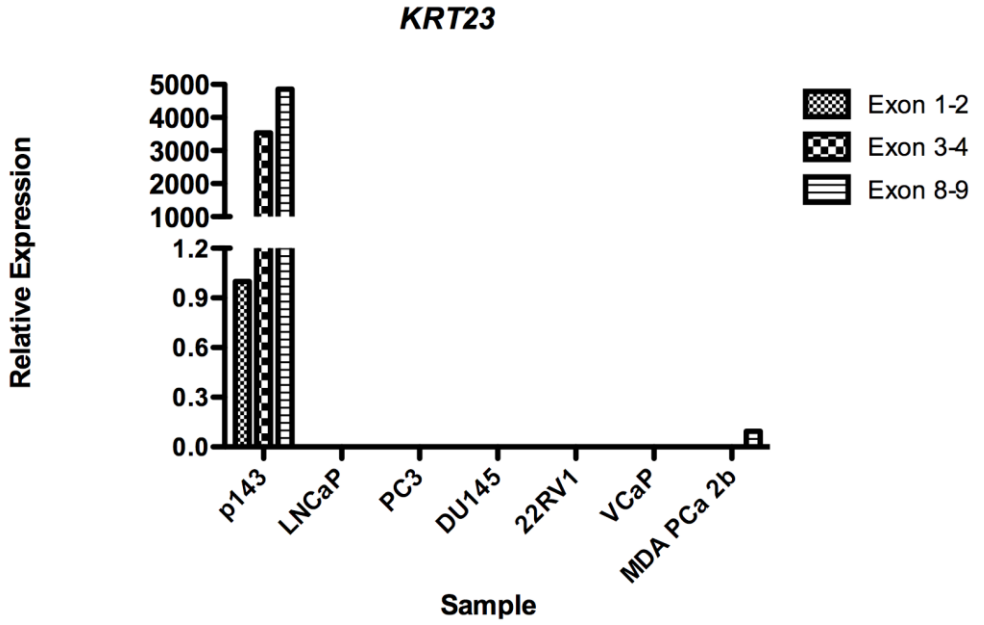

Figure 4.12 Relative expression of *KRT23* exons in BPH and prostate cancer cell lines as measured by qRT-PCR

Using a BPH (p143) and six prostate cancer cell lines (LNCaP, PC3, DU145, VCaP, 22RV1 and MDA PCa 2b), the expression levels of exons 1-2, exons 3-4 and exons 8-9 were measured by qRT-PCR relative to the expression of the housekeeping gene *GAPDH* and normalised to exons 1-2 of p143 as a positive control.

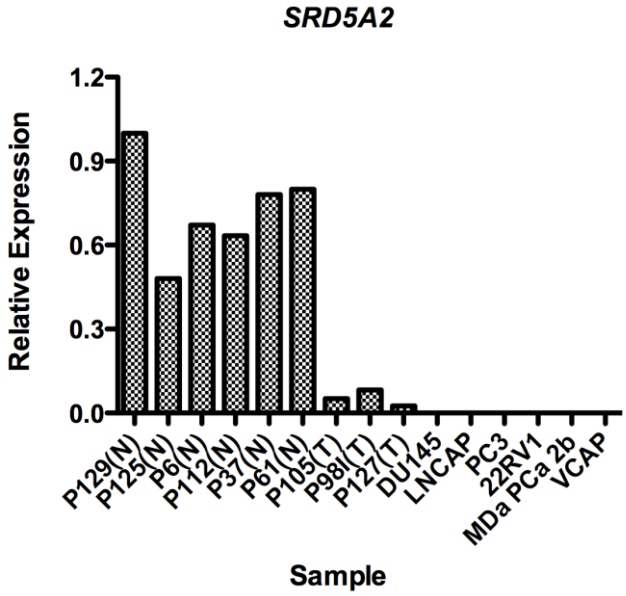

Figure 4.13 Relative expression of *SRD5A2* in prostate cancer cell lines and fresh frozen clinical tissue samples

The expression levels of *SRD5A2* were measured by qRT-PCR relative to the expression of the housekeeping gene *GAPDH* and normalised to the BPH sample p129 as a positive control. N stands for normal BPH sample and T stands for tumour sample.

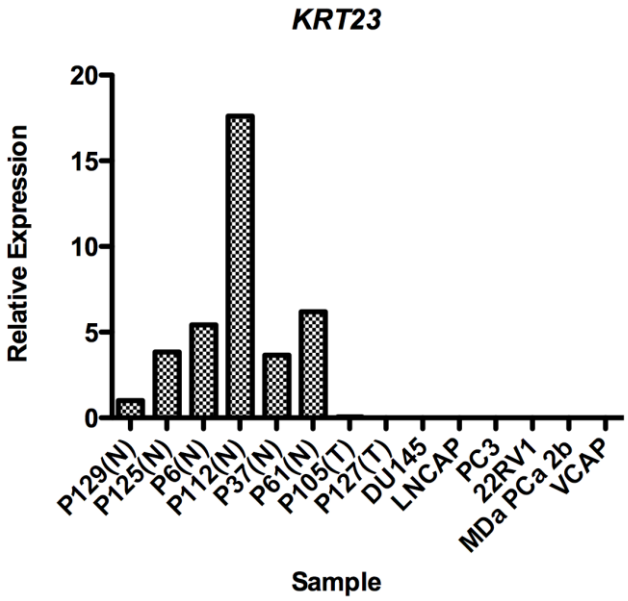

Figure 4.14 Relative expression of *KRT23* in prostate cancer cell lines and fresh frozen clinical tissue samples

The expression levels of *KRT23* were measured by qRT-PCR relative to the expression of the housekeeping gene *GAPDH* and normalised to the BPH sample p129 as a positive control. N stands for normal BPH sample and T stands for tumour sample.

Bioinformatic analysis (as described in **2.6.3.1**) was also applied to identify consistently over-/under-expressed genes in prostate cancer. 1715 and 963 significantly up- or down-regulated genes, respectively, were identified in six prostate cancer cell lines as compared to BPH controls. Nine and 34 significantly up-regulated and down-regulated genes were identified in the clinical prostate cancer samples. Four over-expressed and 34 under-expressed genes were found in both the prostate cancer cell lines and the clinical samples (**Table 4.4**). Analysis of these 38 genes using Ingenuity Pathways Analysis (IPA) software (details in **2.6.3.2**) showed that 15 of the 38 genes were involved in cancer. Further analysis of the 15 genes using IPA revealed that the most significant molecular and cellular function, with 10 of the 15 genes involved, was cell death (**Table 4.5**).

Table 4.4 Up- and down-regulated genes in prostate cancer cell lines and clinical cancer samples

Affy ID	Symbol	Location	Gene name
Down-regulated genes			
3942021	*NEFH*	22q12.2	Neurofilament, heavy polypeptide
2672140	*LTF*	3p21.31	Lactotransferrin
3301263	*SORBS1*	10q23.33	Sorbin and SH3 domain containing 1
3434012	*HSPB8*	12q24.23	Heat shock 22kDa protein 8
3549757	*SERPINA3*	14q32.1	Serpin peptidase inhibitor, clade A (alpha-1 antiproteinase, antitrypsin), member 3
3756591	*KRT23*	17q21.2	Keratin 23 (histone deacetylase inducible)
3367673	*MPPED2*	11p13	Metallophosphoesterase domain containing 2
2840393	*GABRP*	5q33-q34	Gamma-aminobutyric acid (GABA) A receptor, pi
3455186	*KRT6A*	12q12-q13	Keratin 6A
3421511	*LYZ*	12q15	Lysozyme (renal amyloidosis)
3407453	*PDE3A*	12p12	Phosphodiesterase 3A, cGMP-inhibited
3279313	*ITGA8*	10p13	Integrin, alpha 8
4018080	*CHRDL1*	Xq23	Chordin-like 1
3518766	*EDNRB*	13q22	Endothelin receptor type B
2794704	*ASB5*	4q34.2	Ankyrin repeat and SOCS box-containing 5
3908934	*PTGIS*	20q13.13	Prostaglandin I2 (prostacyclin) synthase
2902958	*C4A*	6p21.3	Complement component 4A (Rodgers blood group)
3102372	*SULF1*	8q13.1	Sulfatase 1
2777113	*SPARCL1*	4q22.1	SPARC-like 1 (hevin)
2599153	*TNS1*	2q35-q36	Tensin 1
2591367	*CALCRL*	2q32.1	Calcitonin receptor-like
4018755	*LRCH2*	Xq23	Leucine-rich repeats and calponin homology (CH) domain containing 2
3446919	*ABCC9*	12p12.1	ATP-binding cassette, sub-family C (CFTR/MRP), member 9
3278057	*CCDC3*	10p13	Coiled-coil domain containing 3
4006210	*MAOB*	Xp11.23	Monoamine oxidase B
3411810	*PDZRN4*	12q12	PDZ domain containing ring finger 4
2453006	*PIGR*	1q31-q41	Polymeric immunoglobulin receptor
3310953	*CPXM2*	10q26.13	Carboxypeptidase X (M14 family), member 2
3324447	*LOC387758*	11p14.2	Fin bud initiation factor homolog (zebrafish)
3401704	*CCND2*	12p13	Cyclin D2
3389353	*CASP1*	11q23	Caspase 1, apoptosis-related cysteine peptidase (interleukin 1, beta, convertase)
2521574	*LOC653632*	2q33.1	Similar to 130kDa-Ins(1,4,5)P3 binding protein
3626312	*ALDH1A2*	15q21.3	Aldehyde dehydrogenase 1 family, member A2
3671695	*WFDC1*	16q24.3	WAP four-disulfide core domain 1
Up-regulated genes			
2840664	---		
3749684	---		
2844293	---		
3375307	*CYBASC3*	11q12.2	Cytochrome b, ascorbate dependent 3

Table 4.5 Ten commonly down-regulated genes involved in cell death, determined using IPA

Gene symbol	Location	Name
LTF	3p21.31	Lactotransferrin
SERPINA3	14q32.1	Serpin peptidase inhibitor, clade A (alpha-1 antiproteinase, antitrypsin), member 3
LYZ	12q15	Lysozyme (renal amyloidosis)
PDE3A	12p12	Phosphodiesterase 3A, cGMP-inhibited
EDNRB	13q22	Endothelin receptor type B
PTGIS	20q13.13	Prostaglandin I2 (prostacyclin) synthase
SULF1	8q13.1	Sulfatase 1
CALCRL	2q32.1	Calcitonin receptor-like
CCND2	12p13	Cyclin D2
ALDH1A2	15q21.3	Aldehyde dehydrogenase 1 family, member A2

qRT-PCR analysis was performed to validate the expression of two genes *SULF1* and *PTGIS*. As insufficient cDNA was obtained from BPH sample p143, the cancer sample p127 and prostate cancer cell line MDA PCa 2b, the relative expression of *SULF1* and *PTGIS* was measured from two BPH samples (p125 and WX83I) and five prostate cancer cell lines (LNCaP, PC3, DU145, VCaP and 22RV1). As shown in **Figure 4.15A** and **B**, the expression levels of *SULF1* and *PTGIS* were down-regulated in prostate cancer cell lines as compared to BPH controls. As different BPH samples were applied, and no clinical cancer sample was available, it cannot be said that the qRT-PCR result correlates with the Exon Array data.

qRT-PCR analysis was also performed to validate the expression of *ARMCX1* (armadillo repeat containing, X-linked 1). According to the Exon Array data, *ARMCX1* was down-regulated in both prostate cancer cell lines and the clinical prostate cancer sample (p127) as compared to BPH controls. Using the same samples that were applied to the Exon Array, qRT-PCR analysis validated the Exon Array result (**Figure 4.16**). With an additional five BPH samples (p125, p6, p112, p37, p61) and two primary prostate cancer samples (p105 and p98), *ARMCX1* was still shown to be commonly down-regulated in prostate cancer (**Figure 4.16**).

A

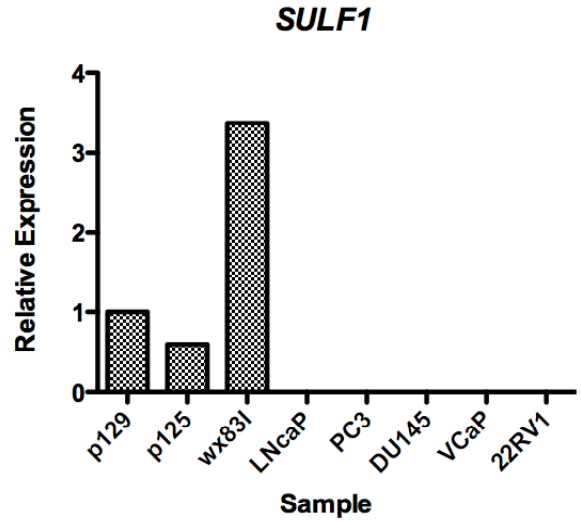

B

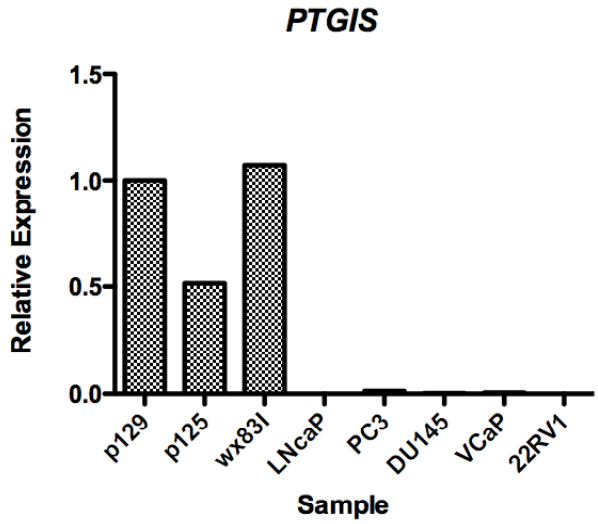

Figure 4.15 Relative expression levels of *SULF1* and *PTGIS* in BPH and prostate cancer cell lines as measured by qRT-PCR.

The expression levels of *SULF1* (A) and *PTGIS* (B) were measured by qRT-PCR relative to the expression of the housekeeping gene *GAPDH* and normalised to the BPH sample p129 as a positive control.

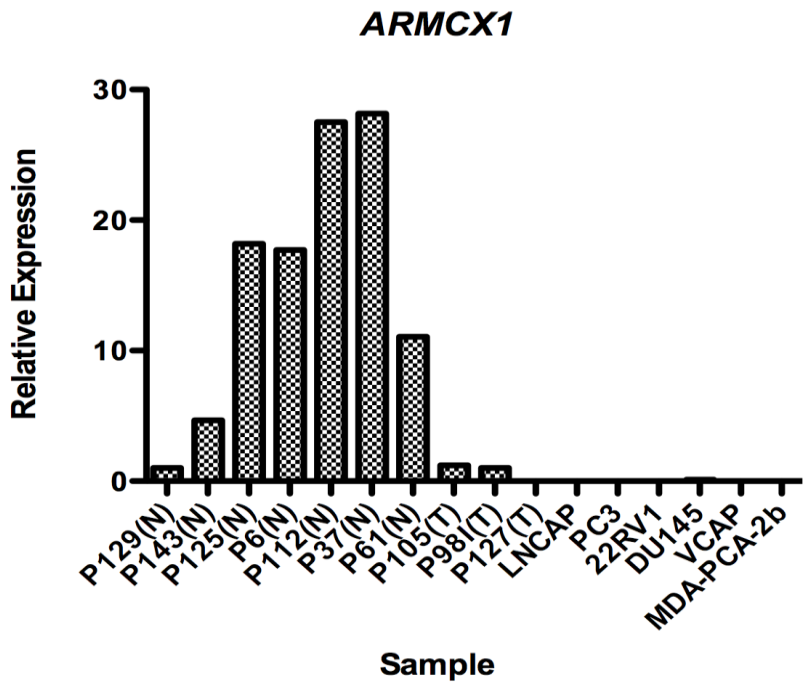

Figure 4.16 Relative expression levels of *ARMCX1* in fresh frozen tissue samples and prostate cancer cell lines as measured by qRT-PCR.

The expression levels of *ARMCX1* were measured by qRT-PCR relative to the expression of the housekeeping gene *GAPDH* and normalised to the BPH sample p129 as a positive control. N stands for normal BPH sample and T stands for tumour sample.

4.4 Discussion

Because of our hypothesis that t(4;6)(q22;q15) may contribute to prostate cancer development through inactivation of tumour suppressor gene(s), I have focused on identifying the potential target gene(s). The micro-deletion on 4q22 and 6q15 is a characteristic of t(4;6) in LNCaP cells and it might contribute to the aggressiveness of prostate cancer. It has been demonstrated that chromosome translocation t(9;22)(q34, q11), coupled with small deletions, is associated with poor prognosis in leukaemia (Lee *et al.*, 2006). Loss of chromosomal regions of 6q has been reported widely as a common occurrence not only in prostate cancer, but also in other cancers such as breast, colon and melanoma (Sun *et al.*, 2006; Sheng *et al.*, 1996; Walker *et al.*, 1994; Tibiletti *et al.*, 2001). A number of studies have subsequently evaluated the frequency of multiple 6q deletions in prostate tumours, with reports of up to 48% in some cases (Verhagen *et al.*, 2002; Sun *et al.*, 2006; Cooney *et al.*, 1996; Srikantan *et al.*, 1999; Alers *et al.*, 2000; Hyytinen *et al.*, 2002; Konishi *et al.*, 2003). In the present study, using tissue microarrays, I found that a similar rate (46%) of prostate cancer samples had specific loss of the 6q15 region. Previous studies indicated that loss of 6q regions might occur at an intermediate stage of disease development with either more locally invasive or metastatic progression (van Dekken *et al.*, 2004; Ribeiro *et al.*, 2006a). In my study, 6q15 deletion seems likely to occur with a high Gleason score (75% with Gleason score between 8-10 vs 43.5% with Gleason score less than 8), however, the number of cases is too small to draw a solid conclusion. Although 6q15 deletion has been widely recognised as a frequent event in prostate cancer (Cooney *et al.*, 1996; Konishi *et al.*, 2003; Liu *et al.*,

2007), the target tumour suppressor gene(s) located in this region are still yet to be identified. Liu et al. applied SNP array analysis on 55 matched prostate cancer and non-malignant tissue samples and identified a minimum overlapped deletion region between 90,3493 and 91,310 Kb (817 Kb), which was shared by 20 tumours. Five genes (*MAP3K*, *CASP8A2*, *CX62*, *MDN1* and *BACH2*) were located in this small region. Further analysis of *MAP3K7* revealed the correlation of its down regulation with high-grade prostate cancer (Liu *et al.*, 2007). It has yet to be determined if *MAP3K7* plays a role in prostate cancer pathogenesis. According to our Exon Array data, *MAP3K7* was not shown to exhibit common down-regulation in prostate cancer cell lines and the clinical cancer sample. In fact, higher expression of *MAP3K7* was shown in PC3 and DU145 cells as compared to BPH controls. Regardless of all the identifications indicating the existence of tumour suppressor genes in 6q15, to date, no strong candidate genes have been discovered relating to prostate cancer.

In this study, I performed Exon Array analysis to interrogate systematically the expression alterations of the genes located in 6q15. Four genes (*CNR1, PNRC1, CX62* and *BACH2*) were identified with common down-regulation in six prostate cancer cell lines and one clinical prostate cancer sample. Followed by qRT-PCR validation of these four genes in enlarged clinical prostate cancer samples, *CNR1* and *BACH2* were still found to be down-regulated but *PNRC1* and *CX62* were not.

CNR1 is one of the two cannabinoid receptors, responsible for the well-known psychotropic effects of cannabinoids. *CNR1* is highly expressed in the central

nervous system, but lower levels are also present in immune cells and peripheral tissues, including prostate. In contrast, cannabinoid receptor 2 (*CNR2*) is expressed predominantly in immune cells. Over past decades, anti-tumourigenic effects of cannabinoids have drawn great attention. Apart from their pro-apoptotic and anti-proliferative action, recent research has shown that cannabinoids may also affect angiogenesis, migration, invasion, adhesion, and metastasis in various cancers (Freimuth *et al.*, 2010). Extensive molecular and pharmacological studies have demonstrated that cannabinoids perform their anti-tumourigenic effect through *CNR1* and *CNR2*. However, whether *CNR1* or *CNR2* specifically exert tumour suppressor effects has not been well-studied. A recent report demonstrated that *CNR1* expression was silenced in human colorectal cancer due to methylation of the *CNR1* promoter and that loss of *CNR1* accelerated intestinal tumour growth *in vivo* (Wang *et al.*, 2008). According to our identification of down-regulation of *CNR1* in clinical prostate cancer samples, it seems promising to investigate further the role of *CNR1* in prostate tumourigenesis.

BACH2 is a B-cell-specific transcription repressor and has been implicated as a B-cell specific tumour suppressor. In non Hodgkin's Lymphoma, a relatively high frequency of loss of heterozygosity was detected for *BACH2* (Sasaki *et al.*, 2000). Moreover, the *BACH2* expression level has proven to be a useful marker to predict disease-free and overall survival of patients with diffuse large B-cell lymphoma, where a favourable prognosis is correlated with a high expression level of *BACH2* (Sakane-Ishikawa *et al.*, 2005). It has also been suggested that loss or down-regulation of *BACH2* expression may contribute to B-cell

lymphomagenesis (Liu *et al.*, 2009). In addition, a recent genome-wide association study identified a risk locus inside of the gene *BACH2* in type 1 diabetes (Cooper *et al.*, 2008). In this study, the down-regulation of *BACH2* was consistent with the genomic deletion in 6q15. Whether it also plays a tumour suppressor role need to be further explored.

As the Exon Array data were available, the expression of *UNC5C* was also investigated in six prostate cancer cell lines, clinical prostate cancer and BPH samples. As illustrated previously, *UNC5C* was the only gene disrupted by breakpoints of t(4;6)(q22;q15). The inactivation of *UNC5C* has been identified in various human tumours, including colorectal, breast, ovary, uterus, stomach, lung, kidney and others (Arakawa, 2004; Furuta *et al.*, 2006; Latil *et al.*, 2003; Thiebault *et al.*, 2003). Inactivation of *UNC5C* has been demonstrated to be associated with colorectal cancer progression (Bernet *et al.*, 2007). Therefore *UNC5C* has been recognised as a putative tumour suppressor gene (Thiebault *et al.*, 2003). In our Exon Array data, the expression of *UNC5C* was down-regulated in all prostate cancer cell lines and one clinical prostate cancer sample. qRT-PCR analysis confirmed the Exon Array data and, with more clinical samples, a trend toward decreased *UNC5C* expression in tumours compared to normal tissue was found.

SRD5A2 and *KRT23* were initially selected from the Exon Array data as potential truncated genes. However, qRT-PCR validation using probes binding to different exons showed that the down-regulation of these two genes was a dominant effect. *SRD5A2* is an isoenzyme of 5-alpha-reductases, which convert

testosterone irreversibly into dihydrotestosterone (DHT). Both normal and pathological growth of the prostate depends on DHT synthesis. It has been demonstrated that *SRD5A2* expression decreases in prostatic intraepithelial neoplasia (PIN) and prostate cancer, compared with non-malignant prostate tissue. However, the expression of another isoenzyme, *SRD5A1*, increases as a complement to these declines in *SRD5A2* levels(Thomas *et al.*, 2008b) (Thomas *et al.*, 2008c). Moreover both isoenzymes appear increased in high-grade, as compared to low-grade localised, cancer (Thomas *et al.*, 2008c). Until now, no study has demonstrated a tumour suppressor role for this gene.

KRT23 is a member of the acidic keratin family. It has been reported that *KRT23* is induced by sodium butyrate in different pancreatic cancer cells through *p21* (WAF1/CIP1), which serves as an important mediator. NaBu was shown to induce cell differentiation and apoptosis in the human pancreatic cancer cell line AsPC-1 (Zhang *et al.*, 2001). It also has been shown that *KRT23* impaired the proliferation of human colon cancer cells significantly, leading to cell death in microsatellite-unstable, but not microsatellite-stable, cell lines (Birkenkamp-Demtroder *et al.*, 2007). There currently is no evidence showing that *KRT23* is associated with prostate cancer.

The Exon Array data were also applied to investigate consistent expression changes of genes located on other chromosome regions. The down-regulation of the gene *ARMCX1* had been reported to be correlated with DNA copy number loss at Xq21.33-q22.2 in primary prostate cancer samples (Jiang *et al.*, 2008). Our SNP array data (unpublished) also showed copy number loss at Xq21.33-

q22.2 in 8 out of 71 (11.3%) clinical prostate cancer samples and also in 22RV1 and VCaP cells. The common down regulation of *ARMCX1* was identified from our Exon Array data. With further clinical samples, the expression of *ARMCX1* was still shown to be down-regulated in prostate cancer cell lines and the clinical prostate cancer samples using qRT-PCR analysis. *ARMCX1* is a member of the armadillo repeat family, which has been implicated in tumourigenesis, embryonic development and maintenance of tissue integrity (Kurochkin *et al.*, 2001). The mRNA expression of *ARMCX1* is lost, or significantly reduced, in various human cancer types including lung, prostate, colon, pancreas, and ovarian carcinomas and also in cell lines established from human carcinomas. It has been speculated that *ARMCX1* may play a role in tumour suppression (Kurochkin *et al.*, 2001); however, no further studies have yet confirmed this possibility.

Fifteen commonly down-regulated genes among prostate cancer cell lines and the clinical prostate cancer sample were shown to be involved in cancer. Ten out of the fifteen genes were shown to be associated with cell death and six of them, (including *LTF* (3p21.31), *EDNRB* (13q22), *CCND2* (12p13) and *ALDH1A2* (15q21.3)), have been reported to be down-regulated in various cancers (Chen *et al.*, 2009; Evron *et al.*, 2001; Frigola *et al.*, 2005; Henrique *et al.*, 2006; Kim *et al.*, 2005; Lai *et al.*, 2008; Phe *et al.*; Shaheduzzaman *et al.*, 2007; Yu *et al.*, 2003). In prostate cancer, *LTF*, *EDNRB*, *CCND2* and *ALDH1A2* have been shown to play a tumour suppressor role (Henrique *et al.*, 2006; Kim *et al.*, 2005; Phe *et al.*; Shaheduzzaman *et al.*, 2007). Down-regulation of *LTF* has been revealed to be associated with reduced PSA recurrence-free survival

(Shaheduzzaman *et al.*, 2007); Hypermethylation of *EDNRB* is correlated with the grade and stage of the primary prostate cancer, and inversely correlated with PSA-free-survival (Bastian *et al.*, 2007; Yegnasubramanian *et al.*, 2004). Inactivation of *CCND2* in prostate cancers correlates with poor prognosis (Padar et al., 2003). Reduction of *ALDH1A2* protein was indicated as an early event in prostate cancer using the transgenic prostate adenocarcinoma mouse model (Touma *et al.*, 2009). As to the gene *SULF1* (8q13.2-q13.3), its down-regulation was observed in the majority of cancer cell lines and its tumour suppressor function was well-documented showing inhibition of cell proliferation, migration and invasion in various cancers, including breast, pancreatic, ovarian, myeloma and hepatocellular carcinoma (Abiatari *et al.*, 2006; Chen *et al.*, 2009; Lai *et al.*, 2003; Lai *et al.*, 2008; Lai *et al.*, 2006; Narita *et al.*, 2006). However, there currently is no study showing its expression and function in prostate cancer. Similarly to *SULF1*, although there is evidence showing frequent hypermethylation of *PTGIS* (20q13.13) observed in colorectal cancer, no study has examined *PTGIS* expression in prostate cancer (Frigola *et al.*, 2005). The qRT-PCR analysis confirmed the down-regulation of *SULF1* and *PTGIS* in prostate cancer cell lines. It would be encouraging to further confirm the expression alterations of these two genes in clinical prostate cancer samples.

In summary, the common down regulation of *CNR1* and *BACH2* in clinical prostate cancer samples was consistent with frequent genomic deletion in 6q15. Therefore *CNR1* and *BACH2* might be target tumour suppressor genes located in 6q15 in prostate cancer. Other genes, including *SRD5A2*, *KRT23*, *ARMCX1*, *SULF1* and *PTGIS* have been shown to exibit common down regulation in

prostate cancer. Whether these genes have a tumour suppressor role in prostate cancer needs to be studied further.

5 FURTHER INVESTIGATION OF *CNR1* AND *BACH2* AT THE PROTEIN LEVEL AND OTHER GENOMIC CHANGES OF *CNR1*

5.1 Introduction

In the previous chapter, I described the identification of putative tumour suppressor genes involved in the recurrent chromosomal translocation, t(4;6)(q22;q15), which are associated with prostate cancer. Using Exon array analysis to examine the expression alterations of the genes located in 6q15 systematically and then using qRT-PCR for confirmation, two genes, *CNR1* and *BACH2* were shown to be commonly down regulated in clinical prostate cancer samples at the RNA level. Using the same approach, there was a trend toward decreased expression of *UNC5C* in clinical prostate cancer samples. However, the function of genes is fulfilled by their encoded proteins and IHC in combination with TMAs is the most efficient method to investigate gene expression in a large cohort of clinical samples.

CNR1 encodes a transmembrane protein belonging to the G-protein coupled receptor family, which possesses seven α-helical transmembrane domains with extracellular amino and intracellullar carboxyl termini (**Figure 5.1A**). Several *CNR1* polyclonal antibodies binding to different protein domains were available through commercial sources. However, concern about the specificity of these *CNR1* antibodies has been generated, since a recent study tested a range of commercial *CNR1* antibodies, none of which were shown to have high specificity (Grimsey *et al.*, 2008). Some of the tested antibodies had been applied

in previously reported studies, thus calling into question the reliability of those studies. It suggested that the selection of *CNR1* antibody to be used needs to be approached cautiously and the specificity should be examined carefully prior to application for such studies.

BACH2 is a transcription factor containing a basic leucine zipper (bZip), a BTB (broad complex Tramtrack bric-a-brac) domain (Vieira *et al.*, 2001). It possesses one nuclear localisation signal (NLS) and one cytoplasmic localisation signal (CLS) (**Figure 5.1B**). *BACH2* mainly is localised in the cytoplasm through its C-terminal evolutionarily conserved CLS. Regarding the protein expression of *BACH2*, so far, only one study on ovarian cancer applied the antibody generated by Santa Cruz on tissue samples (Motamed-Khorasani *et al.*, 2007), others all applied the rabbit polyclonal antibody, F69-2, generated by Prof. Igarashi's group, who discovered the gene *BACH2* in 1996 (Oyake *et al.*, 1996).

In this study, I continued to examine the protein expression alterations of *CNR1* and *BACH2* in primary prostate cancer samples in order to identify whether the protein expression patterns of these three genes are consistent with the RNA expression alterations.

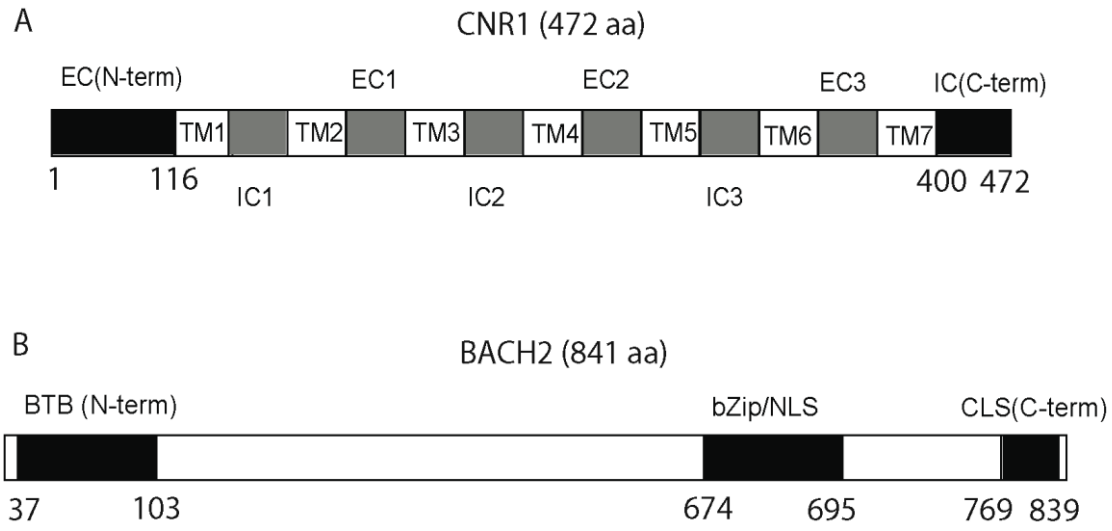

Figure 5.1 Schematic representation of protein regions of CNR1 and BACH2

(A) *CNR1* encodes a transmembrane protein (472 amino acid) possessing seven transmembran domains (TM) with extracellular (EC) domain at N-terminal and intracellular (IC) domain at C-terminal. The CNR1 polyclonal antibody from Abcam is generated by immunizing rabbits with a synthetic peptide against the C-terminal amino acid 461-472. (B) BACH2 encodes a transcription factor (841 amino acid) containing a BTB domain at N-terminal, a bZip/nuclear localisation signal (NLS) domain and a cytoplasmic localisation signal (CLS) domain at C-terminal. The BACH2 polyclonal antibody F69-2 is produced by immunizing rabbits with a fusion protein containing C-terminal 329 amino acids of BACH2.

5.2 Aims

I aimed to investigate the protein expression alterations of the *CNR1*, *BACH2* and *UNC5C* genes in clinical prostate cancer samples using IHC analysis.

5.3 Results

5.3.1 Antibody selection

The specificity of the antibody is crucial for examining protein expression alterations. Therefore the antibodies against *CNR1*, *BACH2* and *UNC5C* products were carefully selected and antibody working conditions were optimised prior to their application to primary prostate cancer samples. A recent study reported a series of *CNR1* antibodies, which were unspecific, therefore the selection of the *CNR1* antibody was even more careful and stringent. One *CNR1* antibody, generated by Abcam Inc. and one antiserum (2814.3), developed by Prof. Maurice's research group (Queen Mary, University of London), were applied, since the specificity of these antibodies has been verified by lack of staining in FFPE *CNR1*$^{-/-}$ mice brain tissue in contrast to the extensive staining in wild-type mice (Chung *et al.*, 2009; Egertova and Elphick, 2000). Moreover, the specificity of the *CNR1* antibody from Abcam has also been demonstrated in FFPE prostate tissue from *CNR1*$^{+/+}$, *CNR1*$^{+/-}$ and *CNR1*$^{-/-}$ mice and shown to provide an appropriate staining pattern in FFPE sections of human cerebellum (Chung *et al.*, 2009). Although human brain tissue, where *CNR1* is highly expressed, would be the best positive control for *CNR1* antibody optimisation, they were not available in our research centre. According to my previous qRT-

PCR analysis result, *CNR1* was shown to be expressed at the RNA level in BPH samples but down-regulated in prostate cancer cell lines (section **4.3.2.3**). In general, the protein expression correlated with the RNA expression level. Therefore *CNR1* antibody specificity examination and working conditions optimisation was done on FFPE BPH samples as a positive control and four FFPE prostate cancer cell lines, including LNCaP, PC3, 22RV1 and DU145, as negative controls. A range of dilutions of the *CNR1* antibody from Abcam (ab23703, Abcam) were used, including 1:50, 1:100, 1:200, 1:300, 1:500. The antibody at 1:100 dilution showed strong staining and weak background on FFPE BPH (**Figure 5.2A**) and very weak or no staining in prostate cancer cell lines (**Figure 5.2C-E**), which was consistent with the RNA expression level determined by qRT-PCR analysis. In contrast, the *CNR1* antiserum (2824.3) showed very weak staining in various dilutions (1:100; 1:300; 1:500; 1:1000; 1:2000). Therefore the *CNR1* antibody from Abcam was applied for further IHC analysis in this study.

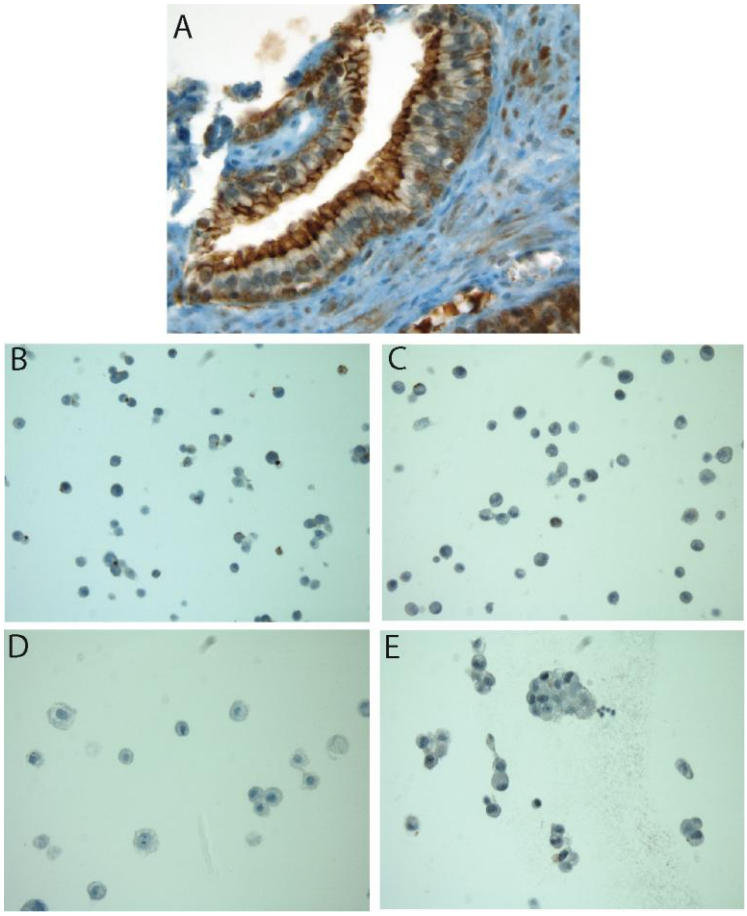

Figure 5.2 *CNR1* antibody specificity for IHC analysis

(A) Representative image of *CNR1* staining in a core of a BPH sample. *CNR1* was localised to the cell membrane of epithelial cells. (B) to (E) Representative images of *CNR1* expression in 22RV1, DU145, PC3 and LNCaP cells, respectively. *CNR1* staining was negative in these four cell lines. The magnification used was 40x.

Regarding the selection of a *BACH2* antibody F69-2, generated by Prof. Igarashi's group, was applied. The antibody working condition was optimised on tonsil tissue, where *BACH2* is highly expressed, and the 1:500 dilution was shown to give strong staining with a low background.

At the time of selection of the *UNC5C* antibody, there was no study reporting the application of a *UNC5C* antibody for IHC and also there were only two commercial antibodies available for IHC: one was from Santa Cruz Int. and the other is from Sigma-Aldrich. The antibody from Santa Cruz was tested on FFPE ovary, uterus and kidney tissue samples, which have been reported to express *UNC5C* (Thiebault *et al.*, 2003), with different concentrations and dilutions, but none of the conditions generated good signals. According to the IHC images using the antibody from Sigma-Aldrich (http://www.proteinatlas.org/), no staining was shown in normal prostate tissue. Therefore the IHC analysis of *UNC5C* could not be performed due to the lack of a good quality commercial antibody.

5.3.2 Protein expression of *CNR1* in primary prostate cancer samples

5.3.2.1 *CNR1* immunoreactivity in non-malignant prostate tissue

CNR1 expression was assessed in a TMA made from 34 BPH cases. Five of them had only stromal tissue without prostate glands and three cases were missing so they were excluded from the analysis. The staining intensity varied between samples, but *CNR1* was localised to the plasma membrane of both basal and

luminal epithelial cells, and with little or no staining of the stroma. An example from a core with a strong *CNR1* staining is shown in **Figure 5.2A**.

5.3.2.2 Comparison of *CNR1* expression in clinical prostate cancer and non-malignant tissue

A total of 68 prostate cancer cases and six BPH cases in two TMAs (details in **2.1.2**) were assessed using IHC analysis. Among the 68 cancer cases, 10 of them were excluded from the interpretation as the tissue cores were missing or contained very few cancer cells. Among the six BPH cases, one case was missing. Therefore 58 cancer cases and five BPH cases were informative for *CNR1* expression evaluation in these two TMAs. Combined with 26 BPH cases from the BPH TMA, 31 BPH cases in total were available to compare the *CNR1* protein expression with the 58 prostate cancer cases. Using the detailed evaluation of IHC staining described in **2.6.2.3**, 3 (10.3%), 16 (55.2%), 10 (34.5%) of 29 BPH samples were shown to have negative (-), weakly positive (+), or strongly positive (++) *CNR1* expression in the cell membrane, respectively. In addition, there were two BPH cases shown with *CNR1* expression at a nuclear localisation. In contrast, 43 (75.4%), 14 (24.6%) and 0 of 57 cancer cases were shown to have negative (-), weakly positive (+) and strongly positive (++) *CNR1* expression in the cell membrane, respectively. There was one cancer case with nuclear staining of *CNR1* (**Table 5.1**). Examples of cancer cores scored as negative (-) and weakly positive (+) are shown in **Figure 5.3A-D**. Based on the membrane staining, cancer cases have a statistically weaker *CNR1* expression than BPH cases ($p<0.001$). Among 58 prostate cancer cases, 45 cases have matched normal glands. 40 out of the 45 cases (88.9%) showed lower expression of *CNR1* in the cancer tissue as

compared with adjacent normal glands. A representative image is shown in **Figure 5.3E**.

Table 5.1 *CNR1* expression in clinical prostate cancer and BPH samples

Immunoreactivity	*CNR1* expression in PCa (% with membrane staining)	*CNR1* expression in BPH (% with membrane staining)	p-value
Membrane staining			<0.001
- (negative)	43 (75.4)	3 (10.3)	
+ (weakly positive)	14 (24.6)	16 (55.2)	
++ (strong positive)	0 (0)	10 (34.5)	
Nuclear staining	1	2	
Missing/not scoreable	10	3	
Total cases	68	34	

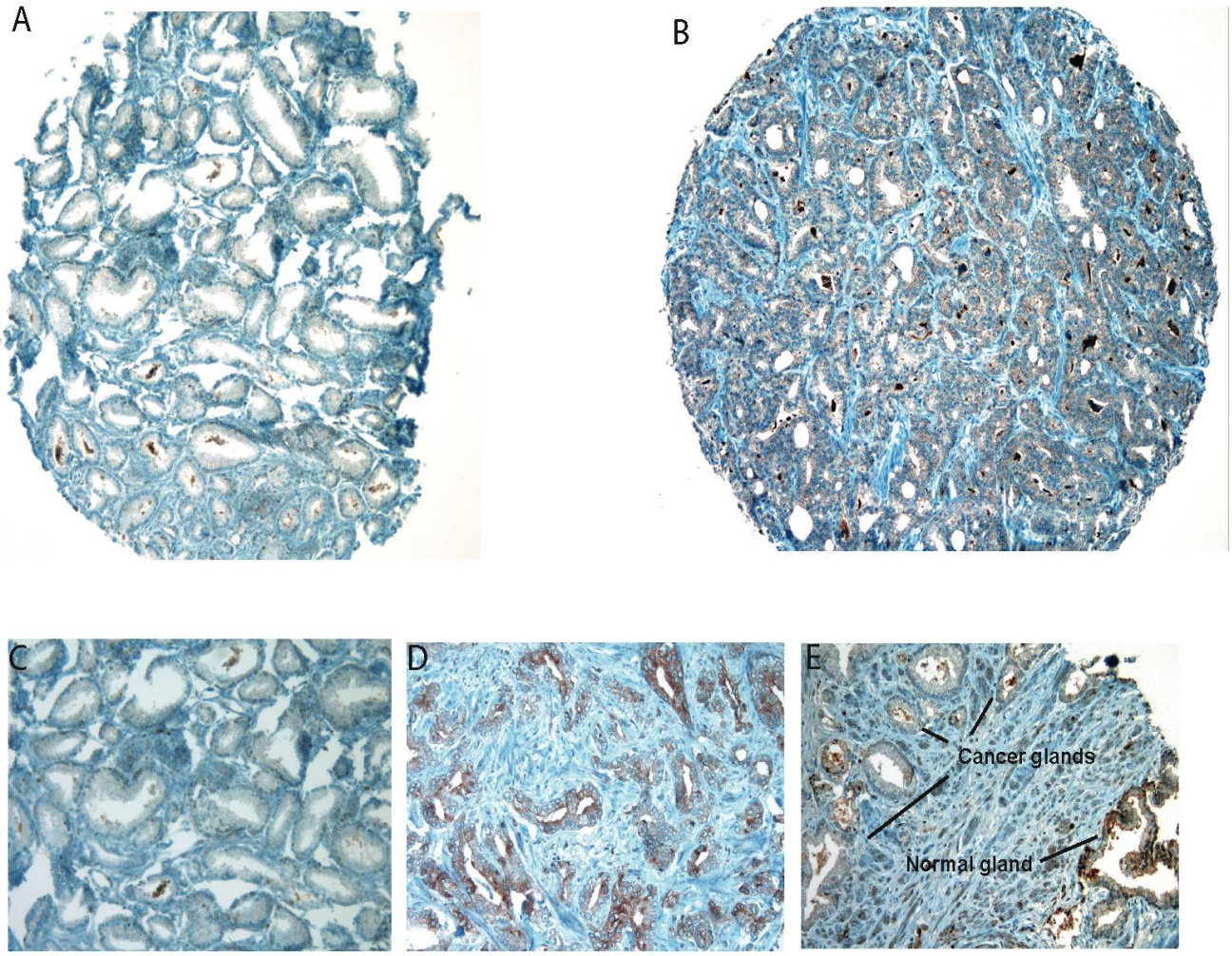

Figure 5.3 *CNR1* immunoreactivity in prostate cancer TMAs.

(A) and (C) Representative images of prostate cancer cores with negative *CNR1* expression at magnification 20x and 40x, respectively. (B) and (D) Representative images of prostate cancer cores with weakly positive *CNR1* expression at magnification 20x and 40x, respectively. (E) Representative image of a tissue core with lower *CNR1* expression in cancer cells compared with adjacent normal glands.

5.3.3 Protein expression of *BACH2* in primary prostate cancer samples

BACH2 expression was assessed in three TMAs containing 124 prostate cancer samples (details in **2.1.2**) and one TMA made from 34 BPH cases. Among 124 prostate cancer samples, 38 of them were excluded from interpretation either because the tissue cores were missing or there were too few cancer cells to be informative. Among 34 BPH samples, three of them had only stromal tissue without prostate glands and two cases were missing so that they were excluded from the analysis. Following detailed evaluation of IHC staining as described in **2.6.2.3,** 22 of 26 BPH samples (84.6%) were shown to have weakly positive (+) staining in the cytoplasm and 3 cases had nuclear staining. In contrast, 39 of 86 informative prostate cancer cases were shown to have nuclear staining (**Figure 5.4D-E**) and 25.5% (12/47), 38.3% (18/47) and 36.2% (17/47) of the cancer samples were shown to have negative (-), weakly positive (+) and strong positive (++) staining of the cytoplasm respectively (**Table 5.2** and **Figure 5.4A-C**).

Table 5.2 *BACH2* expression in clinical prostate cancer and BPH samples

Immunoreactivity	*BACH2* expression in PCa (% with cytoplasmic staining)	*BACH2* expression in BPH (% with cytoplasmic staining)	P value
Cytoplasm staining			0.001
- (negative)	12 (25.5)	2 (7.7)	
+ (weakly positive)	18 (38.3)	22 (84.6)	
++ (strong positive)	17 (36.2)	2 (7.7)	
Nuclear staining			0.001
Positive	39	3	
Negative	47	26	
Missing/not scoreable	38	5	
Total cases	124	34	

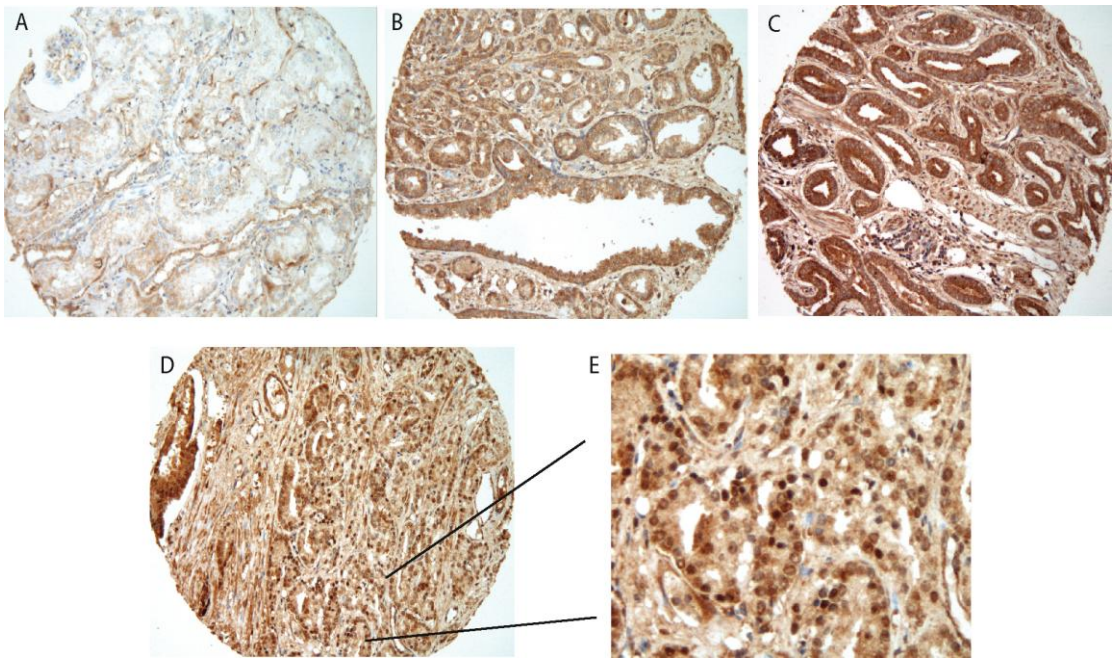

Figure 5.4 *BACH2* immunoreactivity in prostate cancer TMAs.

(A) to (C) Representative images of prostate cancer cores with negative (-), weakly positive (+) and strong positive (++) *CNR1* expression, respectively, at magnification 20x. (D) and (E) Representative images of prostate cancer cores with *BACH2* expression in nuclei at magnification 20x and 40x, respectively.

5.3.4 *CNR1* mutation in prostate cancer

As illustrated above, 43 prostate cancer cases were shown to have negative staining for *CNR1* protein, indicating that the *CNR1* expression might be down-regulated in these samples. The inactivation of a gene can be caused by DNA mutation, genomic deletion or methylation. As *CNR1* is located at 6q15, one of the most frequently deleted regions in prostate cancer, it seems highly likely that the genomic deletion is accounting for the *CNR1* inactivation in some of the 43 cancer samples. Whether mutations also occur in the *CNR1* genomic DNA was further explored. Five prostate cancer cases, which had high purity of cancer cells on the cores of TMAs, were selected from the 43 cancer cases with low or no *CNR1* expression for sequencing. In addition, *CNR1* genomic DNA in 22RV1 cells was also sequenced, as the 22RV1 cell line will be utilised for *CNR1* functional studies due to its better transfection rate compared to other prostate cancer cell lines.

5.3.4.1 PCR amplification and sequencing of *CNR1* genomic coding region

Tumour tissue from the five FFPE prostate cancer cases was micro-dissected and genomic DNA from these five samples and 22RV1 cells was extracted as described in **2.4.1**. As *CNR1* has only one exon, using a pair of primers flanking the genomic coding region (~ 1.4 Kb) of the *CNR1* gene (**Figure 5.5**), PCR analysis was performed on the genomic DNA of the five cancer cases. The coding region of *CNR1* was amplified successfully from 22RV1 cells and four of the five cancer cases except one sample, from which no PCR product was generated using the same primers and PCR working conditions. PCR products

from 22RV1 cells and the four cancer cases were purified and sequenced. A nucleotide change (G-->A) at position 1359 was identified in 22RV1 cells. It is a silent intragenic SNP of the gene *CNR1* in codon 435 (Thr). No mutation was identified from any of the four clinical samples.

The reason for no generated PCR product from the one sample might be that a mutation existed in the primer-binding region or genomic alterations, such as deletion, translocation, occurred in the genomic coding region of *CNR1*. In order to identify any DNA alterations, a series of PCR analyses were performed using the primers, which were designed across the genomic region of *CNR1* with the expected PCR product size ranging from ~120 - 400 bp (details in **2.4.2**). As shown in **Figure 5.6,** no PCR products were generated within a ~5 Kb region, including ~ 4.8 Kb of intron region and ~ 200 bp of coding region. It indicated a homozygous deletion was present in the genomic DNA of *CNR1*. However, using a few different pairs of primers, which flanked the deleted region, no specific PCR product was generated. This was taken to indicate that, apart from the deletion, there might be other genomic alterations that have occurred, such as translocation, inversion or insertion, in this sample. In order to confirm that there was such a genomic alteration, the breakpoints of the deletion need to be mapped and sequenced.

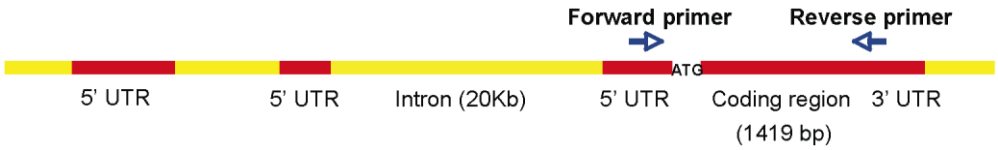

Figure 5.5 Schematic representation of genomic DNA of the gene *CNR1*

CNR1 has one exon with a coding region of 1419 bp. A pair of PCR primers flanking the coding region was designed to amplify *CNR1* for sequencing. Red and yellow bars represent the transciption and intron region, respectively, in the genomic DNA of *CNR1*.

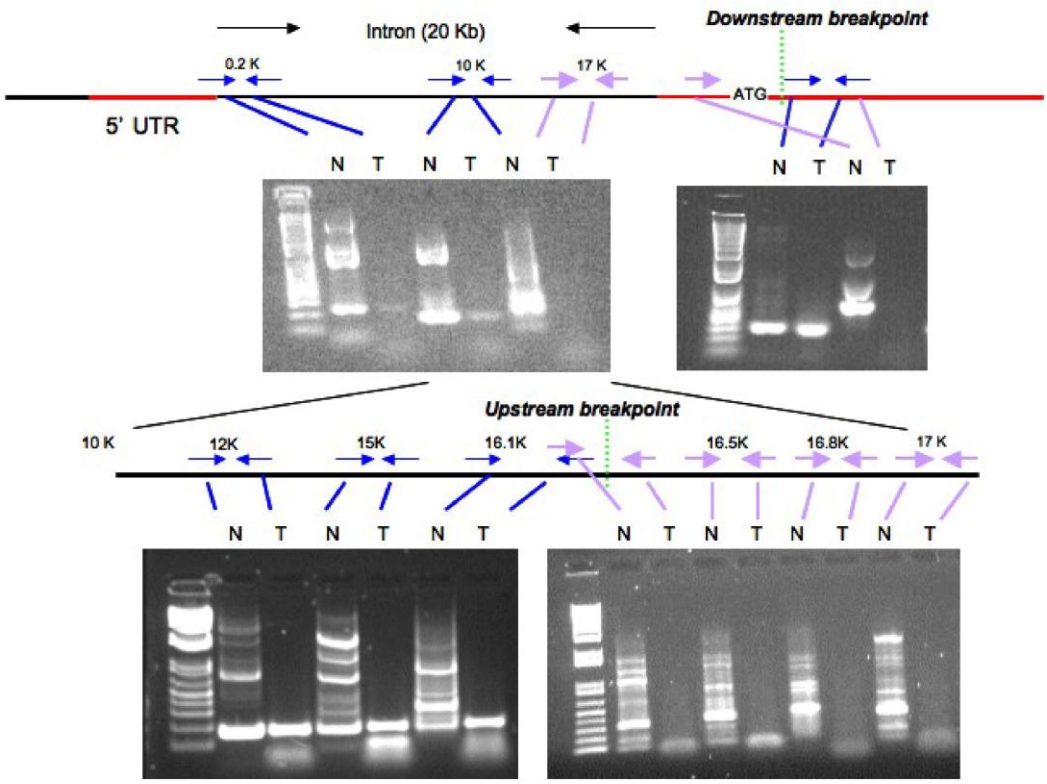

Figure 5.6 Deletion breakpoint mapping in genomic DNA of *CNR1* using PCR analysis

A series of PCR analyses were performed using the primers, which were designed across the genomic region of *CNR1*. No PCR products were generated within a ~5 Kb region including ~ 4.9 Kb of intron region (16.1 Kb- 20 Kb) and ~ 200 bp of coding region. Upstream and downstream deletion breakpoints were indicated with green bars. N stands for normal control sample. T stands for tumour sample (p6363).

5.3.4.2 *CNR1* breakpoint mapping

Genome-walking assay (detailed in **2.4.3**) was performed to map the actual breakpoint of *CNR1* in the clinical cancer case, which had been demonstrated to have an homozygous deletion within *CNR1* genomic DNA. The basic principle of genome-walking analysis is that the genomic DNA is fragmented by different blunt end restriction enzymes and then ligated with adaptors to generate different libraries; from each library, nested PCR was performed with the gene and adaptor specific primers; then the amplified PCR product was purified and sequenced. Two forward primers distal to the *CNR1* intron breakpoint (IFP1, IFP2) and two reverse primers proximal to the *CNR1* coding region breakpoint (CRP1, CRP1) were designed as gene specific primers.

Initially, four genomic libraries were generated with blunt-end restriction enzymes, including *PvuII, EcoRV, DraI* and *StuI*. From each library, two nested PCR were performed: one was using primer pair IFP1/AP1 and IFP2/AP2 to map the intron breakpoint; the other was using primer pair CRP1/AP1 and CRP2/AP2 to map the coding region breakpoint (**Figure 5.7**). For the intron breakpoint mapping, the PCR product was obtained only from the *StuI* library; however, it was too small (<100 bp) to be informative. For the coding region breakpoint mapping, specific PCR products were generated from *DraI* and *EcoRV* libraries with a size around 300 bp (**Figure 5.8**). The PCR product was purified and cloned into the commercial T-vector for sequencing. The sequencing result from the *DraI* library showed that there was 11 bp of unknown sequence (AAACTTAAGCT) fused with genomic *CNR1* and this sequence was 7 bp upstream from the start codon (ATG) of the *CNR1* (**Figure 5.9A**). This fusion

was then confirmed by PCR analysis using primers binding to the boundary of the unknown sequence and the *CNR1* genomic region (**Figure 5.9B**).

Although it was known that the recognition site of *DraI* restriction enzyme is TTT | AAA, 11 bp plus 3 bp of TTT (TTTAAACTTAAGCT) was still too short to align to any specific genomic sequence. Therefore it was not clear at this point which gene or genomic fragment had been fused with *CNR1* in this prostate cancer case. More genomic libraries were generated with blunt end restriction enzymes, including *HincII* and *RsaI*, to map the intron breakpoint. However, so far, no specific PCR product has been characterised.

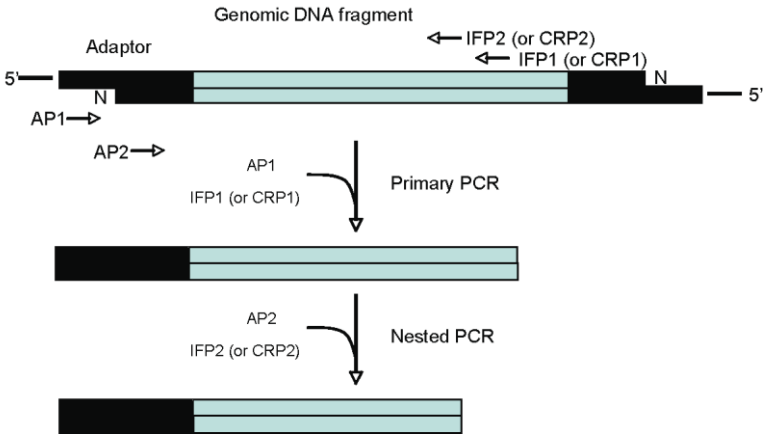

Figure 5.7 Schematic representation of *CNR1* deletion breakpoint mapping using genome walking assay

AP1 and AP2 are adaptor-binding primers for primary and nested PCR respectively. IFP1, IFP2, CRP1 and CRP2 are *CNR1* gene-specific primers. IFP1 and CRP1 are used for primary PCR. IFP2 and CRP2 are applied for nested PCR.

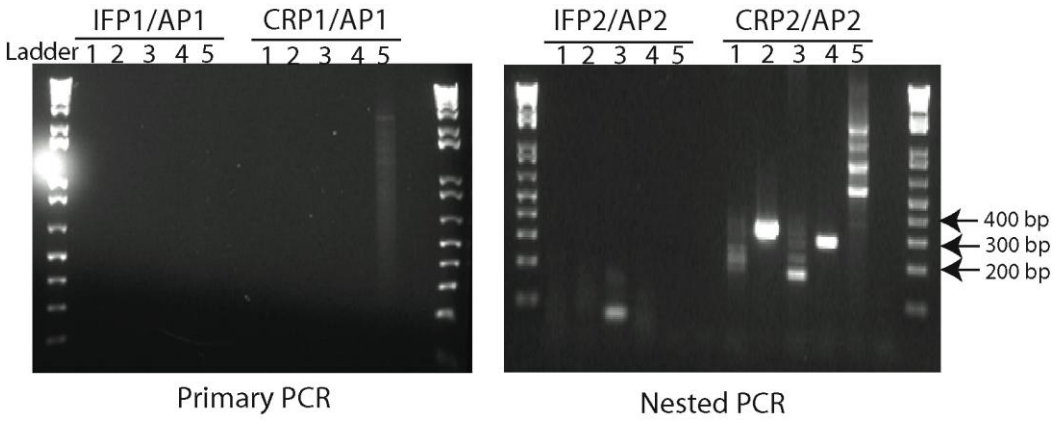

Figure 5.8 Primary and nested PCR for *CNR1* deletion breakpoint mapping

Lanes 1 to 4 represent libraries of *PvuII*, *DraI*, *StuI* and *EcoRV*, respectively, generated using genomic DNA of the prostate cancer patient p6363. Lane 5 represents the *PvuII* library generated from normal control genomic DNA. From each library, primary and nested PCR were performed. Primer pairs IFP1/AP1 and IFP2/AP2 were used for mapping the intron breakpoint; Primer pairs CRP1/AP1 and CRP2/AP2 were applied for mapping the coding region breakpoint. For the coding region breakpoint mapping, a specific PCR product was generated from *DraI* and *EcoRV* libraries with a size between 300 – 400 bp. 1 Kb plus DNA ladder (Invitrogen) was used.

Table 5.3 Primer sequence for confirmation of the *CNR1* fusion

Chimeric fwd	5'-AACTTAAGCTTGAGGTTATG
Chimeric rvsS	5'-AAGGACGAGAGAGACTTG
Chimeric rvsL	5'- TCTATGTCCATGAAGTTCTC

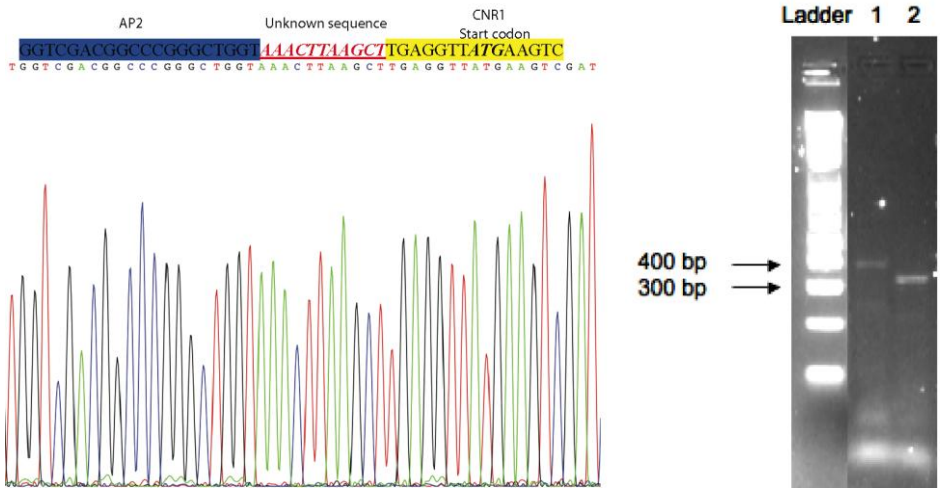

A B

Figure 5.9 *CNR1* fusion from sequencing data and PCR confirmation

(A) Sequencing data of *CNR1* from *DraI* library of the prostate cancer patient p6363; (B) Using forward primer binding to the fusion boundary and two reverse primers binding to downstream of *CNR1* coding region (**Table 5.3**), the *CNR1* fusion was confirmed using PCR analysis. Lane 1 is the PCR product generated using primer pair chimeric fwd and rvsL. Lane 2 is the PCR product generated using primer pair chimeric fwd and rvsS.

5.3.4.3 Exclusion of translocation and large scale chromosome rearrangement affecting *CNR1*

As illustrated above, a homozygous deletion and fusion in genomic DNA of *CNR1* was identified in one prostate cancer sample, which had down-regulated *CNR1* expression. According to the evidence in this case, it seems to fit in with our hypothesis regarding the identification of t(4;6)(q22;q15) and that translocation may contribute to cancer development though inactivation of tumour suppressor gene(s), which locate at breakpoint or adjacent deletion regions.

Whether the fusion is caused by inversion was examined using PCR analysis. As mentioned earlier, 14 bp of unknown sequence (TTTAAACTTAAGCT) was fused with *CNR1* genomic DNA. A minimum of 15 bp is required to blast with the whole human genome from Ensembl database (http://www.ensembl.org/Multi/blastview). Therefore, A, T, G, C was added to the 14 bp respectively and each sequence was blasted with the human genome. Eight regions on chromosome 6 were shown with the matched sequence. Semi-nested PCR analysis was performed with the forward primers binding to the potential fusion region and the two reverse primers, chimeric rvsS and rvsL, which were used to confirm the fusion in *CNR1* (described in the previous section). No specific product was generated after two rounds of PCR reaction indicating that the fusion was not caused by inversion.

Table 5.4 Eight regions on chromosome 6 matching with the 15 bp unknown sequence

Fusion sequence	Region	Strand	Position
ATTTAAACTTAAGCT	6q16	Plus	103846431 - 103846445
TTTTAAACTTAAGCT	6q25	Plus	155118846 - 155118860
	6q22	Plus	129899803 - 29899817
	6p22	Plus	21901382 - 21901396
	6q22.31	Minus	122742768 -122742782
	6q21	Minus	114977922 -114977936
	6p21	Minus	42659850 - 42659864
CTTTAAACTTAAGCT	6q25.3	Minus	155717426 -155717440
GTTTAAACTTAAGCT	No match		

Table 5.5 Forward primers used for investigation of the potential inversion involved in the gene *CNR1*

Primer	Sequence
6q16fwd	5'-CAACTCCTGTCCTAGGATG
6q25fwd	5'-AAAGTGCTGGGATTACAG
6q22fwd	5'-TCCTTCATGTAAGTGTCATC
6p22fwd	5'-CAAGAGTACTGTGCTCCTG
6q22.31fwd	5'-TCAGCTCAAGATGCTCTG
6q21fwd	5'-GAACATTAGTGTAAAACTCACTG
6p21fwd	5'-ACAAGAGAATATCACTGTCTG
6q25.3fwd	5'-CTTCTTGGCTTGAAGTCTC

In order to examine whether the fusion in *CNR1* genomic DNA in the prostate cancer case was caused by chromosomal translocation or large scale chromosome level deletion and insertions, FISH analysis was performed on the TMA containing the cancer case using dual-colour probes binding both sides of the identified *CNR1* breakpoint (**Table 5.6).** The FISH result showed that red and green signals were co-localised rather than split (**Figure 5.10**), suggesting that chromosome translocation or large scale chromosome level deletions or insertions were not responsible for the fusion.

Table 5.6 FISH probes for detection of potential translocation

Probeset	Region	BAC clone	Region	Length (bps)	Labelled	Signal colour
I	Distal *CNR1*	RP1-102H19	88,009,641-88,111,280	101,640	Biotinylated	Red
		RP1-249N8	88,688,904-88,750,812	61,908		
II	Proximal *CNR1*	RP1-72A23	89,632,912-89,781,452	148,540	DIG	Green
		RP3-322A2	90,145,402-90,277,901	132,499		

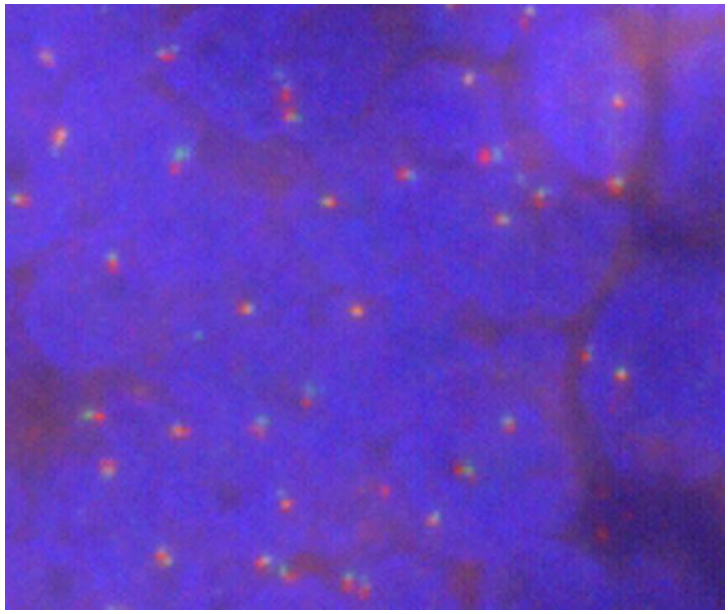

Figure 5.10 Representative FISH image for detection of potential translocation

Using probe sets binding to distal (red) and proximal (green) genomic DNA of *CNR1*, FISH analysis was applied to detect the potential translocation involved in the gene *CNR1* in the patient sample p6363. The representative image above shows all red and green signals to be co-localised in nuclei (blue) demonstrating there was no translocation involved in *CNR1* in this sample.

5.3.5 *CNR1* methylation in prostate cancer

In addition to genomic alterations, I also investigated whether DNA methylation contributed to *CNR1* down-regulation in prostate cancer. Ten BPH samples, 29 prostate cancer samples and 19 pairs of the normal and cancer samples were examined in this study. 24 bp (CGCCAGCGCCTTCCCTTGGCCCGG) of the promoter region (1027 bp) was analysed. There was no significant difference between the matched normal and cancer samples (p=0.922); in order to exclude the possibility that methylation of *CNR1* is a preneoplastic change, so that the methylation can occur in both cancerous and matched noncancerous tissues, we also compared the *CNR1* methylation in all the 48 cancer samples with ten BPH samples. However, there was still no significant difference (p=0.319) (**Table 5.7**).

Table 5.7 *CNR1* methylation status in 10 BPH and 48 clinical prostate cancer samples

No.	Diagnosis	PAI RED	Age	Gleason score	PSA (ng/ml)	Procedure	*CNR1* (% methylation)
1	BPH	No	74	N.A	2.6	(TURP)	0.0
2	BPH	No	73	N.A	6.2	(TURP)	3.1
3	BPH	No	80	N.A	4.2	(TURP)	2.5
4	BPH	No	67	N.A	N.A	(TURP)	1.7
5	BPH	No	85	N.A	N.A	(TURP)	4.1
6	BPH	No	60	N.A	N.A	(TURP)	2.7
7	BPH	No	69	N.A	N.A	(TURP)	3.0
8	BPH	No	65	N.A	N.A	(TURP)	3.8
9	BPH	No	83	N.A	1.57	(TURP)	3.2
10	BPH	No	74	N.A	4.66	(TURP)	2.5
11	Tumour	No	62	3+3=6	N.A	N.A	8.8
12	Tumour	No	62	4+4=8	N.A	N.A	2.9
13	Tumour	No	72	5+4=9	N.A	N.A	12.6
14	Tumour	No	73	4+4=8	N.A	N.A	1.6
15	Tumour	No	52	3+3=6	N.A	Prostatectomy	4.1
16	Tumour	No	77	3+4= 7	N.A	channel TURP	8.5
17	Tumour	No	75	5+5 = 10	14	channel TURP	2.7
18	Tumour	No	77	5+4=9	13	channel TURP	3.2
19	Tumour	No	72	5+4=9	N.A	channel TURP	3.8
20	Tumour	No	58	4+5=9	29	channel TURP	3.4
21	Tumour	No	66	4+5=9	95	channel TURP	8.8
22	Tumour	No	71	4+5=9	N.A	N.A	12.7
23	Tumour	No	64	4+3 = 7	N.A	Prostatectomy	8.3
24	Tumour	No		4+3 = 7	N.A	Prostatectomy	8.9
25	Tumour	No	74	3+3=6	5.2	Prostatectomy	12.5
26	Tumour	No	67	3+4=7	5.6	Prostatectomy	0.0
27	Tumour	No	39	3+3=6	16	Prostatectomy	1.8
28	Tumour	No	65	4+4=8	22.7	Prostatectomy	11.0
29	Tumour	No	65	3+4=7	9.9	Prostatectomy	10.7
30	Tumour	No	57	4+3=7	26.3	Prostatectomy	1.1
31	Tumour	No	70	3+4=7	10.6	Prostatectomy	7.1
32	Tumour	No	60	4+3=7	9.27	Prostatectomy	0.0
33	Tumour	No	74	5+4=9	37.01	Prostatectomy	8.6
34	Tumour	No	58	4+3=7	72.6	Prostatectomy	1.5
35	Tumour	No	53	3+4=7	15.47	Prostatectomy	4.3
36	Tumour	No	67	3+4=7	11.08	Prostatectomy	2.4
37	Tumour	No	78	5+4=9	88.68	Prostatectomy	4.0
38	Tumour	No	53	3+3=6	6.7	Prostatectomy	0.7
39	Tumour	No	50	4+3=7	8.5	Prostatectomy	2.6
40	Normal	Yes	N.A	N.A	N.A	N.A	5.4
41	Normal	YES	N.A	N.A	N.A	Prostatectomy	11.5

42	Normal	YES	N.A	N.A	N.A	Prostatectomy	3.0
43	Normal	YES	N.A	N.A	N.A	Prostatectomy	9.1
44	Normal	YES	N.A	N.A	N.A	Prostatectomy	11.8
45	Normal	YES	N.A	N.A	N.A	Prostatectomy	3.4
46	Normal	YES	N.A	N.A	N.A	Prostatectomy	7.6
47	Normal	YES	N.A	N.A	N.A	Prostatectomy	2.3
48	Normal	YES	N.A	N.A	N.A	Prostatectomy	0.0
49	Normal	YES	N.A	N.A	N.A	Prostatectomy	0.0
50	Normal	YES	N.A	N.A	N.A	Prostatectomy	1.5
51	Normal	YES	N.A	N.A	N.A	Prostatectomy	2.7
52	Normal	YES	N.A	N.A	N.A	Prostatectomy	1.7
53	Normal	YES	N.A	N.A	N.A	Prostatectomy	1.6
54	Normal	YES	N.A	N.A	N.A	Prostatectomy	1.3
55	Normal	YES	N.A	N.A	N.A	Prostatectomy	0.0
56	Normal	YES	N.A	N.A	N.A	Prostatectomy	6.1
57	Normal	YES	N.A	N.A	N.A	Prostatectomy	2.2
58	Normal	YES	N.A	N.A	N.A	Prostatectomy	7.2
59	Tumour	Yes	54	4+3 = 7	N.A	Prostatectomy	3.1
60	Tumour	YES	70	3+4=7	10.3	Prostatectomy	2.3
61	Tumour	YES	50	3+3=6	8.4	Prostatectomy	11.1
62	Tumour	YES	N.A	3+3=6	N.A	Prostatectomy	7.4
63	Tumour	YES	55	3+3=6	6.5	Prostatectomy	4.7
64	Tumour	YES	N.A	3+4=7	N.A	Prostatectomy	7.3
65	Tumour	YES	62	3+4=7	9.3	Prostatectomy	1.6
66	Tumour	YES	69	4+4=8	31.16	Prostatectomy	2.1
67	Tumour	YES	75	3+4=7	11.24	Prostatectomy	3.8
68	Tumour	YES	57	4+3=7	10.74	Prostatectomy	5.7
69	Tumour	YES	77	4+3=7	6.28	Prostatectomy	11.4
70	Tumour	YES	59	4+3=7	26.86	Prostatectomy	0.0
71	Tumour	YES	75	4+4=8	100	Prostatectomy	2.1
72	Tumour	YES	51	3+3=6	13.8	Prostatectomy	3.6
73	Tumour	YES	65	3+4=7	7.38	Prostatectomy	8.5
74	Tumour	YES	75	3+4=7	27.17	Prostatectomy	1.2
75	Tumour	YES	66	3+5=8	8.29	Prostatectomy	0.0
76	Tumour	YES	74	4+3=7	97	Prostatectomy	3.4
77	Tumour	YES	75	5+3=8	22.59	Prostatectomy	1.8

5.4 Discussion

Previously we applied Exon array analysis to examine systematically the expression alterations of all the genes located at the 6q15 deletion region. After qRT-PCR confirmation on enlarged clinical samples, *CNR1*, *BACH2* and *CNR1* showed common down-regulation in the prostate cancer samples. In this study, I further examined *CNR1* and *BACH2* protein expression and other genomic changes of *CNR1*.

Antibody specificity is critical for accurately examining protein localisation and expression while being applied to IHC analysis. In this study, the selection of *CNR1* was very careful as a recent study demonstrated a series of commercial antibodies that were not specific for either Western blot or IHC analysis. The *CNR1* antibody applied here for IHC analysis was purchased from Abcam, and has been demonstrated to have high specificity in prostate tissue (Chung *et al.*, 2009). This specificity was confirmed by my own study. *CNR1* is a cannabinoid receptor localised at the plasma membrane. FFPE prostate cancer cells, including LNCaP, PC3, DU145 and 22RV1, were used as negative controls, as they were demonstrated previously to have very low *CNR1* expression using qRT-PCR analysis. The initial IHC analysis showed no or very weak staining of the prostate cancer cell lines, which was consistent with the low RNA expression. In BPH samples, the staining intensity varied between samples, but this also correlated with previous qRT-PCR results showing different RNA expression levels among BPH samples. In addition, *CNR1* was shown to be localised to the plasma membrane of both basal and luminal epithelial cells, and there was little or no staining of the stroma. Therefore the specificity of the *CNR1* antibody from

Abcam was well demonstrated in this study. None of the 58 cancer cases showed strong *CNR1* expression. In contrast, among 31 informative BPH samples, 32.3% of them showed strong positive expression and 51.6% of them showed weakly positive expression. Only a very small proportion of the 31 BPH samples had negative *CNR1* expression. Moreover, among 58 prostate cancer cases, 45 cases have matched normal glands. The majority of them showed lower expression of *CNR1* in cancer cells compared with adjacent normal glands and none of the 45 cases had higher *CNR1* expression in cancer cells than in the matched normal cells. This study, therefore, demonstrated that the protein expression of *CNR1* frequently was down-regulated in prostate cancer samples. Results in accord with the low levels of RNA expression determined previously by qRT-PCR analysis.

So far, only one reported study has examined *CNR1* expression using IHC analysis in 372 prostate cancer cases and 349 BPH samples (Chung *et al.*, 2009) and this study used the same *CNR1* antibody (Abcam). Using a slightly different scoring for evaluation of *CNR1* staining, the immunoreactive intensity of *CNR1* was scored ranging from 0 – 3 (0 is absent and 3 is high). 61.6% of the BPH samples and 75.3% of the cancer samples were scored ≥ 2. Analysis of 269 prostate cancer patients, who were conservatively managed, for *CNR1* expression showed that a score ≥ 2 was associated with poorer disease specific survival (Chung *et al.*, 2009). Therefore, using the same antibody, an exactly opposite correlation between *CNR1* level and prostate carcinogenesis was observed in my study. I did not find any prostate cancer samples showing strong *CNR1* expression. As *CNR1* activation generally is considered to prevent tumour development (Alexander *et al.*, 2009) and mutation of *CNR1* has been reported

(Gadzicki *et al.*, 1999), the previously observed overexpression of *CNR1* seems counter intuitive but I am unable to explain the reason for the difference between these two investigations.

The inactivation of gene expression can be caused by somatic mutation and epigenetic methylation. PCR and sequencing analysis revealed a nucleotide change in 22RV1 cells and a small deletion (~ 5Kb) in the upstream and 5' UTR region of the *CNR1* gene in one of five clinical prostate cancer samples. After the breakpoint of the deletion was mapped, an 11 bp unknown sequence, 7bp upstream of the *CNR1* start codon (ATG), was identified. Gene fusion (or genomic fragment fusion) can be caused by chromosomal translocations, internal deletions, inversions or insertions. As the possibility of large scale chromosome rearrangements and inversion in causing this gene fusion has been excluded, small deletion and/or insertion might be the possible mechanism to cause this genomic fusion. However, due to the upstream breakpoint of the deletion failing to be mapped, it is difficult to draw this conclusion with any confidence yet.

A silent mutation (1359G-->A) in codon 453 (Thr) of the *CNR1* gene was identified in the genome of 22RV1 cells. This nucleotide change 1359 (G/A) has been reported as a common polymorphism in Caucasian populations (Gadzicki *et al.*, 1999). Recently, a study in colorectal cancer has shown that patients, who had genotype G/A plus A/A, had a shorter overall survival time than G/G wild-type patients (Bedoya *et al.*, 2009b). A similar study in oesophageal cancer has shown that the patients with the A/A type had a reduced survival time in

comparison to the G/G type (Bedoya *et al.*, 2009a). So far, no study has been performed to examine *CNR1* sequence detail in prostate cancer.

The inactivation of the gene *CNR1* due to methylation of the *CNR1* promoter has been reported in colorectal cancer (Wang *et al*., 2008). In this study, the *CNR1* methylation was examined in 48 prostate cancer samples and ten BPH control samples. Some prostate cancer samples were shown to have a higher percentage of cells (> 10%) with *CNR1* promoter methylation than the average of ten BPH samples (2.66%). However, there was no significant difference between BPH and all of the cancer samples (p=0.319). These results were taken to indicate that DNA methylation might account for the *CNR1* inactivation in some of the prostate cancer samples but it is not the prevalent mechanism.

The expression of the gene *BACH2* was also examined in prostate cancer samples in this study. Cytoplasmic expression of *BACH2* was slightly less in the examined cancer cases as compared with BPH samples. However, nuclear expression of *BACH2* was significantly higher in prostate cancer cases than in BPH samples (p=0.001). Therefore, at the protein level, the major difference in *BACH2* expression between prostate cancer and BPH samples seems to be an altered localisation rather than a changed expression level.

The transcription factor *BACH2* is a member of the protein family, which harbours a basic region leucine zipper (bZip) DNA binding domain. In addition, *BACH2* possesses a BTB domain. Both of these domains are involved in forming heterologous protein-protein interactions (Albagli *et al.*, 1995; Vinson *et al.*,

2006). The cytoplasmic localisation of the *BACH2* protein is controlled by the cytoplasmic localisation signal present in the bZip domain and a C-terminal nuclear-export signal (Hoshino *et al.*, 2000). In B-cells, *BACH2* is predominantly cytoplasmic, whereas oxidative stress induces its nuclear accumulation. Once in this subcellular location, it induces expression of genes involved in apoptosis (Kamio *et al.*, 2003; Yoshida *et al.*, 2007). In a study of ovarian cancer, it was shown that cytoplasmic *BACH2* expression was increased significantly in ovarian cancer relative to benign cases. In addition, increased nuclear *BACH2* levels in ovarian cancer samples were associated with decreased time to disease recurrence (Motamed-Khorasani *et al.*, 2007). The full significance of altered *BACH2* expression in ovarian cancer still is unknown. However, it was postulated that the different *BACH2* isoforms localise to different cellular compartments where they may participate in cell processes distinct from transcriptional regulation (Motamed-Khorasani *et al.*, 2007). The results from our study and the ovarian cancer study indicated further analysis of *BACH2* isoform expression and potential cytoplasmic/nuclear function in prostate or ovarian epithelial cells is warranted.

In conclusion, the protein expression of *CNR1* is down-regulated in clinical prostate cancer samples compared with BPH controls, which is consistent with my previous study showing lowered RNA expression in prostate cancer samples. In contrast, the protein expression of *BACH2* was not correlated with previously examined RNA expression patterns in clinical prostate cancer samples. Further study of *CNR1* and *BACH2* cellular function is needed to demonstrate whether, and how, they play a tumour suppressor role in prostate cancer.

6 TUMOUR SUPPRESSOR ROLE OF *CNR1* IN PROSTATE CANCER

6.1 Introduction

In the previous three chapters, I have explained the reasons and processes used for the identification of candidate tumour suppressor genes located at 6q15, which is one of the most frequently deleted regions in prostate cancer. *CNR1* was the only gene identified so far that showed down-regulated expression at both the RNA and protein level in clinical prostate cancer samples.

To date, the majority of studies in the literature reported have supplied only indirect evidence for the relationship between *CNR1* and cancer. The ligands of *CNR1*, such as endocannabinoids and *CNR1* agonists, have been demonstrated by many studies to have an anti-tumourigenic effect, affecting cell growth, apoptosis, angiogenesis, migration, invasion, adhesion, and an ability to metastasise in various cancers (Freimuth *et al.*, 2010). Although it has been demonstrated that cannabinoids exerted their anti-tumourigenic effects through *CNR1* and *CNR2* (Alexander *et al.*, 2009), whether *CNR1* or *CNR2* itself have a tumour suppressor role has not been well studied. The only direct evidence favouring a possible tumour suppressor role for *CNR1* was a recent study in colorectal cancer, which demonstrated that the expression of *CNR1* was silenced due to methylation of its promoter (Wang *et al.*, 2008). Moreover, loss of expression of *CNR1* has been shown to accelerate intestinal tumour growth *in vivo* (Wang *et al.*, 2008). In another study, in hepatocellular carcinoma, over-expression of *CNR1* was shown to correlate with improved prognosis of the

patients (Xu *et al.*, 2006). No previous studies on the role of *CNR1* in prostate cancer have been reported. Because of my identification of the common down-regulation of *CNR1* in clinical prostate cancer samples, I was encouraged to investigate further the cellular function of *CNR1* in prostate cancer.

6.2 Aim

I aimed to examine the cellular function of *CNR1 in vitro* in prostate cancer cells to determine if it has a role as a tumour suppressor.

6.3 Results

6.3.1 *CNR1* transient over-expression

6.3.1.1 Plasmid construction

As described earlier, *CNR1* expression levels were very low in six prostate cancer cell lines. In four immortalised prostate epithelial cell lines available in our group, including PNT1A, PNT2, PNT2-C2 and RWPE, low expression levels of *CNR1* were also revealed by qRT-PCR analysis. The expression of *CNR1* was not detected with 40 cycles of qRT-PCR reaction in these four cell lines. Therefore, it was considered that over-expressing *CNR1* in prostate cancer cell lines would be more feasible than knocking down its expression. In order to over-express *CNR1* in prostate cancer cells, a plasmid incorporating the coding sequence of *CNR1* was constructed. Using cDNA from a BPH sample (p129), which was demonstrated to have a high expression of *CNR1* (section **4.3.2.3**), as

a template, the coding sequence of *CNR1* with a flag tag sequence incorporated before the stop codon of *CNR1* was amplified using PCR analysis (details in **2.7.2.1**). A specific band was obtained (**Figure 6.1**), which was at the expected size of ~1.5 Kb. Then the PCR product was purified, digested with restriction enzymes and ligated to the vector pcDNA3.1 (+) as described in **2.8.2.1**. The ligated plasmids were transformed into competent bacteria cells, which were then cultured until single clones of bacteria were obtained. Five single colonies were inoculated and cultured. Then the plasmids were extracted and sequenced (details in **2.8.2.1**). The plasmid with the correct *CNR1* and flag tag sequence, named pcDNA-CNR1flag, was used for my further study.

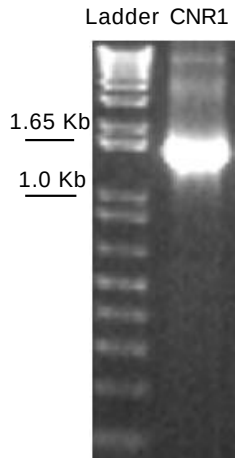

Figure 6.1 *CNR1* coding sequence amplification using PCR analysis.

PCR analysis was performed to amplify the coding sequence of *CNR1* from cDNA of one BPH sample (p129). The expected size of the PCR product is 1467 bp. 1 Kb Plus DNA ladder (Invitrogen) and the PCR product were run on a 1% agarose gel.

6.3.1.2 Transfection efficiency optimisation in 22RV1 cells

Prostate cancer cell lines are known to be difficult to transfect. Four cell lines, LNCaP, PC3, DU145 and 22RV1, commonly are used for studying prostate cancer. However, in terms of DNA transfection, only 22RV1 cells are easily transfected. Therefore 22RV1 cells were chosen to be used in this study as a model to study the function of *CNR1 in vitro*.

Two chemical transfection reagents, JetPEI-RGD and Lipofectamine™ 2000, were used to optimise transfection conditions in 22RV1 cells. JetPEI-RGD was indicated for the transfection of cell lines of epithelial origin that were poorly transfectable. Lipofectamine™ 2000 was commonly used in our laboratory and has been shown to have a high transfection efficiency in various human cell lines.

pcDNA-GFP (described in **2.8.1.1**) was used to determine the transfection efficiency of each reagent in 22RV1 cells. The pcDNA-GFP transfected cells were observed using a fluorescence microscope 48 h after transfection. Less than 5% of 22RV1 cells transfected using JetPEI-RGD reagent expressed visually detectable GFP. In contrast, approximately 40-50% of 22RV1 cells transfected using Lipofectamine™ 2000 reagent expressed visually detectable GFP. Lipofectamine™ 2000 was therefore chosen for further transfection experiments.

6.3.1.3 *CNR1* transient over-expression in 22RV1

The plasmids, pcDNA-CNR1flag and pcDNA3.1(+) (as a control), were transfected into 22RV1 cells using Lipofectamine™ 2000 reagent. The RNA expression of *CNR1* was examined 24 h after transfection. The RNA extracted

from the transfected cells was treated with DNase to remove residual genomic/plasmid DNA contamination before cDNA was synthesised. Since commercial TaqMan gene expression assays are all designed to examine *CNR1* expression using probes binding to the 5'-UTR region (https://www.appliedbiosystems.com/absite/us/en/home.html), they were not appropriate to examine *CNR1* over-expression since the plasmid constructed contained only the coding sequence of *CNR1*. Therefore semi-quantitative RT-PCR analysis was performed, as the primers, which previously were used to map deletion breakpoints of the gene *CNR1* in a clinical prostate cancer sample (section **5.3.2.2**), already were available. Using the housekeeping gene, *β-actin*, as a control, the expression of *CNR1* in pcDNA3.1 and pcDNA-CNR1flag transfected 22RV1 cells was examined. The same amount of cDNA (300 ng) was used in all the PCR reactions. After 35 cycles of amplification, equal volumes of PCR products were loaded on a 1.5% agarose gel. Results showed that *CNR1* was expressed at a markedly higher level in pcDNA-CNR1flag transfected 22RV1 cells than in pcDNA3.1(+) transfected cells (**Figure 6.2**).

The protein expression of *CNR1* was examined at 48 h after transfection using Western blot analysis. The expected molecular weight of *CNR1* is 54 kDa (non-glycosylated) or 63 kDa (glycosylated). 50 μg of total protein from each of the pcDNA3.1(+) and pcDNA-CNR1flag transfected 22RV1 cells was used to detect *CNR1* expression. Using a *CNR1* antibody from Abcam, multiple bands were obtained. Between the molecular weights 52 kDa and 72 kDa, there was one strong band. There were also a few very weak bands between 52 kDa and 72 kDa, but they most probably were artificial bands generated because of the

prolonged exposure. However, none of the bands was shown to have an increased intensity in pcDNA-CNR1flag transfected 22RV1 cells compared with the pcDNA3.1(+) transfected cells (**Figure 6.3A**). In order to examine *CNR1* expression using an anti-Flag antibody, a positive control sample was included to demonstrate that the antibody itself works properly. The positive control consisted of total protein extracted from 293 cells, which were transiently over-expressing pcDNA-DARRP32flag, obtained from Dr Yaohe Wang's group in our Institute (www.cancer.qmul.ac.uk/staff/wang.html). The DARRP32/flag over-expression in these cells previously has been demonstrated, using Western blot analysis with the same anti-Flag antibody, by his group. The expected size of DARRP32flag was 32 kDa. Using the anti-Flag antibody, no band was detected in either pcDNA3.1 or pcDNA-CNR1flag transfected 22RV1 cells, although the positive control showed a strong and specific band (**Figure 6.3B**). It indicated that although *CNR1* was over-expressed in 22RV1 cells at the RNA level, it was not overexpressed at the protein level.

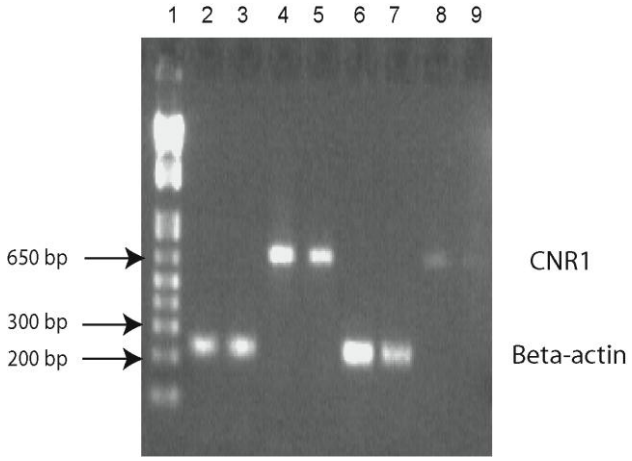

Figure 6.2 *CNR1* expression in transiently transfected 22RV1 cells, measured by semi-quantitative RT-PCR analysis

Semi-quantitative RT-PCR analysis was performed to examine the *CNR1* and β-actin (as a loading control) expression in pcDNA-CNR1flag and pcDNA3.1(+) transfected 22RV1 cells. (1) Invitrogen 1 Kb Plus DNA ladder; (2) and (3) β-actin expression (expected size at 250 bp) in pcDNA-CNR1flag transfected 22RV1 cells as measured in duplicate; (4) and (5) *CNR1* expression in pcDNA-CNR1flag (expected size at 681 bp) transfected 22RV1 cells as measured in duplicate; (6) and (7) β-actin expression in pcDNA3.1(+) transfected 22RV1 cells as measured in duplicate; (8) and (9) *CNR1* expression in pcDNA3.1(+) transfected 22RV1 cells as measured in duplicate. All of the PCR products were run on a 1.5% agarose gel.

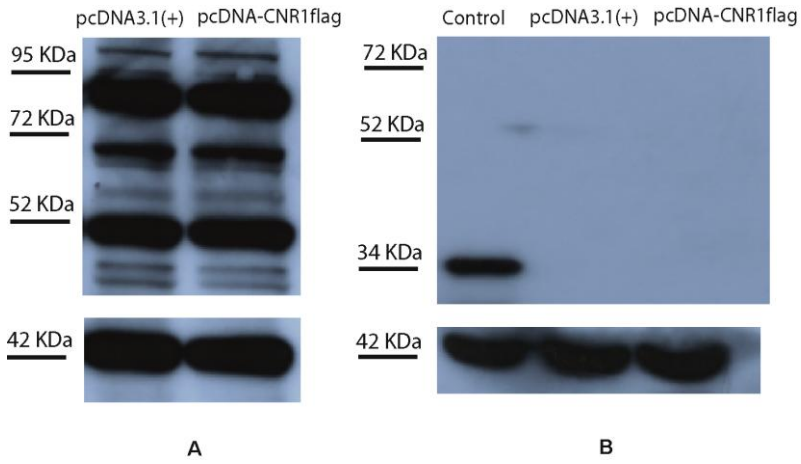

Figure 6.3 Protein expression of *CNR1* in transiently transfected 22RV1 cells examined by Western blot analysis

(A) Using a *CNR1* antibody (Abcam, 1:200 dilution), *CNR1* expression was examined in 22RV1 cells transfected with pcDNA3.1(+) and pcDNA-CNR1flag. (B) Using an anti-Flag antibody (Sigma, 1:1000 dilution), Flag-tag expression was examined in one positive control sample (expected size 32 kDa) and 22RV1 cells transfected with pcDNA3.1(+) and pcDNA-CNR1flag. No protein was detected in pcDNA3.1(+) and pcDNA-CNR1flag transfected 22RV1 cells. β-actin was used as a loading control with an expected size of 43 kDa.

6.3.1.4 *CNR1* transient over-expression using Nucleofector technology

I tried to increase the transfection efficiency, in case the lack of over-expression of *CNR1* was due to a low transfection efficiency, by using the nucleofector transfection method, which has been demonstrated to increase the transfection rate in various types of cells. Using 4 μg of Amaxa's pmaxGFP control vector with the built-in programme, A-020, it was found to result in an approximate 100% transfection efficiency in 22RV1 cells at 48 h after transfection, as observed using a fluorescence microscope. However, using pcDNA-GFP under the same conditions, transfection efficiency reached only approximately 30-40%. This result suggested that the vector itself could affect gene expression efficiency dramatically.

In order to achieve a better transfection efficiency in the 22RV1 cells, the open reading frame sequence of *CNR1* with a Kozak sequence was inserted between KpnI and SacI of the pmaxCloning MCS, which was the same site as the *GFP* sequence in the pmaxCloning vector (pmaxGFP) (details described in **2.8.2.2**). This plasmid was named pmaxCNR1. The pmaxCNR1 plasmid was transfected into 22RV1 cells using the optimised conditions illustrated above. The RNA and protein expression of *CNR1* was examined at 24 h and 48 h respectively after transfection. Similarly to previous observations, *CNR1* was over-expressed at the RNA level in pmaxCNR1 transfected 22RV1 cells compared with pmaxCloning transfected cells (**Figure 6.4**). However, at the protein level, no difference in the intensity of the band (between 52 kDa and 72 kDa) was shown between pmaxCNR1 and pmaxCloning transfected 22RV1 cells using Western blot

analysis (**Figure 6.5**). Whether it was caused by the possibility that 22RV1 cells lost the ability to translate the *CNR1* mRNA to a protein, or it was due to the ineffectiveness of the *CNR1* antibody for Western blot analysis, still needs to be clarified.

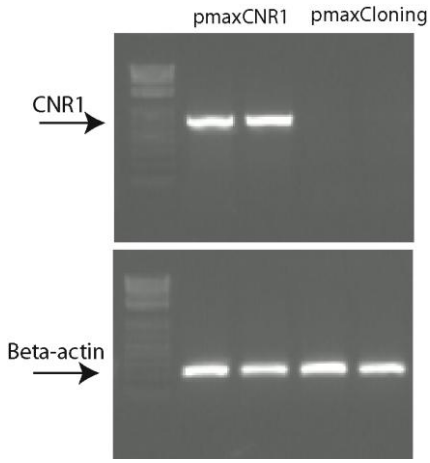

Figure 6.4 *CNR1* expression in transient transfected 22RV1 cells measured by semi-quantitative RT-PCR analysis

Semi-quantitative RT-PCR analysis was performed to examine the *CNR1* and β-actin (as a loading control) expression in pmaxCNR1 and pmaxCloning transfected 22RV1 cells respectively. *CNR1* and β-actin expression in each of the transfected 22RV1 cells were measured in duplicate. Invitrogen 1 Kb Plus DNA ladder was used. All of the PCR products were run on a 1.5% agarose gel.

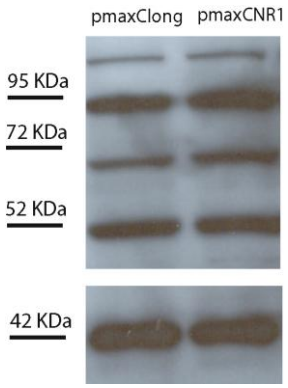

Figure 6.5 Protein expression of *CNR1* in transiently transfected 22RV1 cells, examined by Western blot analysis

Using the *CNR1* antibody (Abcam, 1:200 dilution), *CNR1* expression was examined in 22RV1 cells transfected with pmaxCloning and pmaxCNR1. β-actin was used as a loading control with an expected size of 43 kDa.

6.3.1.5 *CNR1* transient over-expression in 293 cells

In order to reveal whether the lack of detection of the *CNR1* protein over-expression was associated only with the 22RV1 cell line, HEK293 cells were used as a control to demonstrate if *CNR1* can be over-expressed. HEK293 cells are well known for being easy to transfect and have been used widely to express various exogenous genes. Several studies have reported the stable over-expression of *CNR1* in HEK293 cells. Moreover, HEK293 cells were used routinely in our laboratory as a model to study the function of various genes, so the transfection conditions have been optimised. Using the Effectene transfection reagent, a transfection efficiency of approximately 50% can be achieved.

In addition, two commercial plasmids were purchased in case the Flag tag at the C-terminal of *CNR1* affected the translation or reduced the stability of the *CNR1* protein. One of the plasmids, named pcDNA-CNR1, only contains the *CNR1* open reading frame sequence. The other plasmid, named pcDNA-3HA_CNR1, had three HA-tags at the N-terminal of *CNR1*.

The plasmids, pcDNA3.1(+), pcDNA-CNR1, pcDNA-3HA_CNR1 and pmaxCNR1 were transfected into HEK293 cells respectively using the Effectene reagent (details in **2.8.1.1.2**). The RNA and protein expression of *CNR1* was examined at 24 h and 48 h respectively after transfection. Again, the over expression of *CNR1* was detected at the RNA level but not at the protein level. Using a *CNR1* antibody from Abcam, no difference in the intensity of the bands (between 52 kDa and 72 kDa) was detected between *CNR1* over-expressed and control 293 cells using Western blot analysis (**Figure 6.6**). Using an anti-HA

antibody, no band was detected in pcDNA-3HA_CNR1 transfected 293 cells. Accordingly, the non-detection of *CNR1* expression at the protein level was not associated with cell type. It was considered that these inconclusive results most probably were caused by the ineffectiveness of the *CNR1* antibody for Western blot analysis. As for the non-detection of HA-tag, it may have been caused by protein instability, which is due to the extra tag sequence at the N-terminal of *CNR1*.

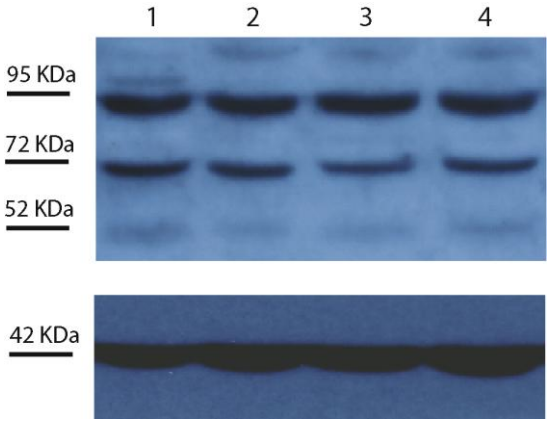

Figure 6.6 Protein expression of *CNR1* in transiently transfected 293 cells examined by Western blot analysis

Using a *CNR1* antibody (Abcam, 1:200 dilution), *CNR1* expression was examined in 293 cells transfected with pcDNA3.1(+) (lane 1), pcDNA-CNR1 (lane 2), pcDNA-3HA_CNR1 (lane 3) and pmaxCNR1 (lane 4), respectively. β-actin was used as a loading control with an expected size of 43 kDa.

6.3.1.6 Functional study of *CNR1* in transiently over-expressed 22RV1 cells

Although the detection of the *CNR1* protein did not prove possible, I considered its expression might still be increased without being detected using the currently

available approach. If *CNR1* expression was increased, it should have played a role in 22RV1 cells. Therefore I took a further step to examine the function of *CNR1* in transiently transfected 22RV1 cells. It was demonstrated previously that the transfection efficiency of the chemical reagent Lipofectamine™ 2000 achieved 40-50% in 22RV1 cells whereas the Nucleofection method reached approximate 100% transfection efficiency in 22RV1 cells. Although chemical reagent transfection was less efficient than the Nucleofection method, 40-50% transfection efficiency should be sufficient to generate distinguishable cellular functional changes (if *CNR*1 indeed was over-expressed) compared with the vector alone in transfected cells. Therefore 22RV1 cells were transfected with pcDNA-CNR1 and pcDNA3.1 using the Lipofectamine™ 2000 reagent and also transfected with pmaxCNR1 and pmaxCloning using the Nucleofection method to examine the functional effects of transiently over-expressing *CNR1* in 22RV1 cells.

I first examined the effects of exogenous *CNR1* on 22RV1 cell viability using an MTS assay. Results from both transfection methods showed no difference in the cell viability of 22RV1 cells (**Figure 6.7**). Next I studied the effect of *CNR1* on the cell proliferation of 22RV1 cells using a colony formation assay. The results from both transfection methods showed fewer colonies formed in *CNR1* putatively over-expressing 22RV1 cells (**Figure 6.8**). I further analysed whether *CNR1* has any effect on the invasion of 22RV1 cells. The results from both transfection methods showed that exogenous *CNR1* led to a decreased number of invading cells (**Figure 6.9**).

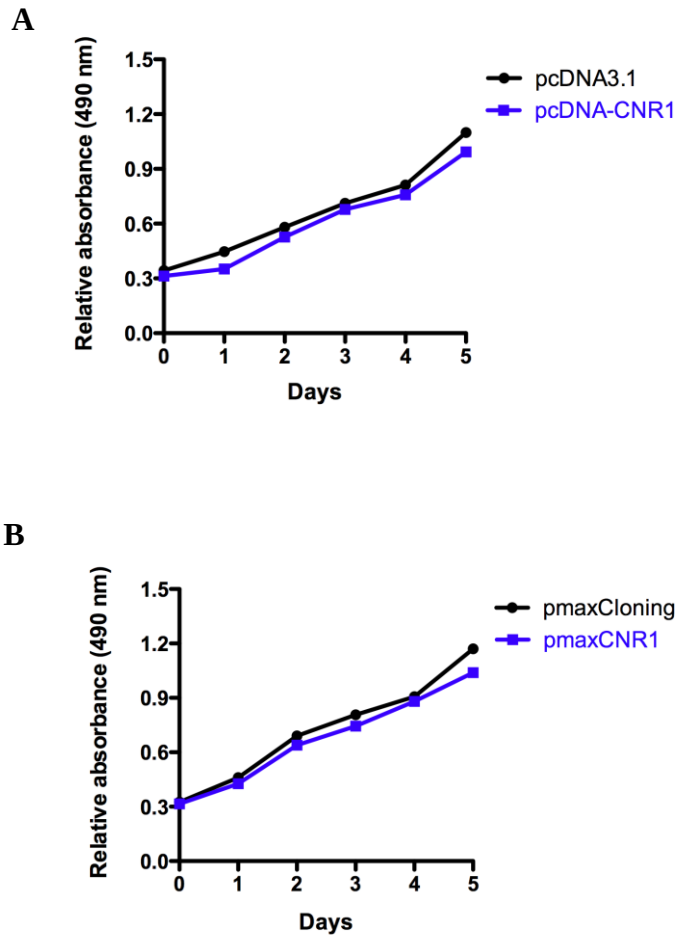

Figure 6.7 Over-expression of *CNR1* in transiently transfected 22RV1 cells does not affect cell viability as assessed by a MTS assay.

(A) Transiently transfected 22RV1 cells with pcDNA3.1 (control) and pcDNA-CNR1 were seeded respectively onto a 96-well plate at 5000 cells/well. The MTS assay was applied every 24 h for 5 days. (B) Transiently transfected 22RV1 cells with pmaxCloning (control) and pmaxCNR1 were seeded onto 96-well plate at 5000 cells/well. The MTS assay was applied every 24 h for 5 days No significant difference was noted between the *CNR1* over-expressing 22RV1 cells and control cells.

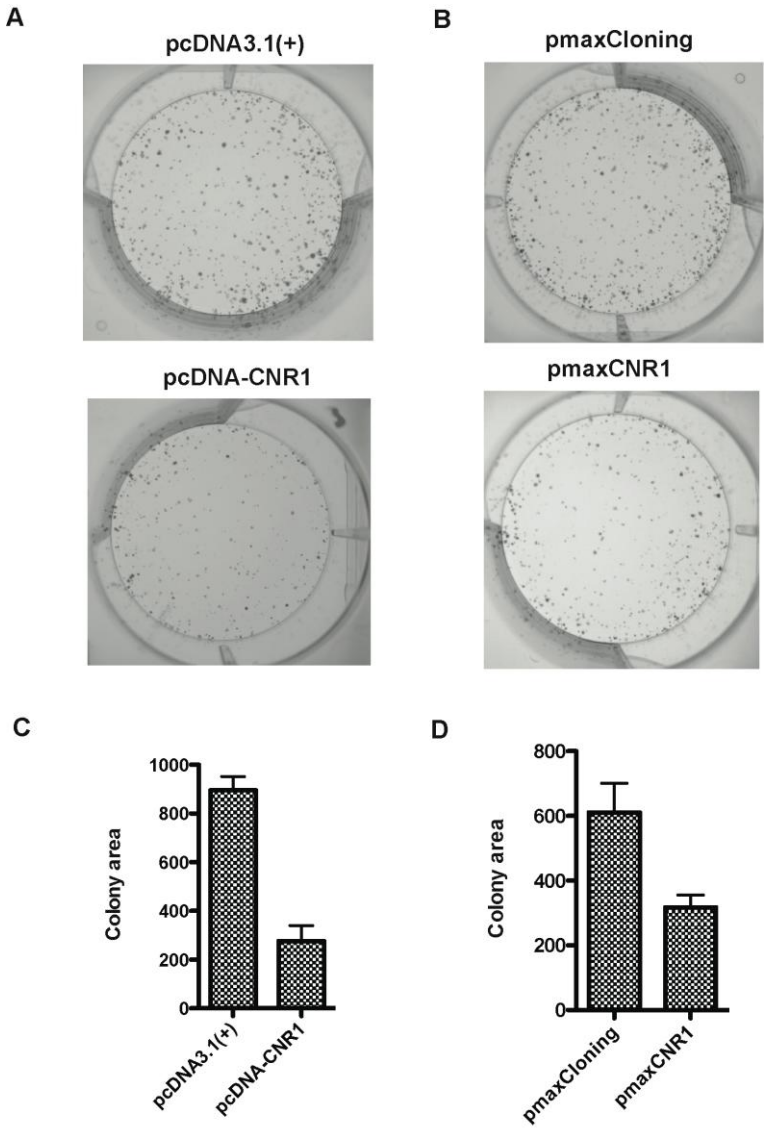

Figure 6.8 The effect of *CNR1* on cell proliferation examined by colony formation assay

(A) and (B) Representative images showing colonies formed from transiently transfected 22RV1 cells with pcDNA3.1(+), pcDNA-CNR1, pmaxCloning, pmaxCNR1, respectively. (C) and (D) Bar charts show the area covered by colonies measured using ImageJ software (details in 2.10.2). The colony area is smaller in pcDNA-CNR1 transiently transfected 22RV1 cells compared with pcDNA3.1(+) transfected cells (C). The colony area is smaller in pmaxCNR1 transiently transfected 22RV1 cells compared with pmaxCloning transfected 22RV1 cells (D). The graph represents an average of three replicates ± standard error.

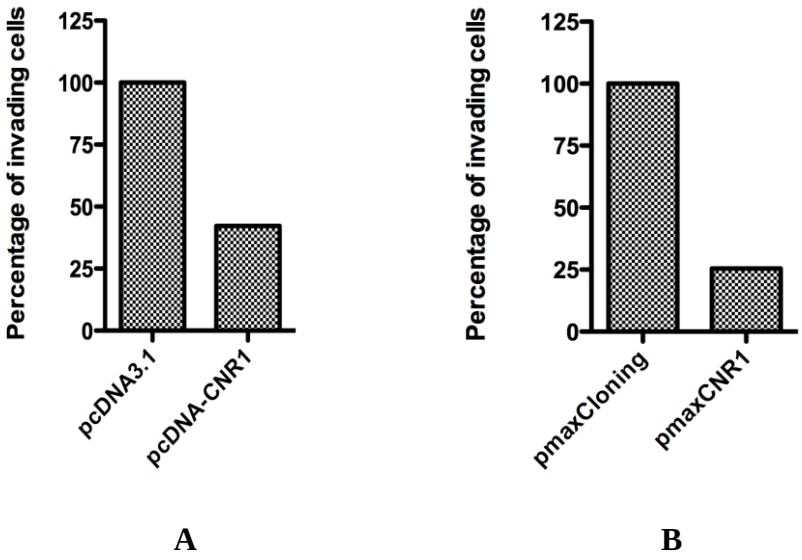

Figure 6.9 The effect of *CNR1* on cell invasion in transiently transfected 22RV1 cells examined by Matrigel invasion assay.

Bar charts show the percentage of invading cells through the Matrigel-coated transwell chambers measured after 48 h. Results are represented normalised to control. (A) Mean value of three replicates of invading cells from pcDNA3.1(+) and pcDNA-CNR1 transfected 22RV1 cells. (B) Mean value of three replicates of invading cells from pmaxCloning and pmaxCNR1 transfected 22RV1 cells.

6.3.2 *CNR1* stable over-expression in 22RV1 cells

6.3.2.1 *CNR1* over-expression confirmation

As *CNR1* has been stably over-expressed in HEK293 cells, but its protein level expression cannot be detected in my transient transfected cells, a 22RV1 cell line with stably over-expressed *CNR1* was deemed necessary to be established in order to demonstrate over-expression of *CNR1* at the protein level and also to further perform cellular functional studies. Four plasmids, pcDNA3.1, pcDNA-CNR1, pcDNA-CNR1flag and pcDNA-3HA_CNR1, were transfected into 22RV1 cells respectively and clones with exogenous *CNR1* expressed were selected using geneticin according to the details described in **2.8.1.3**. The plasmid pmaxCNR1 could not be used for establishing stable transfected cells as the vector itself does not contain the neomycin resistance gene for the selection of stable cells. Three stable cell lines with over-expression of *CNR1*, *CNR1flag* and *3HA_CNR1* respectively and one control stable cell line with pcDNA3.1 vector were generated after approximately six weeks selection. No obvious morphological or proliferative changes were observed in the resistant cells. The RNA expression was examined using SYBR-Green qRT-PCR analysis to measure the precise fold change of *CNR1* expression (details in **2.5.6.2.2**). It showed that *CNR1* expression was 6904, 3381, 2380 fold higher in *CNR1*, *3HA_CNR1* and *CNR1flag* over-expressed 22RV1 cells, respectively, as compared with the control cell line (**Figure 6.10**).

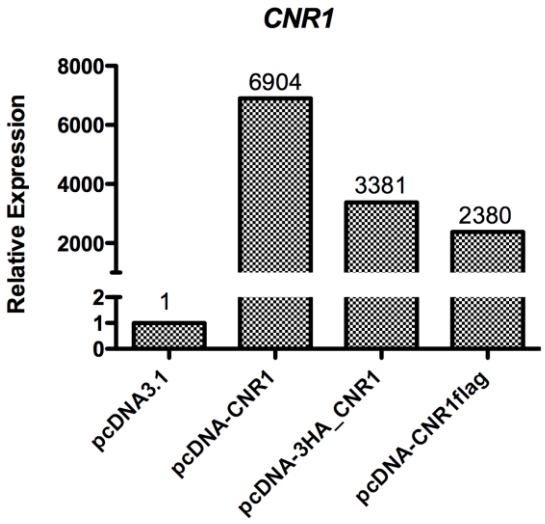

Figure 6.10 Over-expression *CNR1* at the RNA level in stably transfected 22RV1 cells using SYBR green qRT-PCR analysis.

The expression of *CNR1* RNA levels in stably transfected 22RV1 cells with pcDNA-CNR1, pcDNA-3HA-CNR1 and pcDNA-CNRflag, were measured by SYBR green qRT-PCR respectively relative to the expression of the housekeeping gene β-actin and normalised to the pcDNA3.1(+) transfected 22RV1 cells as a control.

The over-expression of *CNR1* was then examined using Western blot analysis. As previously observed in the transiently transfected cells, using *CNR1* antibody,

no difference in intensity of the band (between 52 kDa and 72 kDa) was shown between *CNR1* over-expressing and control cells (**Figure 6.11**).

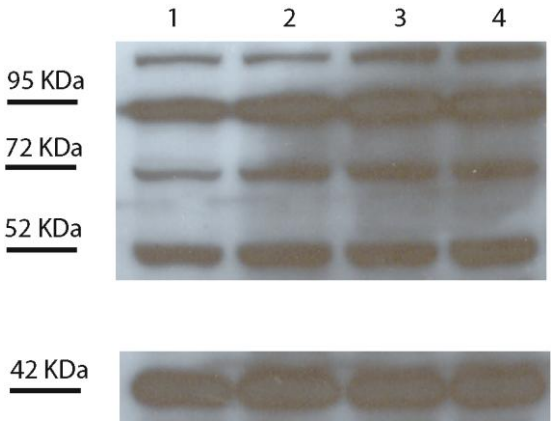

Figure 6.11 Protein expression of *CNR1* in stably transfected 22RV1 cells examined by Western blot analysis

Using *CNR1* antibody (Abcam, 1:200 dilution), *CNR1* expression was examined in 22RV1 cells transfected with pcDNA3.1(+) (lane 1), pcDNA-CNR1 (lane 2), pcDNA-3HA_CNR1 (lane 3) and pcDNA-CNR1flag (lane 4), respectively. β-actin was used as a loading control with expected size at 43 kDa.

Because *CNR1* over-expression could not be demonstrated by Western blot analysis, I performed IHC analysis to detect *CNR1* protein expression. The *CNR1* expression was demonstrated previously in clinical BPH and prostate cancer samples (**Chapter 5**). Therefore, I speculated that the *CNR1* antibody might not be good for Western blot analysis but that it would be fine for IHC or other analysis methods.

Cells from four stable cell lines were paraffin embedded and IHC analysis with *CNR1* antibody from Abcam was performed to examine *CNR1* expression at the

protein level (details in **2.7.2**). The *CNR1* was shown to be over-expressed in pcDNA-CNR1 transfected 22RV1 cells, with the staining intensity and number of stained cells being substantially higher in pcDNA-CNR1 transfected 22RV1 cells as compared with control cells (**Figure 6.12**). In contrast, *CNR1* was not shown to be over-expressed in pcDNA-CNR1flag and pcDNA-3HA_CNR1 transfected cells, although these two cell lines had 2380 and 3381 fold over-expression of *CNR1* at the RNA level respectively.

In order to determine the specificity of the *CNR1* antibody for IHC analysis, siRNA was used to knock down *CNR1* expression in the stably transfected 22RV1 cells. *CNR1*-targeting siRNA and non-targeting siRNA were transfected respectively into pcDNA-CNR1 transfected stable 22RV1 cells (details described in **2.8.2**). Protein expression of *CNR1* was examined using IHC analysis at 96 h of siRNA transfection. It showed that *CNR1* protein expression was down-regulated in *CNR1*-targeting siRNA transfected 22RV1 cells as compared with non-targeting siRNA transfected cells (

Figure 6.13).

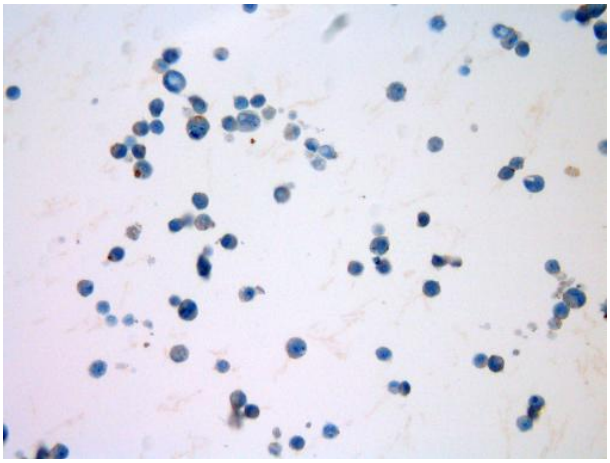

(A) pcDNA3.1

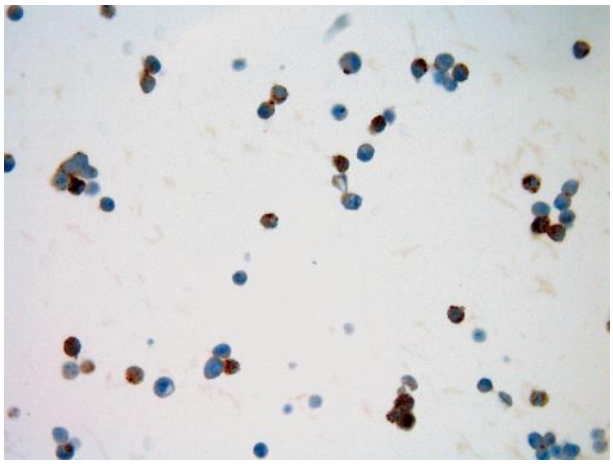

(B) pcDNA-CNR1

Figure 6.12 *CNR1* expression in stably transfected 22RV1 cells using IHC analysis

(A) IHC analysis of *CNR1* expression in stably transfected 22RV1 cells with pcDNA3.1; (B) IHC analysis of *CNR1* expression in stably transfected 22RV1 cells with pcDNA-CNR1.

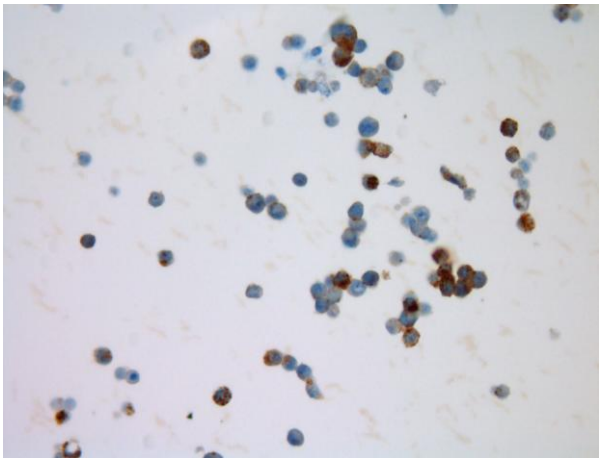

(A) Non-targeting siRNA

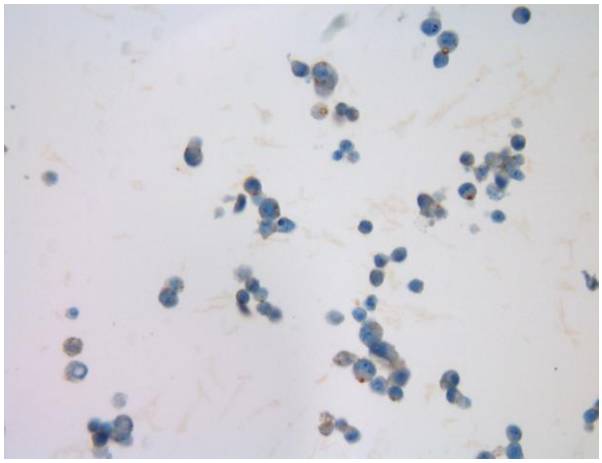

(B) *CNR1*-targeting siRNA

Figure 6.13 *CNR1* expression in siRNA knock down 22RV1 cells using IHC analysis

The siRNA knock down analysis was applied to stably transfected 22RV1 cells with pcDNA-CNR1. (A) *CNR1* expression in the 22RV1 cells transiently transfected with non-targeting siRNA; (B) *CNR1* expression in the 22RV1 cells transiently transfected with *CNR1*-targeting siRNA.

6.4 Discussion

In order to over-express *CNR1* in 22RV1 cells efficiently, chemical transfection reagents, including JetPEI-RGD and Lipofectamine 2000, and Nucleofector Technology were applied in this study. Using the JetPEI-RGD reagent, less than 5% of 22RV1 cells were observed to express *GFP* after 48h transfection with pcDNA-GFP, which was not as expected. As 40-50% of transfection efficiency was achieved using Lipofectamine 2000 in 22RV1 cells, I used the latter rather than spending time trouble shooting the JetPEI-RGD.

Nucleofector Technology (Necleofection) was invented by the biotechnology company Amaxa. Compared with other commonly used non-viral transfection methods, which rely on cell division for the transfer of DNA into the nucleus, Nucleofection is a physical method of electroporation to transfer substrates directly into the cell nucleus and the cytoplasm. Therefore it has been applied to transfer substrates into mammalian cells so far considered difficult, or even impossible, to transfect. In this study, almost 100% of pmaxGFP transfected 22RV1 cells were detected with *GFP* expression after 48 h of transfection, suggesting that Nucleofection potentially is the best technology so far for plasmid transfer in prostate cancer cell lines. It was also noticed that, under the same transfection conditions, pcDNA-GFP only achieved 30-40% transfection efficiency, indicating that the vector itself could dramatically affect gene expression efficiency. One major difference between pmaxCloning vector (backbone of pmaxGFP) and pcDNA3.1 is that there is a 137 bp chimeric intron sequence before the multiple cloning sites (MCS) in pmaxCloning vector to enhance gene expression. There were potentially other ‘tricks’ in the vector to

make such a dramatic difference, but the precise information on plasmid structure as a 'commercial secret' was not available.

Detection of *CNR1* protein using Western blot analysis failed using anti-*CNR1*, anti-flag and anti-HA antibodies in this study. The reason for the failed detection using the *CNR1* antibody proved to be due to the inefficiency of the antibody for Western blot analysis, although it worked very well for IHC analysis. The specificity of this antibody for IHC analysis was also confirmed using siRNA knockdown analysis in this study. The possible explanation for the failed Western blot analysis is that the protein conformation might change during the sample denaturation, and this might affect the antibody recognition of the epitope. As to the failure of Western blot analysis for *CNR1*flag detection using anti-flag antibody, the tag sequence at the C-terminal of *CNR1* might affect *CNR1* protein stability. This possibility was supported by the fact that *CNR1* was over-expressed 2380 fold higher at the RNA level in pcDNA-CNR1flag stably transfected 22RV1 cells compared with the control cells, whereas no increased protein level was detected. Similarly, using anti-HA antibody, no protein was detected using Western blot analysis and no increased protein expression was observed using IHC analysis, although *CNR1* was over-expressed 3381 fold higher at the RNA level in pcDNA-3HA_CNR1 stably transfected 22RV1 cells compared with the control cells. It is possible that the HA tag at the N-terminal of *CNR1* also caused the *CNR1* protein instability.

As mentioned previously a recent study examined a series of commercial *CNR1* antibodies and demonstrated that most of the antibodies were not specific for

either IHC or Western blot analysis. In accordance with my study, even though the *CNR1* antibody was demonstrated to be specific for IHC analysis, it proved to be very difficult to be applied for Western blot analysis. Therefore, a concern regarding the reliability of previously reported studies of *CNR1* in prostate cancer was generated. Several studies have shown that the *CNR1* was highly expressed in prostate cancer cell lines, including LNCaP, PC3 and DU145, using IHC or Western blot analysis (Ruiz-Llorente *et al.*, 2003; Sarfaraz *et al.*, 2005; Czifra *et al.*, 2009). According to our qRT-PCR and IHC analysis in prostate cancer cell lines, none of them showed high expression but, rather, they all exhibited very low or non-detectable levels of the *CNR1* expression. Although it is possible that the differences generated between the studies were caused by different cell lineages or distinct cell culture conditions, such as different media or serum used, the misrecognition of a nonspecific band at the expected size of the *CNR1* protein might well have been the main reason for these conflicting results.

The majority of reported studies regarding *CNR1* have supplied only indirect evidence of the relationship between *CNR1* and cancer. The ligands of *CNR1*, such as endocannabinoids and *CNR1* agonists, have been demonstrated to have anti-tumourigenic effects through activation of *CNR1* in various cancers (Freimuth *et al.*, 2010). In prostate cancer, the treatment with cannabinoid receptor agonists, including R(+)-Methanandamide (MET) and WIN-55,212-2, resulted in inhibition of cell growth in LNCaP and PC3 cells through inhibition of AKT and activation of ERK (Olea-Herrero *et al.*, 2009; Sarfaraz *et al.*, 2006; Sanchez *et al.*, 2003; Sarfaraz *et al.*, 2005). The treatment of cannabinoid

receptor agonists consistently was reported to inhibit cell growth in breast cancer, melanoma and colorectal cancer cells (Qamri *et al.*, 2009; Blazquez *et al.*, 2006; Laezza *et al.*, 2010; Patsos *et al.*, 2010). Different methods have been applied to examine the cell growth, including MTT, MTS, [^{3}H]-thymidine incorporation assays for cell viability, cell counting, colony formation and cell cycle assays for cell proliferation (Takeda *et al.*, 2008; Olea-Herrero *et al.*, 2009; Santoro *et al.*, 2009). In this study, the effect of over-expression of *CNR1* on cell viability was examined in transiently transfected 22RV1 cells using the MTS assay. There was no significant difference between *CNR1* over-expressing and control cells. However the colony formation assay did show that over-expression of *CNR1* inhibited cell proliferation in transiently transfected 22RV1 cells.

Apart from the inhibition of cell growth, the ligand of *CNR1*, endogenous 2-arachidonoylglycerol (2-AG), has also been reported to inhibit invasion of prostate cancer cells. Similar effects, generated by cannabinoid through activating the *CNR1*, have also been identified in gastric, cervical and lung cancer cells (Ramer and Hinz, 2008; Ramer *et al.*, 2010; Xian *et al.*, 2010). In addition, up-regulation of tissue inhibitor of matrix metalloproteinase-1 (TIMP-1) was suggested to mediate the anti-invasive effect of cannabinoids (Ramer and Hinz, 2008; Ramer *et al.*, 2010). In this study, impaired invasion was observed in 22RV1 cells with transient over-expression of the *CNR1* gene. However, due to time limitations, inhibition of proliferation and invasive activity of *CNR1* has not been confirmed in stably transfected 22RV1 cells. Had I had more time available I would have gone on to conduct the experiments.

In conclusion, the accurate examination of *CNR1* expression at the protein level can be achieved by IHC analysis but not the Western blot analysis using the *CNR1* antibody (Abcam). Transient over-expression of *CNR1* in the prostate cancer cell line, 22RV1, was shown to have an anti-invasive effect. Further study is needed to confirm the anti-invasive effect of *CNR1* and also to identify the underlying molecular mechanism.

7 FINAL DISCUSSION AND FUTURE PLANS

7.1 Micro-deletions with unbalanced chromosomal translocation

Since the identification of highly recurrent fusion genes in prostate and lung cancer, gene fusions have been recognised as a common event in almost all types of cancers, including haematological malignancies, sarcomas and carcinomas. In haematological malignancies, fusion genes mainly were caused by chromosomal translocations through juxtaposing promoter/enhancer elements from one gene with the intact coding region of another gene, or recombining the coding regions of two different genes. Due to the low resolution of banding technology, many translocations were originally recognised as balanced chromosomal rearrangements. Whereas with the development of molecular cytogentic technology and microarray technology, sub-microscopic deletions, which are associated with cytogenetically balanced translocations, were detected (Mao *et al.*, 2008; Watson *et al.*, 2007). In a wide range of leukaemias, including CML, AML and ALL, these microdeletions coupled with chromosomal translocations are associated with poor prognosis (Kolomietz *et al.*, 2001).

In prostate cancer, the most common gene fusion is *TMPRSS2-ERG*, present in 50-80% of the cancer patients. This gene fusion falls into the category that an oncogene is fused with promoter elements of another gene: *ERG* belongs to the ETS oncogene family and the promoter of *TMPRSS22* is androgen regulated. *TMPRSS2-ERG* fusion can be caused either by intrachromosomal deletion or

inversion, as the two genes are about 3 Mb apart on chromosome 21. It has been shown that *TMPRSS2-ERG* fusions generated by intrachromosomal deletions tend to correspond with worse prognosis than those created by inversions, suggesting tumour suppressor gene(s) might locate in the deletion region (Attard *et al.*, 2008).

Our group has a long-standing interest in identifying chromosomal translocation and fusion genes in prostate cancer. In 2007, we reported a recurrent chromosomal translocation, t(4;6), in prostate cancer cell lines and a small set of primary prostate tumours (Lane *et al.*, 2007). The breakpoints of the translocation were identified to locate at 4q22 and 6q15 in the LNCaP cell line. In addition, micro-deletions were identified adjacent to both of the breakpoints. The only gene disrupted by the breakpoints was *UNC5C*, a putative tumour suppressor gene, which lost its promoter and the first exon (Lane *et al.*, 2007). In this study, using probes located on distal 4q22 and proximal 6q15, I performed FISH signal co-localisation analysis in a large series of clinical localised prostate cancer samples to examine the prevalence and clinical significance of t(4;6)(q22;q15). It was shown that the t(4;6)(q22;q15) presents in 78 of 667 cases (11.7%). The t(4;6)(q22;q15) was not independently associated with patient outcome, however it occurs more frequently in high clinical T stage, high tumour volume specimens and in those with high baseline PSA (P=0.001, 0.001 and 0.01 respectively). Accordingly, we demonstrated that t(4;6)(q22;q15) is a frequent event in prostate cancer. However, as the recurrent chromosomal rearrangements previously identified mainly lead to gain of functions of genes located at the

breakpoints (Mitelman *et al.*, 2007), the mechanism of action of the t(4;6)(q22;q15) translocation was not clear.

The putative tumour suppressor gene *UNC5C* was shown to be disrupted by the distal breakpoint of the translocation on 4q22 in LNCaP cells. At the genomic level, *UNC5C* lost its promoter and the first exon; at the transcriptional level, the expression of *UNC5C* was not detected by RT-PCR analysis in our previous study; In addition, no fusion transcripts involving *UNC5C* or corresponding to this chromosomal rearrangement have been identified in this cell line by deep sequencing using the next generation sequencing technology (Maher *et al.*, 2009). Therefore, t(4;6)(q22;q15) might cause the inactivation of *UNC5C*. Moreover, micro-deletions on 4q22 and 6q15 were also identified to be associated with t(4;6)(q22;q15) in LNCaP cells. 4q and 6q are among the most frequently deleted chromosome regions in human tumours. 6q15, particularly, is one of the most frequently deleted regions in prostate cancer, indicating that tumour suppressor gene(s) might locate in this region. Therefore, we hypothesised that the t(4;6)(q22;q15) may contribute to prostate cancer development through inactivation of tumour suppressor genes at the breakpoint or/and micro-deletion region rather than gain of function by forming fusion genes. As illustrated above, microdeletions coupled with chromosomal translocations have been identified in leukaemias and prostate cancer associated with poor prognosis, indicating that any tumour suppressor gene(s) are located in the deletion region. Tumour suppressor genes inactivated through disruption of translocation/deletion breakpoints have been well demonstrated in breast cancer

(Howarth *et al.*, 2008; Huang *et al.*, 2004). For example, translocation/deletion breakpoints in neuregulin 1 (*NRG1*) are present in at least 6% of breast cancers (Huang *et al.*, 2004). Cell lines with breakpoints in the *NRG1* gene express less *NRG1* transcript than normal breast epithelial cells, and most breast cancer cell lines express none at all, often as a result of promoter methylation (Chua *et al.*, 2009). Now it is believed that *NRG1* is a tumour suppressor gene on 8p and that the breaks within the gene are one of several ways of reducing its activity (Chua *et al.*, 2009; Pole *et al.*, 2006).

7.2 Identification of tumour suppressor genes in prostate cancer

Deletion is one of the most frequent genetic alterations detected in cancer cells. Non-random deletions detected in certain regions have been widely interrogated to identify tumour suppressor genes. In prostate cancer, most commonly deleted regions were summarised in **1.6.3.1**. Recently, an integrated oncogenomic analysis was applied on 218 primary and metastatic prostate cancer cases as well as 12 cell lines and xenografts. The assessment of DNA copy number changes in these samples confirmed the frequent deletion in 6q15 in prostate cancer (Taylor *et al*., 2010). However, the tumour suppressor gene(s) in this region has not been identified.

In this study, we combined different approaches to identify candidate tumour suppressor genes in 6q15. Using high resolution SNP array analysis, two minimum overlapping deletion regions within 87.21-90.35 Mbp and 90.88-91.35 Mbp in 6q15 were detected in 33 and 34 out of 71 clinical prostate cancer

samples, respectively. In order to examine systematically the expression alterations of all the genes located in these two regions, we applied Exon array analysis to six prostate cancer cell lines and one clinical prostate cancer sample. Use of cell lines has been questioned, because the process of immortalisation *in vitro* could generate artificial events when compared to native tissue (Dairkee *et al.*, 2004). A solution is to use cell lines for their purity and convenience, and at the same time, include primary prostate cancer samples to exclude the artefacts. The difficulties in obtaining pure prostate cancer cells and also extracting good quality RNA from those cancer cells hampered the number of primary samples applied for Exon array analysis. First, the instability of RNA requires the cancer tissue to be fresh frozen immediately after being removed from the patients; second, micro-dissection is needed to obtain pure malignant epithelial cells. Micro-dissection is a time consuming process and the degradation of RNA during the dissection is inevitable. In addition, the quantity of RNA is not guaranteed from the limited amount of dissected cancer cells available. Therefore, only one primary prostate cancer sample with more than 70% purity of cancer cells was included in the Exon array analysis. We decided to identify commonly down-regulated genes at 6q15 in prostate cancer cell lines and one clinical cancer sample; and then confirm the features in enlarged clinical prostate cancer samples. Four genes, *CNR1*, *PNRC1*, *GJA10* and *BACH2*, were identified with common down-regulation located at 6q15. Using qRT-PCR analysis, *CNR1* and *BACH2* were still shown to exhibit down-regulated expression in the enlarged cancer samples, which were macro-dissected with relatively pure populations of cancer cells.

Whether protein expression of these two genes are correlated with RNA expression was examined further in FFPE prostate cancer samples using IHC analysis. *CNR1* was still shown to exhibit down-regulated protein expression in prostate cancer cases as compared with BPH or adjacent normal tissue. In contrast, *BACH2* protein was shown to have an altered cellular localisation in prostate cancer samples compared with BPH controls. Cytoplasmic localisation of *BACH2* was detected in the majority of BPH samples (89.7%), whereas nuclear localisation of *BACH2* was shown in 45.3% of prostate cancer cases. It has been shown that nuclear accumulation of *BACH2* in B-cells was caused by oxidative stress and associated with induction of apoptosis (Kamio *et al.*, 2003; Yoshida *et al.*, 2007). However, increased nuclear expression of *BACH2* in ovarian cancer has been associated with decreased time to disease recurrence (Motamed-Khorasani *et al.*, 2007). The full significance of altered *BACH2* expression still is unknown. Further analysis of *BACH2* isoform expression and potential cytoplasmic function in prostate cells is needed.

As down-regulated expression of *CNR1* at the RNA and protein level was consistent with the identification of frequent genomic deletions in 6q15, we wondered if other mechanisms, such as mutation or methylation, also play a role in the inactivation of *CNR1*. Random sequencing of five prostate cancer cases, which did not express CNR1, revealed a homozygous deletion inside the *CNR1* genome in one of the five samples. Therefore it is considered this is an encouraging finding for examining more cancer samples to identify if there are other mutations present and also to investigate the prevalence of these mutations in a wider series of cases. Methylation analysis showed that, in some prostate

cancer samples, *CNR1* promoter methylation occurred in a higher percentage of cells (> 10%) compared with the methylation in the average percentage of cells (2.66%) in ten BPH samples. However, there was no significant difference between BPH and all of the cancer samples (p= 0.319). It is possible that DNA methylation might only account for the *CNR1* inactivation in some of the prostate cancer samples; or, since only very short (24 bp) of the promoter region (1027 bp) was analysed, the methylation status of other promoter regions, which are unknown, might be important. It is plausible to investigate the other promoter regions to finally draw a conclusion regarding the frequency of *CNR1* mehtylation in prostate cancer.

From genomic study to transcript and protein expression analysis, *CNR1* was shown as a potential tumour suppressor gene in 6q15. In order to confirm and clarify its tumour suppressor role, *CNR1* was further studied at the cellular level. As RNA expression of *CNR1* was very low in prostate cancer cell lines and immortalised prostate epithelial cells, the siRNA knock down analysis was not considered suitable for studying *CNR1* in prostate cancer cells. Therefore transient/stable over-expression of *CNR1* was the only approach to investigate its cellular function.

We are now in the stage that I have obtained stably transfected 22RV1 cells with over-expression of *CNR1*. The MTS analysis demonstrated that *CNR1* over-expression does not affect cell proliferation in transiently and stably transfected 22RV1 cells. Using Matrigel invasion assay, over-expression of *CNR1* was shown to decrease cell invasion in transiently transfected 22RV1. However, it

needs to be further confirmed in the stably transfected cells and this is the type of additional study I would conduct if I had more time available.

7.3 Future plans

7.3.1 *CNR1* protein expression and clinical significance of *CNR1* inactivation in prostate cancer

In this study, different approaches were combined to identify candidate tumour suppressor genes in the 6q15 deletion region. So far, multiple lines of evidence indicate that *CNR1* might be the target gene. The preliminary IHC analysis on two prostate cancer TMAs showed that protein expression of *CNR1* was down regulated in cancer samples. In the next step, I will continue to perform IHC analysis on other batches of TMAs (details in **2.1.1**) to further confirm the altered expression of *CNR1* in the cancer samples.

Using FISH analysis, I demonstrated a frequent 6q15 deletion (46%) in prostate cancer and also correlated the deletion status with the Gleason score. It was shown that 6q15 deletion might occur in cases with a high Gleason score, but more cases are required to draw a firm conclusion. If the gene *CNR1* was the target tumour suppressor in 6q15, in theory, the expression of *CNR1* should be associated with clinical and/or patient outcome. Therefore, the expression status of *CNR1* obtained from IHC analysis on TMAs will be correlated with clinical significance in prostate cancer.

7.3.2 *CNR1* mutation and methylation

In this study, a small deletion inside of *CNR1* genomic DNA was identified in one of the five clinical prostate cancer samples with inactivated protein expression of *CNR1*. Whether there are other mutations in *CNR1* genomic DNA, and the frequency of the mutations, will be investigated through sequencing of the *CNR1* coding region in more clinical cancer samples; specifically thoses which were shown with down regulated protein expression. In the meanwhile, the methylation of *CNR1* in prostate cancer will continue to be investigated in more regions of the entire promoter sequence.

7.3.3 Cellular functional study of the gene *CNR1* in 22RV1 cells

7.3.3.1 Separation of *CNR1* expressed and unexpressed cells from stably transfected 22RV1 cells

According to the IHC analysis of stably transfected 22RV1 cells, *CNR1* was not shown with uniform over-expression in every 22RV1 cell. There were some cells with very weak or no expression of *CNR1*. In order to clearly define the function of *CNR1* in prostate cancer, first of all, cells with or without *CNR1* expression will be sorted from stably transfected 22RV1 cells using FACS analysis.

7.3.3.2 Cellular functional analysis and molecular mechanism identification

A series of functional assays will be applied to investigate the tumour suppressor role of *CNR1* in prostate cancer. It has been shown in this study that *CNR1* over-expression did not affect cell viability, using the MTS assay. After cells with or

without *CNR1* expression are sorted, the MTS assay will be repeated to draw a final conclusion regarding the role of *CNR1* in cell viability. In parallel, Matrigel invasion and Transwell migration assays will be applied to examine the role of *CNR1* in cell invasion and migration; soft agar colony formation assay will be performed to investigate the role of *CNR1* in cell adhesion, in terms of anchorage independent growth. According to the tumour suppressor role of *CNR1*, which I have identified, the corresponding molecular mechanisms regarding the cell signalling pathways affected will be investigated.

7.3.3.3 *CNR1* agonist treatment on stably transfected 22RV1 cells

The majority of reported studies regarding the gene *CNR1* have focused on the anti-tumour effect of *CNR1* agonists and not much attention has been paid to the potential tumour suppressing effect of *CNR1*. Whether *CNR1* expression is essential for the anti-tumour effects of *CNR1* agonists will be examined. Different dosages of a *CNR1* agonist, (i.e HU210), will be applied to treat 22RV1 cells with or without *CNR1* expression. Ideally, a certain dose of the agonist, which has no cell toxicity effect on 22RV1 cells without *CNR1* expression but which induces death of the cells with *CNR1* expression, will be identified.

7.3.4 Functional study of *CNR1 in vivo*

If cellular function studies *in vitro* suggest that *CNR1* plays a tumour suppressor role, further functional study of *CNR1* will be performed *in vivo*. For more accurate measurement and stable expression of *CNR1*, a Tet-Off inducible gene expression system will be established, which permits the modulation of gene expression both *in vitro* and *in vivo* (http://www.clontech.com). First of all,

tetracycline transactivator-producing 22RV1 cell line will be established. Next the complete open reading frame of *CNR1* will be incorporated into pTet-Off vector (named pTet-CNR1) before being transfected in the presence of doxycycline into the 22RV1 cells constitutively producing the tetracycline transactivator. Finally, cell clones, which show the best tetracycline regulation (at least 100-fold difference of *CNR1* expression between induced and repressed state), will be selected. Using the established inducible gene expression system, *CNR1* will be expressed in the absence, but not in the presence, of tetracycline or its analog doxycycline. For *in vivo* study, a total of 10^7 established 22RV1 cells would be injected in different sites in nude mice. The tumour formation and size will be investigated and compared among nude mice with or without *CNR1* expression.

7.3.5 Investigation of *BACH2* isoforms and the corresponding protein localisation

In this study, *BACH2* protein was shown with altered cellular localisation in prostate cancer samples compared with BPH controls. It was postulated that the different *BACH2* isoforms localise to different cellular compartments where they may participate in cell processes distinct from transcriptional regulation. In the following step, we will apply IHC analysis on prostate cancer cell lines and immortalised prostate epithelial cell lines to detect the localisation of *BACH2*. If the different localisation of *BACH2* is identified among the cell lines, the mRNA splicing isoforms of *BACH2* will be investigated and the protein isoforms will be examined using Western blot analysis. If the different isoforms of *BACH2*

account for the altered cellular localisation, the function of the different isoforms will be further studied.

7.4 The potential clinical implications of *CNR1* in prostate cancer

The initial goal of this project was to investigate the clinical significance of t(4;6)(q15;q22) in prostate cancer. Although the result showed that t(4;6)(q15;q22) did not correlate with clinical outcome, it might contribute to prostate cancer development through inactivation of TSG(s) which are associated with the common 6q15 deletion in prostate cancer. Based on the information from the literature and my study, *CNR1* is likely to be the target gene associated with 6q abnormalities in prostate cancer. Although a few steps are required to confirm the tumour suppressor role of *CNR1*, here I would like to postulate the potential significance and clinical implications of *CNR1* in prostate cancer.

Clinically, there are three major problems in managing prostate cancer. First of all, although PSA has been widely used for screening of prostate cancer, more specific and sensitive early diagnostic markers are still needed to avoid over-diagnosis of prostate cancer. Second, as illustrated previously, the clinically localised prostate cancers are biologically diverse, ranging from indolent tumours to a subset of aggressive tumours with a potential for recurrence and metastasis. Prognosis markers that can accurately identify and stratify these subsets of clinically localised cancer need to be identified in order to refrain from over-treatment of the cancer patients. Third, there is no effective treatment of androgen-resistant prostate cancer. Because *CNR1* encodes a trans-membrane

protein, which is not secreted into human fluids (such as serum and urine) for easy collection from the patients, it will not be an ideal marker for early diagnosis. However, as 6q deletion is commonly but not universally presented in prostate cancer and the expression of *CNR1* was frequently down-regulated in clinical prostate cancer samples in my study, *CNR1* might have a prognostic value if it is differentially expressed in indolent and aggressive cancers (van Dekken *et al*., 2004; Ribeiro *et al*., 2006). The association of *CNR1* expression with clinical outcome need to be investigated in order to identify whether expression status of *CNR1* could supplement Gleason score to distinguish indolent from clinically aggressive prostate cancer. Moreover, there is a greater chance that *CNR1* will serve as a therapeutic target. Currently, various *CNR1* agonists have been developed and are commercially available. The ligands of *CNR1*, such as endocannabinoids and *CNR1* agonists, have been demonstrated by many studies to have an anti-tumourigenic effect, affecting cell growth, apoptosis, angiogenesis, migration, invasion, adhesion, and an ability to metastasise in various cancers (Freimuth *et al.*, 2010). As my study strongly supports the tumour suppressor role of *CNR1*, clinically approved *CNR1* agonists could be applied to the cancer patients with down-regulated *CNR1* expression. For those who carry cancer cells without, or with very low level of, *CNR1* expression, gene therapy might be applied to deliver exogenous *CNR1*. Other approaches, such as targeting the down-stream gene(s) of *CNR1*-involved pathway(s), could also be considered. However, more studies and solid evidence are required to prove all above possibilities.

8 REFERENCES

Abdel-Rahman WM, Katsura K, Rens W, Gorman PA, Sheer D, Bicknell D, Bodmer WF, Arends MJ, Wyllie AH, Edwards PA (2001). Spectral karyotyping suggests additional subsets of colorectal cancers characterized by pattern of chromosome rearrangement. *Proc Natl Acad Sci U S A* **98:** 2538-43.

Abiatari I, Kleeff J, Li J, Felix K, Buchler MW, Friess H (2006). Hsulf-1 regulates growth and invasion of pancreatic cancer cells. *J Clin Pathol* **59:** 1052-8.

Al-Tassan N, Chmiel NH, Maynard J, Fleming N, Livingston AL, Williams GT, Hodges AK, Davies DR, David SS, Sampson JR, Cheadle JP (2002). Inherited variants of MYH associated with somatic G:C-->T:A mutations in colorectal tumors. *Nat Genet* **30:** 227-32.

Albagli O, Dhordain P, Deweindt C, Lecocq G, Leprince D (1995). The BTB/POZ domain: a new protein-protein interaction motif common to DNA- and actin-binding proteins. *Cell Growth Differ* **6:** 1193-8.

Albertsen PC, Hanley JA, Fine J (2005). 20-year outcomes following conservative management of clinically localized prostate cancer. *JAMA* **293:** 2095-101.

Albertson DG (2006). Gene amplification in cancer. *Trends Genet* **22:** 447-55.

Albertson DG, Collins C, McCormick F, Gray JW (2003). Chromosome aberrations in solid tumors. *Nat Genet* **34:** 369-76.

Alers JC, Rochat J, Krijtenburg PJ, Hop WC, Kranse R, Rosenberg C, Tanke HJ, Schroder FH, van Dekken H (2000). Identification of genetic markers for prostatic cancer progression. *Lab Invest* **80:** 931-42.

Alexander A, Smith PF, Rosengren RJ (2009). Cannabinoids in the treatment of cancer. *Cancer Lett* **285:** 6-12.

Alison M (2002). *The cancer handbook*. Nature Publishing Group: London

Amundadottir LT, Sulem P, Gudmundsson J, Helgason A, Baker A, Agnarsson BA, Sigurdsson A, Benediktsdottir KR, Cazier JB, Sainz J, Jakobsdottir M, Kostic J, Magnusdottir DN, Ghosh S, Agnarsson K, Birgisdottir B, Le Roux L, Olafsdottir A, Blondal T, Andresdottir M, Gretarsdottir OS, Bergthorsson JT, Gudbjartsson D, Gylfason A, Thorleifsson G, Manolescu A, Kristjansson K, Geirsson G, Isaksson H, Douglas J, Johansson JE, Balter K, Wiklund F, Montie JE, Yu X, Suarez BK, Ober C, Cooney KA, Gronberg H, Catalona WJ, Einarsson GV, Barkardottir RB, Gulcher JR, Kong A, Thorsteinsdottir U, Stefansson K (2006). A common variant associated with prostate cancer in European and African populations. *Nat Genet* **38:** 652-8.

ar-Rushdi A, Nishikura K, Erikson J, Watt R, Rovera G, Croce CM (1983). Differential expression of the translocated and the untranslocated c-myc oncogene in Burkitt lymphoma. *Science* **222:** 390-3.

Arakawa H (2004). Netrin-1 and its receptors in tumorigenesis. *Nat Rev Cancer* **4:** 978-87.

Atkin NB, Baker MC (1985). Chromosome study of five cancers of the prostate. *Hum Genet* **70:** 359-64.

Attard G, Clark J, Ambroisine L, Fisher G, Kovacs G, Flohr P, Berney D, Foster CS, Fletcher A, Gerald WL, Moller H, Reuter V, De Bono JS, Scardino P, Cuzick J, Cooper CS (2008). Duplication of the fusion of TMPRSS2 to ERG sequences identifies fatal human prostate cancer. *Oncogene* **27:** 253-63.

Attard G, Jameson C, Moreira J, Flohr P, Parker C, Dearnaley D, Cooper CS, de Bono JS (2009a). Hormone-sensitive prostate cancer: a case of ETS gene fusion heterogeneity. *J Clin Pathol* **62:** 373-6.

Attard G, Swennenhuis JF, Olmos D, Reid AH, Vickers E, A'Hern R, Levink R, Coumans F, Moreira J, Riisnaes R, Oommen NB, Hawche G, Jameson C, Thompson E, Sipkema R, Carden CP, Parker C, Dearnaley D, Kaye SB, Cooper CS, Molina A, Cox ME, Terstappen LW, de Bono JS (2009b). Characterization of ERG, AR and PTEN gene status in circulating tumor cells from patients with castration-resistant prostate cancer. *Cancer Res* **69:** 2912-8.

Aubin SM, Reid J, Sarno MJ, Blase A, Aussie J, Rittenhouse H, Rittmaster R, Andriole GL, Groskopf J (2010). PCA3 Molecular Urine Test for Predicting Repeat Prostate Biopsy Outcome in Populations at Risk: Validation in the Placebo Arm of the Dutasteride REDUCE Trial. *J Urol*.

Aus G, Nordenskjold K, Robinson D, Rosell J, Varenhorst E (2003). Prognostic factors and survival in node-positive (N1) prostate cancer-a prospective study based on data from a Swedish population-based cohort. *Eur Urol* **43:** 627-31.

Azar GM, DiPillo F, Gogineni SK, Godec CJ, Verma RS (1997). Highly complex chromosomal aberrations in bone marrow of a patient with metastatic prostate neoplasm. *Cancer Genet Cytogenet* **99:** 116-20.

Banez LL, Sun L, van Leenders GJ, Wheeler TM, Bangma CH, Freedland SJ, Ittmann MM, Lark AL, Madden JF, Hartman A, Weiss G, Castanos-Velez E (2010). Multicenter clinical validation of PITX2 methylation as a prostate specific antigen recurrence predictor in patients with post-radical prostatectomy prostate cancer. *J Urol* **184:** 149-56.

Barrett IP (2010). Cancer genome analysis informatics. *Methods Mol Biol* **628:** 75-102.

Bastian PJ, Ellinger J, Heukamp LC, Kahl P, Muller SC, von Rucker A (2007). Prognostic value of CpG island hypermethylation at PTGS2, RAR-beta, EDNRB, and other gene loci in patients undergoing radical prostatectomy. *Eur Urol* **51:** 665-74; discussion 674.

Bastian PJ, Yegnasubramanian S, Palapattu GS, Rogers CG, Lin X, De Marzo AM, Nelson WG (2004). Molecular biomarker in prostate cancer: the role of CpG island hypermethylation. *Eur Urol* **46:** 698-708.

Bayani J, Selvarajah S, Maire G, Vukovic B, Al-Romaih K, Zielenska M, Squire JA (2007). Genomic mechanisms and measurement of structural and numerical instability in cancer cells. *Semin Cancer Biol* **17:** 5-18.

Bayani J, Squire J (2004). Multi-color FISH techniques. *Curr Protoc Cell Biol* **Chapter 22:** Unit 22 5.

Bedoya F, Meneu JC, Macias MI, Moreno A, Enriquez-De-Salamanca R, Gonzalez EM, Vegh I (2009a). Mutation in CNR1 gene and VEGF expression in esophageal cancer. *Tumori* **95:** 68-75.

Bedoya F, Rubio JC, Morales-Gutierrez C, Abad-Barahona A, Lora Pablos D, Meneu JC, Moreno-Gonzalez E, Enriquez de Salamanca R, Vegh I (2009b). Single nucleotide change in the cannabinoid receptor-1 (CNR1) gene in colorectal cancer outcome. *Oncology* **76:** 435-41.

Belloni E, Trubia M, Mancini M, Derme V, Nanni M, Lahortiga I, Riccioni R, Confalonieri S, Lo-Coco F, Di Fiore PP, Pelicci PG (2004). A new complex rearrangement involving the ETV6, LOC115548, and MN1 genes in a case of acute myeloid leukemia. *Genes Chromosomes Cancer* **41:** 272-7.

Berger R, Busson M, Baranger L, Helias C, Lessard M, Dastugue N, Speleman F (2006). Loss of the NPM1 gene in myeloid disorders with chromosome 5 rearrangements. *Leukemia* **20:** 319-21.

Bernet A, Mazelin L, Coissieux MM, Gadot N, Ackerman SL, Scoazec JY, Mehlen P (2007). Inactivation of the UNC5C Netrin-1 receptor is associated with tumor progression in colorectal malignancies. *Gastroenterology* **133:** 1840-8.

Berney DM (2010). Biomarkers for prostate cancer detection and progression: Beyond prostate-specific antigen. *Drug News Perspect* **23:** 185-94.

Bethel CR, Faith D, Li X, Guan B, Hicks JL, Lan F, Jenkins RB, Bieberich CJ, De Marzo AM (2006). Decreased NKX3.1 protein expression in focal prostatic atrophy, prostatic intraepithelial neoplasia, and adenocarcinoma: association with gleason score and chromosome 8p deletion. *Cancer Res* **66:** 10683-90.

Birkenkamp-Demtroder K, Mansilla F, Sorensen FB, Kruhoffer M, Cabezon T, Christensen LL, Aaltonen LA, Verspaget HW, Orntoft TF (2007). Phosphoprotein Keratin 23 accumulates in MSS but not MSI colon cancers in vivo and impacts viability and proliferation in vitro. *Mol Oncol* **1:** 181-95.

Blazquez C, Carracedo A, Barrado L, Real PJ, Fernandez-Luna JL, Velasco G, Malumbres M, Guzman M (2006). Cannabinoid receptors as novel targets for the treatment of melanoma. *FASEB J* **20:** 2633-5.

Bower M, Wasman J (2006). Oncology. *The scientific basis of cancer* **15:** 22-23.

Brandes AA, Franceschi E, Tosoni A, Hegi ME, Stupp R (2008). Epidermal growth factor receptor inhibitors in neuro-oncology: hopes and disappointments. *Clin Cancer Res* **14:** 957-60.

Bratt O (2002). Hereditary prostate cancer: clinical aspects. *J Urol* **168:** 906-13.

Brooks JD, Weinstein M, Lin X, Sun Y, Pin SS, Bova GS, Epstein JI, Isaacs WB, Nelson WG (1998). CG island methylation changes near the GSTP1 gene in prostatic intraepithelial neoplasia. *Cancer Epidemiol Biomarkers Prev* **7:** 531-6.

Bruns I, Czibere A, Fischer JC, Roels F, Cadeddu RP, Buest S, Bruennert D, Huenerlituerkoglu AN, Stoecklein NH, Singh R, Zerbini LF, Jager M, Kobbe G, Gattermann N, Kronenwett R, Brors B, Haas R (2009). The hematopoietic stem cell in chronic phase CML is characterized by a transcriptional profile resembling normal myeloid progenitor cells and reflecting loss of quiescence. *Leukemia* **23:** 892-9.

Buckland PR, Hoogendoorn B, Coleman SL, Guy CA, Smith SK, O'Donovan MC (2005). Strong bias in the location of functional promoter polymorphisms. *Hum Mutat* **26:** 214-23.

Bussemakers MJ, van Bokhoven A, Verhaegh GW, Smit FP, Karthaus HF, Schalken JA, Debruyne FM, Ru N, Isaacs WB (1999). DD3: a new prostate-specific gene, highly overexpressed in prostate cancer. *Cancer Res* **59:** 5975-9.

Caceres W, Cruz-Amy M, Diaz-Melendez V (2010). AIDS-related malignancies: revisited. *P R Health Sci J* **29:** 70-5.

Cahill DP, Kinzler KW, Vogelstein B, Lengauer C (1999). Genetic instability and darwinian selection in tumours. *Trends Cell Biol* **9:** M57-60.

Cai C, Hsieh CL, Omwancha J, Zheng Z, Chen SY, Baert JL, Shemshedini L (2007). ETV1 is a novel androgen receptor-regulated gene that mediates prostate cancer cell invasion. *Mol Endocrinol* **21:** 1835-46.

Calin GA, Sevignani C, Dumitru CD, Hyslop T, Noch E, Yendamuri S, Shimizu M, Rattan S, Bullrich F, Negrini M, Croce CM (2004). Human microRNA genes are frequently located at fragile sites and genomic regions involved in cancers. *Proc Natl Acad Sci U S A* **101:** 2999-3004.

Campbell PJ, Stephens PJ, Pleasance ED, O'Meara S, Li H, Santarius T, Stebbings LA, Leroy C, Edkins S, Hardy C, Teague JW, Menzies A, Goodhead I, Turner DJ, Clee CM, Quail MA, Cox A, Brown C, Durbin R, Hurles ME, Edwards PA, Bignell GR, Stratton MR, Futreal PA (2008). Identification of somatically acquired rearrangements in cancer using genome-wide massively parallel paired-end sequencing. *Nat Genet* **40:** 722-9.

Capdeville R, Krahnke T, Hatfield A, Ford JM, Van Hoomissen I, Gathmann I (2008). Report of an international expanded access program of imatinib in adults with Philadelphia chromosome positive leukemias. *Ann Oncol* **19:** 1320-6.

Carter P, Presta L, Gorman CM, Ridgway JB, Henner D, Wong WL, Rowland AM, Kotts C, Carver ME, Shepard HM (1992). Humanization of an anti-p185HER2 antibody for human cancer therapy. *Proc Natl Acad Sci U S A* **89:** 4285-9.

Carvalho JR, Filipe L, Costa VL, Ribeiro FR, Martins AT, Teixeira MR, Jeronimo C, Henrique R (2010). Detailed analysis of expression and promoter methylation status of apoptosis-related genes in prostate cancer. *Apoptosis* **15:** 956-65.

Carvalho-Salles AB, Mesquita JC, Tajara EH (2000). Deletion (1)(q12) and double minutes in a metastatic adenocarcinoma of the prostate. *Cancer Genet Cytogenet* **116:** 50-3.

Chen Z, Fan JQ, Li J, Li QS, Yan Z, Jia XK, Liu WD, Wei LJ, Zhang FZ, Gao H, Xu JP, Dong XM, Dai J, Zhou HM (2009). Promoter hypermethylation correlates with the Hsulf-1 silencing in human breast and gastric cancer. *Int J Cancer* **124:** 739-44.

Cheng I, Plummer SJ, Jorgenson E, Liu X, Rybicki BA, Casey G, Witte JS (2008). 8q24 and prostate cancer: association with advanced disease and meta-analysis. *Eur J Hum Genet* **16:** 496-505.

Choi YL, Takeuchi K, Soda M, Inamura K, Togashi Y, Hatano S, Enomoto M, Hamada T, Haruta H, Watanabe H, Kurashina K, Hatanaka H, Ueno T, Takada S, Yamashita Y, Sugiyama Y, Ishikawa Y, Mano H (2008). Identification of novel isoforms of the EML4-ALK transforming gene in non-small cell lung cancer. *Cancer Res* **68:** 4971-6.

Chua YL, Ito Y, Pole JC, Newman S, Chin SF, Stein RC, Ellis IO, Caldas C, O'Hare MJ, Murrell A, Edwards PA (2009). The NRG1 gene is frequently silenced by methylation in breast cancers and is a strong candidate for the 8p tumour suppressor gene. *Oncogene* **28:** 4041-52.

Chung SC, Hammarsten P, Josefsson A, Stattin P, Granfors T, Egevad L, Mancini G, Lutz B, Bergh A, Fowler CJ (2009). A high cannabinoid CB(1) receptor immunoreactivity is associated with disease severity and outcome in prostate cancer. *Eur J Cancer* **45:** 174-82.

Clark J, Attard G, Jhavar S, Flohr P, Reid A, De-Bono J, Eeles R, Scardino P, Cuzick J, Fisher G, Parker MD, Foster CS, Berney D, Kovacs G, Cooper CS (2008). Complex patterns of ETS gene alteration arise during cancer development in the human prostate. *Oncogene* **27:** 1993-2003.

Coleman WB, Tsongalis GJ (1999). The role of genomic instability in human carcinogenesis. *Anticancer Res* **19:** 4645-64.

Colotta F, Allavena P, Sica A, Garlanda C, Mantovani A (2009). Cancer-related inflammation, the seventh hallmark of cancer: links to genetic instability. *Carcinogenesis* **30:** 1073-81.

Cooney KA, Wetzel JC, Consolino CM, Wojno KJ (1996). Identification and characterization of proximal 6q deletions in prostate cancer. *Cancer Res* **56:** 4150-3.

Cooper JD, Smyth DJ, Smiles AM, Plagnol V, Walker NM, Allen JE, Downes K, Barrett JC, Healy BC, Mychaleckyj JC, Warram JH, Todd JA (2008). Meta-analysis of genome-wide association study data identifies additional type 1 diabetes risk loci. *Nat Genet* **40:** 1399-401.

Cowell JK, Lo KC (2009). Application of oligonucleotides arrays for coincident comparative genomic hybridization, ploidy status and loss of heterozygosity studies in human cancers. *Methods Mol Biol* **556:** 47-65.

Cox D, Oakes D (1984). analysis of survival data. *Chapman & Hall: London, New York*.

Croce CM (2008). Oncogenes and cancer. *N Engl J Med* **358:** 502-11.

Crundwell MC, Chughtai S, Knowles M, Takle L, Luscombe M, Neoptolemos JP, Morton DG, Phillips SM (1996). Allelic loss on chromosomes 8p, 22q and 18q (DCC) in human prostate cancer. *Int J Cancer* **69:** 295-300.

Cuzick J, Fisher G, Kattan MW, Berney D, Oliver T, Foster CS, Moller H, Reuter V, Fearn P, Eastham J, Scardino P (2006). Long-term outcome among men with conservatively treated localised prostate cancer. *Br J Cancer* **95:** 1186-94.

Czepulkowski B (2001). *Analyzing chromoses.* Bios Scientific Publishers Ltd.

Czifra G, Varga A, Nyeste K, Marincsak R, Toth BI, Kovacs I, Kovacs L, Biro T (2009). Increased expressions of cannabinoid receptor-1 and transient receptor potential vanilloid-1 in human prostate carcinoma. *J Cancer Res Clin Oncol* **135:** 507-14.

Dairkee SH, Ji Y, Ben Y, Moore DH, Meng Z, Jeffrey SS (2004). A molecular 'signature' of primary breast cancer cultures; patterns resembling tumor tissue. *BMC Genomics* **5:** 47.

Dalla-Favera R, Bregni M, Erikson J, Patterson D, Gallo RC, Croce CM (1982). Human c-myc onc gene is located on the region of chromosome 8 that is translocated in Burkitt lymphoma cells. *Proc Natl Acad Sci U S A* **79:** 7824-7.

Damania B (2007). DNA tumor viruses and human cancer. *Trends Microbiol* **15:** 38-44.

Damber JE, Aus G (2008). Prostate cancer. *Lancet* **371:** 1710-21.

de Bono JS, Scher HI, Montgomery RB, Parker C, Miller MC, Tissing H, Doyle GV, Terstappen LW, Pienta KJ, Raghavan D (2008). Circulating tumor cells predict survival benefit from treatment in metastatic castration-resistant prostate cancer. *Clin Cancer Res* **14:** 6302-9.

de Kok JB, Verhaegh GW, Roelofs RW, Hessels D, Kiemeney LA, Aalders TW, Swinkels DW, Schalken JA (2002). DD3(PCA3), a very sensitive and specific marker to detect prostate tumors. *Cancer Res* **62:** 2695-8.

de la Chapelle A (2003). Microsatellite instability. *N Engl J Med* **349:** 209-10.

De Marzo AM, Meeker AK, Zha S, Luo J, Nakayama M, Platz EA, Isaacs WB, Nelson WG (2003). Human prostate cancer precursors and pathobiology. *Urology* **62:** 55-62.

Demichelis F, Fall K, Perner S, Andren O, Schmidt F, Setlur SR, Hoshida Y, Mosquera JM, Pawitan Y, Lee C, Adami HO, Mucci LA, Kantoff PW, Andersson SO, Chinnaiyan AM, Johansson JE, Rubin MA (2007). TMPRSS2:ERG gene fusion associated with lethal prostate cancer in a watchful waiting cohort. *Oncogene* **26:** 4596-9.

Deng G, Lu Y, Zlotnikov G, Thor AD, Smith HS (1996). Loss of heterozygosity in normal tissue adjacent to breast carcinomas. *Science* **274:** 2057-9.

Deubler DA, Williams BJ, Zhu XL, Steele MR, Rohr LR, Jensen JC, Stephenson RA, Changus JE, Miller GJ, Becich MJ, Brothman AR (1997). Allelic loss detected on chromosomes 8, 10, and 17 by fluorescence in situ hybridization using single-copy P1 probes on isolated nuclei from paraffin-embedded prostate tumors. *Am J Pathol* **150:** 841-50.

Dianat SS, Margreiter M, Eckersberger E, Finkelstein J, Kuehas F, Herwig R, Ayati M, Lepor H, Djavan B (2009). Gene polymorphisms and prostate cancer: the evidence. *BJU Int* **104:** 1560-72.

Duggan D, Zheng SL, Knowlton M, Benitez D, Dimitrov L, Wiklund F, Robbins C, Isaacs SD, Cheng Y, Li G, Sun J, Chang BL, Marovich L, Wiley KE, Balter K, Stattin P, Adami HO, Gielzak M, Yan G, Sauvageot J, Liu W, Kim JW, Bleecker ER, Meyers DA, Trock BJ, Partin AW, Walsh PC, Isaacs WB, Gronberg H, Xu J, Carpten JD (2007). Two genome-wide association studies of aggressive prostate cancer implicate putative prostate tumor suppressor gene DAB2IP. *J Natl Cancer Inst* **99:** 1836-44.

Dutt A, Beroukhim R (2007). Single nucleotide polymorphism array analysis of cancer. *Curr Opin Oncol* **19:** 43-9.

Eagle LR, Yin X, Brothman AR, Williams BJ, Atkin NB, Prochownik EV (1995). Mutation of the MXI1 gene in prostate cancer. *Nat Genet* **9:** 249-55.

Edlund S, Bu S, Schuster N, Aspenstrom P, Heuchel R, Heldin NE, ten Dijke P, Heldin CH, Landstrom M (2003). Transforming growth factor-beta1 (TGF-beta)-induced apoptosis of prostate cancer cells involves Smad7-dependent activation of p38 by TGF-beta-activated kinase 1 and mitogen-activated protein kinase kinase 3. *Mol Biol Cell* **14:** 529-44.

Edwards PA (2010). Fusion genes and chromosome translocations in the common epithelial cancers. *J Pathol* **220:** 244-54.

Eeles RA, Kote-Jarai Z, Giles GG, Olama AA, Guy M, Jugurnauth SK, Mulholland S, Leongamornlert DA, Edwards SM, Morrison J, Field HI, Southey MC, Severi G, Donovan JL, Hamdy FC, Dearnaley DP, Muir KR, Smith C, Bagnato M, Ardern-Jones AT, Hall AL, O'Brien LT, Gehr-Swain BN, Wilkinson RA, Cox A, Lewis S, Brown PM, Jhavar SG, Tymrakiewicz M, Lophatananon A, Bryant SL, Horwich A, Huddart RA, Khoo VS, Parker CC, Woodhouse CJ, Thompson A, Christmas T, Ogden C, Fisher C, Jamieson C, Cooper CS, English DR, Hopper JL, Neal DE, Easton DF (2008). Multiple newly identified loci associated with prostate cancer susceptibility. *Nat Genet* **40:** 316-21.

Egertova M, Elphick MR (2000). Localisation of cannabinoid receptors in the rat brain using antibodies to the intracellular C-terminal tail of CB. *J Comp Neurol* **422:** 159-71.

El Gammal AT, Bruchmann M, Zustin J, Isbarn H, Hellwinkel OJ, Kollermann J, Sauter G, Simon R, Wilczak W, Schwarz J, Bokemeyer C, Brummendorf TH, Izbicki JR, Yekebas E, Fisch M, Huland H, Graefen M, Schlomm T (2010). Chromosome 8p deletions and 8q gains are associated with tumor progression and poor prognosis in prostate cancer. *Clin Cancer Res* **16:** 56-64.

Evron E, Umbricht CB, Korz D, Raman V, Loeb DM, Niranjan B, Buluwela L, Weitzman SA, Marks J, Sukumar S (2001). Loss of cyclin D2 expression in the majority of breast cancers is associated with promoter hypermethylation. *Cancer Res* **61:** 2782-7.

Feldser DM, Hackett JA, Greider CW (2003). Telomere dysfunction and the initiation of genome instability. *Nat Rev Cancer* **3:** 623-7.

Fernandez TV, Garcia-Gonzalez IJ, Mason CE, Hernandez-Zaragoza G, Ledezma-Rodriguez VC, Anguiano-Alvarez VM, E'Vega R, Gutierrez-Angulo M, Maya ML, Garcia-Bejarano HE, Gonzalez-Cruz M, Barrios S, Atorga R, Lopez-Cardona MG, Armendariz-Borunda J, State MW, Davalos NO (2008). Molecular characterization of a patient with 3p deletion syndrome and a review of the literature. *Am J Med Genet A* **146A:** 2746-52.

Franceschi S (1998). Iodine intake and thyroid carcinoma--a potential risk factor. *Exp Clin Endocrinol Diabetes* **106 Suppl 3:** S38-44.

Freedman ML, Haiman CA, Patterson N, McDonald GJ, Tandon A, Waliszewska A, Penney K, Steen RG, Ardlie K, John EM, Oakley-Girvan I, Whittemore AS, Cooney KA, Ingles SA, Altshuler D, Henderson BE, Reich D (2006). Admixture mapping identifies 8q24 as a prostate cancer risk locus in African-American men. *Proc Natl Acad Sci U S A* **103:** 14068-73.

Freimuth N, Ramer R, Hinz B (2010). Antitumorigenic effects of cannabinoids beyond apoptosis. *J Pharmacol Exp Ther* **332:** 336-44.

Frigola J, Munoz M, Clark SJ, Moreno V, Capella G, Peinado MA (2005). Hypermethylation of the prostacyclin synthase (PTGIS) promoter is a frequent event in colorectal cancer and associated with aneuploidy. *Oncogene* **24:** 7320-6.

Fujita T, Igarashi J, Okawa ER, Gotoh T, Manne J, Kolla V, Kim J, Zhao H, Pawel BR, London WB, Maris JM, White PS, Brodeur GM (2008). CHD5, a tumor suppressor gene deleted from 1p36.31 in neuroblastomas. *J Natl Cancer Inst* **100:** 940-9.

Furuta J, Nobeyama Y, Umebayashi Y, Otsuka F, Kikuchi K, Ushijima T (2006). Silencing of Peroxiredoxin 2 and aberrant methylation of 33 CpG islands in putative promoter regions in human malignant melanomas. *Cancer Res* **66:** 6080-6.

Gadzicki D, Muller-Vahl K, Stuhrmann M (1999). A frequent polymorphism in the coding exon of the human cannabinoid receptor (CNR1) gene. *Mol Cell Probes* **13:** 321-3.

Gaidano G, Pastore C, Gloghini A, Volpe G, Ghia P, Saglio G, Carbone A (1996). AIDS-related non-Hodgkin's lymphomas: molecular genetics, viral infection and cytokine deregulation. *Acta Haematol* **95:** 193-8.

Ganem NJ, Storchova Z, Pellman D (2007). Tetraploidy, aneuploidy and cancer. *Curr Opin Genet Dev* **17:** 157-62.

Gardina PJ, Clark TA, Shimada B, Staples MK, Yang Q, Veitch J, Schweitzer A, Awad T, Sugnet C, Dee S, Davies C, Williams A, Turpaz Y (2006). Alternative splicing and differential gene expression in colon cancer detected by a whole genome exon array. *BMC Genomics* **7:** 325.

Garzon R, Calin GA, Croce CM (2009). MicroRNAs in Cancer. *Annu Rev Med* **60:** 167-79.

Gayther SA, de Foy KA, Harrington P, Pharoah P, Dunsmuir WD, Edwards SM, Gillett C, Ardern-Jones A, Dearnaley DP, Easton DF, Ford D, Shearer RJ, Kirby RS, Dowe AL, Kelly J, Stratton MR, Ponder BA, Barnes D, Eeles RA (2000). The frequency of germ-line mutations in the breast cancer predisposition genes BRCA1 and BRCA2 in familial prostate cancer. The Cancer Research Campaign/British Prostate Group United Kingdom Familial Prostate Cancer Study Collaborators. *Cancer Res* **60:** 4513-8.

Geigl JB, Obenauf AC, Schwarzbraun T, Speicher MR (2008). Defining 'chromosomal instability'. *Trends Genet* **24:** 64-9.

Gentleman RC, Carey VJ, Bates DM, Bolstad B, Dettling M, Dudoit S, Ellis B, Gautier L, Ge Y, Gentry J, Hornik K, Hothorn T, Huber W, Iacus S, Irizarry R, Leisch F, Li C,

Maechler M, Rossini AJ, Sawitzki G, Smith C, Smyth G, Tierney L, Yang JY, Zhang J (2004). Bioconductor: open software development for computational biology and bioinformatics. *Genome Biol* **5:** R80.

Ghoussaini M, Song H, Koessler T, Al Olama AA, Kote-Jarai Z, Driver KE, Pooley KA, Ramus SJ, Kjaer SK, Hogdall E, DiCioccio RA, Whittemore AS, Gayther SA, Giles GG, Guy M, Edwards SM, Morrison J, Donovan JL, Hamdy FC, Dearnaley DP, Ardern-Jones AT, Hall AL, O'Brien LT, Gehr-Swain BN, Wilkinson RA, Brown PM, Hopper JL, Neal DE, Pharoah PD, Ponder BA, Eeles RA, Easton DF, Dunning AM (2008). Multiple loci with different cancer specificities within the 8q24 gene desert. *J Natl Cancer Inst* **100:** 962-6.

Gibas Z, Pontes JE, Sandberg AA (1985). Chromosome rearrangements in a metastatic adenocarcinoma of the prostate. *Cancer Genet Cytogenet* **16:** 301-4.

Gleason DF (1966). Classification of prostatic carcinomas. *Cancer Chemother Rep* **50:** 125-8.

Gleason DF, Mellinger GT (1974). Prediction of prognosis for prostatic adenocarcinoma by combined histological grading and clinical staging. *J Urol* **111:** 58-64.

Gollin SM (2004). Chromosomal instability. *Curr Opin Oncol* **16:** 25-31.

Gollin SM (2005). Mechanisms leading to chromosomal instability. *Semin Cancer Biol* **15:** 33-42.

Gopalan A, Leversha MA, Satagopan JM, Zhou Q, Al-Ahmadie HA, Fine SW, Eastham JA, Scardino PT, Scher HI, Tickoo SK, Reuter VE, Gerald WL (2009). TMPRSS2-ERG gene fusion is not associated with outcome in patients treated by prostatectomy. *Cancer Res* **69:** 1400-6.

Grimsey NL, Goodfellow CE, Scotter EL, Dowie MJ, Glass M, Graham ES (2008). Specific detection of CB1 receptors; cannabinoid CB1 receptor antibodies are not all created equal! *J Neurosci Methods* **171:** 78-86.

Gronberg H (2003). Prostate cancer epidemiology. *Lancet* **361:** 859-64.

Gudmundsson J, Sulem P, Manolescu A, Amundadottir LT, Gudbjartsson D, Helgason A, Rafnar T, Bergthorsson JT, Agnarsson BA, Baker A, Sigurdsson A, Benediktsdottir KR, Jakobsdottir M, Xu J, Blondal T, Kostic J, Sun J, Ghosh S, Stacey SN, Mouy M, Saemundsdottir J, Backman VM, Kristjansson K, Tres A, Partin AW, Albers-Akkers MT, Godino-Ivan Marcos J, Walsh PC, Swinkels DW, Navarrete S, Isaacs SD, Aben KK, Graif T, Cashy J, Ruiz-Echarri M, Wiley KE, Suarez BK, Witjes JA, Frigge M, Ober C, Jonsson E, Einarsson GV, Mayordomo JI, Kiemeney LA, Isaacs WB, Catalona WJ, Barkardottir RB, Gulcher JR, Thorsteinsdottir U, Kong A, Stefansson K (2007a). Genome-wide association study identifies a second prostate cancer susceptibility variant at 8q24. *Nat Genet* **39:** 631-7.

Gudmundsson J, Sulem P, Rafnar T, Bergthorsson JT, Manolescu A, Gudbjartsson D, Agnarsson BA, Sigurdsson A, Benediktsdottir KR, Blondal T, Jakobsdottir M, Stacey SN, Kostic J, Kristinsson KT, Birgisdottir B, Ghosh S, Magnusdottir DN, Thorlacius S, Thorleifsson G, Zheng SL, Sun J, Chang BL, Elmore JB, Breyer JP, McReynolds KM, Bradley KM, Yaspan BL, Wiklund F, Stattin P, Lindstrom S, Adami HO, McDonnell SK, Schaid DJ, Cunningham JM, Wang L, Cerhan JR, St Sauver JL, Isaacs SD, Wiley KE, Partin AW, Walsh PC, Polo S, Ruiz-Echarri M, Navarrete S, Fuertes F, Saez B,

Godino J, Weijerman PC, Swinkels DW, Aben KK, Witjes JA, Suarez BK, Helfand BT, Frigge ML, Kristjansson K, Ober C, Jonsson E, Einarsson GV, Xu J, Gronberg H, Smith JR, Thibodeau SN, Isaacs WB, Catalona WJ, Mayordomo JI, Kiemeney LA, Barkardottir RB, Gulcher JR, Thorsteinsdottir U, Kong A, Stefansson K (2008). Common sequence variants on 2p15 and Xp11.22 confer susceptibility to prostate cancer. *Nat Genet* **40:** 281-3.

Gudmundsson J, Sulem P, Steinthorsdottir V, Bergthorsson JT, Thorleifsson G, Manolescu A, Rafnar T, Gudbjartsson D, Agnarsson BA, Baker A, Sigurdsson A, Benediktsdottir KR, Jakobsdottir M, Blondal T, Stacey SN, Helgason A, Gunnarsdottir S, Olafsdottir A, Kristinsson KT, Birgisdottir B, Ghosh S, Thorlacius S, Magnusdottir D, Stefansdottir G, Kristjansson K, Bagger Y, Wilensky RL, Reilly MP, Morris AD, Kimber CH, Adeyemo A, Chen Y, Zhou J, So WY, Tong PC, Ng MC, Hansen T, Andersen G, Borch-Johnsen K, Jorgensen T, Tres A, Fuertes F, Ruiz-Echarri M, Asin L, Saez B, van Boven E, Klaver S, Swinkels DW, Aben KK, Graif T, Cashy J, Suarez BK, van Vierssen Trip O, Frigge ML, Ober C, Hofker MH, Wijmenga C, Christiansen C, Rader DJ, Palmer CN, Rotimi C, Chan JC, Pedersen O, Sigurdsson G, Benediktsson R, Jonsson E, Einarsson GV, Mayordomo JI, Catalona WJ, Kiemeney LA, Barkardottir RB, Gulcher JR, Thorsteinsdottir U, Kong A, Stefansson K (2007b). Two variants on chromosome 17 confer prostate cancer risk, and the one in TCF2 protects against type 2 diabetes. *Nat Genet* **39:** 977-83.

Guffanti A, Iacono M, Pelucchi P, Kim N, Solda G, Croft LJ, Taft RJ, Rizzi E, Askarian-Amiri M, Bonnal RJ, Callari M, Mignone F, Pesole G, Bertalot G, Bernardi LR, Albertini A, Lee C, Mattick JS, Zucchi I, De Bellis G (2009). A transcriptional sketch of a primary human breast cancer by 454 deep sequencing. *BMC Genomics* **10:** 163.

Gurel B, Iwata T, Koh CM, Jenkins RB, Lan F, Van Dang C, Hicks JL, Morgan J, Cornish TC, Sutcliffe S, Isaacs WB, Luo J, De Marzo AM (2008). Nuclear MYC protein overexpression is an early alteration in human prostate carcinogenesis. *Mod Pathol* **21:** 1156-67.

Haffner MC, Aryee MJ, Toubaji A, Esopi DM, Albadine R, Gurel B, Isaacs WB, Bova GS, Liu W, Xu J, Meeker AK, Netto G, De Marzo AM, Nelson WG, Yegnasubramanian S (2010). Androgen-induced TOP2B-mediated double-strand breaks and prostate cancer gene rearrangements. *Nat Genet* **42:** 668-75.

Haiman CA, Le Marchand L, Yamamato J, Stram DO, Sheng X, Kolonel LN, Wu AH, Reich D, Henderson BE (2007a). A common genetic risk factor for colorectal and prostate cancer. *Nat Genet* **39:** 954-6.

Haiman CA, Patterson N, Freedman ML, Myers SR, Pike MC, Waliszewska A, Neubauer J, Tandon A, Schirmer C, McDonald GJ, Greenway SC, Stram DO, Le Marchand L, Kolonel LN, Frasco M, Wong D, Pooler LC, Ardlie K, Oakley-Girvan I, Whittemore AS, Cooney KA, John EM, Ingles SA, Altshuler D, Henderson BE, Reich D (2007b). Multiple regions within 8q24 independently affect risk for prostate cancer. *Nat Genet* **39:** 638-44.

Hanahan D, Weinberg RA (2000). The hallmarks of cancer. *Cell* **100:** 57-70.

Henrique R, Costa VL, Cerveira N, Carvalho AL, Hoque MO, Ribeiro FR, Oliveira J, Teixeira MR, Sidransky D, Jeronimo C (2006). Hypermethylation of Cyclin D2 is associated with loss of mRNA expression and tumor development in prostate cancer. *J Mol Med* **84:** 911-8.

Herbst RA, Weiss J, Ehnis A, Cavenee WK, Arden KC (1994). Loss of heterozygosity for 10q22-10qter in malignant melanoma progression. *Cancer Res* **54:** 3111-4.

Hibi K, Mizukami H, Shirahata A, Goto T, Sakata M, Saito M, Ishibashi K, Kigawa G, Nemoto H, Sanada Y (2009). Aberrant methylation of the UNC5C gene is frequently detected in advanced colorectal cancer. *Anticancer Res* **29:** 271-3.

Holcomb IN, Grove DI, Kinnunen M, Friedman CL, Gallaher IS, Morgan TM, Sather CL, Delrow JJ, Nelson PS, Lange PH, Ellis WJ, True LD, Young JM, Hsu L, Trask BJ, Vessella RL (2008). Genomic alterations indicate tumor origin and varied metastatic potential of disseminated cells from prostate cancer patients. *Cancer Res* **68:** 5599-608.

Holcomb IN, Young JM, Coleman IM, Salari K, Grove DI, Hsu L, True LD, Roudier MP, Morrissey CM, Higano CS, Nelson PS, Vessella RL, Trask BJ (2009). Comparative analyses of chromosome alterations in soft-tissue metastases within and across patients with castration-resistant prostate cancer. *Cancer Res* **69:** 7793-802.

Holland AJ, Cleveland DW (2009). Boveri revisited: chromosomal instability, aneuploidy and tumorigenesis. *Nat Rev Mol Cell Biol* **10:** 478-87.

Hoshino H, Kobayashi A, Yoshida M, Kudo N, Oyake T, Motohashi H, Hayashi N, Yamamoto M, Igarashi K (2000). Oxidative stress abolishes leptomycin B-sensitive nuclear export of transcription repressor Bach2 that counteracts activation of Maf recognition element. *J Biol Chem* **275:** 15370-6.

Howarth KD, Blood KA, Ng BL, Beavis JC, Chua Y, Cooke SL, Raby S, Ichimura K, Collins VP, Carter NP, Edwards PA (2008). Array painting reveals a high frequency of balanced translocations in breast cancer cell lines that break in cancer-relevant genes. *Oncogene* **27:** 3345-59.

Howe JR, Roth S, Ringold JC, Summers RW, Jarvinen HJ, Sistonen P, Tomlinson IP, Houlston RS, Bevan S, Mitros FA, Stone EM, Aaltonen LA (1998). Mutations in the SMAD4/DPC4 gene in juvenile polyposis. *Science* **280:** 1086-8.

Huang HE, Chin SF, Ginestier C, Bardou VJ, Adelaide J, Iyer NG, Garcia MJ, Pole JC, Callagy GM, Hewitt SM, Gullick WJ, Jacquemier J, Caldas C, Chaffanet M, Birnbaum D, Edwards PA (2004). A recurrent chromosome breakpoint in breast cancer at the NRG1/neuregulin 1/heregulin gene. *Cancer Res* **64:** 6840-4.

Humphrey PA (2004). Gleason grading and prognostic factors in carcinoma of the prostate. *Mod Pathol* **17:** 292-306.

Hyytinen ER, Saadut R, Chen C, Paull L, Koivisto PA, Vessella RL, Frierson HF, Jr., Dong JT (2002). Defining the region(s) of deletion at 6q16-q22 in human prostate cancer. *Genes Chromosomes Cancer* **34:** 306-12.

Ishkanian AS, Mallof CA, Ho J, Meng A, Albert M, Syed A, van der Kwast T, Milosevic M, Yoshimoto M, Squire JA, Lam WL, Bristow RG (2009). High-resolution array CGH identifies novel regions of genomic alteration in intermediate-risk prostate cancer. *Prostate* **69:** 1091-100.

Jalava SE, Porkka KP, Rauhala HE, Isotalo J, Tammela TL, Visakorpi T (2009). TCEB1 promotes invasion of prostate cancer cells. *Int J Cancer* **124:** 95-102.

Jiang M, Li M, Fu X, Huang Y, Qian H, Sun R, Mao Y, Xie Y, Li Y (2008). Simultaneously detection of genomic and expression alterations in prostate cancer using cDNA microarray. *Prostate* **68:** 1496-509.

Johansson JE, Andren O, Andersson SO, Dickman PW, Holmberg L, Magnuson A, Adami HO (2004). Natural history of early, localized prostate cancer. *JAMA* **291:** 2713-9.

Johnson CD, Esquela-Kerscher A, Stefani G, Byrom M, Kelnar K, Ovcharenko D, Wilson M, Wang X, Shelton J, Shingara J, Chin L, Brown D, Slack FJ (2007). The let-7 microRNA represses cell proliferation pathways in human cells. *Cancer Res* **67:** 7713-22.

Johnson SM, Grosshans H, Shingara J, Byrom M, Jarvis R, Cheng A, Labourier E, Reinert KL, Brown D, Slack FJ (2005). RAS is regulated by the let-7 microRNA family. *Cell* **120:** 635-47.

Jones MH, Koi S, Fujimoto I, Hasumi K, Kato K, Nakamura Y (1994). Allelotype of uterine cancer by analysis of RFLP and microsatellite polymorphisms: frequent loss of heterozygosity on chromosome arms 3p, 9q, 10q, and 17p. *Genes Chromosomes Cancer* **9:** 119-23.

Jones PA, Baylin SB (2002). The fundamental role of epigenetic events in cancer. *Nat Rev Genet* **3:** 415-28.

Jones PA, Baylin SB (2007). The epigenomics of cancer. *Cell* **128:** 683-92.

Jorgenson E, Witte JS (2007). Genome-wide association studies of cancer. *Future Oncol* **3:** 419-27.

Joshua AM, Evans A, Van der Kwast T, Zielenska M, Meeker AK, Chinnaiyan A, Squire JA (2008). Prostatic preneoplasia and beyond. *Biochim Biophys Acta* **1785:** 156-81.

Kallioniemi A, Kallioniemi OP, Sudar D, Rutovitz D, Gray JW, Waldman F, Pinkel D (1992). Comparative genomic hybridization for molecular cytogenetic analysis of solid tumors. *Science* **258:** 818-21.

Kamio T, Toki T, Kanezaki R, Sasaki S, Tandai S, Terui K, Ikebe D, Igarashi K, Ito E (2003). B-cell-specific transcription factor BACH2 modifies the cytotoxic effects of anticancer drugs. *Blood* **102:** 3317-22.

Karan D, Lin MF, Johansson SL, Batra SK (2003). Current status of the molecular genetics of human prostatic adenocarcinomas. *Int J Cancer* **103:** 285-93.

Karenko L, Hahtola S, Paivinen S, Karhu R, Syrja S, Kahkonen M, Nedoszytko B, Kytola S, Zhou Y, Blazevic V, Pesonen M, Nevala H, Nupponen N, Sihto H, Krebs I, Poustka A, Roszkiewicz J, Saksela K, Peterson P, Visakorpi T, Ranki A (2005). Primary cutaneous T-cell lymphomas show a deletion or translocation affecting NAV3, the human UNC-53 homologue. *Cancer Res* **65:** 8101-10.

Kearney L (2006). Multiplex-FISH (M-FISH): technique, developments and applications. *Cytogenet Genome Res* **114:** 189-98.

Khayat AS, Guimaraes AC, Calcagno DQ, Seabra AD, Lima EM, Leal MF, Faria MH, Rabenhorst SH, Assumpcao PP, Demachki S, Smith MA, Burbano RR (2009). Interrelationship between TP53 gene deletion, protein expression and chromosome 17 aneusomy in gastric adenocarcinoma. *BMC Gastroenterol* **9:** 55.

Kiemeney LA, Thorlacius S, Sulem P, Geller F, Aben KK, Stacey SN, Gudmundsson J, Jakobsdottir M, Bergthorsson JT, Sigurdsson A, Blondal T, Witjes JA, Vermeulen SH, Hulsbergen-van de Kaa CA, Swinkels DW, Ploeg M, Cornel EB, Vergunst H, Thorgeirsson TE, Gudbjartsson D, Gudjonsson SA, Thorleifsson G, Kristinsson KT, Mouy M, Snorradottir S, Placidi D, Campagna M, Arici C, Koppova K, Gurzau E, Rudnai P, Kellen E, Polidoro S, Guarrera S, Sacerdote C, Sanchez M, Saez B, Valdivia G, Ryk C, de Verdier P, Lindblom A, Golka K, Bishop DT, Knowles MA, Nikulasson S, Petursdottir V, Jonsson E, Geirsson G, Kristjansson B, Mayordomo JI, Steineck G, Porru S, Buntinx F, Zeegers MP, Fletcher T, Kumar R, Matullo G, Vineis P, Kiltie AE, Gulcher JR, Thorsteinsdottir U, Kong A, Rafnar T, Stefansson K (2008). Sequence variant on 8q24 confers susceptibility to urinary bladder cancer. *Nat Genet* **40:** 1307-12.

Kim H, Lapointe J, Kaygusuz G, Ong DE, Li C, van de Rijn M, Brooks JD, Pollack JR (2005). The retinoic acid synthesis gene ALDH1a2 is a candidate tumor suppressor in prostate cancer. *Cancer Res* **65:** 8118-24.

Kim JH, Dhanasekaran SM, Mehra R, Tomlins SA, Gu W, Yu J, Kumar-Sinha C, Cao X, Dash A, Wang L, Ghosh D, Shedden K, Montie JE, Rubin MA, Pienta KJ, Shah RB, Chinnaiyan AM (2007). Integrative analysis of genomic aberrations associated with prostate cancer progression. *Cancer Res* **67:** 8229-39.

Kinzler KW, Vogelstein B (1997). Cancer-susceptibility genes. Gatekeepers and caretakers. *Nature* **386:** 761-3.

Kinzler KW, Vogelstein B (1998). Landscaping the cancer terrain. *Science* **280:** 1036-7.

Klein CA (2009). Parallel progression of primary tumours and metastases. *Nat Rev Cancer* **9:** 302-12.

Klein CA, Blankenstein TJ, Schmidt-Kittler O, Petronio M, Polzer B, Stoecklein NH, Riethmuller G (2002). Genetic heterogeneity of single disseminated tumour cells in minimal residual cancer. *Lancet* **360:** 683-9.

Knudson AG, Jr. (1971). Mutation and cancer: statistical study of retinoblastoma. *Proc Natl Acad Sci U S A* **68:** 820-3.

Kobayashi M, Ishida H, Shindo T, Niwa S, Kino M, Kawamura K, Kamiya N, Imamoto T, Suzuki H, Hirokawa Y, Shiraishi T, Tanizawa T, Nakatani Y, Ichikawa T (2008). Molecular analysis of multifocal prostate cancer by comparative genomic hybridization. *Prostate* **68:** 1715-24.

Kohno T, Yokota J (2006). Molecular processes of chromosome 9p21 deletions causing inactivation of the p16 tumor suppressor gene in human cancer: deduction from structural analysis of breakpoints for deletions. *DNA Repair (Amst)* **5:** 1273-81.

Kolomietz E, Al-Maghrabi J, Brennan S, Karaskova J, Minkin S, Lipton J, Squire JA (2001). Primary chromosomal rearrangements of leukemia are frequently accompanied by extensive submicroscopic deletions and may lead to altered prognosis. *Blood* **97:** 3581-8.

Konig JJ, Teubel W, Kamst E, Romijn JC, Schroder FH, Hagemeijer A (1998). Cytogenetic analysis of 39 prostate carcinomas and evaluation of short-term tissue culture techniques. *Cancer Genet Cytogenet* **101:** 116-22.

Konishi N, Nakamura M, Kishi M, Ishida E, Shimada K, Matsuyoshi S, Nagai H, Emi M (2003). Genetic mapping of allelic loss on chromosome 6q within heterogeneous prostate carcinoma. *Cancer Sci* **94:** 764-8.

Kron KJ, Liu L, Pethe VV, Demetrashvili N, Nesbitt ME, Trachtenberg J, Ozcelik H, Fleshner NE, Briollais L, van der Kwast TH, Bapat B (2010). DNA methylation of HOXD3 as a marker of prostate cancer progression. *Lab Invest* **90:** 1060-7.

Kurochkin IV, Yonemitsu N, Funahashi SI, Nomura H (2001). ALEX1, a novel human armadillo repeat protein that is expressed differentially in normal tissues and carcinomas. *Biochem Biophys Res Commun* **280:** 340-7.

Laezza C, Malfitano AM, Proto MC, Esposito I, Gazzerro P, Formisano P, Pisanti S, Santoro A, Caruso MG, Bifulco M (2010). Inhibition of 3-hydroxy-3-methylglutaryl-coenzyme A reductase activity and of Ras farnesylation mediate antitumor effects of anandamide in human breast cancer cells. *Endocr Relat Cancer* **17:** 495-503.

Lai J, Chien J, Staub J, Avula R, Greene EL, Matthews TA, Smith DI, Kaufmann SH, Roberts LR, Shridhar V (2003). Loss of HSulf-1 up-regulates heparin-binding growth factor signaling in cancer. *J Biol Chem* **278:** 23107-17.

Lai JP, Sandhu DS, Shire AM, Roberts LR (2008). The tumor suppressor function of human sulfatase 1 (SULF1) in carcinogenesis. *J Gastrointest Cancer* **39:** 149-58.

Lai JP, Yu C, Moser CD, Aderca I, Han T, Garvey TD, Murphy LM, Garrity-Park MM, Shridhar V, Adjei AA, Roberts LR (2006). SULF1 inhibits tumor growth and potentiates the effects of histone deacetylase inhibitors in hepatocellular carcinoma. *Gastroenterology* **130:** 2130-44.

Lambros MB, Simpson PT, Jones C, Natrajan R, Westbury C, Steele D, Savage K, Mackay A, Schmitt FC, Ashworth A, Reis-Filho JS (2006). Unlocking pathology archives for molecular genetic studies: a reliable method to generate probes for chromogenic and fluorescent in situ hybridization. *Lab Invest* **86:** 398-408.

Lane TM, Strefford JC, Yanez-Munoz RJ, Purkis P, Forsythe E, Nia T, Hines J, Lu YJ, Oliver RT (2007). Identification of a recurrent t(4;6) chromosomal translocation in prostate cancer. *J Urol* **177:** 1907-12.

Lapointe J, Li C, Giacomini CP, Salari K, Huang S, Wang P, Ferrari M, Hernandez-Boussard T, Brooks JD, Pollack JR (2007). Genomic profiling reveals alternative genetic pathways of prostate tumorigenesis. *Cancer Res* **67:** 8504-10.

Latil A, Chene L, Cochant-Priollet B, Mangin P, Fournier G, Berthon P, Cussenot O (2003). Quantification of expression of netrins, slits and their receptors in human prostate tumors. *Int J Cancer* **103:** 306-15.

Lee WH, Morton RA, Epstein JI, Brooks JD, Campbell PA, Bova GS, Hsieh WS, Isaacs WB, Nelson WG (1994). Cytidine methylation of regulatory sequences near the pi-class glutathione S-transferase gene accompanies human prostatic carcinogenesis. *Proc Natl Acad Sci U S A* **91:** 11733-7.

Lee YK, Kim YR, Min HC, Oh BR, Kim TY, Kim YS, Cho HI, Kim HC, Lee YS, Lee DS (2006). Deletion of any part of the BCR or ABL gene on the derivative chromosome 9 is a poor prognostic marker in chronic myelogenous leukemia. *Cancer Genet Cytogenet* **166:** 65-73.

Lengauer C, Kinzler KW, Vogelstein B (1998). Genetic instabilities in human cancers. *Nature* **396:** 643-9.

Lewis BP, Burge CB, Bartel DP (2005). Conserved seed pairing, often flanked by adenosines, indicates that thousands of human genes are microRNA targets. *Cell* **120:** 15-20.

Lin C, Yang L, Tanasa B, Hutt K, Ju BG, Ohgi K, Zhang J, Rose DW, Fu XD, Glass CK, Rosenfeld MG (2009). Nuclear receptor-induced chromosomal proximity and DNA breaks underlie specific translocations in cancer. *Cell* **139:** 1069-83.

Liu J, Sorensen AB, Wang B, Wabl M, Nielsen AL, Pedersen FS (2009). Identification of novel Bach2 transcripts and protein isoforms through tagging analysis of retroviral integrations in B-cell lymphomas. *BMC Mol Biol* **10:** 2.

Liu W, Chang B, Sauvageot J, Dimitrov L, Gielzak M, Li T, Yan G, Sun J, Adams TS, Turner AR, Kim JW, Meyers DA, Zheng SL, Isaacs WB, Xu J (2006). Comprehensive assessment of DNA copy number alterations in human prostate cancers using Affymetrix 100K SNP mapping array. *Genes Chromosomes Cancer* **45:** 1018-32.

Liu W, Chang BL, Cramer S, Koty PP, Li T, Sun J, Turner AR, Von Kap-Herr C, Bobby P, Rao J, Zheng SL, Isaacs WB, Xu J (2007). Deletion of a small consensus region at 6q15, including the MAP3K7 gene, is significantly associated with high-grade prostate cancers. *Clin Cancer Res* **13:** 5028-33.

Liu X, Adams AL (2007). Mucoepidermoid carcinoma of the bronchus: a review. *Arch Pathol Lab Med* **131:** 1400-4.

Lotan TL, Epstein JI (2010). Clinical implications of changing definitions within the Gleason grading system. *Nat Rev Urol* **7:** 136-42.

Lu YJ, Birdsall S, Summersgill B, Smedley D, Osin P, Fisher C, Shipley J (1999). Dual colour fluorescence in situ hybridization to paraffin-embedded samples to deduce the presence of the der(X)t(X;18)(p11.2;q11.2) and involvement of either the SSX1 or SSX2 gene: a diagnostic and prognostic aid for synovial sarcoma. *J Pathol* **187:** 490-6.

Lundgren R, Kristoffersson U, Heim S, Mandahl N, Mitelman F (1988). Multiple structural chromosome rearrangements, including del(7q) and del(10q), in an adenocarcinoma of the prostate. *Cancer Genet Cytogenet* **35:** 103-8.

Lundgren R, Mandahl N, Heim S, Limon J, Henrikson H, Mitelman F (1992). Cytogenetic analysis of 57 primary prostatic adenocarcinomas. *Genes Chromosomes Cancer* **4:** 16-24.

Lynch ED, Ostermeyer EA, Lee MK, Arena JF, Ji H, Dann J, Swisshelm K, Suchard D, MacLeod PM, Kvinnsland S, Gjertsen BT, Heimdal K, Lubs H, Moller P, King MC (1997). Inherited mutations in PTEN that are associated with breast cancer, cowden disease, and juvenile polyposis. *Am J Hum Genet* **61:** 1254-60.

Macleod K (2000). Tumor suppressor genes. *Curr Opin Genet Dev* **10:** 81-93.

Maher CA, Kumar-Sinha C, Cao X, Kalyana-Sundaram S, Han B, Jing X, Sam L, Barrette T, Palanisamy N, Chinnaiyan AM (2009). Transcriptome sequencing to detect gene fusions in cancer. *Nature* **458:** 97-101.

Mani RS, Tomlins SA, Callahan K, Ghosh A, Nyati MK, Varambally S, Palanisamy N, Chinnaiyan AM (2009). Induced chromosomal proximity and gene fusions in prostate cancer. *Science* **326:** 1230.

Manolio TA (2010). Genomewide association studies and assessment of the risk of disease. *N Engl J Med* **363:** 166-76.

Mao X, James SY, Yanez-Munoz RJ, Chaplin T, Molloy G, Oliver RT, Young BD, Lu YJ (2007). Rapid high-resolution karyotyping with precise identification of chromosome breakpoints. *Genes Chromosomes Cancer* **46:** 675-83.

Mao X, Young BD, Chaplin T, Shipley J, Lu YJ (2008). Subtle genomic alterations and genomic instability revealed in diploid cancer cell lines. *Cancer Lett* **267:** 49-54.

Mao X, Yu Y, Boyd LK, Ren G, Lin D, Chaplin T, Kudahetti SC, Stankiewicz E, Xue L, Beltran L, Gupta M, Oliver RT, Lemoine NR, Berney DM, Young BD, Lu YJ (2010). Distinct genomic alterations in prostate cancers in Chinese and Western populations suggest alternative pathways of prostate carcinogenesis. *Cancer Res* **70:** 5207-12.

Mardis ER (2008). Next-generation DNA sequencing methods. *Annu Rev Genomics Hum Genet* **9:** 387-402.

Margolis RL, Lohez OD, Andreassen PR (2003). G1 tetraploidy checkpoint and the suppression of tumorigenesis. *J Cell Biochem* **88:** 673-83.

Mayr C, Hemann MT, Bartel DP (2007). Disrupting the pairing between let-7 and Hmga2 enhances oncogenic transformation. *Science* **315:** 1576-9.

McMichael AJ (2008). Food, nutrition, physical activity and cancer prevention. Authoritative report from World Cancer Research Fund provides global update. *Public Health Nutr* **11:** 762-3.

McNeal JE (1981). Normal and pathologic anatomy of prostate. *Urology* **17:** 11-6.

McNeal JE (1988). Normal anatomy of the prostate and changes in benign prostatic hypertrophy and carcinoma. *Semin Ultrasound CT MR* **9:** 329-34.

McWhirter JR, Wang JY (1991). Activation of tyrosinase kinase and microfilament-binding functions of c-abl by bcr sequences in bcr/abl fusion proteins. *Mol Cell Biol* **11:** 1553-65.

Medina PP, Slack FJ (2008). microRNAs and cancer: an overview. *Cell Cycle* **7:** 2485-92.

Mehra R, Han B, Tomlins SA, Wang L, Menon A, Wasco MJ, Shen R, Montie JE, Chinnaiyan AM, Shah RB (2007a). Heterogeneity of TMPRSS2 gene rearrangements in multifocal prostate adenocarcinoma: molecular evidence for an independent group of diseases. *Cancer Res* **67:** 7991-5.

Mehra R, Tomlins SA, Shen R, Nadeem O, Wang L, Wei JT, Pienta KJ, Ghosh D, Rubin MA, Chinnaiyan AM, Shah RB (2007b). Comprehensive assessment of TMPRSS2 and ETS family gene aberrations in clinically localized prostate cancer. *Mod Pathol* **20:** 538-44.

Mertens F, Antonescu CR, Hohenberger P, Ladanyi M, Modena P, D'Incalci M, Casali PG, Aglietta M, Alvegard T (2009). Translocation-related sarcomas. *Semin Oncol* **36:** 312-23.

Milasin J, Micic S (1994). Double minute chromosomes in an invasive adenocarcinoma of the prostate. *Cancer Genet Cytogenet* **72:** 157-9.

Mitelman F (1995). *ISCN (1995):An international system for human cytogenetic nomenclature*. S. Karger: Basel.

Mitelman F, Johansson B, Mertens F (2007). The impact of translocations and gene fusions on cancer causation. *Nat Rev Cancer* **7:** 233-45.

Mitelman F, Johansson B, Mertens F (2010). Mitelman Database of Chromosome Aberrations and Gene Fusions in Cancer (online), http://cgap.nci.nih.gov/Chromosomes/Mitelman.

Mitra AV, Bancroft EK, Barbachano Y, Page EC, Foster CS, Jameson C, Mitchell G, Lindeman GJ, Stapleton A, Suthers G, Evans DG, Cruger D, Blanco I, Mercer C, Kirk J, Maehle L, Hodgson S, Walker L, Izatt L, Douglas F, Tucker K, Dorkins H, Clowes V, Male A, Donaldson A, Brewer C, Doherty R, Bulman B, Osther PJ, Salinas M, Eccles D, Axcrona K, Jobson I, Newcombe B, Cybulski C, Rubinstein WS, Buys S, Townshend S, Friedman E, Domchek S, Ramon YCT, Spigelman A, Teo SH, Nicolai N, Aaronson N, Ardern-Jones A, Bangma C, Dearnaley D, Eyfjord J, Falconer A, Gronberg H, Hamdy F, Johannsson O, Khoo V, Kote-Jarai Z, Lilja H, Lubinski J, Melia J, Moynihan C, Peock S, Rennert G, Schroder F, Sibley P, Suri M, Wilson P, Bignon YJ, Strom S, Tischkowitz M, Liljegren A, Ilencikova D, Abele A, Kyriacou K, Van Asperen C, Kiemeney L, Easton DF, Eeles RA (2010). Targeted prostate cancer screening in men with mutations in BRCA1 and BRCA2 detects aggressive prostate cancer: preliminary analysis of the results of the IMPACT study. *BJU Int*.

Molenaar WM, Stoepker ME, de Ruiter AJ, Hoekstra HJ, van den Berg E (1996). Cytogenetic support for primary prostatic cancer in a patient presenting with a soft tissue mass in the leg. *Cancer Genet Cytogenet* **86:** 147-9.

Moller-Levet CS, Betts GN, Harris AL, Homer JJ, West CM, Miller CJ (2009). Exon array analysis of head and neck cancers identifies a hypoxia related splice variant of LAMA3 associated with a poor prognosis. *PLoS Comput Biol* **5:** e1000571.

Montironi R, Mazzucchelli R, Scarpelli M, Lopez-Beltran A, Mikuz G, Algaba F, Boccon-Gibod L (2006). Prostate carcinoma II: prognostic factors in prostate needle biopsies. *BJU Int* **97:** 492-7.

Moolgavkar SH, Luebeck EG (2003). Multistage carcinogenesis and the incidence of human cancer. *Genes Chromosomes Cancer* **38:** 302-6.

Morita R, Saito S, Ishikawa J, Ogawa O, Yoshida O, Yamakawa K, Nakamura Y (1991). Common regions of deletion on chromosomes 5q, 6q, and 10q in renal cell carcinoma. *Cancer Res* **51:** 5817-20.

Motamed-Khorasani A, Jurisica I, Letarte M, Shaw PA, Parkes RK, Zhang X, Evangelou A, Rosen B, Murphy KJ, Brown TJ (2007). Differentially androgen-modulated genes in ovarian epithelial cells from BRCA mutation carriers and control patients predict ovarian cancer survival and disease progression. *Oncogene* **26:** 198-214.

Nakayama M, Bennett CJ, Hicks JL, Epstein JI, Platz EA, Nelson WG, De Marzo AM (2003). Hypermethylation of the human glutathione S-transferase-pi gene (GSTP1) CpG island is present in a subset of proliferative inflammatory atrophy lesions but not in normal or hyperplastic epithelium of the prostate: a detailed study using laser-capture microdissection. *Am J Pathol* **163:** 923-33.

Narita K, Staub J, Chien J, Meyer K, Bauer M, Friedl A, Ramakrishnan S, Shridhar V (2006). HSulf-1 inhibits angiogenesis and tumorigenesis in vivo. *Cancer Res* **66:** 6025-32.

Neal JA, Hoskin JP (2009). Clinical oncology: basic principles and practice. *Pathogenesis of cancer* **1:** 3-4.

Negrini S, Gorgoulis VG, Halazonetis TD (2010). Genomic instability--an evolving hallmark of cancer. *Nat Rev Mol Cell Biol* **11:** 220-8.

Nogueira L, Corradi R, Eastham JA (2010). Other biomarkers for detecting prostate cancer. *BJU Int* **105:** 166-9.

Nowell PC, Hungerford DA (1960). A minute chromosome in human chronic granulocytic leukemia. *Science* **132:** 1497-1501.

Oba K, Matsuyama H, Yoshihiro S, Kishi F, Takahashi M, Tsukamoto M, Kinjo M, Sagiyama K, Naito K (2001). Two putative tumor suppressor genes on chromosome arm 8p may play different roles in prostate cancer. *Cancer Genet Cytogenet* **124:** 20-6.

Olea-Herrero N, Vara D, Malagarie-Cazenave S, Diaz-Laviada I (2009). Inhibition of human tumour prostate PC-3 cell growth by cannabinoids R(+)-Methanandamide and JWH-015: involvement of CB2. *Br J Cancer* **101:** 940-50.

Olschwang S, Serova-Sinilnikova OM, Lenoir GM, Thomas G (1998). PTEN germ-line mutations in juvenile polyposis coli. *Nat Genet* **18:** 12-4.

Ota A, Tagawa H, Karnan S, Tsuzuki S, Karpas A, Kira S, Yoshida Y, Seto M (2004). Identification and characterization of a novel gene, C13orf25, as a target for 13q31-q32 amplification in malignant lymphoma. *Cancer Res* **64:** 3087-95.

Oyake T, Itoh K, Motohashi H, Hayashi N, Hoshino H, Nishizawa M, Yamamoto M, Igarashi K (1996). Bach proteins belong to a novel family of BTB-basic leucine zipper transcription factors that interact with MafK and regulate transcription through the NF-E2 site. *Mol Cell Biol* **16:** 6083-95.

Padar A, Sathyanarayana UG, Suzuki M, Maruyama R, Hsieh JT, Frenkel EP, Minna JD, Gazdar AF (2003). Inactivation of cyclin D2 gene in prostate cancers by aberrant promoter methylation. *Clin Cancer Res* **9:** 4730-4.

Panagopoulos I, Strombeck B, Isaksson M, Heldrup J, Olofsson T, Johansson B (2006). Fusion of ETV6 with an intronic sequence of the BAZ2A gene in a paediatric pre-B acute lymphoblastic leukaemia with a cryptic chromosome 12 rearrangement. *Br J Haematol* **133:** 270-5.

Paris PL, Hofer MD, Albo G, Kuefer R, Gschwend JE, Hautmann RE, Fridyland J, Simko J, Carroll PR, Rubin MA, Collins C (2006). Genomic profiling of hormone-naive lymph node metastases in patients with prostate cancer. *Neoplasia* **8:** 1083-9.

Park J, Betel D, Gryfe R, Michalickova K, Di Nicola N, Gallinger S, Hogue CW, Redston M (2002). Mutation profiling of mismatch repair-deficient colorectal cncers using an in silico genome scan to identify coding microsatellites. *Cancer Res* **62:** 1284-8.

Park WS, Oh MJ, Lee HK, Lee KO, Rhyu MG, Dong SM, Lee JY, Kim SH (1996). Deletions of 9p21 and TP53 in bladder cancer. *J Korean Med Sci* **11:** 233-8.

Patsos HA, Greenhough A, Hicks DJ, Al Kharusi M, Collard TJ, Lane JD, Paraskeva C, Williams AC (2010). The endogenous cannabinoid, anandamide, induces COX-2-dependent cell death in apoptosis-resistant colon cancer cells. *Int J Oncol* **37:** 187-93.

Peiffer SL, Herzog TJ, Tribune DJ, Mutch DG, Gersell DJ, Goodfellow PJ (1995). Allelic loss of sequences from the long arm of chromosome 10 and replication errors in endometrial cancers. *Cancer Res* **55:** 1922-6.

Perner S, Demichelis F, Beroukhim R, Schmidt FH, Mosquera JM, Setlur S, Tchinda J, Tomlins SA, Hofer MD, Pienta KG, Kuefer R, Vessella R, Sun XW, Meyerson M, Lee C, Sellers WR, Chinnaiyan AM, Rubin MA (2006). TMPRSS2:ERG fusion-associated deletions provide insight into the heterogeneity of prostate cancer. *Cancer Res* **66:** 8337-41.

Pession A, Tonelli R (2005). The MYCN oncogene as a specific and selective drug target for peripheral and central nervous system tumors. *Curr Cancer Drug Targets* **5:** 273-83.

Petersen I, Langreck H, Wolf G, Schwendel A, Psille R, Vogt P, Reichel MB, Ried T, Dietel M (1997). Small-cell lung cancer is characterized by a high incidence of deletions on chromosomes 3p, 4q, 5q, 10q, 13q and 17p. *Br J Cancer* **75:** 79-86.

Phe V, Cussenot O, Roupret M (2010). Methylated genes as potential biomarkers in prostate cancer. *BJU Int* **105**: 1364-70.

Pierotti MA, Santoro M, Jenkins RB, Sozzi G, Bongarzone I, Grieco M, Monzini N, Miozzo M, Herrmann MA, Fusco A, et al. (1992). Characterization of an inversion on the long arm of chromosome 10 juxtaposing D10S170 and RET and creating the oncogenic sequence RET/PTC. *Proc Natl Acad Sci U S A* **89:** 1616-20.

Pole JC, Courtay-Cahen C, Garcia MJ, Blood KA, Cooke SL, Alsop AE, Tse DM, Caldas C, Edwards PA (2006). High-resolution analysis of chromosome rearrangements on 8p in breast, colon and pancreatic cancer reveals a complex pattern of loss, gain and translocation. *Oncogene* **25:** 5693-706.

Pomerantz MM, Ahmadiyeh N, Jia L, Herman P, Verzi MP, Doddapaneni H, Beckwith CA, Chan JA, Hills A, Davis M, Yao K, Kehoe SM, Lenz HJ, Haiman CA, Yan C, Henderson BE, Frenkel B, Barretina J, Bass A, Tabernero J, Baselga J, Regan MM, Manak JR, Shivdasani R, Coetzee GA, Freedman ML (2009a). The 8q24 cancer risk variant rs6983267 shows long-range interaction with MYC in colorectal cancer. *Nat Genet* **41:** 882-4.

Pomerantz MM, Beckwith CA, Regan MM, Wyman SK, Petrovics G, Chen Y, Hawksworth DJ, Schumacher FR, Mucci L, Penney KL, Stampfer MJ, Chan JA, Ardlie KG, Fritz BR, Parkin RK, Lin DW, Dyke M, Herman P, Lee S, Oh WK, Kantoff PW, Tewari M, McLeod DG, Srivastava S, Freedman ML (2009b). Evaluation of the 8q24 prostate cancer risk locus and MYC expression. *Cancer Res* **69:** 5568-74.

Popovici C, Basset C, Bertucci F, Orsetti B, Adelaide J, Mozziconacci MJ, Conte N, Murati A, Ginestier C, Charafe-Jauffret E, Ethier SP, Lafage-Pochitaloff M, Theillet C, Birnbaum D, Chaffanet M (2002). Reciprocal translocations in breast tumor cell lines: cloning of a t(3;20) that targets the FHIT gene. *Genes Chromosomes Cancer* **35:** 204-18.

Powell IJ, Bock CH, Ruterbusch JJ, Sakr W (2010). Evidence supports a faster growth rate and/or earlier transformation to clinically significant prostate cancer in black than in white American men, and influences racial progression and mortality disparity. *J Urol* **183:** 1792-6.

Prensner JR, Chinnaiyan AM (2009). Oncogenic gene fusions in epithelial carcinomas. *Curr Opin Genet Dev* **19:** 82-91.

Price CM (1993). Fluorescence in situ hybridization. *Blood Rev* **7:** 127-34.

Qamri Z, Preet A, Nasser MW, Bass CE, Leone G, Barsky SH, Ganju RK (2009). Synthetic cannabinoid receptor agonists inhibit tumor growth and metastasis of breast cancer. *Mol Cancer Ther* **8:** 3117-29.

Qi H, Dal Cin P, Van de Voorde W, Elgamal AA, Van Poppel H, Baert L, Van Den Berghe H (1996). del(1)(q12) in adenocarcinomas of the prostate. *Cancer Genet Cytogenet* **87:** 79-81.

Rabbitts TH (2009). Commonality but diversity in cancer gene fusions. *Cell* **137:** 391-5.

Rajput AB, Miller MA, De Luca A, Boyd N, Leung S, Hurtado-Coll A, Fazli L, Jones EC, Palmer JB, Gleave ME, Cox ME, Huntsman DG (2007). Frequency of the TMPRSS2:ERG gene fusion is increased in moderate to poorly differentiated prostate cancers. *J Clin Pathol* **60:** 1238-43.

Ramer R, Hinz B (2008). Inhibition of cancer cell invasion by cannabinoids via increased expression of tissue inhibitor of matrix metalloproteinases-1. *J Natl Cancer Inst* **100:** 59-69.

Ramer R, Merkord J, Rohde H, Hinz B (2010). Cannabidiol inhibits cancer cell invasion via upregulation of tissue inhibitor of matrix metalloproteinases-1. *Biochem Pharmacol* **79:** 955-66.

Ransom DT, Ritland SR, Moertel CA, Dahl RJ, O'Fallon JR, Scheithauer BW, Kimmel DW, Kelly PJ, Olopade OI, Diaz MO, et al. (1992). Correlation of cytogenetic analysis and loss of heterozygosity studies in human diffuse astrocytomas and mixed oligo-astrocytomas. *Genes Chromosomes Cancer* **5:** 357-74.

Raptis S, Bapat B (2006). Genetic instability in human tumors. *EXS***:** 303-20.

Rempel SA, Schwechheimer K, Davis RL, Cavenee WK, Rosenblum ML (1993). Loss of heterozygosity for loci on chromosome 10 is associated with morphologically malignant meningioma progression. *Cancer Res* **53:** 2386-92.

Ribeiro FR, Diep CB, Jeronimo C, Henrique R, Lopes C, Eknaes M, Lingjaerde OC, Lothe RA, Teixeira MR (2006a). Statistical dissection of genetic pathways involved in prostate carcinogenesis. *Genes Chromosomes Cancer* **45:** 154-63.

Ribeiro FR, Jeronimo C, Henrique R, Fonseca D, Oliveira J, Lothe RA, Teixeira MR (2006b). 8q gain is an independent predictor of poor survival in diagnostic needle biopsies from prostate cancer suspects. *Clin Cancer Res* **12:** 3961-70.

Ricke RM, van Ree JH, van Deursen JM (2008). Whole chromosome instability and cancer: a complex relationship. *Trends Genet* **24:** 457-66.

Rikova K, Guo A, Zeng Q, Possemato A, Yu J, Haack H, Nardone J, Lee K, Reeves C, Li Y, Hu Y, Tan Z, Stokes M, Sullivan L, Mitchell J, Wetzel R, Macneill J, Ren JM, Yuan J, Bakalarski CE, Villen J, Kornhauser JM, Smith B, Li D, Zhou X, Gygi SP, Gu TL, Polakiewicz RD, Rush J, Comb MJ (2007). Global survey of phosphotyrosine signaling identifies oncogenic kinases in lung cancer. *Cell* **131:** 1190-203.

Rodriguez C, Jacobs EJ, Patel AV, Calle EE, Feigelson HS, Fakhrabadi-Shokoohi D, Thun MJ (2002). Jewish ethnicity and prostate cancer mortality in two large US cohorts. *Cancer Causes Control* **13:** 271-7.

Ross JS, Fletcher JA (1998). The HER-2/neu oncogene in breast cancer: prognostic factor, predictive factor, and target for therapy. *Stem Cells* **16:** 413-28.

Ruiz-Llorente L, Sanchez MG, Carmena MJ, Prieto JC, Sanchez-Chapado M, Izquierdo A, Diaz-Laviada I (2003). Expression of functionally active cannabinoid receptor CB1 in the human prostate gland. *Prostate* **54:** 95-102.

Sakane-Ishikawa E, Nakatsuka S, Tomita Y, Fujita S, Nakamichi I, Takakuwa T, Sugiyama H, Fukuhara S, Hino M, Kanamaru A, Soma T, Tsukaguchi M, Igarashi K, Kanakura Y, Aozasa K (2005). Prognostic significance of BACH2 expression in diffuse large B-cell lymphoma: a study of the Osaka Lymphoma Study Group. *J Clin Oncol* **23:** 8012-7.

Sakr WA, Grignon DJ, Haas GP, Heilbrun LK, Pontes JE, Crissman JD (1996). Age and racial distribution of prostatic intraepithelial neoplasia. *Eur Urol* **30:** 138-44.

Sampson VB, Rong NH, Han J, Yang Q, Aris V, Soteropoulos P, Petrelli NJ, Dunn SP, Krueger LJ (2007). MicroRNA let-7a down-regulates MYC and reverts MYC-induced growth in Burkitt lymphoma cells. *Cancer Res* **67:** 9762-70.

Sanchez MG, Ruiz-Llorente L, Sanchez AM, Diaz-Laviada I (2003). Activation of phosphoinositide 3-kinase/PKB pathway by CB(1) and CB(2) cannabinoid receptors expressed in prostate PC-3 cells. Involvement in Raf-1 stimulation and NGF induction. *Cell Signal* **15:** 851-9.

Santoro A, Pisanti S, Grimaldi C, Izzo AA, Borrelli F, Proto MC, Malfitano AM, Gazzerro P, Laezza C, Bifulco M (2009). Rimonabant inhibits human colon cancer cell growth and reduces the formation of precancerous lesions in the mouse colon. *Int J Cancer* **125:** 996-1003.

Saramaki OR, Porkka KP, Vessella RL, Visakorpi T (2006). Genetic aberrations in prostate cancer by microarray analysis. *Int J Cancer* **119:** 1322-9.

Sarfaraz S, Afaq F, Adhami VM, Malik A, Mukhtar H (2006). Cannabinoid receptor agonist-induced apoptosis of human prostate cancer cells LNCaP proceeds through sustained activation of ERK1/2 leading to G1 cell cycle arrest. *J Biol Chem* **281:** 39480-91.

Sarfaraz S, Afaq F, Adhami VM, Mukhtar H (2005). Cannabinoid receptor as a novel target for the treatment of prostate cancer. *Cancer Res* **65:** 1635-41.

Sasaki S, Ito E, Toki T, Maekawa T, Kanezaki R, Umenai T, Muto A, Nagai H, Kinoshita T, Yamamoto M, Inazawa J, Taketo MM, Nakahata T, Igarashi K, Yokoyama M (2000). Cloning and expression of human B cell-specific transcription factor BACH2 mapped to chromosome 6q15. *Oncogene* **19:** 3739-49.

Savelyeva L, Schwab M (2001). Amplification of oncogenes revisited: from expression profiling to clinical application. *Cancer Lett* **167:** 115-23.

Schaid DJ (2004). The complex genetic epidemiology of prostate cancer. *Hum Mol Genet* **13 Spec No 1:** R103-21.

Schatz P, Dietrich D, Koenig T, Burger M, Lukas A, Fuhrmann I, Kristiansen G, Stoehr R, Schuster M, Lesche R, Weiss G, Corman J, Hartmann A (2010). Development of a diagnostic microarray assay to assess the risk of recurrence of prostate cancer based on PITX2 DNA methylation. *J Mol Diagn* **12:** 345-53.

Scher HI, Jia X, de Bono JS, Fleisher M, Pienta KJ, Raghavan D, Heller G (2009). Circulating tumour cells as prognostic markers in progressive, castration-resistant prostate cancer: a reanalysis of IMMC38 trial data. *Lancet Oncol* **10:** 233-9.

Schroder FH, Hugosson J, Roobol MJ, Tammela TL, Ciatto S, Nelen V, Kwiatkowski M, Lujan M, Lilja H, Zappa M, Denis LJ, Recker F, Berenguer A, Maattanen L, Bangma CH, Aus G, Villers A, Rebillard X, van der Kwast T, Blijenberg BG, Moss SM, de Koning HJ, Auvinen A (2009). Screening and prostate-cancer mortality in a randomized European study. *N Engl J Med* **360:** 1320-8.

Sessions J (2007). Chronic myeloid leukemia in 2007. *J Manag Care Pharm* **13:** 4-7.

Shah RB, Chinnaiyan AM (2009). The discovery of common recurrent transmembrane protease serine 2 (TMPRSS2)-erythroblastosis virus E26 transforming sequence (ETS) gene fusions in prostate cancer: significance and clinical implications. *Adv Anat Pathol* **16:** 145-53.

Shaheduzzaman S, Vishwanath A, Furusato B, Cullen J, Chen Y, Banez L, Nau M, Ravindranath L, Kim KH, Mohammed A, Ehrich M, Srikantan V, Sesterhenn IA, McLeod D, Vahey M, Petrovics G, Dobi A, Srivastava S (2007). Silencing of Lactotransferrin expression by methylation in prostate cancer progression. *Cancer Biol Ther* **6:** 1088-95.

Shen MM, Abate-Shen C (2003). Roles of the Nkx3.1 homeobox gene in prostate organogenesis and carcinogenesis. *Dev Dyn* **228:** 767-78.

Sheng ZM, Marchetti A, Buttitta F, Champeme MH, Campani D, Bistocchi M, Lidereau R, Callahan R (1996). Multiple regions of chromosome 6q affected by loss of heterozygosity in primary human breast carcinomas. *Br J Cancer* **73:** 144-7.

Slamon DJ, Clark GM, Wong SG, Levin WJ, Ullrich A, McGuire WL (1987). Human breast cancer: correlation of relapse and survival with amplification of the HER-2/neu oncogene. *Science* **235:** 177-82.

Slamon DJ, Godolphin W, Jones LA, Holt JA, Wong SG, Keith DE, Levin WJ, Stuart SG, Udove J, Ullrich A, et al. (1989). Studies of the HER-2/neu proto-oncogene in human breast and ovarian cancer. *Science* **244:** 707-12.

Soda M, Choi YL, Enomoto M, Takada S, Yamashita Y, Ishikawa S, Fujiwara S, Watanabe H, Kurashina K, Hatanaka H, Bando M, Ohno S, Ishikawa Y, Aburatani H, Niki T, Sohara Y, Sugiyama Y, Mano H (2007). Identification of the transforming EML4-ALK fusion gene in non-small-cell lung cancer. *Nature* **448:** 561-6.

Solinas-Toldo S, Lampel S, Stilgenbauer S, Nickolenko J, Benner A, Dohner H, Cremer T, Lichter P (1997). Matrix-based comparative genomic hybridization: biochips to screen for genomic imbalances. *Genes Chromosomes Cancer* **20:** 399-407.

Srikantan V, Sesterhenn IA, Davis L, Hankins GR, Avallone FA, Livezey JR, Connelly R, Mostofi FK, McLeod DG, Moul JW, Chandrasekharappa SC, Srivastava S (1999). Allelic loss on chromosome 6Q in primary prostate cancer. *Int J Cancer* **84:** 331-5.

Steck PA, Pershouse MA, Jasser SA, Yung WK, Lin H, Ligon AH, Langford LA, Baumgard ML, Hattier T, Davis T, Frye C, Hu R, Swedlund B, Teng DH, Tavtigian SV (1997). Identification of a candidate tumour suppressor gene, MMAC1, at chromosome 10q23.3 that is mutated in multiple advanced cancers. *Nat Genet* **15:** 356-62.

Summersgill B, Clark J, Shipley J (2008). Fluorescence and chromogenic in situ hybridization to detect genetic aberrations in formalin-fixed paraffin embedded material, including tissue microarrays. *Nat Protoc* **3:** 220-34.

Sun J, Liu W, Adams TS, Li X, Turner AR, Chang B, Kim JW, Zheng SL, Isaacs WB, Xu J (2007). DNA copy number alterations in prostate cancers: a combined analysis of published CGH studies. *Prostate* **67:** 692-700.

Sun J, Purcell L, Gao Z, Isaacs SD, Wiley KE, Hsu FC, Liu W, Duggan D, Carpten JD, Gronberg H, Xu J, Chang BL, Partin AW, Walsh PC, Isaacs WB, Zheng SL (2008). Association between sequence variants at 17q12 and 17q24.3 and prostate cancer risk in European and African Americans. *Prostate* **68:** 691-7.

Sun M, Srikantan V, Ma L, Li J, Zhang W, Petrovics G, Makarem M, Strovel JW, Horrigan SG, Augustus M, Sesterhenn IA, Moul JW, Chandrasekharappa S, Zou Z, Srivastava S (2006). Characterization of frequently deleted 6q locus in prostate cancer. *DNA Cell Biol* **25:** 597-607.

Takamizawa J, Konishi H, Yanagisawa K, Tomida S, Osada H, Endoh H, Harano T, Yatabe Y, Nagino M, Nimura Y, Mitsudomi T, Takahashi T (2004). Reduced expression of the let-7 microRNAs in human lung cancers in association with shortened postoperative survival. *Cancer Res* **64:** 3753-6.

Takeda S, Yamaori S, Motoya E, Matsunaga T, Kimura T, Yamamoto I, Watanabe K (2008). Delta(9)-Tetrahydrocannabinol enhances MCF-7 cell proliferation via cannabinoid receptor-independent signaling. *Toxicology* **245:** 141-6.

Taylor BS, Schultz N, Hieronymus H, Gopalan A, Xiao Y, Carver BS, Arora VK, Kaushik P, Cerami E, Reva B, Antipin Y, Mitsiades N, Landers T, Dolgalev I, Major JE,

Wilson M, Socci ND, Lash AE, Heguy A, Eastham JA, Scher HI, Reuter VE, Scardino PT, Sander C, Sawyers CL, Gerald WL (2010). Integrative genomic profiling of human prostate cancer. *Cancer Cell* **18:** 11-22.

Team RDC (2009). *R: A language and environment for statistical computing*. R Foundation for Statistical Computing: Vienna, Austria.

Teixeira MR, Waehre H, Lothe RA, Stenwig AE, Pandis N, Giercksky KE, Heim S (2000). High frequency of clonal chromosome abnormalities in prostatic neoplasms sampled by prostatectomy or ultrasound-guided needle biopsy. *Genes Chromosomes Cancer* **28:** 211-9.

Thiebault K, Mazelin L, Pays L, Llambi F, Joly MO, Scoazec JY, Saurin JC, Romeo G, Mehlen P (2003). The netrin-1 receptors UNC5H are putative tumor suppressors controlling cell death commitment. *Proc Natl Acad Sci U S A* **100:** 4173-8.

Thomas G, Jacobs KB, Yeager M, Kraft P, Wacholder S, Orr N, Yu K, Chatterjee N, Welch R, Hutchinson A, Crenshaw A, Cancel-Tassin G, Staats BJ, Wang Z, Gonzalez-Bosquet J, Fang J, Deng X, Berndt SI, Calle EE, Feigelson HS, Thun MJ, Rodriguez C, Albanes D, Virtamo J, Weinstein S, Schumacher FR, Giovannucci E, Willett WC, Cussenot O, Valeri A, Andriole GL, Crawford ED, Tucker M, Gerhard DS, Fraumeni JF, Jr., Hoover R, Hayes RB, Hunter DJ, Chanock SJ (2008a). Multiple loci identified in a genome-wide association study of prostate cancer. *Nat Genet* **40:** 310-5.

Thomas LN, Douglas RC, Lazier CB, Gupta R, Norman RW, Murphy PR, Rittmaster RS, Too CK (2008b). Levels of 5alpha-reductase type 1 and type 2 are increased in localized high grade compared to low grade prostate cancer. *J Urol* **179:** 147-51.

Thomas LN, Douglas RC, Lazier CB, Too CK, Rittmaster RS, Tindall DJ (2008c). Type 1 and type 2 5alpha-reductase expression in the development and progression of prostate cancer. *Eur Urol* **53:** 244-52.

Thompson IM, Pauler DK, Goodman PJ, Tangen CM, Lucia MS, Parnes HL, Minasian LM, Ford LG, Lippman SM, Crawford ED, Crowley JJ, Coltman CA, Jr. (2004). Prevalence of prostate cancer among men with a prostate-specific antigen level < or =4.0 ng per milliliter. *N Engl J Med* **350:** 2239-46.

Thorsen K, Sorensen KD, Brems-Eskildsen AS, Modin C, Gaustadnes M, Hein AM, Kruhoffer M, Laurberg S, Borre M, Wang K, Brunak S, Krainer AR, Torring N, Dyrskjot L, Andersen CL, Orntoft TF (2008). Alternative splicing in colon, bladder, and prostate cancer identified by exon array analysis. *Mol Cell Proteomics* **7:** 1214-24.

Tibiletti MG, Bernasconi B, Furlan D, Bressan P, Cerutti R, Facco C, Franchi M, Riva C, Cinquetti R, Capella C, Taramelli R (2001). Chromosome 6 abnormalities in ovarian surface epithelial tumors of borderline malignancy suggest a genetic continuum in the progression model of ovarian neoplasms. *Clin Cancer Res* **7:** 3404-9.

Tognon C, Knezevich SR, Huntsman D, Roskelley CD, Melnyk N, Mathers JA, Becker L, Carneiro F, MacPherson N, Horsman D, Poremba C, Sorensen PH (2002). Expression of the ETV6-NTRK3 gene fusion as a primary event in human secretory breast carcinoma. *Cancer Cell* **2:** 367-76.

Tomlins SA, Rhodes DR, Perner S, Dhanasekaran SM, Mehra R, Sun XW, Varambally S, Cao X, Tchinda J, Kuefer R, Lee C, Montie JE, Shah RB, Pienta KJ, Rubin MA,

Chinnaiyan AM (2005). Recurrent fusion of TMPRSS2 and ETS transcription factor genes in prostate cancer. *Science* **310:** 644-8.

Tomlins SA, Laxman B, Dhanasekaran SM, Helgeson BE, Cao X, Morris DS, Menon A, Jing X, Cao Q, Han B, Yu J, Wang L, Montie JE, Rubin MA, Pienta KJ, Roulston D, Shah RB, Varambally S, Mehra R, Chinnaiyan AM (2007). Distinct classes of chromosomal rearrangements create oncogenic ETS gene fusions in prostate cancer. *Nature* **448:** 595-9.

Tomlins SA, Laxman B, Varambally S, Cao X, Yu J, Helgeson BE, Cao Q, Prensner JR, Rubin MA, Shah RB, Mehra R, Chinnaiyan AM (2008). Role of the TMPRSS2-ERG gene fusion in prostate cancer. *Neoplasia* **10:** 177-88.

Tost J, Gut IG (2007). DNA methylation analysis by pyrosequencing. *Nat Protoc* **2:** 2265-75.

Touma SE, Perner S, Rubin MA, Nanus DM, Gudas LJ (2009). Retinoid metabolism and ALDH1A2 (RALDH2) expression are altered in the transgenic adenocarcinoma mouse prostate model. *Biochem Pharmacol* **78:** 1127-38.

Trosko JE, Ruch RJ (1998). Cell-cell communication in carcinogenesis. *Front Biosci* **3:** d208-36.

Trybus TM, Burgess AC, Wojno KJ, Glover TW, Macoska JA (1996). Distinct areas of allelic loss on chromosomal regions 10p and 10q in human prostate cancer. *Cancer Res* **56:** 2263-7.

van Dekken H, Paris PL, Albertson DG, Alers JC, Andaya A, Kowbel D, van der Kwast TH, Pinkel D, Schroder FH, Vissers KJ, Wildhagen MF, Collins C (2004). Evaluation of genetic patterns in different tumor areas of intermediate-grade prostatic adenocarcinomas by high-resolution genomic array analysis. *Genes Chromosomes Cancer* **39:** 249-56.

van Heemst D, den Reijer PM, Westendorp RG (2007). Ageing or cancer: a review on the role of caretakers and gatekeepers. *Eur J Cancer* **43:** 2144-52.

Varghese JS, Easton DF (2010). Genome-wide association studies in common cancers--what have we learnt? *Curr Opin Genet Dev* **20:** 201-9.

Ventura A, Jacks T (2009). MicroRNAs and cancer: short RNAs go a long way. *Cell* **136:** 586-91.

Ventura RA, Martin-Subero JI, Jones M, McParland J, Gesk S, Mason DY, Siebert R (2006). FISH analysis for the detection of lymphoma-associated chromosomal abnormalities in routine paraffin-embedded tissue. *J Mol Diagn* **8:** 141-51.

Verhagen PC, Hermans KG, Brok MO, van Weerden WM, Tilanus MG, de Weger RA, Boon TA, Trapman J (2002). Deletion of chromosomal region 6q14-16 in prostate cancer. *Int J Cancer* **102:** 142-7.

Veronese ML, Bullrich F, Negrini M, Croce CM (1996). The t(6;16)(p21;q22) chromosome translocation in the LNCaP prostate carcinoma cell line results in a tpc/hpr fusion gene. *Cancer Res* **56:** 728-32.

Vieira SA, Deininger MW, Sorour A, Sinclair P, Foroni L, Goldman JM, Melo JV (2001). Transcription factor BACH2 is transcriptionally regulated by the BCR/ABL oncogene. *Genes Chromosomes Cancer* **32:** 353-63.

Vinson C, Acharya A, Taparowsky EJ (2006). Deciphering B-ZIP transcription factor interactions in vitro and in vivo. *Biochim Biophys Acta* **1759:** 4-12.

Vogt N, Lefevre SH, Apiou F, Dutrillaux AM, Cor A, Leuraud P, Poupon MF, Dutrillaux B, Debatisse M, Malfoy B (2004). Molecular structure of double-minute chromosomes bearing amplified copies of the epidermal growth factor receptor gene in gliomas. *Proc Natl Acad Sci U S A* **101:** 11368-73.

Walker GJ, Palmer JM, Walters MK, Nancarrow DJ, Parsons PG, Hayward NK (1994). Simple tandem repeat allelic deletions confirm the preferential loss of distal chromosome 6q in melanoma. *Int J Cancer* **58:** 203-6.

Walker M, Aronson KJ, King W, Wilson JW, Fan W, Heaton JP, MacNeily A, Nickel JC, Morales A (2005). Dietary patterns and risk of prostate cancer in Ontario, Canada. *Int J Cancer* **116:** 592-8.

Wang D, Wang H, Ning W, Backlund MG, Dey SK, DuBois RN (2008). Loss of cannabinoid receptor 1 accelerates intestinal tumor growth. *Cancer Res* **68:** 6468-76.

Wang J, Cai Y, Ren C, Ittmann M (2006). Expression of variant TMPRSS2/ERG fusion messenger RNAs is associated with aggressive prostate cancer. *Cancer Res* **66:** 8347-51.

Warmuth M, Danhauser-Riedl S, Hallek M (1999). Molecular pathogenesis of chronic myeloid leukemia: implications for new therapeutic strategies. *Ann Hematol* **78:** 49-64.

Watson SK, Deleeuw RJ, Horsman DE, Squire JA, Lam WL (2007). Cytogenetically balanced translocations are associated with focal copy number alterations. *Hum Genet* **120:** 795-805.

Watson SK, Woolcock BW, Fee JN, Bainbridge TC, Webber D, Kinahan TJ, Lam WL, Vielkind JR (2009). Minimum altered regions in early prostate cancer progression identified by high resolution whole genome tiling path BAC array comparative hybridization. *Prostate* **69:** 961-75.

Weaver BA, Cleveland DW (2006). Does aneuploidy cause cancer? *Curr Opin Cell Biol* **18:** 658-67.

Webb HD, Hawkins AL, Griffin CA (1996). Cytogenetic abnormalities are frequent in uncultured prostate cancer cells. *Cancer Genet Cytogenet* **88:** 126-32.

Weinberg RA (2007). *The biology of cancer*. Garland Science.

Weisenberger DJ, Siegmund KD, Campan M, Young J, Long TI, Faasse MA, Kang GH, Widschwendter M, Weener D, Buchanan D, Koh H, Simms L, Barker M, Leggett B, Levine J, Kim M, French AJ, Thibodeau SN, Jass J, Haile R, Laird PW (2006). CpG island methylator phenotype underlies sporadic microsatellite instability and is tightly associated with BRAF mutation in colorectal cancer. *Nat Genet* **38:** 787-93.

Whitaker HC, Warren AY, Eeles R, Kote-Jarai Z, Neal DE (2010). The potential value of microseminoprotein-beta as a prostate cancer biomarker and therapeutic target. *Prostate* **70:** 333-40.

Witte JS (2007). Multiple prostate cancer risk variants on 8q24. *Nat Genet* **39:** 579-80.

Xian XS, Park H, Cho YK, Lee IS, Kim SW, Choi MG, Chung IS, Han KH, Park JM (2010). Effect of a synthetic cannabinoid agonist on the proliferation and invasion of gastric cancer cells. *J Cell Biochem* **110:** 321-32.

Xu X, Liu Y, Huang S, Liu G, Xie C, Zhou J, Fan W, Li Q, Wang Q, Zhong D, Miao X (2006). Overexpression of cannabinoid receptors CB1 and CB2 correlates with improved prognosis of patients with hepatocellular carcinoma. *Cancer Genet Cytogenet* **171:** 31-8.

Yanaihara N, Caplen N, Bowman E, Seike M, Kumamoto K, Yi M, Stephens RM, Okamoto A, Yokota J, Tanaka T, Calin GA, Liu CG, Croce CM, Harris CC (2006). Unique microRNA molecular profiles in lung cancer diagnosis and prognosis. *Cancer Cell* **9:** 189-98.

Yeager M, Orr N, Hayes RB, Jacobs KB, Kraft P, Wacholder S, Minichiello MJ, Fearnhead P, Yu K, Chatterjee N, Wang Z, Welch R, Staats BJ, Calle EE, Feigelson HS, Thun MJ, Rodriguez C, Albanes D, Virtamo J, Weinstein S, Schumacher FR, Giovannucci E, Willett WC, Cancel-Tassin G, Cussenot O, Valeri A, Andriole GL, Gelmann EP, Tucker M, Gerhard DS, Fraumeni JF, Jr., Hoover R, Hunter DJ, Chanock SJ, Thomas G (2007). Genome-wide association study of prostate cancer identifies a second risk locus at 8q24. *Nat Genet* **39:** 645-9.

Yegnasubramanian S, Kowalski J, Gonzalgo ML, Zahurak M, Piantadosi S, Walsh PC, Bova GS, De Marzo AM, Isaacs WB, Nelson WG (2004). Hypermethylation of CpG islands in primary and metastatic human prostate cancer. *Cancer Res* **64:** 1975-86.

Yoshida C, Yoshida F, Sears DE, Hart SM, Ikebe D, Muto A, Basu S, Igarashi K, Melo JV (2007). Bcr-Abl signaling through the PI-3/S6 kinase pathway inhibits nuclear translocation of the transcription factor Bach2, which represses the antiapoptotic factor heme oxygenase-1. *Blood* **109:** 1211-9.

Yoshimoto M, Joshua AM, Cunha IW, Coudry RA, Fonseca FP, Ludkovski O, Zielenska M, Soares FA, Squire JA (2008). Absence of TMPRSS2:ERG fusions and PTEN losses in prostate cancer is associated with a favorable outcome. *Mod Pathol* **21:** 1451-60.

Yu J, Leung WK, Ebert MP, Leong RW, Tse PC, Chan MW, Bai AH, To KF, Malfertheiner P, Sung JJ (2003). Absence of cyclin D2 expression is associated with promoter hypermethylation in gastric cancer. *Br J Cancer* **88:** 1560-5.

Zanke BW, Greenwood CM, Rangrej J, Kustra R, Tenesa A, Farrington SM, Prendergast J, Olschwang S, Chiang T, Crowdy E, Ferretti V, Laflamme P, Sundararajan S, Roumy S, Olivier JF, Robidoux F, Sladek R, Montpetit A, Campbell P, Bezieau S, O'Shea AM, Zogopoulos G, Cotterchio M, Newcomb P, McLaughlin J, Younghusband B, Green R, Green J, Porteous ME, Campbell H, Blanche H, Sahbatou M, Tubacher E, Bonaiti-Pellie C, Buecher B, Riboli E, Kury S, Chanock SJ, Potter J, Thomas G, Gallinger S, Hudson TJ, Dunlop MG (2007). Genome-wide association scan identifies a colorectal cancer susceptibility locus on chromosome 8q24. *Nat Genet* **39:** 989-94.

Zhang JS, Wang L, Huang H, Nelson M, Smith DI (2001). Keratin 23 (K23), a novel acidic keratin, is highly induced by histone deacetylase inhibitors during differentiation of pancreatic cancer cells. *Genes Chromosomes Cancer* **30:** 123-35.

Zitzelsberger H, Szucs S, Robens E, Weier HU, Hofler H, Bauchinger M (1996). Combined cytogenetic and molecular genetic analyses of fifty-nine untreated human prostate carcinomas. *Cancer Genet Cytogenet* **90:** 37-44.